Implications of global warming for African climate

RACHEL JAMES

Hertford College

A thesis submitted for the degree of Doctor of Philosophy

University of Oxford

Michaelmas Term 2013

Abstract

A 2°C increase in global mean temperature (ΔT_g) has been widely adopted as a benchmark for dangerous climate change. However, there has been a lack of research into the implications of 2°C, or any other degree of warming, for Africa. In this thesis changes in African temperature and precipitation associated with 1°C, 2°C, 3°C, 4°C, and beyond are investigated for the first time, using output from 350 climate model experiments: a collection of simulations from international modelling centres (CMIP3), two Perturbed Physics Ensembles (PPEs), and a group of five regional models. The models project temperature and precipitation anomalies which increase in magnitude and spatial extent as global temperature rises, including a wet signal in East Africa, and drier conditions for African rainforests. The models consistently show that the evolution of change with global warming is gradual, even at 4°C and beyond; but the amplitude and direction of precipitation change at each ΔT_g increment vary between models and between datasets. The PPEs project precipitation signals which are not represented by CMIP3, in particular a large drying (>0.5 mm day^{-1} $°C^{-1}$) of western Africa. There are also important differences between global and regional models, especially in southern and West Africa (>1 mm day^{-1}). Analysis of atmospheric circulation responses suggests that the higher resolution projections are no more credible in this case. Some of the variation between models can be understood as the result of untrustworthy simulations, leading to constraints on the PPEs, and casting doubt on the strong drying of west Sahel; but model evaluation is found to be limited by observations in the case of the Congo Basin. The implications of global warming are different depending on which models are consulted. The findings emphasise that caution should be exercised in the application of climate model data to inform mitigation debates.

Table of Contents

Acknowledgements

The research described in this thesis would not have been possible without the generous support of Hertford College and the Julia, Bruce, and Mortimer May Senior Scholarship, which funded me through three stimulating years as a DPhil student. I will be eternally grateful to the benefactors.

The thesis is based on climate model data and it is only right that I acknowledge the countless people and institutions that have worked for many years to develop the models, and to make them available for analysis. Specific acknowledgements for each dataset will be provided in the relevant chapters. I am also thankful to those people who have assisted me personally with accessing and downloading data, often sharing considerable time and expertise, in particular Carlo Buontempo, Karina Williams, Jagadishwor Karmacharya, and Simon Driscoll. Gil Lizcano provided vital technical support and training for the initial data analysis and Sebastian Engelstaedter has offered extremely helpful advice and assistance.

The research has greatly benefited from collaboration with some excellent scientists. Dave Rowell has played a fundamental role in this project, both in initiating the use of the QUMP dataset, and by contributing useful insights throughout the analysis. It has been a pleasure working with him, and I am very grateful for all of the time, feedback, and advice he has offered over the last couple of years. I am also much obliged to Richard Jones, who has somehow always found the time in his unfathomable schedule to answer my questions, and who made an essential contribution to the investigation of regional models in this thesis. I hope we can continue working together in future.

Conversations with many other scientists have been enormously helpful, including Myles Allen, Yadvinder Malhi, Mark New, Mxolisi Shongwe, Wilfried Pokam, Camilla Mathison, Carol McSweeney, Wilfran Moufouma-Okia, Peter Good, and William Ingram. In particular, I'd like to thank Richard Allan, whose readiness to help me early in the project was very motivating, and David Sexton, who generously offered his time and expertise to help guide the research of perturbed physics ensembles.

I would also like to mention Giles Wiggs, my undergraduate tutor at Brasenose College, for encouraging me to pursue research, and for his continued support. Additionally, I would like to acknowledge the organisers of the Boulder summer school which I attended in my second year: Linda Mearns, Hayley Fowler, and Chris Forest. The workshop allowed me to view my research in a broader context, and has motivated me to pursue more

integrated research beyond my doctorate. Others who have inspired me to think about the use of climate information include Rosalind Cornforth, Emma Visman, Rebecca Darbyshire, and Fai Fung.

Many superb friends have made the last three years a joy, and also dealt with some severe neglect over the latter six months. My sister, I want to thank for being an excellent friend, for inspiring me to work on the things that matter, and for the frequent deliveries of cake and perspective whilst I was writing up. I am very glad to have taken on Niel as a friend and brother. He has played a crucial role in helping me to finish this thesis, by reminding me of the world beyond my DPhil, and introducing me to task management software! Enormous thanks to Rio, not least for taking me on adventures away from Oxford when I needed it most. I am also very appreciative of the many wonderful inhabitants of both Hurst Street and Rectory Road, in particular Lucy for her continued interest in my daily routine, and Will for some very energising breakfast conversations. My fellow students and colleagues in the Climate Research Lab and the School of Geography have also greatly enhanced my time in Oxford. I am especially keen to thank Andika, for an education in chocolate and the English language. Big thanks to Hugo and Amy: Friday lunch transformed many a week of coding.

My Mum and Dad deserve a particularly special mention. They provided an essential proportion of the funding for this project, and have offered me so much else besides, supporting me financially, intellectually, and emotionally (!) through twenty-one years of education. Any of the qualities which helped me to complete this thesis were inherited from them. It was their conviction that I should take up this opportunity which persuaded me to begin the DPhil, and their persistent words of wisdom which have carried me this far. I am incredibly lucky to have such magnificent people as parents and friends.

Finally, I would like to recognise Richard Washington's immeasurable contribution to this thesis and to my induction into scientific research. I have benefited immensely from his ideas, insights, and advice over the years. I feel very fortunate to work with a supervisor with such an ability to identify what is important, as well as the best teacher I've ever had. I have also never encountered another scientist with such a poetic way with words. It was Richard who first inspired me to undertake climate research, and who has continued to motivate me throughout, whilst also enduring my endless lists of questions with good humour! It has been an absolute pleasure to work with him and I hope there are many years of collaboration ahead.

xx

List of Tables

List of Figures

List of Acronyms and Abbreviations

ΔT_g	Global mean temperature increase
ω	Omega/vertical velocity
1xCO_2	Preindustrial CO_2
2xCO_2	Double preindustrial CO_2
4xCO_2	Quadruple preindustrial CO_2
20C3M	Emissions scenario with 20th century forcings
A1B	SRES scenario with increasing emissions in a more integrated world
A1FI	SRES scenario with fossil fuel intensive emissions
A2	SRES scenario with increasing emissions in a more divided world
AEJ	African Easterly Jet
AEWs	African Easterly Waves
AMDAR	Aircraft Meteorological Data Relay
AMMA	African Monsoon Multidisciplinary Analysis
AOGCM	Atmosphere-Ocean General Circulation Model
AO-PPE	MOHC PPE of 17 AOGCMs (see section 2.2.2)
AOSIS	Association of Small Island States
AR4	Fourth Assessment Report (of the IPCC)
AR5	Fifth Assessment Report (of the IPCC)
ASGCM	Atmosphere-Slab ocean General Circulation Model
AS-PPE	MOHC PPE of 280 ASGCMs (see section 2.2.2)
AWJ	African Westerly Jet
BADC	British Atmospheric Data Centre
CFSR	Climate Forecast System Reanalysis
CMAP	Climate Prediction Centre Merged Analysis of Precipitation
CMIP	Coupled Model Intercomparison Project
CMIP3	Coupled Model Intercomparison Project phase 3
CMIP5	Coupled Model Intercomparison Project phase 5
CMORPH	NOAA CPC Morphing Technique
CORDEX	Coordinated Regional Downscaling Experiment
CRU	Climate Research Unit (University of East Anglia)

CSC	Climate Service Center (Hamburg)
DAI	Dangerous Anthropogenic Interference
DECC	Department for Energy and Climate Change (UK)
Defra	Department for Environment, Food and Rural Affairs (UK)
DFID	Department for International Development (UK)
DJF	December-January-February
DJFM	December-January-February-March
ECMWF	European Centre for Medium-Range Weather Forecasts
ENSO	El Nino Southern Oscillation
EOF	Empirical Orthogonal Function
ERA-40	ECMWF 40 year reanalysis
ERA-I	ERA-Interim (ECMWF Interim reanalysis)
ESM	Earth System Model
EU	European Union
GCM	Global Climate Model/General Circulation Model
GHG	Greenhouse Gas
GPCP	Global Precipitation Climatology Project
IOD	Indian Ocean Dipole
IPCC	Intergovernmental Panel on Climate Change
ISM	Indian Summer Monsoon
ITCZ	Inter-Tropical Convergence Zone
JAS	July-August-September
JFM	January-February-March
JJA	June-July-August
JJAS	June-July-August-September
LBA	Large-Scale Biosphere Atmosphere Experiment
LLWs	Low Level Westerlies
MAM	March-April-May
MCS	Mesoscale Convective Systems
MCWD	Maximum Climatological Water Deficit
MME	Multi-Model Ensemble
MOHC	Met Office Hadley Centre
MOSES	Met Office Surface Exchange Scheme
NCAR	National Centre for Atmospheric Research (USA)

NCEP	National Centers for Environmental Prediction (USA) – here used to refer to the NCEP/NCAR reanalysis 1
NGO	Non-Govermental Organisation
NH	Northern Hemisphere
NOAA	National Oceanic and Atmospheric Adminstration (USA)
OND	October-November-December
PC	Principal Component
PCA	Principal Component Analysis
PCMDI	Programme for Climate Model Diagnosis and Intercomparison
PPE	Perturbed Physics Ensemble
q	Specific humidity
QCCCE	Queensland Climate Change Centre of Excellence
QUMP	Quantifying Uncertainty in Model Projections
qV	Moisture flux
PRECIS	Providing Regional Climates for Impact Studies
PRECIS-GCM	MOHC PPE of 5 AOGCMs (see section 2.2.2)
PRECIS-RCM	MOHC ensemble of 5 RCMs (see section 2.3)
RCM	Regional Climate Model
RCP	Representative Concentration Pathway
RCP2.6	RCP with radiative forcing of approximately 2.6 $W.m^{-2}$ in 2100
RCP8.5	RCP with radiative forcing of approximately 8.5 $W.m^{-2}$ in 2100
SAMBBA	South American Biomass Burning Analysis
SAR	Second Assessment Report
SH	Southern Hemisphere
SHL	Saharan Heat Low
SICZ	South Indian Convergence Zone
SLP	Sea Level Pressure
SON	September-October-November
S-PPE-S	First part of AS-PPE
S-PPE-M	Second part of AS-PPE
S-PPE-E	Third part of AS-PPE
SRES	Special Report on Emissions Scenarios
SST	Sea-Surface Temperature
SWIOD	South West Indian Ocean Dipole

TAMSAT	Tropical Applications of Meteorology using SATellite data and ground-based observations
TARCAT	TAMSAT African Rainfall Climatology and Time-Series
TEJ	Tropical Easterly Jet
TRMM	Tropical Rainfall Measuring Mission
TTCB	Tropical-Temperate Cloud Band
TTT	Tropical-Temperate Trough
u	Zonal wind
UKCP09	United Kingdom Climate Projections 2009
UN	United Nations
UNFCCC	United Nations Framework Convention on Climate Change
v	Meridional wind
WAM	West African Monsoon
WCRP	World Climate Research Programme
WG1	Working Group 1 (of the IPCC)

1 Introduction

1.1 Motivation for research

1.1.1 Background and Rationale

Human activity has now led to the emission of over 500 PgC into the atmosphere (Ciais et al. 2013) and anthropogenic Greenhouse Gas (GHG) emissions continue to rise (Le Quéré et al. 2012; Peters et al. 2012). The growth in the concentration of CO_2 and other GHGs has contributed to an observed increase in global mean temperature (ΔT_g) of approximately 0.89°C since the 19th century (Forster and Rahmstorf 2011; Hartmann et al. 2013), and global warming is expected to continue in future if CO_2 emissions are not reduced to zero (Matthews and Weaver 2010). Higher global temperatures might be associated with changes in regional climate which pose a threat to ecosystems, economies, and societies; particularly in regions which are the most vulnerable to climate change; many of which are in Africa (Boko et al. 2007).

Policy-makers from 195 countries have pledged to stabilise atmospheric GHG concentrations so as to prevent dangerous anthropogenic interference with the climate system, under the United Nations Framework Convention on Climate Change (UN 1992; UNFCCC 2013). Much of the debate surrounding the UNFCCC concerns how to avoid a 2°C global mean temperature increase (ΔT_g), which has largely been adopted as a benchmark for dangerous climate change (Randalls et al. 2010). Yet 2°C is not a scientific goal (Jaeger and Jaeger 2010). There is a lack of scientific research which can be used to judge whether 2°C would be safe from a regional perspective, particularly for Africa.

Climate models offer the potential to investigate the influence of anthropogenic forcing on regional climate systems (Randall et al. 2007; Collins et al. 2013). Tens of climate research centres around the world have run models of the Earth's atmosphere in experiments with increasing GHG emissions (Meehl et al. 2007a; Taylor et al. 2012a); to investigate how climate might change in future, and explore the associated uncertainties (Murphy et al. 2004; Stainforth et al. 2005). Output from many of these simulations is widely available, including data from global and regional models which vary in terms of grid-spacing, core physics, and parameterisation. However, there has been very little research using climate model output to identify regional changes associated with specific ΔT_g intervals. Most experiments are run through the twenty-first century, and the majority of climate projection and climate impacts research, including for Africa, inspects changes in time-slices (Kaplan and New 2006), such as 2075-2100 (e.g. Giannini et al. 2008). Using these studies, policy-makers can develop adaptation strategies for specific decades, but cannot determine what degree of global warming might be dangerous from a regional perspective.

1.1.2 Aims and Objectives

In this thesis data from existing climate model experiments run with increasing GHG emissions are exploited to investigate changes in African temperature and precipitation at 1°C, 2°C, 3°C, 4°C ΔT_g and beyond. For the first time, projections will be presented at specific degrees of global warming across the African continent. Important policy-relevant questions will be asked of the models:

what changes in regional climate are associated with different levels of ΔT_g? Will local climate change be amplified progressively as global temperature increases? Will the rate of change with global warming imply that incremental adaptation is possible, or will there be non-linear transformations which would require early mitigation to avoid?

The principal research question is therefore:

- How do temperature and precipitation in Africa evolve with anthropogenic global warming in climate models?

The ability of the models to realistically simulate responses to warming should also be considered. The value of climate projections is a huge topic (e.g. Räisänen 2007), a full treatment of which is beyond the scope of this thesis. However by comparing projections from three different datasets, and investigating sources of variation between models; this thesis will seek to make a small contribution towards understanding the credibility of the evidence base. Are the implications of global warming different depending on which types of models are consulted? Can any of the precipitation responses be judged to be untrustworthy? Does variation between models result from limited understanding or identifiable model errors?

The central aim is therefore:

- To identify and interrogate changes in African temperature and precipitation associated with degrees of anthropogenic global warming in climate model experiments.

1.1.3 Relevance to policy

The importance of the thesis will not be manifest in a direct contribution to mitigation policy. The focus is on changes in mean climate, and it is difficult to judge how these will influence society without investigation of extremes, variability, or impacts (IPCC 2012). Analysis of changes in the mean is therefore only the first step towards generating information to support the selection of a mitigation goal; but it is a crucial one. It is useful to know whether there are thresholds or nonlinearities in the evolution of mean climate: any abrupt changes could be used as initial evidence for mitigating to a ΔT_g increment which avoids the onset of rapid change. Conversely, if change is linear, there will be limited potential for distinguishing between ΔT_g increments on the basis of seasonal climate, and impacts assessment becomes even more important. In this case, the projected changes in mean temperature and precipitation found here would be an essential starting point for research into changes in, for example, water availability, agriculture, or health.

The key reason for focusing on mean changes, though, is the importance of understanding uncertainty in climate before proceeding to impacts assessment; particularly in the case of precipitation since it is so difficult to model (e.g. Dai 2006). Impacts studies are often based on a range of model projections (e.g. Thornton et al. 2011), but to what extent is this a good representation of uncertainty in future climate? Does the modelled range include implausible projections? Or exclude alternative possible futures? The inferences from the thesis about the credibility of the evidence base might be the more useful output of relevance to mitigation debates: potentially delivering insights into the extent to which impacts assessment to support decision

making can rely on climate model data to provide a measure of uncertainty in the response to each degree of ΔT_g.

1.1.4 Thesis structure

The investigation is arranged into two main sections. The first and longer section is an analysis of pan-African projections at 1°C, 2°C, 3°C, 4°C ΔT_g and beyond from three types of climate model ensemble. In the second and shorter section of the thesis, a case study is presented to address the potential to use climate model data to understand the implications of global warming for the Congo Basin.

The present chapter is intended to make the case for this analysis. First it will explore the rationale for the project in more depth, by examining the importance of research and limitations of previous literature with regard to the two key knowledge gaps: the influence of anthropogenic GHG forcing on African climate, and the regional implications of specific increases in global mean temperature (2°C, 4°C, etc.). Then the approaches used to tackle these knowledge gaps will be justified. Climate model data are the basis of the research, and it is thus important to discuss existing climate modelling infrastructure, and the criteria for the selection of the three datasets which support the first three substantive chapters. The rationale for the case study will also be examined, before a detailed summary of the research questions including a chapter-by-chapter outline.

1.2 The Knowledge Gaps

This thesis addresses the lack of information about the implications of specific *degrees of global warming*, but also the limited understanding of projected *future change in African climate*. Whilst there has been previous research into the influence of GHGs on African climate, the focus has largely been restricted to East Africa, southern Africa, and the Sahel. By presenting changes at 1°C, 2°C, 3°C, etc. throughout the continent, the thesis will provide additional information about these domains, but also deliver understanding of projections in regions which have been neglected to date.

In this section the importance of research into each of the two knowledge gaps is clarified. First the large potential impact of temperature and especially precipitation change in African regions is highlighted, and literature which might provide insights into how African climate would be influenced by global warming is surveyed. The rationale for identifying regional changes at specific ΔT_g intervals is also further developed, and any existing work which has sought to achieve this beyond Africa is reviewed.

1.2.1 Future change in African climate

1.2.1.1 Rationale

The need to advance African climate research has been recognised internationally in recent years: the Intergovernmental Panel on Climate Change (IPCC)

identified Africa as a focus region for the Fifth Assessment Report (AR5), and the Coordinated Regional Downscaling Experiment (CORDEX) has also put emphasis on regional modelling for Africa (Hewitson et al. 2012). This attention is justified by the vulnerability of African regions to changes in climate, the central role played by Africa in the global Earth system, and the lack of previous research into African climate relative to other continents.

There are multiple reasons that Africa is especially vulnerable to climate change. Vulnerability is a function of exposure, sensitivity, and adaptive capacity (Parry et al. 2007). Many African regions are already *exposed* to high interannual (e.g. Rodhe and Virji 1976; Nicholson 1986; Nicholson and Entekhabi 1986; Balas et al. 2007) and interdecadal (e.g. Tyson et al. 1975; Folland et al. 1986; Dai et al. 2004) variations in rainfall, and climate models suggest that they could face large changes in temperature (Mahlstein et al. 2011) and precipitation (e.g. Held et al. 2005) in future. African societies also have high *exposure* to these changes due to dependence on subsistence farming and rain-fed agriculture (Dixon et al. 2003), which enhances risks associated with drought and flooding (Morton 2007). A quarter of the population of the continent already experiences high water stress (Boko et al. 2007). In addition, some African ecosystems are particularly *sensitive* to changes in climate: parts of West and Central Africa have been identified as hotspots for interaction between the atmosphere and land surface (Koster et al. 2004), an important example being the Niger inland delta (Dadson et al. 2010; Taylor 2010). Finally, *adaptive capacity*, which is influenced by factors such as governance, wealth, technology, literacy, and infrastructure, is also low in many sub-Saharan African countries (Dixon et al. 2003; Brooks et al. 2005). The combination of these elements means that variability in

climate, particularly precipitation, often has large socio-economic implications (Conway et al. 2005). Whilst there is currently little evidence to support claims about climatic control on GDP and civil war (Conway 2011; Conway and Schipper 2011), the vulnerability of African economies and societies to extreme weather events is undisputed.

In selecting a benchmark for dangerous climate change, it is important to consider the impacts of anthropogenic interference for regions which are vulnerable, but also for regions which play an important role in the larger Earth system, and where atmospheric changes might have feedback effects. Africa contains at least two regions which qualify. The Sahara is the world's largest source of mineral aerosols, contributing >50% of global emissions (Tanaka and Chiba 2006), with half of this input estimated to be produced from one former lake bed: the Bodele Depression (Washington et al. 2003). Small changes in regional climate could influence dust emission with subsequent impacts on the Saharan Heat Low, the West African Monsoon, convection over the Atlantic (Washington et al. 2009), and possibly the fertility of the Amazon rainforest (Prospero and Lamb 2003; Koren et al. 2006). The Congo Basin is another African region of global importance, containing the second largest area of rainforest globally, with a vital function in the regulation of river flow, atmospheric carbon, and global atmospheric circulation (Webster 1981; Williams et al. 2007; Zelazowski et al. 2011; Malhi et al. 2013). This ecological prominence is one reason that the Congo Basin has been identified as a case study in this thesis and its importance is discussed further in section 1.4.

Understanding how African environments might be influenced by global warming is therefore a pressing concern. This importance has not been matched by scientific research attention. African climate is generally poorly comprehended relative to the mid-latitudes, and there are many limitations of the existing literature on future projections, as will be discussed below.

1.2.1.2 Previous research

Research into generalised responses of tropical precipitation to anthropogenic global warming (e.g. Chou and Neelin 2004; Allan et al. 2007) will be discussed here as a starting point. Studies directly addressing African climate change projections from Global Climate Models (GCMs) (e.g. Hoerling et al. 2006; Shongwe et al. 2009; Shongwe et al. 2011) and Regional Climate Models (RCMs) (e.g. Patricola and Cook 2010, 2011; Paeth et al. 2011; Laprise et al. 2013) has largely been restricted to three regions, which are also the most well understood in terms of fundamental climate dynamics (Washington et al. 2006): East Africa, southern Africa, and the Sahel. A summary of literature on each domain will be offered here, as a basis for interpreting the projected changes identified in this thesis, and to highlight issues which still require further investigation. The existing state of knowledge for the rest of the continent will also be outlined.

Tropical Precipitation

There is a growing body of work into the generalised response of tropical precipitation and circulation to anthropogenic GHG forcing. Maps of projected precipitation change for the global tropics show large variation between models in the spatial pattern of change (Dai 2006; Rowell 2012), but this is at least partly due to biases in their twentieth century climatologies. When local responses to warming are examined in climatologically wet/dry regions in each model, some consistent changes are revealed. Chou and Neelin (2004) describe the most important mechanisms as the "rich-get-richer" mechanism and the "upped-ante" mechanism. Throughout the tropics, wet regions are expected to become wetter and dry regions drier in a warming world. Moisture increases associated with higher tropospheric temperatures reduce gross moist stability, enhancing convection and precipitation in convective regions, whilst stability increases in regions of subsidence (Chou and Neelin 2004; Chou et al. 2006). This "rich-get-richer" response has been identified in historical observations and model runs for the twentieth and twenty-first centuries (Trenberth et al. 2003; Allan and Soden 2007; May 2008; Allan et al. 2012). The mechanism may also enhance seasonality, leading to longer dry seasons (Chou et al. 2007). According to the recently published IPCC AR5 Working Group 1 (WG1) report, there is now "high confidence" that the contrast between wet and dry regions, and wet and dry seasons, will increase as temperature rises (Collins et al. 2013).

At the same time, drought may be induced at the margins of convective regions, due to the "upped-ante" mechanism (Neelin et al. 2003; Neelin et al. 2006), evidence for which has been found in modelling studies (Chou and Neelin 2004;

Chou et al. 2006). In a warmer atmosphere, the convective threshold is increased: greater specific humidity is required before convection can occur. This restriction does not prevent uplift in the middle of convective zones, but at the edges there may be less moisture available if there is low level inflow from regions of subsidence, which are getting drier due to the rich-get-richer mechanism. The situation is complicated further by "secondary mechanisms" (Chou and Neelin 2004), a useful summary of which is given in Chou et al. (2009); as well as changes in tropical circulation, namely a weakening of the Hadley and Walker circulations (Held and Soden 2006; Vecchi et al. 2006; Vecchi and Soden 2007; Chadwick et al. 2013), and a broadening of the Hadley cell (Hu and Fu 2007).

On the basis of this literature one might expect global warming to lead to large increases in precipitation in the wettest African regions (see Figure 1.1, 1.2), particularly the Congo Basin, and decreases in subtropical regions; albeit offset by weakened circulation, and with drought on the margins of convective regions. However, it is unclear which of these effects will dominate: Chadwick et al. (2013) find that weakening of circulation almost cancels out the rich-get-richer mechanism. Furthermore, the general thermodynamic changes may interact with shifts in regional climate dynamics. The review of climate projections for Africa in the IPCC Fourth Assessment Report (AR4) (Christensen et al. 2007), based on models from the Coupled Model Intercomparison Project (CMIP) phase 3 (CMIP3), suggests that there is generally an increase or little change in precipitation in the tropics, and decreases in precipitation in the subtropics (Figure 1.3). Projections from the newest generation of models (CMIP5), published in the AR5, are similar (Christensen et al. 2013; Figure 1.4). This large scale response could be partly due to the rich-get-richer

mechanism; but there are some changes, notably the strong wet signal in East Africa, which cannot easily be explained by the literature into generalised tropical responses, and demand regionally-focused investigation.

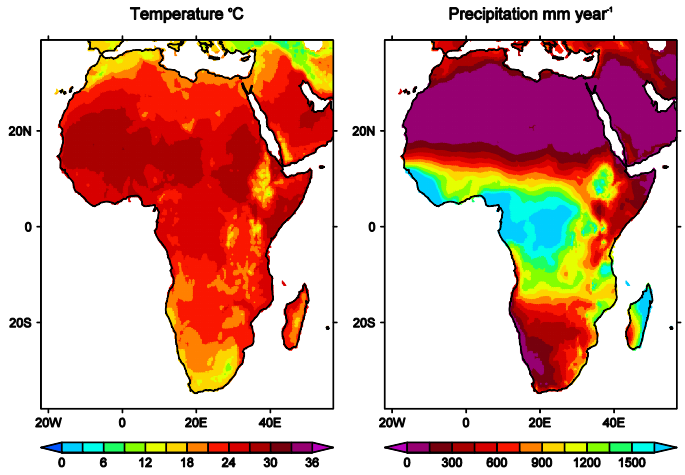

Figure 1.1 Maps of annual mean temperature (°C) and precipitation (mm year^{-1}) based on data from CRU (Climate Research Unit; Harris et al. 2013).

East Africa

East Africa, here referring to the Greater Horn of Africa, encompassing land regions approximately 10°N to 10°S and east of 30°E, has a dry climate relative to its tropical latitude (Waliser and Gautier 1993), with mean rainfall <1000 mm year^{-1} outside highland areas (Figure 1.1). The annual cycle of precipitation is dominated by the migration of tropical convection, with the "long rains" in March-April-May and "short rains" in October-November (Figure 1.2), though seasonality varies by location (Herrmann and Mohr 2011). East Africa experiences pronounced interannual

variability (e.g. Rodhe and Virji 1976), which is also spatially heterogeneous (e.g. Conway et al. 2004; Bewkett and Conway 2007), partly due to variation in teleconnections (Diro et al. 2011). The correlation between rainfall over Ethiopia and India is long established (Walker 1910; Williams et al. 2011); changes in the Somali Jet being linked to precipitation in eastern Africa during JJAS as well as the Indian Summer Monsoon (ISM). Interannual variability is also influenced by the Indian Ocean Dipole (IOD) (Goddard and Graham 1999; Clark et al. 2003; Black et al. 2003; Behera et al. 2005; Hastenrath et al. 2011) and the El Nino Southern Oscillation (ENSO) (Ropelewski and Halpert 1987; Hastenrath et al. 1993; Mason and Goddard 2001; Mistry and Conway 2003; Giannini et al. 2008). Both of these relationships are more robust in the short rains than the long rains season (Lyon and DeWitt 2012).

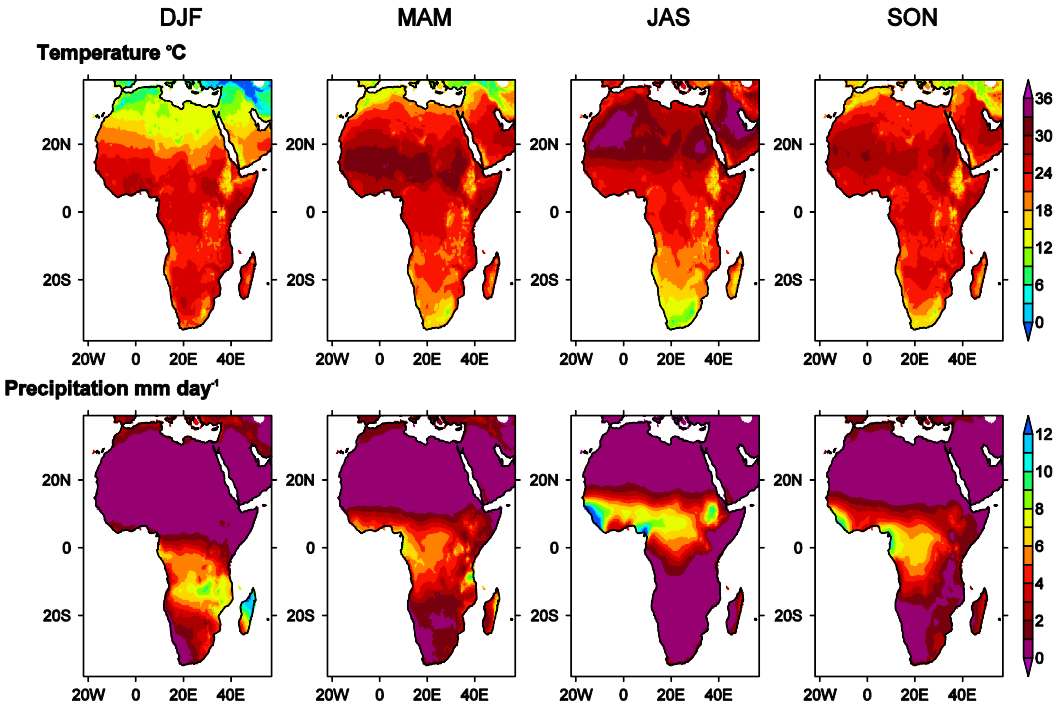

Figure 1.2 Maps of seasonal mean temperature (°C) and precipitation (mm day^{-1}) for four seasons of relevance to precipitation in Africa, DJF, MAM, JAS, and SON (denoted by the initial letter of each month). Based on CRU data.

GCM experiments from CMIP3 suggest that East Africa will become wetter in future in the annual mean and DJF (Figure 1.3), and in both MAM and OND in terms of an increase in mean precipitation, more intense wet events, and less severe droughts (Shongwe et al. 2011). The wet signal to the east of the Great Lakes is one of the most robust projections from this set of models anywhere on the continent, with 18 of 21 models experiencing positive anomalies (Figure 1.3; Christensen et al. 2007); although further north, in Ethiopia, there is less agreement (Conway and Schipper 2011). Most CMIP5 models also project wetter futures (Taylor et al. 2012b; Figure 1.4). Shongwe et al. (2011) investigate atmospheric dynamics and Sea-Surface Temperature (SST) anomalies associated with the wet signal in OND in CMIP3, and find positive SST anomalies near the east African coast accompanied by a change in the IOD which explains 30% of the response. The modification of overturning in the Indian Ocean is consistent with the general weakening of the Walker circulation which is expected in response to global warming (Held and Soden 2006). In addition, the Indian Ocean is likely to experience particularly large changes in future: warming of Indian Ocean SSTs has been observed since the mid twentieth century (Copsey et al. 2006; Williams and Funk 2011) and is projected to continue (Cook and Vizy 2006). The IPCC AR5 concludes that the change in the IOD and wetting of East Africa is a "likely" (66% probability) future response (Christensen et al. 2013). However, this inference is potentially inconsistent with observational studies which have found recent Indian Ocean warming to be associated with reduced precipitation.

Droughts in the Greater Horn of Africa, including the consecutive failure of the short (2010) and long (2011) rains which led to a humanitarian crisis in 2011, have catalysed research into mechanisms for drying (Williams and Funk 2011;

Williams et al. 2011; Lyon and Dewitt 2012; Lott et al. 2013). This work has demonstrated a decline in MAM precipitation in recent decades (Williams and Funk 2011) and an abrupt decrease since 1999 (Lyon and Dewitt 2012). Lyon and Dewitt (2012) suggest that this drying is due to changes in Pacific Ocean SSTs, whilst Williams and Funk (2011) highlight the role of Indian Ocean warming, which is associated with local enhancement of precipitation, and subsidence over southern Somalia, eastern Ethiopia, and northern Kenya, as well as suppression of convection over central Ethiopia and eastern Sudan (Williams and Funk 2011). Williams et al. (2011) also find a link between Indian Ocean SSTs and drying in northern East Africa during JJAS. The authors conclude that drying of East Africa is likely to continue as the Indian Ocean becomes warmer.

Several studies have therefore highlighted a potentially important role for the Indian Ocean, but the direction of its influence on East African precipitation is unclear, and there are now efforts to explain the apparent "East African Climate Paradox" (Rowell et al. 2013). It may be that models have a poor simulation of this teleconnection. Whilst many can reproduce the statistical relationship between East African precipitation and Indian Ocean SSTs in the twentieth century (Conway et al. 2007; Rowell 2013), the relevant processes may not be sufficiently well represented to simulate change over time. Copsey et al. (2006) find that recent increases in SSTs were associated with local increases in Sea Level Pressure (SLP) in observations, but when models are forced with fixed SST they show the opposite SLP anomalies. It is also possible that the role of the Indian Ocean will be seasonally variable, or contingent on the location of the warming, meaning the results from Shongwe et al. (2009) and Williams and Funk (2011) are not necessarily contradictory. Recent RCM

studies by Cook and Vizy (2012; 2013) show increases in precipitation in the short rains season, in agreement with Shongwe et al. (2011), which they attribute to a shift in the South Indian Convergence Zone (SICZ) (Cook 2000), potentially related to Indian Ocean warming; but also drying in MAM, in keeping with Williams and Funk (2011).

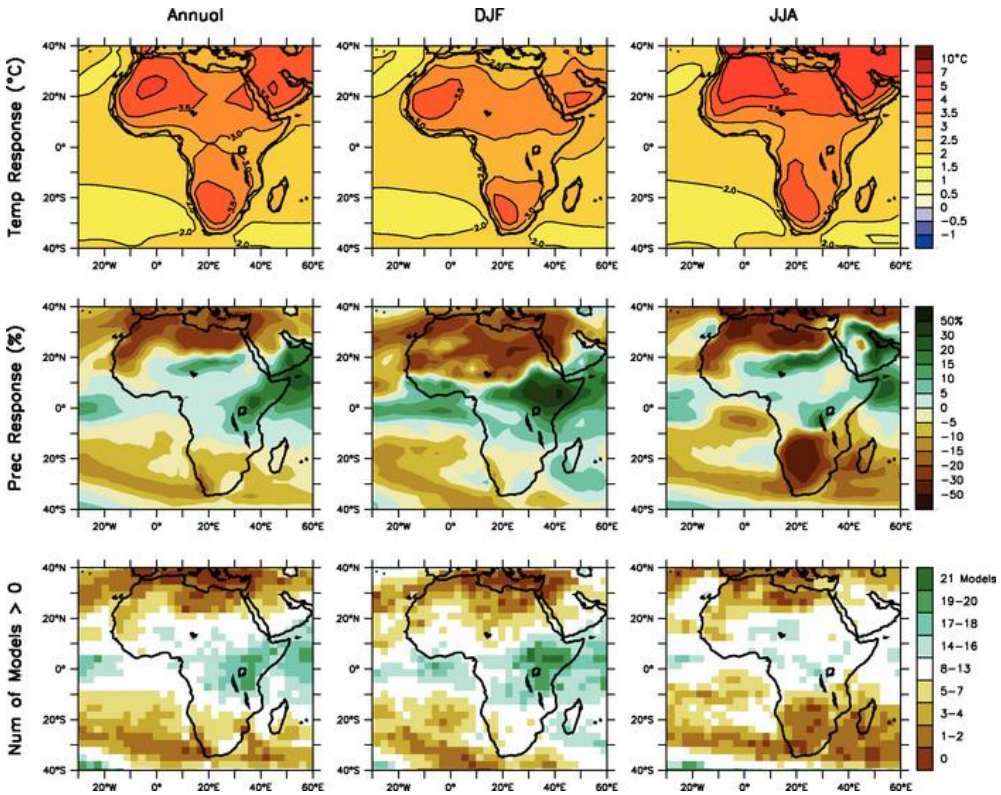

Figure 1.3 Temperature and Precipitation projections as presented in the IPCC AR4, based on 21 CMIP3 models run in SRES A1B. Top row: ensemble mean temperature change between 1980 to 1999 and 2080 to 2099. Middle row: as top, but for fractional change in precipitation. Bottom row: number of models out of 21 that project increases in precipitation. Source: Christensen et al. (2007).

Southern Africa

Southern Africa, here referring to the continent south of approximately 10°S, is a predominantly semi-arid region, influenced by both tropical and mid-latitude climate systems. The south-western tip of the continent, or "winter-rainfall region", receives precipitation from transient eddies in austral winter (Tyson and Preston-Whyte 2000; Figure 1.2), but the rest of southern Africa is very dry (<1 mm day^{-1}) during this season, and wettest during JFM, when much of the precipitation is generated by Tropical-Temperate Troughs (TTTs) which produce cloud bands (TTCBs) extending in a northwest-southeast orientation from the southeast Atlantic to the southwest Indian Ocean (Kuhnel 1989; Washington and Todd 1999), likely modulated by the heat low over Angola and Namibia (Cook et al. 2004). The region is characterised by marked interannual and interdecadal variability (Mason and Jury 1997). The link to ENSO is long documented (Lindesay 1988; Ropelewski and Halpert 1987; Reason et al. 2000). Precipitation variability is also controlled by Indian Ocean SSTs. Both the zonal IOD (Goddard and Graham 1999; Reason 2002), and the meridional dipole between the northern and southern southwest Indian Ocean (Washington and Preston 2006), or South West Indian Ocean Dipole (SWIOD) (Kay and Washington 2008), are important.

Model projections indicate a robust dry signal across southern Africa during JJA (Shongwe et al. 2009; Figure 1.3, 1.4), which is likely associated with a broader poleward shift in the storm tracks across the South Atlantic and Indian Oceans (Christensen et al. 2007), but may have limited societal impact given that this is already a very dry season. During SON, there is also a decrease in precipitation in

most CMIP3 models (Christensen et al. 2007), as well as downscaled GCM projections (Tadross et al. 2005b), and some RCM experiments (Cook and Vizy 2012). Cook and Vizy (2012) find a 40-80% reduction in growing season days over Angola and to the south of the Congo Basin. The decline in spring precipitation could signify a delay in the main rainfall season (Shongwe et al. 2009), possibly symptomatic of a generalised delay in rainfall seasons in a warmer atmosphere. A late onset has been observed for most regions in Africa over recent decades (Kniveton et al. 2009), and specifically for the maize growing season in parts of southern Africa (Tadross et al. 2005a, b). New et al. (2006) find that an increase in dry season duration is one of the only precipitation indicators with a statistically significant change over Central and southern Africa from 1961-2000. As noted above, longer dry seasons might be expected due to the rich-get-richer mechanism (Chou et al. 2007). Seth et al. (2011) suggest that more intense dry seasons would increase stability and reduce surface moisture, decreasing spring convection in monsoon regions, including West and southern Africa.

In the case of the CMIP3 projections, Shongwe et al. (2009) find that SON precipitation is likely inhibited in part by the reduced soil moisture associated with drier winters (JJA), but more importantly by anomalous moisture divergence, which causes the climatological moisture influx from the southwest Indian Ocean to be diverted further north into East Africa. Cook and Vizy (2013) also describe a shift of moisture convergence to the east in RCM simulations. They explain the wetting in East Africa and drying in southern Africa during SON in terms of shift in the SICZ, as noted in the previous section. They liken this circulation anomaly to an observed mode of variability which has been associated with warming in the Indian Ocean,

emphasising further the potential link to changes in the East African short rains season.

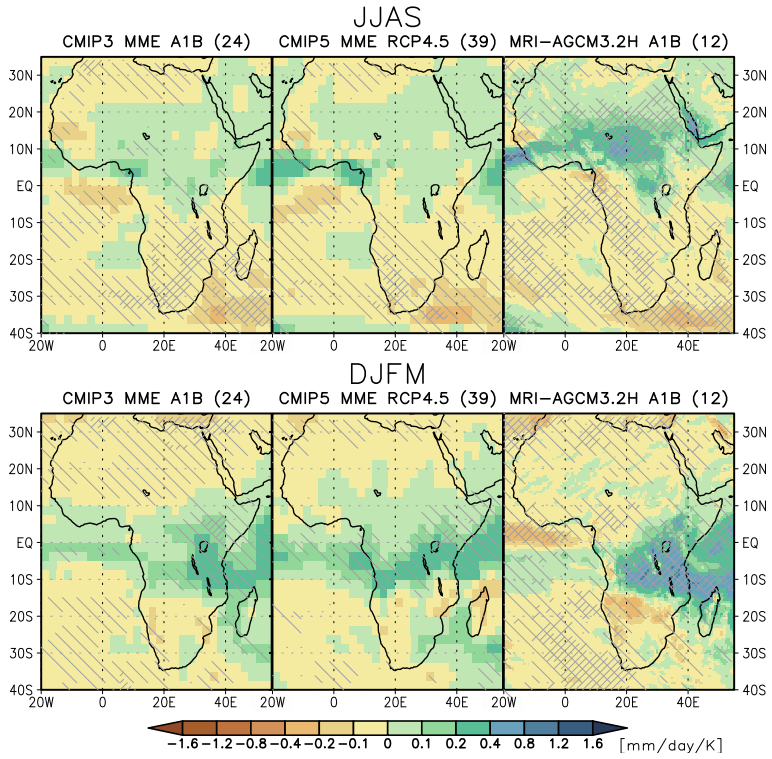

Figure 1.4 Precipitation projections as presented in the IPCC AR5. The first two columns are for 2080-2099 with respect to 1986-2005 in JJAS and DJFM, for 24 CMIP3 models run in SRES A1B, 39 CMIP5 models run in RCP4.5. The right column are for 2075-2099 with respect to 1979-2003 for the 12 member 60km mesh MRI-AGCM3.2 multi-physics, multi-SST ensembles (Endo et al. 2012), run in SRES A1B. Precipitation changes are normalized by the global annual mean surface air temperature changes in each scenario. Light hatching denotes where more than 66% of models (or members) have the same sign with the ensemble mean changes, while dense hatching denotes where more than 90% of models (or members) have the same sign with the ensemble mean changes. Source: Christensen et al. (2013).

During the main southern African rainfall season (DJF), there is a lack of agreement between CMIP3 models in the direction of precipitation change (Figure 1.3), although Shongwe et al. (2009) find an early cessation of the rains in many parts of southern Africa. Empirical downscaling has revealed greater consensus for South Africa. Hewitson and Crane (2006) use circulation data from 3 GCM simulations with contrasting precipitation responses to produce high resolution precipitation projections, and find agreement for an increase in summer rainfall in the interior and east of the country, with a slight drying in the western Cape. This result suggests that the GCMs have consistent circulation anomalies. Tadross et al (2006) use the same downscaling technique for 7 models and also find summer precipitation increases.

The Sahel

The Sahel has been studied more than any other African region, principally due to the drought of the 1970s and early 1980s (Hulme 1992; Folland et al. 1986). This spatially coherent decline in water availability was recorded in rainfall and river flow data across West Africa (Conway et al. 2009), and was, on average, a 40% reduction in precipitation from the 1950s to 1980s (Held et al. 2005), which has few if any parallels observed anywhere in the world. It was associated with severe human impacts, including a depletion of the natural resource base for Sahelian pastoralists (Mortimore and Adams 2001; Tarhule and Lamb 2003) and millions of fatalities (Cook 2008).

The Sahel lies between the tropical Guinea Coast (>1200 mm year^{-1}, Figure 1.1) and the subtropical Sahara (<150 mm year^{-1}), and is characterised by steep meridional precipitation gradients. The vast majority (75-90%) of precipitation is delivered during one rainfall season from late June to September (Lebel et al. 2003; Figure 1.2). The onset of precipitation is linked to the southerly moisture flux of the West African Monsoon (WAM), but other circulation features may be more important in controlling precipitation variability and change (Nicholson 2009), including the African Easterly Jet (AEJ) (Nicholson and Grist 2003; Jenkins et al. 2005) and associated African Easterly Waves (AEWs) (Duvel 1990; Leroux and Hall 2009), the Tropical Easterly Jet (TEJ) (Koteswaram 1958; Caminade et al. 2006), and the West African Westerly Jet (AWJ) (Nicholson and Grist 2003; Vizy et al. 2013). The Saharan Heat Low (SHL) (Biasutti et al. 2009; Vizy et al. 2013) and Atlantic cold tongue (Thorncroft et al. 2011; Tokinaga and Xie 2011) are also known to have a strong control on Sahel precipitation; and the region has been associated with global SST teleconnections (e.g. Folland et al. 1986; Giannini et al. 2003; Mohino et al. 2011). It is also thought to be characterised by large land surface feedbacks (Zeng et al. 1999).

The interplay between these factors is associated with complex interannual and interdecadal variability (clarified by Ward 1998), and creates a challenge for research into the potential influence of anthropogenic interference on Sahel precipitation. Despite the relatively large amount of work on the drought of the 1970s and 1980s there are still many unanswered questions about its causes, and the role of GHGs and global warming is still debated. The importance of inter-hemispheric SST gradients (Folland et al. 1986) is widely accepted (e.g. Hoerling et al. 2006;

Christensen et al. 2007; Cook 2008; Druyan 2011; Vizy et al. 2013). The contrast between the cooler north Atlantic and warmer south Atlantic temperatures which likely hindered the northward migration of precipitation has been attributed to spatially varying aerosol forcing: the higher concentration of sulphates in northern hemisphere (NH) is thought to have induced a decrease in SST via perturbation to cloud albedo and lifetime (Rotstayn and Lohman 2002; Biasutti and Giannini 2006). The reduction in NH sulphates since the 1980s (Skeie et al. 2011) and concurrent partial recovery of the Sahel drought (Nicholson 2005; Lebel and Ali 2009; Ben Mohamed 2010), in the presence of continued increase in GHGs and global temperature (Hartmann et al. 2013), might imply that GHG-induced warming was not responsible for the drought. Indeed some have suggested the opposite: that GHGs may have driven any recent increase in Sahel precipitation and may continue to increase it in future (Paethe and Hense 2004). Yet other studies using idealised experiments have found a drying response to global SST warming (Herceg et al. 2007), suggesting that GHGs may have contributed towards the dry conditions of the 1970s and 1980s. Mohino et al. (2011) attribute 10% of the observed Sahel drought to global warming.

Future projections for the Sahel from both CMIP3 and CMIP5 are divided between wetter and drier conditions (Hoerling et al. 2006; Christensen et al. 2013). The many studies of these simulations, including those which are designed to understand the projections mechanistically and/or to select the most reliable models (e.g. Cook and Vizy 2006; Lau et al. 2006), have failed to generate consensus, as highlighted in a review by Druyan (2011). The IPCC AR5 concluded that there is "low confidence" in projected change in the WAM: lower than for any other

monsoon system globally (Christensen et al. 2013). The uncertainty partly arises from the difficulty in simulating teleconnections to this region: even when models are run with the uniform SSTs they produce different conditions (Held et al. 2005). The diverse influences on the Sahel also make assessment of future change difficult: a range of mechanisms can be invoked to explain wetting or drying responses.

Given the importance of inter-hemispheric SST gradients in the twentieth century, a warming of the NH relative to the SH, which is a conceivable response to increasing GHGs, could induce wetter conditions in the Sahel (Hoerling et al. 2006). The monsoon may also be amplified by an increase in the temperature contrast between the African continent and the Atlantic (Haarsma et al. 2005), which is expected as a result of the general difference in the rate of warming between land and ocean (Joshi et al. 2007). The Sahara is projected to experience particularly large temperature anomalies in response to increasing greenhouse gases, especially in boreal summer (Figure 1.3), and this warming may be associated with a deepening of the heat low which could also act to strengthen the monsoon (Biasutti et al. 2009). Conversely, warming of Indo-Pacific SST could generate warming of the entire tropical atmosphere and enhanced stability over Africa (Herceg et al. 2007). Warming of the Indian Ocean in particular has been found to dry western Africa in idealised experiments (Hoerling et al. 2006; Mohino et al. 2011), and, as already discussed, further warming is projected in future.

The understanding of modelled responses has been clarified by recent studies demonstrating more consensus between the CMIP3 models than was previous recognised. By examining projections on a monthly rather than seasonal (JAS) basis,

Biasutti and Sobel (2009) reveal that many models show a decrease in precipitation at the beginning of the monsoon season, and an increase at the end. Fontaine et al. (2011) and Monerie et al (2012b) find further agreement by examining the spatial variation of change. When averaged across the Sahel there is divergence between modelled changes, but most models show a dry signal in west Sahel and a wet signal in central and east Sahel. This pattern is also found in CMIP5 (Monerie et al. 2012a; Vizy et al. 2013; Roehrig et al. 2013), and some RCMs (Cook and Vizy 2012; Diallo et al. 2012). The zonal contrast might be explained in terms of an increase in the monsoon, but with anomalous subsidence suppressing precipitation over west Sahel (Monerie et al. 2012a, b).

Other regions

The largest knowledge gaps exist beyond East Africa, southern Africa, and the Sahel. Much of the problem can be traced to a scarcity of observational data (Washington et al. 2006; see Figure 1.5) which inhibits understanding of present day conditions and creates an obstacle for climate projection research, as models' twentieth century runs cannot be validated. Continent-wide reviews of African climate change projections (Hulme et al 2001; Christensen et al 2007; Giannini et al. 2008; Christensen et al. 2013) have provided a cursory overview of modelled changes in other regions. One of the most robust projections is a dry signal at the Mediterranean coast throughout the year, and most CMIP3 models show drying of North Africa during DJF. In the Congo Basin there is a modest increase in precipitation in the CMIP3 ensemble mean but with little agreement between models

(Figure 1.3). This region has received a particular lack of research attention (Todd and Washington 2004) (with the exception of a recently published study by the Climate Service Center [CSC 2013]), which is another reason that it has been selected as a case study in this thesis. A more detailed summary of existing literature of relevance to Central Africa will be provided in Chapter 7.

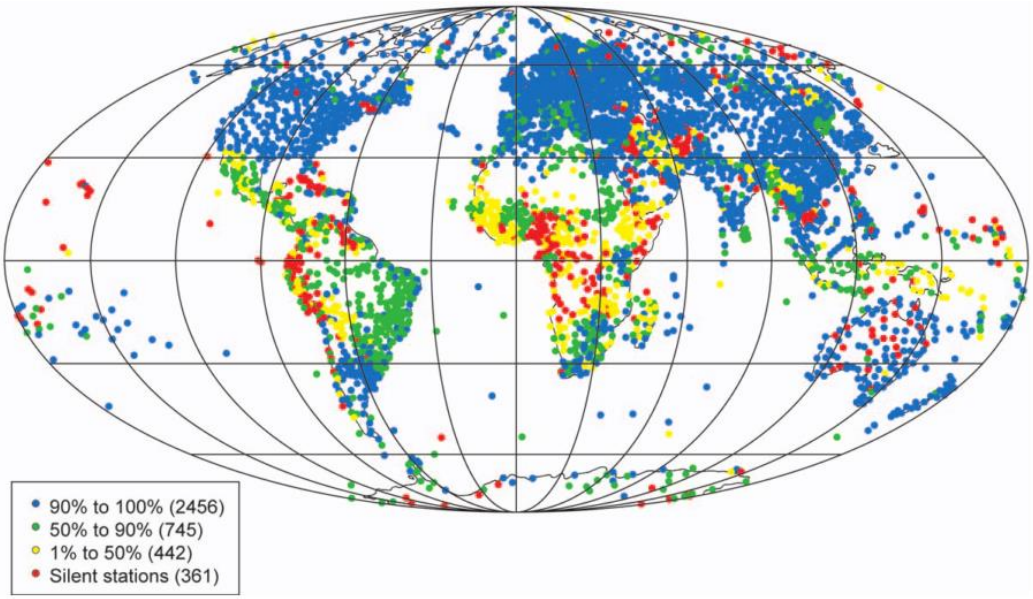

Figure 1.5 The global network of World Weather Watch stations, colour coded to show reporting rates. Data-sparse areas and low reporting rates for Africa are clearly visible. Source: Washington et al. (2006) (data from WMO 2003).

1.2.1.3 Justification for further research

There have been considerable advances in understanding potential climate changes for East Africa, southern Africa and the Sahel; but there is still no consensus

on how precipitation is likely to be influenced by anthropogenic GHGs. Further examination of model projections has the potential to lead to new insights, and in this thesis two model ensembles are studied which have never before been applied to investigate African climate change. The thesis also intends to address the lack of research for other regions, in examining pan-African projections, and focusing on one of the most neglected domains: the Congo Basin. The summary above emphasises that analysis of mechanisms for precipitation change is particularly important for interpreting modelled responses, thus atmospheric dynamics associated with selected responses will be considered. At the same time the projected changes in African climate will be re-evaluated by presenting anomalies as a function of global temperature.

1.2.2 Degrees of global warming

1.2.2.1 Rationale

There are multiple reasons that investigating climate projections at 1°C, 2°C, 3°C, 4°C ΔT_g and beyond might be useful. The dominant motivation here is political.

Political rationale

Over the past two decades, climate change mitigation policy has focused on 'Dangerous Anthropogenic Interference' (DAI), a narrative formalised in international resolutions (Liverman 2009); most prominently the UNFCCC, which in

Article 2 declares its goal as the "stabilization of GHG concentrations in the atmosphere at a level that would prevent DAI with the climate system" (UN 1992:4). A definition of DAI is not included in the text (Lorenzoni et al. 2005). Many authors have highlighted the need for a definition in order to find a rational solution to global warming (e.g. Dessai et al. 2004; Lieserowitz 2005; Gupta and van Asselt 2006); but it is unclear what the most appropriate metric for danger should be, whether a rate of GHGs emissions, level of GHG concentrations, sum of cumulative CO_2 emissions (Allen et al. 2009), quantity of radiative forcing (Lenton 2011a), or degree of global warming.

The difficulty in selecting a global mitigation goal is partly due to uncertainty: the relationship between emissions, concentrations, global temperature, and impacts is not fully understood (as highlighted by O'Neill and Oppenheimer 2002; Liverman 2009). Yet even with perfect knowledge of the Earth system it would, in theory, be difficult to agree upon a global benchmark for danger, since the severity of impacts will vary from region to region, and of course within regions. The choice of a definition for danger is therefore not a scientific endeavour but a political issue (Lorenzoni et al. 2005; Schneider and Manstrandrea 2005). The role of scientists is arguably (Parry et al. 1996; Oppenheimer 2005) to investigate the risks associated with varying amounts of anthropogenic interference, enabling an informed political debate about the level of risk which is tolerable.

Since 1992, policy-makers have converged on a benchmark for danger (Randalls et al. 2010). A 2°C global warming relative to preindustrial conditions is widely used as the limit beyond which further anthropogenic interference should be

prevented. The EU officially adopted this goal in 1996, and it has been reaffirmed by the EU since (May 2008; Randalls et al. 2010), as well as being accepted by over 100 countries (Meinshausen et al. 2009), and recently included in UNFCCC documentation (UNFCCC 2011). Its prevalence in policy has also led climate science which aims to support mitigation debates to employ 2°C as a baseline for calculating emissions targets (Macintosh 2010; van Vuuren et al. 2011; Rogelj et al. 2011; 2012a) or allowable cumulative carbon (Meinshausen et al. 2009; Allen et al. 2009). However, 2°C does not have a robust scientific origin (Jaeger and Jaeger 2010). Tol (2007) argues that its selection relied on a narrow set of studies. According to Liverman (2009), it was founded on the results of the IPCC Second Assessment Report (SAR) (Watson et al. 1995), which projected serious impacts from a scenario that had a 2°C warming by 2100. Other research has suggested that there would be dangerous impacts at less than 2°C (e.g. Hansen et al. 2008), and the Association Of Small Island States (AOSIS) and other developing countries have called for the threshold to be reduced to 1.5°C, appealing for "1.5 to stay alive" (Caricom 2009; Simpson et al. 2009). Many Non-Govermental Organisations (NGOs) have backed this call, for example 350.org. As a result the UNFCCC is currently conducting a review to consider strengthening or changing the long term goal (UNFCCC 2010, 2011, 2012, 2013; Jordan 2013).

There is thus a demand for scientific evidence about the implications of 1.5°C and 2°C. It is also important to make the comparison between 2°C and higher degrees of warming. Global temperatures have already increased as a result of anthropogenic emissions (Stott et al. 2000; Forster and Rahmstorf 2011; Bindoff et al.

2013): 2°C above the preindustrial is actually equivalent to a further increase from the early twenty-first century of approximately 1.2°C (IPCC 2007; Schmidt and Archer 2009). Some studies suggest that if no further CO_2 was emitted, a warming >2°C would be possible from previous anthropogenic activity alone (e.g. Ramanathan and Feng 2008). Emissions are still rising (Peters et al. 2012; Le Quéré et al. 2012), therefore it is increasingly likely that 4°C or higher will be reached without mitigation (New et al. 2009). If the costs and benefits of limiting to 2°C are to be fully appreciated, it is important to understand the implications of unmitigated warming; and if mitigation is unsuccessful, evidence about the impacts of higher degrees of warming could provide information for adaptation.

The majority of climate projection research is, however, unhelpful for assessing the regional implications of 2°C, 4°C, or any other degree of ΔT_g. Most climate model experiments to examine the role of GHGs are run with increasing emissions through the twenty-first century, and most projection and impacts research selects time-slices from these data (e.g. Hoerling et al. 2006; Conway and Schipper 2011), such as 2081-2100 (e.g. Collins et al. 2013). In studies which use multiple models, the ensemble mean or range of projections is calculated for the time-slice. Information is therefore compared from models which have consistent GHG concentrations, but their global temperature anomalies are not necessarily consistent. Variation in ΔT_g in a time-slice is largely due to differences in the models' climate sensitivity to GHG forcing: some models have stronger feedbacks associated with water vapour, lapse rates, clouds, snow, and sea-ice (Bony et al. 2006). The ΔT_g in a time-slice may also vary between models due to disparities in aerosol forcing (Kiehl

2007; Andrews et al. 2012). Time-slices are therefore usually of limited relevance for investigating uncertainty in regional climate changes associated with degrees of ΔT_g (as illustrated in Figure 1.6).

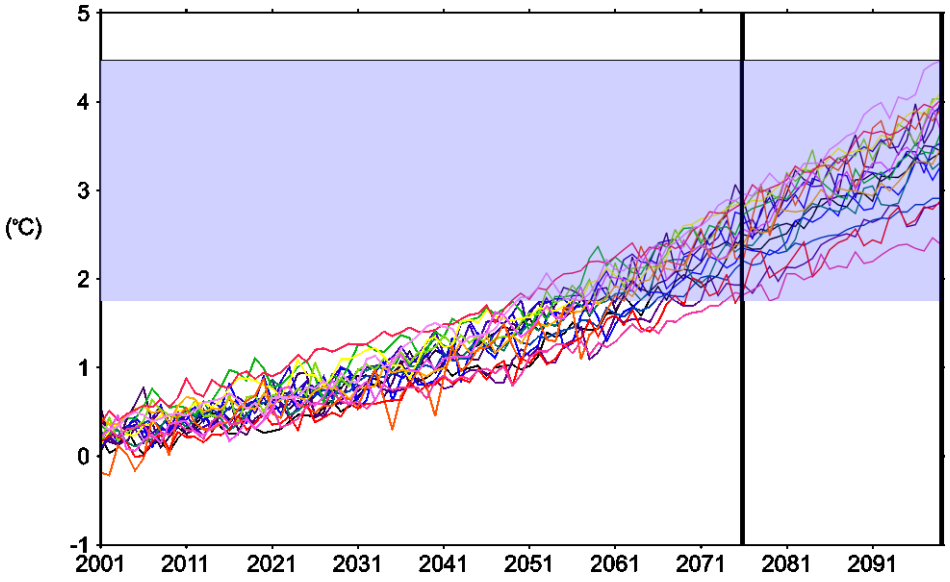

Figure 1.6 Schematic diagram to illustrate the difficulty of investigating ΔT_g increments using time-slices. Global mean temperature anomaly time-series relative to 1985-99 are shown for 19 CMIP3 models run in SRES A2. In a 1975-2100 time-slice (illustrated by the thick black lines) the models would have inconsistent ΔT_g: their global mean temperature anomalies range from <2°C to >4°C (as illustrated by the blue shading).

Scientific rationale

There is also scientific justification for presenting projections at 1°C, 2°C, 3°C ΔT_g etc. As explained above, the majority of climate projection research

compares models with the same GHG forcing. GHGs influence precipitation directly (Allen and Ingram 2002; Bala et al. 2009; Good et al. 2012), but this effect is smaller than their indirect influence via global temperature (Andrews et al. 2010). Comparing models with consistent ΔT_g might therefore develop understanding of the important radiative impact of temperature on precipitation.

Using ΔT_g also removes the dependence on emissions scenarios (Tang and Lettenmaier 2012; Darbyshire et al. 2013). When impacts are presented for time-slices, for example the end of the twenty-first century, the results will vary depending on which emissions scenario is used (e.g. Hulme et al 2001). A range of scenarios are therefore required to understand risk, and it can be challenging to communicate such results to stakeholders (e.g. Darbyshire 2012, *pers comm.*). It is also difficult to compare simulations from models run with different forcings. Presenting changes at 1°C, 2°C, 3°C ΔT_g etc. should produce results which are comparable with future research regardless of the emissions scenario employed, and which are easier to communicate. The assumption here is that regional climate changes associated with each ΔT_g increment will be the same regardless of the emissions trajectory which forces the modelled global warming, and this uncertainty will also be discussed further during the course of this thesis.

1.2.2.2 Previous research

The vast majority of new climate change research is still based on time-slices, but there has been an increase in the number of studies which present regional

projections in relation to global temperature (the main methodologies for which are discussed further in Chapter 3). The development of the CMIP5 database and the AR5 has been associated with some progress in this regard. The SRES (Special Report on Emissions Scenarios) scenarios used for CMIP3 did not include any mitigation scenarios, limiting analysis of stabilisation to a small number of research projects (Tubiello and Fischer 2007; Hayashi et al. 2009; Arnell et al. 2013); but one of the RCPs (Representative Concentration Pathways) prescribed for the CMIP5 models, RCP2.6, is designed to restrict global temperature to approximately 2°C (van Vuuren et al. 2011). This has facilitated research into the impacts of 2°C using RCP2.6 (e.g. Schellnhuber et al. 2013). The need to compare projections from CMIP3 and CMIP5, and the lack of overlap between SRES scenarios and RCPs (Rogelj et al. 2012b), has also motivated the presentation of regional projections as a function of global temperature (per °C) in parts of the AR5 (Collins et al. 2013; Christensen et al. 2013) and elsewhere (Markovic et al. 2013). In addition, there have been a number of other projects investigating changes associated with ΔT_g, predominantly focusing on 2°C and 4°C.

Implications of 2°C

Research into changes associated with 2°C (Kaplan and New 2006; May 2008; Giannakopoulos et al. 2009; Anderson 2011; Lang and Yue 2012; Elkin et al. 2013) suggests that there could be severe impacts in some regions. Anderson (2011) finds that in many locations worldwide seasonal mean temperatures in most years would exceed the values which were extreme in the late twentieth century (Anderson

2011). Elkin et al. (2013) conclude that 2°C is not a safe target from the perspective of ecosystem services in the European Alps. To the author's knowledge, the only existing peer reviewed paper addressing changes of 2°C and focusing on Africa is Thornton et al. (2011)'s assessment of agriculture and food systems in sub-Saharan Africa, which concludes that successful adaptation strategies would be crucial at 2°C. The EU FP7 funded IMPACT2C project promises to deliver analysis of the impacts of 2°C for the Nile and Niger Basins (as well as for Europe, Bangladesh, and the Maldives); however to the authors knowledge the results are yet to be published. A recent World Bank report on the implications of 2°C also includes analysis of sub-Saharan Africa, concluding that there would be large regional risks to food production (Schellnhuber et al. 2013).

Implications of 4°C

The regional implications of 4°C global warming have perhaps received more attention than 2°C, partly driven by conferences on this theme in Oxford in 2009 and Melbourne in 2011, and a special issue in Philosophical Transactions A (including Fung et al. 2011; Thornton et al. 2011; Zelazowski et al. 2011). More has been written in the grey literature (e.g. World Bank 2012; Schellnhuber et al. 2013). The UK government developed a Google Earth layer showing impacts at 4°C, researchers at Oxford University have created an interface allowing the CMIP3 model projections to be presented at 4°C. Most of the research indicates that impacts at 4°C would be difficult to adapt to (New et al. 2011; World Bank 2012), and in the case of

farming in sub-Saharan Africa, might require a transformation of agricultural systems (Thornton et al. 2011); although the implications of other changes are more ambiguous and might even be beneficial, such as the potential expansion of African rainforests (Zelazowski et al. 2011).

Comparison between ΔT_g increments

Comparison between ΔT_g increments is all important in order to identify the relative merits of 2°C relative to other mitigation limits; however not all of the studies have taken this step. Noteworthy exceptions include a report for the Caribbean which compares 1.5°C and 2°C (Simpson et al. 2009), and several studies of ecosystems (Warren et al. 2010; Frieler et al. 2012). Frieler et al. (2012) find that warming must be limited to <1.5°C to save more than 10% of coral reefs. Studies which compare 2°C with 4°C consistently show that impacts would be larger at 4°C, including for coastal cities, agriculture, water stress, ecosystems, and migration (New et al. 2011). Yet many of these analyses make the distinction between ΔT_g levels using pattern scaling (e.g. Thornton et al. 2011; Zelazowski et al. 2011).

Pattern scaling techniques (Huntingford and Cox 2000; Mitchell et al. 2003) can be applied to quickly derive changes at different ΔT_g increments based on the assumption of a linear relationship between global temperature and local climate. Changes associated with one ΔT_g increment (for example 2°C) may be multiplied to compute changes at other ΔT_g increments (such as 4°C); or global temperature can be linearly regressed against local change to generate a "pattern" or rate of change, which

might then be used to compute change at any level of ΔT_g. The Queensland Climate Change Centre of Excellence (QCCCE) has produced pattern scaled projections from CMIP3 over Australia, standardising their use in impacts assessment nationally (e.g. Darbyshire et al. 2013); and the AR5 projections presented per °C (e.g. Figure 1.4) are also derived using pattern scaling.

It may be problematic to assume a linear response to global warming, particularly if the "patterns" are extrapolated to higher levels of anthropogenic forcing. Experts suggest that the response to warming might be nonlinear, and there could be tipping points in the Earth system, which are more likely to be reached at higher global temperatures (Kriegler and Hall 2009). Good et al. (2012) use step experiments to compare regional climate changes at $2xCO_2$ and $4xCO_2$, and find nonlinear change in West Africa. Neupane and Cook (2013) find a different precipitation response in the Sahel for a 1°C versus a 2°C warming of the Atlantic Ocean. May (2011) compares ΔT_g increments using different stabilisation scenarios rather than pattern scaling techniques, demonstrating that the impacts of unmitigated warming are more complex than a linear amplification of the anomalies associated with 2°C. This evidence would imply that directly investigating how local changes evolve with global temperature is necessary in order to understand differences between ΔT_g levels.

1.2.2.3 Justification for further research

A minority of projection studies have investigated regional changes at 2°C and 4°C, but much of this work has failed to thoroughly compare ΔT_g intervals, either focusing on one level of warming, or relying on pattern scaling techniques. And, despite the recognition that it is important to prioritise research into vulnerable systems and regions, there has been little work which focuses on Africa. In this thesis changes in African temperature and precipitation associated with 1°C, 2°C, 3°C, 4°C ΔT_g and beyond will be extracted directly from model output allowing a comparison between many ΔT_g increments which does not assume a linear relationship with global temperature.

1.3 The Evidence Base

The preceding section clarifies the prospective value in understanding how African climate would evolve with global warming. Climate model experiments with increasing GHG emissions are an available resource, which have so far mainly been used to present projections for time-slices, but which could equally be applied to investigate changes associated with ΔT_g increments; and for all of Africa including the understudied regions. However, if the models are to be applied to support policy, the quality of the evidence base they provide deserves examination. The value of future simulations is a subject for debate (e.g. Räisänen 2007). Projecting how climate might change over decades and centuries is a very difficult task. Even with a perfect model it would be impossible to predict the exact anomalies at 1°C, 2°C, 3°C, etc., due to

natural variability in the climate system and uncertainty in the changing concentrations of GHGs relative to other atmospheric forcing agents (thorough discussions [e.g. Collins 2007; Tebaldi and Knutti 2007; Knutti 2008] and analyses [e.g. Hawkins and Sutton 2009; Yip et al. 2011] of the different sources of uncertainty are provided in previous work). Furthermore, current climate models are far from perfect. They are based on an incomplete theoretical understanding of climate, partly limited by observations; and certain simplifying assumptions are unavoidable in their construction (Reichler and Kim 2008).

Comparison of models' twentieth century simulations with observations reveals many biases (Flato et al. 2013), even in the most state of the art models. An important example for Africa is the persistent warm bias in the Gulf of Guinea (Cook and Vizy 2006; Roehrig et al. 2013). Models' future simulations might also be expected to have many errors. A more fundamental problem is that their future projections cannot be evaluated (Tebaldi and Knutti 2007): there are, of course, no future observations, and also no well-observed historical analogues for GHG-induced warming (Räisänen 2007). Forced with the same GHGs, model projections of future change diverge substantially, particularly for tropical (Dai 2006) and African (e.g. Hoerling et al. 2006) precipitation, but it is not possible to establish which, if any, of the modelled responses would be realised.

How to deal with modelling uncertainty is the subject of much deliberation (Frame 2007; Knutti 2010; Knutti et al. 2010). Given variation between model projections it seems clear that more than one simulation should be consulted (Knutti 2008). Experiments with increasing GHGs have been run with many different models

and model versions, including global (Meehl et al. 2007a; Taylor et al. 2012a) and regional (Giorgi et al. 2009) models, with varied grids, core physics, and parameter values (Stainforth et al. 2005; Murphy et al. 2007; Collins et al. 2010); providing hundreds of simulations which could potentially be analysed. Using all of these data may not be the best way to understand the risks associated with global warming, however. Some, or all of the simulations available may be unreliable or provide implausible projections; and they may be other plausible futures which are not represented.

In this thesis, projections from a Multi-Model Ensemble (MME), Perturbed Physics Ensembles (PPEs), and a group of Regional Climate Models (RCMs) are compared to establish whether they produce different responses at each ΔT_g increment. The findings could be used to judge which kinds of model datasets should be consulted in regional climate change assessments, and may also generate insights into whether the available data are sufficient to understand uncertainty, and what kind of further experiments might be useful. In this section the status of current climate projection infrastructure is examined, to situate the three datasets in the wider context. First MMEs, PPEs, and RCMs are dealt with in turn, and then the specific ensembles employed here are summarised and their selection justified. Technical information is saved for Chapter 2.

1.3.1 Multi-model ensembles

Climate models have been developed by approximately twenty research centres worldwide (Easterbrook 2012), each of which has one or more global and/or regional models, and continually work to improve them. The models may be distinct in terms of their horizontal and vertical resolutions, basic physics, and parameterisation schemes. They also differ in level of complexity. Most climate projection work is based on global models which have a coupled atmosphere-ocean (AO-GCMs), but some state-of-the-art global models, known as Earth System Models (ESMs), also include dynamic vegetation, carbon cycle components, interactive ice sheets, or atmospheric chemistry (Friedlingstein and Jones 2011).

The importance of comparing results from different models, and the successful use of ensembles to improve forecast skill in a variety of applications from weather prediction to public health (Tebaldi and Knutti 2007), has motivated the development of MMEs for climate research (Meehl et al. 2007b; Collins et al. 2011). For over twenty years the World Climate Research Programme (WCRP) has been coordinating experiments from modelling centres around the world to create MMEs through the Programme for Climate Model Diagnosis and Intercomparison (PCMDI). Each modelling centre is encouraged to run experiments with their own models following guidelines from the WCRP, and to submit the output to be distributed online. The relevant experiments for future projection are collected under the Coupled Model Intercomparison Project (CMIP), which is now in the fifth phase (Taylor et al. 2012a). The vast majority of projection studies to date have been based on CMIP3 (Meehl et al. 2007a), including many of the African studies referred to in

section 1.2.1; and there are an increasing number using CMIP5 (e.g. Monerie et al. 2012a; Taylor et al. 2012b). More recently future simulations from RCMs are also being compiled through CORDEX (Jones et al. 2011).

MMEs have been instrumental in facilitating research into future climate and climate impacts which incorporates modelling uncertainty. However, an enduring challenge for researchers is how to combine information from the different models. Which statistics should be presented, and which models should be included remain controversial issues (e.g. Frame 2007; Tebaldi and Knutti 2007; Knutti 2010). Much of the work based on MMEs uses an ensemble mean or median to summarise projections from individual models (e.g. Hoerling et al. 2006; Christensen et al. 2007; Giannini et al. 2008). When twentieth century simulations are compared to observations, the ensemble mean often outperforms all individual models, in terms of the global scale long term mean climate (Reichler and Kim 2008), and on a regional basis: the multi-model mean of ten CORDEX RCMs run over Africa has been found to produce more realistic precipitation climatologies than individual models (Nikulin et al. 2012; Kim et al. 2013). However, the correspondence of the ensemble mean with twentieth century observations does not imply that it will be more reliable in terms of projected change.

The level of agreement between models is also assessed in many projection studies, and they often focus on the changes for which there is consensus, as the most "robust" responses (e.g. Christensen et al. 2007). For precipitation, agreement in the direction of change is often examined, sometimes using a "one model one vote" approach which is determined entirely by the sign of change rather than the

magnitude (Santer et al. 2009; Monerie et al. 2012b). More recently, emphasis has been placed on considering the statistical significance of change as well as the direction, and distinguishing between areas for which there is a lack of agreement between models and areas where the models agree that there is little change (Power et al. 2011; Tebaldi et al. 2011; McSweeney and Jones 2013). Recent statistical approaches for summarising projections therefore provide scope for a better understanding of the dominant responses from an ensemble, but it is important not to rely entirely on the ensemble mean and measures of consensus to understand the risks associated with global warming. The most common response is not necessarily the most trustworthy (Knutti 2010), particularly given that the models in a MME are not independent: they often share data and algorithms and sometimes parameterisation schemes, meaning similar responses may be due to similar model composition (Jun et al. 2008; Knutti et al. 2010; Masson and Knutti 2011).

Many studies have instead sought to weight models according to their skill, usually through evaluation of their twentieth century hindcasts relative to observations (e.g. Cook and Vizy 2006), and often using Bayesian statistics to produce probabilistic projections (e.g. Giorgi and Mearns 2002, 2003; Tebaldi et al 2005; Shongwe et al. 2009; 2011). However, this work is based on the assumption that there is a relationship between the ability to model historical conditions and future change, which is not necessarily the case (Abe et al. 2009; Giorgi and Coppola 2010). It is also difficult to choose the metrics to evaluate, and to decide how poor the fit has to be to observations to warrant exclusion. Furthermore, models in a MME are different from each other in myriad ways, so whilst it might be possible to show contrasts between model simulations, it is difficult to understand why these occur, so it is usually unclear

whether the constraint has been applied to the right parameter. Constraining MMEs is therefore problematic, and different approaches can lead to different models being excluded, for example for the Sahel (Cook and Vizy 2006; Lau et al. 2006).

A more cautious, or more conservative, approach is to consider any projection which has not been found to be implausible, allowing a spread of possible responses to be factored into adaptation and mitigation decisions. For this reason the range of projections is often presented (Stainforth et al. 2007), referred to as a frequentist "bounding box" approach by Frame (2007). Regional climate change impacts assessments sometimes incorporate uncertainty in future climate change using the range of projections from GCMs (e.g. Thornton et al. 2011), or by selecting a subset of models which represent the full range of the MME (e.g. Darbyshire et al. 2013, Paton et al. 2013; following Watterson 2011; Whetton et al. 2012).

In this thesis, projections are presented from CMIP3. An attempt is made to represent the dominant responses in the ensemble, using the mean and measures of consensus; but the range of model projections is also presented. Yet this range should be treated critically, due to the way in which CMIP3 has been assembled. MMEs are "ensembles of opportunity": results are collected from any modelling centre which is willing to contribute (Tebaldi and Knutti 2007). The size and composition of an MME is therefore determined by unscientific factors, such as the computational resources available to each modelling group. It is neither a random nor a systematic sample (Knutti 2010). Many of the models are related (Masson and Knutti 2011), and each model is designed to produce a best fit of recent observations (Knutti 2010), meaning MMEs are likely to under-sample uncertainty. There could be

other hypothetical models which have not been created, which would produce alternative and equally plausible futures. This issue is difficult to overcome: it is not feasible to generate all possible models. However, it is possible to investigate uncertainty more systematically using PPEs.

1.3.2 Perturbed physics ensembles

PPEs are designed to explore uncertainty in future climate change, and to contribute towards quantification of this uncertainty (Collins et al. 2011). In models which are submitted to CMIP, parameter values have been set for certain processes which are poorly understood (Meehl et al. 2007b), including those relating to convection, clouds, radiation, and sea-ice (Barnett et al. 2006). The range of projections from any MME might be different if alternative parameter values had been chosen (Allen and Stainforth 2002). PPEs test the uncertainty in future change resulting from parameterisations. Expert elicitation is used to define the range of plausible values for each uncertain parameter, and then the same base model is run multiple times with slightly different parameter values (Rougier et al. 2009).

The most prominent examples of PPEs have been developed by the Met Office Hadley Centre (MOHC) as part of the QUMP (Quantifying Uncertainty in Model Projections) project, (Murphy et al. 2007) and by climateprediction.net (Stainforth et al. 2005). The latter uses distributed computing to run experiments on volunteers personal computers (Allen 1999), and has produced the largest, multi-thousand member, ensembles. Both projects originally focused on examining

uncertainty in climate sensitivity: the temperature change expected for a doubling of CO_2. The range of modelled climate sensitivities from PPEs was shown to be much larger than from MMEs, with warming greater than 11°C in some model versions produced by climateprediction.net (Stainforth et al. 2005). This range has since been constrained (Piani et al. 2005), but PPEs have gone on to be used to explore uncertainty in regional climate, including for the UK Climate Projections 2009 (UKCP09) (Murphy et al. 2007), and continue to reveal risks which are not represented by MMEs (Fung et al. 2011; McSweeney et al. 2012). The application of PPEs to understand African climate projections has been very limited (to the author's knowledge the only relevant study is Buontempo et al. 2013 which focuses on a small selection of model versions).

PPEs are therefore an important and as yet unexploited resource to investigate uncertainty in the implications of anthropogenic forcing for African climate. The range of projected futures from CMIP3 does not necessarily represent the range of all possible futures given current understanding. Using PPEs, it will be possible to test the extent to which parameter perturbations produce projections which are outside the CMIP3 range. Here two PPEs from the MOHC QUMP project are employed. These ensembles will not necessarily produce all possible futures: they only explore uncertainty for a range of atmospheric parameters in one base model (HadAM3), but the experiments will provide an insight into the extent to which it is important to include PPEs as well as MMEs to understand the risks associated with global warming.

A further benefit of using PPEs is that they are easier to constrain. As noted above, one of the challenges in selecting models from MMEs is that differences between them are difficult to diagnose. In a PPE the differences between models are small and well understood; and the large size of the ensemble facilitates understanding of the influence of different parameters (e.g. Sanderson et al. 2008a, b; Rougier et al. 2009; Collins et al. 2011; Sexton et al. 2012). Therefore as well as testing whether there are alternative futures which should be included in the range of projections, the MOHC PPEs can be used to assess whether any projections within the range should be excluded.

1.3.3 Regional Climate Models

The MME (CMIP3) and the PPEs used in this thesis are made up of GCMs. Most existing climate projection work, for Africa and elsewhere, has also been based on global models (e.g. Christensen et al. 2007; Collins et al. 2013). GCMs have a coarse resolution: each grid-point can represent hundreds of kilometres. Whilst some state-of-the-art GCMs have higher resolution, the grid-spacing is still 1° or greater in most CMIP5 simulations (Taylor et al. 2012a).

There are two reasons that low resolution might be problematic for understanding the implications of global warming for African climate. The first is that the large grid-spacing of GCMs can inhibit their ability to represent processes and features with a strong control on precipitation, such as topography and coastlines (e.g. Sylla et al. 2012), and it may limit their capacity to respond reliably to global warming.

The second reason is that finer scale data are required for impacts assessment and decision making (e.g. Wilby and Wigley 1997). RCMs allow experiments to be run at a higher resolution without incurring a prohibitive computational cost. They may produce more trustworthy projections, and can generate outputs at a scale which is more policy-relevant. There has recently been an international effort organised by CORDEX to produce twenty-first century simulations using RCMs, particularly over Africa (Giorgi et al. 2009; Jones et al. 2012; Hewitson et al. 2012). Should these experiments therefore be the basis for analysis to support the selection of a ΔT_g threshold?

RCMs are often viewed as a tool for downscaling projections from GCMs (Wilby and Wigley 1997; Fowler et al. 2007). In the traditional conception of impacts assessment (Figure 1.7; as critiqued by Wilby and Dessai 2010), GCMs are used as boundary conditions for RCMs, which then produce output for impacts models. However, the difference between GCM and RCM projections is not only in the resolution of their output. Existing comparisons reveal that RCMs show different future responses to their driving GCMs (Sylla et al. 2012; Diallo et al. 2012; Laprise et al. 2013; Saeed et al. 2013). The output from RCMs should therefore only replace the GCM projections if it is judged to be more credible. There has been very little work to diagnose the disparities between GCM and RCM projections and to assess their relative value. Saeed et al. (2013) find that REMO alters the signal of MPI-ESM over the Congo Basin due differences in the simulation of extreme rainfall events. Mariotti et al. (2011) and Sylla et al. (2012) infer that RegCM3 produces more trustworthy projections than its driving GCM (ECHAM5) over West Africa, since it is better able to incorporate soil moisture feedbacks and topography. More work is needed to

develop these process-based understandings and investigate projections from other RCMs. In this thesis an ensemble of five GCM and RCM projections will be compared, and their atmospheric dynamics assessed against reanalysis data, to judge the extent to which RCMs can be considered more credible, and therefore the preferred tool for understanding the risks associated with anthropogenic forcing.

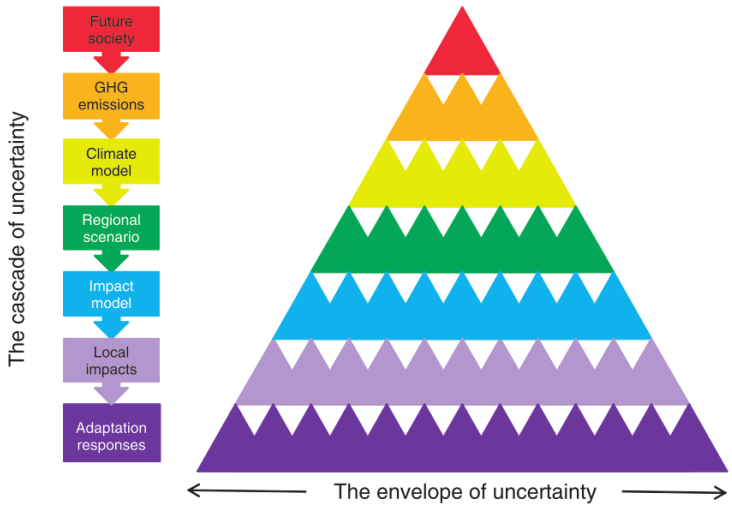

Figure 1.7 Schematic diagram to illustrate the "cascade of uncertainty", taken from Wilby and Dessai (2010). In the traditional conception of impacts assessment, RCMs are used to downscale GCMs, shown here as the "climate models" feeding through to "regional scenarios" (although note that statistical approaches may be required to downscale RCM data further). 'The increasing number of triangles at each level symbolise the growing number of permutations and hence expanding envelope of uncertainty' Wilby and Dessai (2010: 181). This conception, critiqued by Wilby and Dessai, does not anticipate that RCMs may produce different projections to their driving GCMs, meaning some potential changes in large scale climate may not be represented in the resulting "envelope of uncertainty".

1.3.4 Datasets used in this thesis

The first three research chapters in this thesis present pan-African projections from three types of model ensemble in turn: a MME (CMIP3), two PPEs, and a group of RCMs (Table 1.1). Technical information and full references for each are provided in Chapter 2, along with information about additional data which are used to support the analysis of projections.

Table 1.1 Summary of datasets used for projections, including reference to the key chapters which analyse their projections.

Group	Chapter	Ensemble	Members	Type of Model
CMIP3	Chapter 4	CMIP3	24	AOGCM
PPEs	Chapter 5	AS-PPE	280	ASGCM
		AO-PPE	17	AOGCM
RCMs	Chapter 6	PRECIS-GCM	5	AOGCM
		PRECIS-RCM	5	RCM

1.3.4.1 CMIP3

CMIP3 (Meehl et al. 2007b) is a multi-model ensemble (MME) of global models with a coupled atmosphere-ocean (AOGCMs). This dataset is used to provide an initial assessment of changes in African temperature and precipitation associated with 1°C, 2°C, 3°C, and 4°C ΔT_g. It was selected because it is the most widely used climate projection ensemble to date, and is therefore a good starting point, allowing

an assessment of the contribution of the ΔT_g approach used here relative to previous literature on African climate projections based on CMIP3. Analysis of projections from CMIP5 might provide a useful addition to this work, but it was not considered the highest priority here. Existing studies of CMIP5 projections suggest little change from CMIP3 over Africa (Monerie et al. 2012a; Taylor et al. 2012b; Roehrig et al. 2013; Haensler et al. 2013; Christensen et al. 2013) and across the globe (Knutti and Sedlacek 2012; Collins et al. 2013). Furthermore, being an MME and "ensemble of opportunity" CMIP5 suffers from many of the same problems as CMIP3 in that it does not explore uncertainty systematically. Analysis of PPEs was therefore considered more important.

1.3.4.2 PPEs

Two global perturbed physics ensembles (PPEs) developed by the Met Office Hadley Centre (MOHC) (Murphy et al. 2007) are used to test the results from CMIP3; specifically: to examine whether the PPEs extend the range of projections from the MME, and to establish whether they are easier to constrain. The MOHC PPEs were chosen because they have advantages over experiments from climateprediction.net in terms of the spatial resolution and number of variables which have been stored, allowing for analysis across the African continent and in atmospheric dynamics as well as temperature and precipitation responses.

The two PPEs have different benefits. One is a coupled model (AOGCM) ensemble of 17 members run in a high emission scenario (Betts et al. 2011), enabling

investigation of change at 4°C and beyond, and direct comparison with CMIP3. The other ensemble is made up of slab model (ASGCM) equilibrium experiments which are not directly comparable to CMIP3; but it has a larger number of members (280) (Rougier et al. 2009), which might facilitate analysis of variation between models, including mechanisms associated with contrasting precipitation responses in different ensemble members.

1.3.4.3 RCMs

The final dataset is an ensemble of five GCM and RCM simulations. The experiments were produced by the MOHC (Buontempo et al. 2013), using members of the coupled model PPE above (AO-PPE) to force a regional model (PRECIS) over Africa. These represent some of the first century-long simulations run over the whole African continent (at the time of writing CORDEX twenty-first century simulations were gradually becoming available), and output is available from a wide selection of variables allowing for analysis of atmospheric dynamics.

The ensemble is used to assess the extent to which RCMs produce different, and more reliable, climate information than GCMs. Such appraisal will be difficult using CORDEX as it is a matrix of GCM and RCM experiments from different modelling centres (Giorgi et al. 2008): the RCMs have different physics from one another and from their driving GCMs making it problematic to diagnose distinctions between them. In the ensemble used here, the five runs differ from each other only in small perturbations to the driving GCM, meaning it is possible to make inferences

about the difference between the GCM and RCM based on consistency between the ensemble members.

1.4 Case Study

The primary approach in the thesis will be to identify modelled changes across the continent, and to examine regional signals which are found to exhibit the greatest amplitude or largest contrast between models. However, it is also useful to include a case study to be investigated in more detail, including examination of the variation between models and the mechanisms associated with precipitation responses; as well as changes in metrics which are more impacts relevant. As noted in section 1.1, the focus of the thesis is on understanding the uncertainty in seasonal means, but for this test region there is a step towards more decision-appropriate projections.

The dominant motivation for the case study, though, is to investigate the extent to which climate model data can provide useful information for one region, and to explore the difficulties in assessing the implications of global warming given large uncertainty. The Congo Basin is a fitting example because it exemplifies the dilemma faced for the continent as a whole. For all of Africa, there is an urgent need to understand the implications of global warming, but it is difficult to investigate due to the relative lack of previous research and problems with data availability (see section 1.2.1). For Central Africa, understanding the implications of global warming has global significance, but there is a severe scarcity of observations even in comparison to other African regions.

The Congo Basin is the third largest tropical convective zone worldwide (Webster 1981) and contains one of the largest rainforests (Zelazowski et al. 2011). Whilst measurements of carbon stocks and fluxes are limited (Lewis et al. 2009), and it is unknown whether the biome is a net sink or source of CO_2, it is evident that African rainforests play a crucial role, dominating interannual variability in terrestrial carbon cycling (Williams et al. 2007). Changes in the forest therefore have the potential for global feedbacks. Modifications in forest distribution could be generated by changes in the availability of water: drier periods have led to large ecological shifts on millennial timescales (Malhi et al. 2004; Oslisly et al 2013). There is thus considerable interest in understanding how precipitation in the Congo Basin will be influenced by global warming.

Research into Central African precipitation has been severely restricted by the dearth of high quality long term gauge datasets, as highlighted by McCollum et al. (2000), Camberlin et al. (2001), and Todd and Washington (2004); and shown in Figure 1.5. The lack of data has limited understanding of the background climatology, and also presents a problem for evaluating climate models, which has understandably deterred some scientists from examining projections over the region (e.g. Shongwe et al. 2009).

The aim of the case study is to establish the level of understanding which can be gleaned from climate projections in spite of the uncertainties and lack of observations. Where previously there has been little attempt to evaluate models in this region due to the paucity of data; here those data which are available (including satellite and reanalysis products) are examined and compared, to assess the extent of

the observational uncertainty, and the extent to which it might be possible to evaluate hindcasts from climate models. As has already been noted (section 1.3.1), comparing models to observations is not sufficient for validation or for constraining ensembles, but an understanding of their biases is important, so an assessment of whether it is possible to define biases is useful. The investigation of historical climatologies gives a context for subsequent analysis of projected changes in indices of relevance to rainforests; which are further assessed through examination of atmospheric dynamics.

1.5 Summary of aims and objectives

The principal objective of this thesis is to find out how African temperature and precipitation evolve with anthropogenic global warming in climate models, delivering a foundation for evidence-based comparison of mitigation targets. If the model data are to inform policy decisions, it is also important to address the credibility of their representation of uncertainty. As well as identifying modelled changes at 1°C, 2°C, 3°C, 4°C ΔT_g and beyond, the thesis will begin to interrogate these projections, providing insights into the extent to which available model experiments constitute a trustworthy evidence base.

1.5.1 Identifying modelled changes

For each of the datasets outlined in section 1.3.4, and specifically for the Congo Basin case study, the thesis will characterise changes in African temperature

and precipitation, and examine how these evolve with global warming. The focus here is not on the specific temperature and precipitation anomalies calculated for each model, in each region, at each degree of global mean temperature increase (ΔT_g). Rather, the aim is to investigate the range of projections and how these develop from 1°C to 4°C ΔT_g and beyond.

African climate projections will be explored in more detail than in previous studies, through examination of changes across the continent and in all seasons. Precipitation will be given more attention than temperature, due to the greater divergence between model projections (e.g. Dai 2006) and the vulnerability of African regions to change in this variable (see section 1.2.1). The objective is to present what the models show, and in general there will be an attempt to describe the largest anomalies. Whilst there would also be rationale for focusing on regions which are most ecologically sensitive or most populous, here the analysis is driven by the models. There will additionally be an emphasis on describing the changes which show the most agreement between models. Consensus does not indicate credibility, and a large part of the thesis will explore variation between models, but it is also helpful to identify the dominant responses from the model ensembles.

In presenting projections at ΔT_g increments, the first objective is to evaluate the utility of this approach relative to the use of time-slices, and this goal will be addressed in the first paper using CMIP3. Assuming there is a basis for the ΔT_g approach, the central aim from the perspective of mitigation is to investigate how changes develop with global warming: whether anomalies are amplified progressively, there are accelerations in the rate of change, or there are trend reversals. Importantly,

the evolution of change at higher degrees of warming (4°C and beyond) will also be analysed using AO-PPE. As a result of this work, conclusions can be made about the extent to which there is a basis for distinguishing between ΔT_g levels in terms of seasonal climate, with potential implications for policy.

1.5.2 Interrogating modelled changes

The consistency of modelled responses to global warming will be investigated through comparison between the MME, PPEs, and RCMs. There will be a particular focus on the range of projections from each ensemble; to establish whether the uncertainty at each degree of warming differs between the sources of evidence. The results will have implications for the type of datasets which should be included in order to characterise the range of possible futures in impacts assessments. Is it important to consult MMEs and PPEs, GCMs and RCMs in order to produce the most conservative (cautious) error bar for decision makers?

The thesis will also explore techniques for appraising the credibility of specific models and specific precipitation signals. In the case of the large PPE, the size and systematic nature of the ensemble will be exploited to characterise and diagnose sources of variation between model versions, and to examine whether there are any ensemble members whose simulations can be identified as implausible. For the Congo Basin, observational uncertainty will be inspected to ascertain whether there is a basis for distinguishing between models using their climatologies. Evaluation of twentieth century hindcasts is insufficient to assess the trustworthiness

of the climate change signal, however. In order to appraise the projections directly, atmospheric dynamics associated with precipitation responses will be analysed, for those wetting and drying signals which are the largest or show most divergence between models. If the mechanisms for precipitation change can be identified, it may be possible to gauge their plausibility by comparing the responses to warming with circulation anomalies associated with twentieth century interannual variability.

1.5.3 Aims of each research chapter

The thesis objectives are addressed through five substantive chapters, and the relevant research questions for each are outlined below. The first three papers (Chapters 4, 5, and 6) analyse pan-African projections from each of the datasets in turn, and the last two papers (Chapters 8 and 9) focus on the Congo Basin. Between these sections Chapter 7 introduces the Congo Basin case study, and provides further explanation of the objectives for Chapters 8 and 9.

Chapter 4: CMIP3

Chapter 4 presents changes in African temperature and precipitation at 1°C, 2°C, 3°C, and 4°C ΔT_g from CMIP3 models. It provides an initial assessment of the utility of an approach using ΔT_g increments, and a basis for further work.

- To what extent does an approach using time-slices conceal differences between ΔT_g intervals?
- What changes in regional climate are associated with different levels of ΔT_g?

- What are the largest changes in temperature and precipitation projected for Africa by CMIP3 models?
- Which temperature and precipitation anomalies exhibit the most agreement between CMIP3 models?
- How does local climate evolve with global warming?

Chapter 5: PPEs

In this paper two PPEs are used to critically re-evaluate the projections from CMIP3, exploring uncertainties which were not possible in Chapter 4, namely changes at higher degrees of warming, and the influence of parameter perturbations on the range of projections.

- How do changes in African temperature and precipitation evolve at 4°C and beyond?
- Do parameter perturbations modify the range of projected futures?
- Does variation between models result from limitations in understanding or model error? Can any models be justifiably excluded?

Chapter 6: RCMs

Projections from RCMs are compared to their driving GCMs in Chapter 6, to assess the extent to which they provide different, and more reliable, information.

- Are there important differences between GCM and RCM projections?
- Can the differences between GCM and RCM be understood in terms of differences in atmospheric dynamics?
- To what extent can GCM or RCM projections be considered more credible?

Chapter 8: Congo Basin climatologies

After the Congo Basin case study has been introduced in Chapter 7, Chapter 8 presents precipitation and moisture flux climatologies from a range of datasets over the Congo Basin to assess the extent of the observational uncertainty.

- To what extent can available observed and reanalysis datasets be used to assess the credibility of climate models over the Congo Basin?

Chapter 9: Congo Basin projections

In Chapter 9, changes in the climate of African rainforests associated with global warming are presented from CMIP3 and the MOHC PPEs.

- What changes of relevance to rainforests are projected for the Congo Basin?

1.6 Notes on thesis format

This thesis takes the form of the "paper route", whereby the substantive research chapters are academic papers, provided as submitted to, or published in, peer reviewed journals. A minimum of four articles are required, and in this case four first author papers and one second author paper are included. The total of five papers presents a coherent body of research investigating the implications of global warming for African climate. At the time of writing, three of these papers have been published and two submitted, as follows:

Published

James, R., & Washington, R. (2013) Changes in African temperature and precipitation associated with degrees of global warming. *Climatic Change* **117** (4) 859-872 doi:10.1007/s10584-012-0581-7

James, R., Washington, R., & Rowell, D. P. (2013) Implications of global warming for the climate of African rainforests. *Philosophical transactions of the Royal Society of London. Series B, Biological sciences* **368** (1625) 20120298 doi:10.1098/rstb.2012.0298

Washington, R., James, R., Pearce, H., Pokam, W. M., & Moufouma-Okia, W. (2013) Congo Basin rainfall climatology: can we believe the climate models? *Philosophical transactions of the Royal Society of London. Series B, Biological sciences* **368** (1625) 20120296. doi:10.1098/rstb.2012.0296

Submitted

James, R., Washington, R., & Rowell, D. P. (2013) African climate change uncertainty in perturbed physics ensembles: implications of warming to 4°C and beyond *Submitted to: Journal of Climate.*

James, R., Washington, R., & Jones, R. (2013) African climate change in global and regional models: a comparison of precipitation responses to global warming Submitted to: Climate Dynamics

The text, figures, and tables in each paper are the same as published or represented in the submitted version. The references to figures and citations have been standardised to provide a coherent format throughout the thesis. The references have been summarised into a single list at the end of the thesis. Supplementary information which is provided online for each journal article has been included in the thesis at the end of the relevant chapter, and is referred to using the letter S (Table 4.S1, Figure 4.S1, etc.).

2 Data

2.1 Introduction

This chapter provides technical details for all data utilised in the thesis, including model ensembles used for projections (the selection of which has already been discussed in section 1.3.4), and other datasets which have been applied to investigate the value of the projections. Their uses are summarised in Table 2.1 and 2.2. For each dataset, the relevant section will also offer a short overview of existing work examining its ability to represent African climate. GCMs, RCMs, reanalyses, and observations will be covered in turn.

Table 2.1 Summary of model ensembles and their applications.

Ensemble	Members	Model	Scenarios	Summary of applications
CMIP3	24	AOGCM	20C3M SRES A2 SRES A1B	Chapter 4: Projections at 1-4°C Chapter 5: Comparison of projections with PPEs Chapter 8: Comparison of Congo Basin precipitation climatology with other datasets Chapter 9: Projections for African rainforests
CMIP5	9	AOGCM ESM	historical	Chapter 8: Comparison of Congo Basin climatology with other datasets (precipitation and moisture flux)
AS-PPE	280	ASGCM	1 x CO_2 2 x CO_2	Chapter 5: Comparison of projections with CMIP3 and AO-PPE Chapter 9: Projections for African rainforests
AO-PPE	17	AOGCM	historical SRES A1FI	Chapter 5: Comparison of projections with CMIP3 and AS-PPE Chapter 9: Projections for African rainforests
PRECIS-GCM	5	AOGCM	historical SRES A1B	Chapter 6: Comparison of projections with PRECIS-RCM
PRECIS-RCM	5	RCM	historical SRES A1B	Chapter 6: Comparison of projections with PRECIS-GCM

Table 2.2 Summary of observed, satellite, and reanalysis datasets and their applications.

Dataset	Type of data	Summary of applications
NCEP	reanalysis	Chapter 6: Comparison of wet and dry year dynamics with GCMs and RCMs Chapter 8: Congo Basin climatology (precipitation and moisture flux)
CFSR	reanalysis	Chapter 8: Congo Basin climatology
ERA-40	reanalysis	Chapter 8: Congo Basin climatology
ERA-I	reanalysis	Chapter 6: Comparison of wet and dry year dynamics with GCMs and RCMs Chapter 8: Congo Basin climatology (precipitation and moisture flux)
CRU	gauge data	Chapter 8: Congo Basin climatology
CMAP	satellite data	Chapter 8: Congo Basin climatology
TAMSAT	satellite data	Chapter 8: Congo Basin climatology
CMORPH	satellite data	Chapter 8: Congo Basin climatology
GPCP	merged satellite and gauge data	Chapter 8: Congo Basin climatology
TRMM	merged satellite and gauge data	Chapter 8: Congo Basin climatology

2.2 Global Climate Models

In total five ensembles of GCMs have been analysed in this thesis: two MMEs and three PPEs.

2.2.1 Multi-Model Ensembles

2.2.1.1 CMIP3

The Coupled Model Intercomparison Project phase 3 (CMIP3) is a collection of AOGCM experiments from different modelling centres, organised by the WCRP and freely available for download via PCMDI (http://esg.llnl.gov:8080/index.jsp; Meehl et al. 2007b). Monthly data for precipitation rate and temperature at the surface were analysed from historical and future simulations. The historical scenario (20C3M) is forced with twentieth century estimates of variables known to be important for climate: GHGs and sulphate aerosols, and in some models volcanic eruptions and solar variability. The twenty-first century scenarios used were SRES A2 and A1B (Nakicenovic et al. 2000). A2 is characterised by economic development which continues to be reliant on fossil fuels, but in a more divided world. A1B assumes rapid economic growth from a balance of energy sources in a more integrated world. Of the scenarios prioritised for CMIP3, A2 and A1B offer the greatest potential for large global warming: A2 has the highest GHG forcing by 2100, and A1B was run to 2200 or longer in many models meaning global temperature has longer to adjust to radiative forcing. All models available in each scenario were analysed. Each model has been developed separately and different

ensemble members have different parameterisation schemes and resolutions. Data were interpolated to allow comparison on a common grid (as detailed in the relevant chapters). One initialisation of each model was included: either the first integration available or the longest integration in the case of A1B. Details of each model run are provided in Table 2.3.

CMIP3 was prepared for the IPCC AR4 (2007). In terms of the representation of historical climatologies, models of this generation show a substantial improvement in skill relative to their predecessors (Reichler and Kim 2008); but still struggle to simulate tropical precipitation, due to uncertainties in scientific understanding, a lack of observations, and the difficulty in representing small scale convective systems at coarse resolution (Dai 2006; Randall et al. 2007). The models' ability to reproduce African precipitation climatologies is impeded by some large and common biases. In particular, SSTs in the Gulf of Guinea are too warm, by almost 3°C in some models (Cook and Vizy 2006), indicating a failure to represent the cold tongue, which is problematic for simulating the West African Monsoon (WAM), preventing the migration of the precipitation maximum as far north as in observations. Another important issue is that many models overestimate precipitation in the Southern Hemisphere mid-latitude storm tracks during JJA (Neelin et al. 2006). Christensen et al. (2007) find precipitation is overestimated in southern Africa in 90% of models, by >20% on average, which could have an important influence on the response to warming. In Giorgi and Coppola's (2010) analysis, southern Africa during JJA is the only African region where the twentieth century bias in CMIP3 models is significantly correlated with projected precipitation change.

Table 2.3 CMIP3 models used in this thesis, including the range of years analysed from each SRES experiment.

Model Name[a]	Country	Resolution[b]	A2	A1B
BCCR-BCM2.0	Norway	1.9°x1.9° L16	2001-2099	2001-2099
CCSM3.0	USA	1.4°x1.4° L26	2001-2099	2000-2349
CGCM3.1 (T47)	Canada	2.8°x2.8° L31	2001-2099	2001-2300
CGCM3.1 (T63)	Canada	1.9°x1.9° L31	-	2001-2300
CNRM-CM3	France	1.9°x1.9° L45	2001-2099	2000-2299
CSIRO-Mk3.0	Australia	1.9°x1.9° L18	2001-2099	2001-2200
CSIRO-Mk3.5	Australia	1.9°x1.9° L18	2001-2099	2001-2300
ECHAM5/MPI-OM	Germany	1.9°x1.9° L31	2001-2099	2001-2300
ECHO-G	Germany/Korea	3.9°x3.9° L19	2001-2099	2001-2300
FGOALS-g1.0	China	2.8°x2.8° L26	-	2000-2199
GFDL-CM2.0	USA	2.0°x2.5° L24	2001-2099	2001-2300
GFDL-CM2.1	USA	2.0°x2.5° L24	2001-2099	2001-2300
GISS-AOM	USA	3.0°x4.0° L12	-	2001-2100
GISS-EH	USA	4.0°x5.0° L20	-	2001-2099
GISS-ER	USA	4.0°x5.0° L20	2004-2099	2004-2199
INGV-SXG	Italy	1.1°x1.1° L19	2001-2099	2001-2099
INM-CM3.0	Russia	4.0°x5.0° L21	2001-2099	2001-2200
IPSL-CM4	France	2.5°x3.75° L19	2001-2099	2000-2230
MIROC3.2(hires)	Japan	1.1°x1.1° L56	-	2001-2099
MIROC3.2(medres)	Japan	2.8°x2.8° L20	2001-2099	2001-2300
MRI-CGCM2.3.2a	Japan	2.8°x2.8° L30	2001-2099	2001-2300
PCM	USA	2.8°x2.8° L26	2001-2099	2000-2299
UKMO-HadCM3	UK	2.5°x3.75° L19	2001-2099	2000-2199
UKMO-HadGEM1	UK	1.3°x1.9° L38	2001-2099	2000-2199

[a]Naming conventions are taken from the IPCC www-pcmdi.llnl.gov/ipcc/model_documentation/ipcc_model_documentation.php

[b]Horizontal resolution is expressed as approximate degrees latitude by longitude. Vertical resolution (L) is the number of vertical levels.

Research into the models' ability to simulate local circulation features has paid most attention to the Sahel. Some generate the Saharan Heat Low (SHL) too far east, and many do not reproduce the southward outflow from the Saharan high which is linked to the African Easterly Jet (AEJ) (Cook and Vizy 2006). Sylla et al. (2010) demonstrate large variation between members of CMIP3 in the ability to reproduce zonal wind features over West Africa. A further consideration is the extent to which models can simulate modes of variability which are all important in many African regions (see section 1.2.1). Cook and Vizy (2006) find that only 4 out of 18 members of CMIP3 can realistically model the dipole between the Sahel and Guinea Coast associated with SST variability in the Gulf of Guinea. Rowell (2013) investigates teleconnections across the African continent, finding that some are reproduced well, for example the link between the Indian Ocean Dipole (IOD) and the Greater Horn of Africa in OND; whilst others are more difficult to model, such as the IOD's impact on south-east Africa. Given that climate change is expected to be manifest through modes of variability (Corti et al. 1999; Stone et al. 2001), these limitations could determine the extent to which the models can produce realistic responses to warming.

It is also important to note that the models may fail to represent some feedbacks associated with anthropogenic climate change, due to their limited complexity. The majority of CMIP3 models do not include indirect aerosol effects (Albrecht 1989; Randall et al. 2007); and all have prescribed vegetation (see e.g. Betts et al. 2004 on the influence of dynamic vegetation), meaning potential feedbacks associated with the strong coupling between the land surface and atmosphere in many African regions (e.g. Koster et al. 2004) cannot be incorporated. There are also

remote influences which may be overlooked: importantly many models do not include interactive ice sheets (Lenton 2011b).

In spite of these limitations, assessment of simulations from CMIP3 is arguably an important component of any projection study which seeks to make comparisons across ensembles, as a result of its widespread use in previous climate projection work (Easterbrook 2013). Furthermore, despite recent advances in climate modelling, the differences in output from CMIP3 and CMIP5 are small (as will be discussed below), indicating that CMIP3 models remain some of the best available in so far as they can be evaluated.

2.2.1.2 CMIP5

CMIP5 is the most recent MME of AOGCMs organised by the WCRP, prepared for the IPCC AR5, freely available via PCMDI (http://cmip-pcmdi.llnl.gov/cmip5/index.html), and documented by Hurrell et al. (2011) and Taylor et al. (2012a). Monthly data for precipitation rate, specific humidity (q), zonal wind (u), and meridional wind (v) on pressure levels, were analysed from historical simulations. Nine models were used (Table 2.4), with one initialisation for each. Data were interpolated to a 1.9x1.9° grid-spacing to allow comparison between models and to reanalysis on a common grid.

Table 2.4 CMIP5 models used in this thesis.

Model Name[a]	Modelling Group	Resolution[b]
CanESM2	CCCMA, Canada	2.8°x2.8° L35
CNRM-CM5	CNRM-CERFACS, France	1.4°x1.4° L31
CSIRO-Mk3.6.0	CSIRO-QCCCE, Australia	1.9°x1.9° L18
GISS-E2-H	NASA GISS, USA	2.0°x2.5° L40
GISS-E2-R	NASA GISS, USA	2.0°x2.5° L40
HadGEM1-ES	MOHC, UK	1.3°x1.9° L38
MPI-ESM-LR	MPI-M, Germany	1.9°x1.9° L47
MRI-CGCM3	MRI, Japan	1.1°x1.1° L48
NorESM1-M	NCC, Norway	1.9°x2.5° L26

[a]Naming conventions are taken from PCMDI http://cmip-pcmdi.llnl.gov/cmip5/docs/CMIP5_modeling_groups.pdf

[b]Horizontal resolution is expressed as approximate degrees latitude by longitude. Vertical resolution (L) is the number of vertical levels.

Whilst CMIP5 does include some of the same models as CMIP3 (e.g. HadCM3), most are new versions, with updated parameterisations or alternative parameterisation schemes, and in many cases higher horizontal and vertical resolution (Taylor et al. 2012a). Many of the models also have greater complexity relative to CMIP3 (Friedlingstein and Jones 2011). Some are described as Earth System Models (ESMs), including 4 of the 9 models used in this thesis, although ESM has no rigid definition. Different earth system components are incorporated into different CMIP5 members, including aerosol-chemistry climate models, dynamic vegetation, land and ocean carbon cycles, and interactive ice sheets.

Existing work to evaluate CMIP5 suggests that, despite these advances, many of the biases in the representation of African precipitation remain (Monerie et al. 2012a), including the warm SSTs in the Gulf of Guinea (Roehrig et al. 2013). There has been no discernable improvement in the representation of teleconnections (Rowell 2013). Projected changes in precipitation are also consistent between CMIP3 and CMIP5: for Africa (Monerie et al. 2012a; Taylor et al. 2012b; Christensen et al. 2013; Haensler et al. 2013; Roerhig et al. 2013) and across the globe (Knutti and Sedlacek 2012; Collins et al. 2013).

2.2.2 Perturbed Physics Ensembles

The PPEs used here were developed by the Met Office Hadley Centre (MOHC) as part of the "QUMP" project: for Quantifying Uncertainty in Model Projections. The project investigated uncertainty in future climate by varying atmospheric, land surface, oceanic, and carbon cycle parameters within Hadley Centre models (Rowell 2012). In this thesis the focus is on perturbations to atmospheric and land surface parameters due to the direct association with precipitation. Three ensembles are employed: a large ensemble of slab models (AS-PPE), a smaller ensemble of coupled models (AO-PPE), and also a subensemble of AO-PPE members which were applied as boundary conditions in RCM experiments using PRECIS. For clarity this third ensemble is referred to as PRECIS-GCM and the corresponding RCMs PRECIS-RCM.

2.2.2.1 AS-PPE

The basis for AS-PPE is HadSM3: HadAM3 (Pope et al. 2000) coupled to a 50m mixed layer or "slab" ocean. HadAM3 has a horizontal resolution of 2.5° latitude and 3.75° longitude, with 19 vertical levels. The ensemble of 280 members was created through perturbations to 31 atmospheric and land surface parameters; in three stages, which are described in detail in Collins et al. (2011) as S-PPE-S, S-PPE-M, and S-PPE-E. The first stage used single parameter perturbations to create an ensemble of 52 models, which do not have an interactive sulphur cycle, and are not tuned to observations (Murphy et al. 2004). In the second stage multiple parameters were perturbed in each version, producing 128 ensemble members (Webb et al. 2006). These versions have an interactive sulphur cycle and the parameters were selected to maximise model performance relative to observations. The third stage generated 100 model versions with single and multiple parameter perturbations, designed to explore parts of parameter space which were not covered in the first two stages (Rougier et al. 2009). The parameters and range of expert specified values are provided in Barnett et al. (2006).

Each of the model versions was run three times. The first run is a 25 year calibration phase, in which heat convergences are calculated for each ensemble member: heat sources which are added to slab oceans during the experimental phase to simulate heat transport and correct for top of atmosphere flux imbalances. Then two equilibrium experiments were run with preindustrial ($1xCO_2$) and doubled CO_2 ($2xCO_2$). These runs continue for 20 years beyond equilibrium and 20 year monthly

means from this period were the basis for analysis; for temperature at 2m, precipitation rate, *u*, *v*, *q*, vertical velocity (ω), SST, and SLP.

Slab models were used for AS-PPE because the lower computational expense allows a large number of model versions to be tested. Models with a mixed layer ocean may have a less realistic response to anthropogenic forcing than coupled models, because atmosphere-ocean interactions are represented in a superficial manner (Dickinson et al. 1995), and such processes are known to be important in tropical climate, not least for the El Nino Southern Oscillation (ENSO). However, despite previous wisdom (Kattenberg et al. 1995; Luo et al. 2011), slab models can produce the Southern Oscillation and associated global connections to some extent (Clement et al. 2010), and projections of tropical precipitation change show similarity between slab models and coupled models outside of the Pacific (Chou et al. 2006); suggesting that slab models have the potential to be a useful tool for exploring African precipitation projections.

It is worth noting that after producing the ensemble a coding error was discovered in all experiments from the second stage (S-PPE-M) and some experiments from the third stage (S-PPE-E) of ensemble development (Collins et al. 2011). The heat convergences specified in the $1xCO_2$ and $2xCO_2$ simulations were selected from one year of the calibration phase, when they should have been averaged over many years. This error could introduce SST biases. Collins et al. (2011) conclude that the impact on SSTs is small. They also note that after selected experiments were repeated with the error removed, there was little change in non-SST related variables or in feedbacks at $2xCO_2$, suggesting that the experiments are suitable for quantifying

uncertainty and examining feedbacks. Given the focus on regional climate in this thesis, the SST biases were re-examined to establish whether the anomalies from observations were particularly large in any region which might influence African precipitation. Seasonal SSTs from the control period ($1xCO_2$) were differenced from HadISST (Rayner et al. 2003) and the biases of individual ensemble members were inspected. Differences from observed SSTs were evident, but it is difficult to establish whether these anomalies result from parameter perturbations or the calibration error. As found by Collins et al., the biases are smaller than the biases of non-flux adjusted coupled models (such as those in CMIP3), and on this basis AS-PPE was deemed suitable to investigate uncertainty in African climate change.

Another important consideration is the perturbation of parameters in the third stage of AS-PPE's construction. This stage was designed to build an emulator and not to produce realistic model versions (Rougier et al. 2009). The exploration of parameter space is a key motivation for using the ensemble, allowing the range of projections from CMIP3 to be tested; and the dataset has been shown to reveal more about sources of uncertainty in future tropical precipitation than smaller ensembles (Rowell 2012). However, AS-PPE might include unrealistic model versions. The ensemble has previously been used in Bayesian frameworks to develop probabilistic projections (Sexton et al 2012), and this analysis has delivered information about the validity of certain parameter values; but there has been little previous work to directly evaluate the output on a regional basis, and none for Africa (to the author's knowledge). Therefore, before using AS-PPE to investigate uncertainty in African projections, the plausibility of ensemble members will be examined in Chapter 5.

2.2.2.2 AO-PPE

AO-PPE was created to explore uncertainty in future climate projections from a coupled model: HadCM3 (Collins et al. 2001). HadCM3, like HadSM3, is based on HadAM3 but in this case coupled to a fully dynamical ocean. The model is the same as in CMIP3 except with flux adjustments included at the sea-surface, to ensure baseline sea-surface temperatures and sea-ice are close to observed, and an interactive sulphur cycle. Due to greater computational expense of the dynamical ocean it was not possible to run all 280 atmospheric configurations from AS-PPE; therefore 17 versions were chosen. As well as the standard model, the variant with the best simulation of present day climate was used, and 15 others were selected to span a range of climate sensitivities and parameter values (Murphy et al. 2007; Collins et al. 2011). The ensemble has been run with a number of forcing scenarios. Here SRES A1FI is used, which assumes rapid economic growth with an emphasis on fossil fuels (Nakicenovic et al. 2000). It has the highest GHG forcing of the SRES scenarios, generating global warming >4°C in some ensemble members (Betts et al. 2011). The A1FI experiment was compared to a preindustrial control: a reference period was selected 40 years into the run to avoid spin-up issues. Monthly data for temperature at 2m and precipitation rate were analysed.

HadCM3 is now over ten years old. It has a coarse horizontal resolution and limited complexity relative to the state-of-the-art models in CMIP5. However, its endurance from CMIP2 to CMIP5 is testament to its capabilities relative to other GCMs. Prior to the development of the latest MOHC GCM (HadGEM3), HadCM3 outperformed more complex MOHC models (HadGEM1) in terms of variability in

Pacific SSTs, ENSO, and monsoon rainfall (Pope et al. 2007). Validation of HadCM3 over Africa has concentrated on the Sahel, suggesting that the model captures the zonal circulation over West Africa well relative to other CMIP3 models (Sylla et al. 2010), but produces too much precipitation prior to the monsoon season (Biasutti et al. 2008; Monerie et al. 2012b), and simulates the precipitation maximum too far south during JAS (Cook and Vizy 2006; Monerie et al. 2012b). HadCM3 also fails to reproduce the 1970s-80s Sahel drought (Lau et al. 2006), possibly indicating poor representation of teleconnections: Rowell (2013) shows that HadCM3 has a relatively low ranking in this regard, when compared to models from CMIP3 and CMIP5; although it can reproduce some important correlations with SSTs such as between the IOD and East African short rains (Conway et al. 2007).

The ability of the AO-PPE ensemble to simulate African climatologies has also been evaluated by Buontempo et al. (2013), who find that the representation of annual cycles of temperature and precipitation compares well to observations relative to other CMIP3 models. The simulation of climatological wind fields is also relatively close to observations. However, the ensemble as a whole shares some biases found in HadCM3, for example there is too much precipitation in central Sahel prior to the climatological rainfall season. AO-PPE also overestimates near surface temperatures in hotter regions (Buontempo et al. 2013). Aside from these findings which apply to the whole ensemble, there are also biases in individual ensemble members, and the spread in climatological temperature, precipitation, SLP, and geopotential height at 500mb, is large relative to other continents (Sanderson 2008).

2.2.2.3 PRECIS-GCM

PRECIS-GCM is a sub-ensemble of the HadCM3 PPE. Using experiments in which the 17 model versions were run with historical emissions and SRES A1B, Buontempo et al. (2013) selected five members to be used as boundary conditions for regional downscaling using PRECIS. The model versions are the same as those in AO-PPE, but due to the restricted ensemble size (5 rather than 17) and the difference in emission scenario (A1B rather than A1FI) this group is referred to here as PRECIS-GCM for clarity.

The selection of the sub-ensemble was motivated by the computational expense associated with century-long RCM integrations. The regional downscaling and impacts communities are often forced to constrain ensembles for this reason. For PRECIS-GCM, the model sub-selection followed a framework developed by McSweeney et al. (2012) for Southeast Asia, and applied to Africa by Buontempo et al. (2013). The approach aims first to eliminate ensemble members which have a poor simulation of the key features of regional climate, and second to select model versions which capture the range of future responses in temperature and precipitation from the full ensemble. This process is not straightforward, as the ensemble members with the highest skill or the most extreme projections are not necessarily the same in different regions; therefore those models which have outlying projections in the most regions and a reasonable simulation of the annual cycle of temperature and precipitation are generally selected. In this case, the five models chosen include the standard model and four others, which together represent the hotter and colder, and

wetter and dryer projections. In general, the group of five models has some improvements in background climatology relative to the larger 17 member ensemble.

Monthly data were analysed from historical and SRES A1B runs from 1949-2100, for temperature at 2m, precipitation rate, SLP, and the following variables on pressure levels: u, v, q, ω, and temperature.

2.3 Regional Climate Models

One ensemble of RCMs has been used in this thesis, known here as PRECIS-RCM.

2.3.1.1 PRECIS-RCM

The basis of this ensemble is HadRM3P: the same formulation of the Hadley Centre regional model used for the PRECIS Regional Climate Modelling System (through which the RCM is given a simple user interface and provided to climate centres in developing countries). The HadRM3P physics is based on HadAM3, but with some structural changes to the representation of clouds, and other parameters optimised to deliver improved model performance over land regions when run as a global atmospheric model at double the standard atmospheric resolution of HadAM3/HadCM3. Details are provided in Jones et al. (2004).

The RCM was run over the CORDEX Africa domain (Giorgi et al. 2008) at a grid-spacing of 50km, with 19 vertical levels, and the land surface scheme MOSES

2.2 (Met Office Surface Exchange Scheme version 2.2). Boundary conditions were taken from the five versions of HadCM3 in PRECIS-GCM. The physics of the RCM was not perturbed to match each driving global model, meaning the only difference between the five RCM experiments is in slight changes to the parameters of the corresponding GCM. Note that the boundary conditions were provided directly, following the standard procedure for regional modelling, rather than as an anomaly to reanalysis (an approach which has applied recently over Africa e.g. Patricola and Cook 2010; Cook and Vizy 2012; Vizy et al. 2013). As in the case of the GCMs, monthly data were analysed from historical and SRES A1B runs from 1949-2100, for temperature at 2m, precipitation rate, SLP, and the following variables on pressure levels: u, v, q, ω, and temperature.

The MOHC has developed more advanced regional models since HadRM3P, but this RCM has many advantages, including that it has been widely used, and is designed to be adaptable to any area of the globe. The CORDEX Africa domain is, however, controversial. Whilst some authors highlight the potential importance of large domains encompassing the entire African continent due to the complex interplay between different circulation systems (Mariotti et al. 2011), others have suggested that the domain might be too large. Another potential limitation is the 50km resolution, which may not be sufficient for improvement over GCMs: it is still coarse relative to the scale of convective processes governing tropical precipitation (see Marsham et al. 2013).

Several recent studies have evaluated the ability of RCMs run over the CORDEX Africa domain at 50km resolution with reanalysis for boundary conditions,

including HadRM3P (Nikulin et al. 2012; Kim et al. 2013; Endris et al. 2013; Kalognomou et al. 2013; Gbobaniyi et al. 2013). All of the ten RCMs investigated generate reasonably accurate precipitation in terms of the seasonal mean and annual cycle (Nikulin et al. 2012), and also capture the basic climatological features of temperature and cloudiness (Kim et al. 2013). Whilst Nikulin et al. (2012), Endris et al. (2013), and Kalognomou et al. (2013) conclude that these RCMs can provide useful information for climate projection; Kim et al. (2013) highlight the need for evaluation for each region, variable, and metric if RCMs are to be used for climate change impact assessment. Buontempo et al. (2013) have conducted an evaluation of PRECIS-RCM across Africa, comparing the historical climatology from the RCMs with the driving GCMs, observations, and reanalysis, on a continental and regional scale, for temperature, precipitation, and wind. Their paper suggests that the background precipitation climatology of the RCMs is improved relative to the 17 member HadCM3 ensemble. The RCMs generate a more reliable simulation of the magnitude and timing of the rainfall season in the Sahel than the GCMs. However, there is little difference in the general circulation between GCMs and RCMs, and the RCMs overestimate precipitation for much of the continent relative to observations. They also have a bias over Lake Victoria, but this error is understood to have little relevance beyond the lake itself. The RCMs do not show an improvement in the representation of orographic precipitation maxima relative to GCMs: there is still no maximum over the Cameroon highlands in JJA.

2.4 Reanalysis data

Monthly data from four reanalysis projects have been employed. From the US National Centers for Environmental Prediction: NCEP/NCAR reanalysis 1 (Kalnay et al. 1996), and the NCEP Climate Forecast System Reanalysis (CFSR) (Saha et al. 2010). From the European Centre for Medium-Range Weather Forecasts: the ECMWF 40 year reanalysis (ERA-40) (Uppala et al. 2005) and ERA-interim (Dee et al. 2011). The resolution and variables used are summarised in Table 2.5.

Table 2.5 Reanalysis datasets: information about atmospheric resolution, variables used, and time periods available. Note that resolution refers to the standard archive resolution rather than model resolution.

Dataset	Variables	Resolution	Levels	Time period
NCEP	precipitation rate on pressure levels: temperature, u, v, q, ω	approx. 1.9x1.9° for precipitation; 2.5x2.5° for other variables	17	1948-2013
CFSR	precipitation rate	0.5x0.5°	37	1979-2010
ERA-40	precipitation rate	2.5x2.5°	23	1957-2002
ERA-I	precipitation rate on pressure levels: temperature, u, v, q, ω	0.75x0.75°	37	1979-2013

Reanalysis datasets allow investigation of many variables across the African continent. Whilst they are a useful means to overcome gaps in observed records;

some regions, time periods, and variables have very few observations (see Figure 1.5), and therefore the reanalysis data must rely heavily on the numerical model and assimilation scheme. Given that the regions with limited observations (such as the Congo Basin) also tend to be poorly understood, the models may also be less reliable over these domains. The key problem is that neither the model nor the reanalysis output can be fully evaluated; also due to the lack of observations.

2.5 Ground-based and satellite data

Monthly precipitation data were analysed from ground based, satellite, and merged products (Table 2.6). The only gauge data used were CRU (Climate Research Unit time-series version 3.20) (Mitchell et al. 2004; Harris et al. 2013). Monthly station counts were also examined for this dataset: using the actual number of all stations reporting in each cell, rather than the number of stations which could have influenced the cell.

The following satellite products were employed. CMAP (the Climate Prediction Centre Merged Analysis of Precipitation), which combines estimates from five satellites (Xie and Arkin 1997): the standard version is used, rather than the version which is enhanced with NCEP reanalysis. TAMSAT (Tropical Applications of Meteorology using SATellite data and ground-based observations) data were also used from TARCAT (TAMSAT African Rainfall Climatology and Time-Series) version 2.0 (Tarnavsky et al. 2013). Finally, CMORPH (NOAA CPC Morphing Technique) time-series were analysed (Joyce et al. 2004). The merged products used were GPCP

(Global Precipitation Climatology Project) (Adler et al. 2003), and TRMM (Tropical Rainfall Measuring Mission) 3B43v7 (ftp://meso-a.gsfc.nasa.gov/pub/trmmdocs/3B42_3B43_doc.pdf).

Table 2.6 Ground-based and satellite datasets: information about atmospheric resolution and available time period.

Dataset	Type of data	Resolution	Time period
CRU	gauge	0.5x0.5°	1901-2011
CMAP	satellite	2.5x2.5°	1979-2011
TAMSAT	satellite	0.0375x0.0375°	1983-2011
CMORPH	satellite	0.07277x0.07277°	2002-2013
GPCP	merged satellite and gauge	2.5x2.5°	1979-2013
TRMM	merged satellite and gauge	0.25x0.25°	1998-2013

The availability of gauge data is limited for many African regions, which might bring the CRU dataset into question and also suggests that the merged products are likely to rely more heavily on satellite than gauge data. Rowell (2013) shows that the availability of CRU data has declined since the 1980s in all regions analysed: the Sahel, the Guinea Coast, and parts of southern and East Africa; and Conway et al. (2009) find similar results for major river basins in sub-Saharan Africa.

3 Methods

3.1 Introduction

This chapter will outline the techniques used to identify and interrogate modelled changes in African climate associated with global warming. First, approaches to relate local climate changes to global temperature will be described, before a summary of methods which are employed to characterise projected warming, wetting, and drying signals: from individual models, and from different models and model ensembles. Then, analysis tools for investigating sources of uncertainty, and for developing process-based understanding of projected precipitation responses, are examined. Throughout the thesis there is a preference for simple and transparent techniques rather than more complex statistics, and an emphasis on sensitivity tests of methodological decisions.

3.2 Deriving local change as a function of global temperature

Existing efforts to investigate climate changes associated with specific degrees of global mean temperature increase (ΔT_g) have employed four main approaches for relating local conditions to global warming. The first approach is to select only those models which reach the specified ΔT_g interval by the end of the 21st century (Betts et al. 2011; Fung et al. 2011; Sanderson et al. 2011; World Bank 2012). The second involves pattern scaling, whereby changes per °C are calculated, and then multiplied to find changes at other ΔT_g intervals (Thornton et al. 2011; Zelazowski et al. 2011). A third method is to compare emissions scenarios/concentration pathways

which produce different levels of warming (May 2011; Huebener et al. 2013; Schellnhuber et al. 2013). Finally it is possible to directly extract the time of each degree of global warming, and examine regional climate changes which correspond to this date (Kaplan and New 2006; Giannakopoulos et al. 2009; Tang and Lettenmaier 2012). This latter approach allows for each ΔT_g increment to be examined directly and therefore provides greater potential to compare different levels of ΔT_g, and this is the primary technique adopted here. However, there are limitations associated with the time-based sampling approach and a second method of presenting local change as a function of global temperature using linear regression was also employed, which is similar to pattern scaling. Both are described in this section.

3.2.1 Time-based samples at 1°C, 2°C, 3°C, 4°C and beyond

In order to find the time of each degree of ΔT_g, annual global mean temperature anomaly time-series must be constructed for each model. Historical and future data for temperature at the surface or screen temperature are weighted by grid-box area and then spatially averaged annual global means are calculated. The annual means for a historical baseline period of m years are temporally averaged to create a reference climatology (T_{g1}). Each annual mean in the future time-series (T_{g2}) is differenced from the baseline as follows:

$$T_{g1} = \frac{\sum_1^m \left(\frac{\sum_1^n T_1}{n}\right)}{m}$$

$$T_{g2} = \frac{\sum_1^n T_2}{n}$$

$$\Delta T_g = T_{g2} - T_{g1}$$

where T_1 and T_2 are the annual temperatures in each grid-box, for the historical and future scenarios respectively, and n is the number of grid-boxes. The resulting time-series are then smoothed to remove interannual variability. This smoothing ensures that the time of each ΔT_g sample represents a long term change to this higher global temperature, and not an extreme hot year after which the global temperature recovers. The technique used to smooth the time-series was contingent on the emissions scenario. For each scenario different regression techniques were tested and the type of regression with the best fit to the data (according to the highest value of r^2) was employed, except in the case of SRES A1B for which a 15 year running mean was found to be more appropriate. Where projections from different emission scenarios are directly compared, the smoothing technique is standardised.

For each model, the date at which the regressed time-series crossed 1°C, 2°C, 3°C, 4°C, 5°C, and 6°C of ΔT_g was extracted and defined as the median of a

climatological period, to be used to analyse local temperature and precipitation change. A 15 year period was used in order to eliminate interannual variability, whilst also maintaining a difference between ΔT_g intervals. A longer time period might inhibit comparison between ΔT_g increments, particularly for higher emissions scenarios under which models can experience >1°C or >2°C change in a 30 year period. The reference period was also set to 15 years for consistency.

There are two limitations of time-based samples. First, due to different climate sensitivities, each model reaches a different ΔT_g threshold by 2100 (or by 2350 in A1B); therefore a different number of models are available at 1°C, 2°C, 3°C, etc. Thus when considering an ensemble as a whole, differences between ΔT_g increments may be due to the inclusion of different models, and not exclusively due to the different level of anthropogenic forcing. The results were tested for sensitivity to this issue, by including only those models which reach the highest ΔT_g increment in the ensemble mean at 1°C, 2°C, 3°C, etc.. The findings were unchanged. Another reason that the time-based sampling approach might not be considered optimal is that selecting 15 year periods from a 100+ year run generally leaves many years of the experiment un-analysed. In theory, the remaining years might provide additional information about evolving regional climate signals, and therefore it would be more robust to incorporate all years from the experiment. The second technique for investigating local change as a function of global temperature is based on all models, and all years from the future simulations.

3.2.2 Rate of local change per °C ΔT_g

Local change in temperature or precipitation was linearly regressed against global temperature change using ordinary least squares, and the slope of the regression line used to represent local change per °C $\measuredangle T_g$. Individual datapoints were overlapping 20 year time periods: 2000-2019, 2010-2029, etc. The exact time periods used varied slightly between ensembles due to data availability. The baseline was not included as a data point, i.e. the regression line was not forced to pass through [0, 0]. The results are therefore insensitive to the reference climatology, allowing for direct comparison between datasets with different baselines. The regression slope was computed for each grid-point.

The regression based approach has two main advantages. As noted above, all models and all simulation data are included. In addition, calculating the rate of change facilitates comparison between model ensembles: the projections can be presented using one map showing change per °C, rather than separate maps at 1°C, 2°C, 3°C, etc. However, the technique assumes a linear relationship between global temperature and local climate change, which does not necessarily apply (see section 1.2.2), particularly for precipitation. Scatterplots for individual grid-boxes were examined to provide an initial assessment of the linearity of the relationship between local change and global temperature. This cursory analysis revealed a close fit to the regression line as well as small and evenly distributed residuals, indicative of a strong correlation and a linear relationship respectively. The symmetry of residuals suggested that the parametric t-test on the slope of the regression line would be appropriate, and this was conducted following Wilks (2006). This tests the gradient of the

regression line but also the standard deviation of the residuals: grid-points will be insignificant if there is minimal change in local climate per °C of warming, and/or if there is a large scatter about the regression line. The test therefore gives an indication of the magnitude of the rate of change with warming, but also the strength of the relationship between global temperature and local precipitation.

3.3 Measuring projected changes from each model

3.3.1 The "delta change" approach

The majority of climate projection studies and regional climate change assessments examine projected changes from climate models (Δx), rather than the models' future climatology (x_2):

$$\Delta x = x_2 - x_1$$

where x_1 is a historical reference climatology. This is true of research which directly addresses the change in climatological variables (including all of the studies cited in section 1.2.1), as well as impacts assessment whereby Δx from climate models are added to observed climatologies or time-series (usually at a finer scale) before being used as input for hydrological or impacts models (e.g. Tate et al. 2004; Delire et

al. 2008), in what is known as a "factor of change" (Lafon et al. 2012) or "delta change" approach (Fowler et al. 2007). Using deltas is a basic form of bias correction on the models' mean state. There is no reason to trust modelled changes more than their background conditions, meaning it is still necessary to critically examine the credibility of this output; but it is useful to isolate the response to GHGs or global temperature in each model and to compare models' changes (Δx) independently from variation in their climatologies (x_1). This thesis will focus on local change (Δx) at 1°C, 2°C, 3°C, etc., rather than the future climate (x_2) at each ΔT_g interval.

3.3.2 Absolute and relative precipitation change

When examining precipitation projections it may be advantageous to present change as a ratio (R), proportional to the reference climatology:

$$R = \frac{\Delta x}{x_1}$$

Many projection studies express precipitation change as a percentage (e.g. Hulme et al. 2001; Christensen et al. 2007 [Figure 1.3]; Sylla et al. 2012). In comparison to the anomaly (Δx), the ratio (R) highlights changes in climatologically dry (versus wet) regions. This measure can be useful, due to the greater potential implications of precipitation variations in semi-arid parts of Africa (Dixon et al. 2003; Morton 2007). However, R can also be misleading for very arid regions, where a

negligible absolute change in precipitation can constitute a 100% increase or decrease. For this reason some authors have presented proportional precipitation change with a mask over hyper-arid regions (e.g. Patricola and Cook 2011; Diallo et al. 2012). In this thesis both absolute and relative change are presented where possible. Masks were applied to R for grid-boxes with precipitation <150 mm year^{-1}, although in the final papers these were superseded by masks on areas with a lack of significant change or a lack of agreement between models, which in general concealed hyper-arid regions, further demonstrating that the large proportional changes in hyper-arid regions (e.g. Christensen et al. 2007; Figure 1.3) do not indicate a consistent shift away from present day conditions.

3.3.3 Regional area-averaging

As well as examining gridded changes across the continent, area-averages were used to quantify mean temperature and precipitation change in selected regions. Gridded historical (x_1) and future (x_2) climatologies for the chosen domains were weighted by grid-box area then spatially averaged. The difference between historical (x_{r1}) and future (x_{r2}) regional climatologies was calculated to generate the regional anomaly (Δx_r) as:

$$x_{r1} = \frac{\sum_1^n x_1}{n}$$

$$x_{r2} = \frac{\sum_1^n x_2}{n}$$

$$\Delta x_r = x_{r2} - x_{r2}$$

Proportional change relative to the historical regional climatology was also calculated:

$$R_r = \frac{\Delta_{x_r}}{x_{r1}}.$$

Selecting regions for analysis and delimiting their domains involves non-trivial decisions. Regionalisation is a fundamental practice in climatology, and various techniques have been developed (see Wilks 2006), for example using cluster analysis (e.g. Ward 1963) or principal component analysis (Joliffe 2002), to identify domains which are homogenous with respect to modes of variability or teleconnections. Examples of studies which define sub-regions in Africa include Nicholson & Palao (1993), Indege et al. (2001), Balas et al. (2007), Dezfuli (2010), and Rowell (2013).

In an investigation of projected climate change, it may be constructive to use regions which have consistent seasonal and interannual variability and similar controls: examining a domain with a coherent climate system might facilitate process-

based understanding of projections. However, it is also important to select regions which will best characterise signals from the climate models. Given the large grid-spacing of GCMs, and lack of confidence in model output at the native grid-scale (Masson and Knutti 2011; McSweeney and Jones 2013), the domains might need to be larger than those used to investigate observed data (Giorgi and Francisco 2000). Yet it is also unhelpful to define domains which are so large as to obscure spatial heterogeneity (as highlighted by Shongwe et al. 2011). Many global scale projection studies (e.g. Christensen et al. 2007; Giorgi and Coppola 2011) have used the "Giorgi regions" (Giorgi and Francisco 2000; Giorgi and Bi 2005), and some research into African climate change has been based on very large domains (e.g. Hoerling et al. 2006 for southern Africa), which average together several distinct African climate systems to generate one regional projection, and may therefore be unhelpful. Another consideration is that there may be contrasting signals within a region which has exhibited covariance in observations. In the case of the Sahel, an average over the latitudinal band which experienced a spatially homogenous drought in the twentieth century obscures zonal contrast in future projections, as discussed in section 1.2.1. It might therefore be useful to delimit additional regions on the basis of modelled patterns of change.

In this thesis, the choice of regions was determined by the understanding of large scale, spatially coherent, climate systems in the literature; as well as interest in climate change signals identified from gridded analysis. The domains were delimited loosely based on existing research (in the case of East Africa, Central Africa, southern Africa, and the Sahel: following Todd and Washington 2004; Jenkins et al. 2005; Kay and Washington 2008; Pokam et al. 2011; Shongwe et al. 2011); or defined following

inspection of maps of projected change. The sensitivity of the results to the precise coordinates of each region was tested by varying the boundaries. The domains are described in the relevant chapters.

3.3.4 Significance relative to natural variability

Discriminating between variability and change is an important challenge for research into past and future climate. Many authors highlight the importance of differentiating the climate change signal from noise in presenting model projections (Tebaldi et al. 2011; Power et al. 2012; McSweeney and Jones 2013). To establish whether the models project change which is distinct from natural variability, the difference between historical and future time periods was tested for significance. A non-parametric test was chosen due to the focus on precipitation: the interannual distribution of seasonal precipitation in domains with high rainfall receipt may be close to normal, but this is unlikely to be the case for drier regions and seasons. The Mann Whitney U test was applied, to precipitation change and, for consistency, also to changes in other variables. As difference is tested between 15 year time periods, constituting a small sample, the direct method was applied. For each year in the historical period, the number of years in the future period with a smaller value is counted, and the sum of these counts becomes the U statistic (U_1). This is repeated for the future time period to get U_2, and the smaller of U_1 and U_2 is compared to the critical value.

The test was undertaken on a grid-point by grid-point basis, and for regional area-averages. Other authors have also conducted significance testing of projections at the grid-point scale (Tebaldi et al. 2011; Power et al. 2012). However, McSweeney and Jones (2013) suggest that applying smoothing techniques to the data before significance testing may be more appropriate given the lack of skill in GCMs at the grid-cell scale (Masson and Knutti 2011). They show that the proportion of the globe with detectable change is increased when smoothing is applied. There might therefore be an increase in the area over which significance would be detected if such smoothing were applied to the projections presented here; but this would be at the expense of spatial detail.

This significance test was conducted on 15 year time periods and was therefore predominantly a check on signal relative to interannual variability. Many African regions are also prone to interdecadal rainfall variability (e.g. Tyson et al. 1975; Ward 1998). To establish whether changes were distinct from long term fluctuations, multiple baseline periods were used.

3.4 Combining information from multiple models

As discussed in section 1.3.1, there is no standard approach for presenting information from multiple models. In this thesis several statistical tools were employed to understand the dominant responses from each ensemble. Variation

between models in each dataset was also quantified, and comparisons were made between ensembles.

3.4.1 Identifying dominant responses

Ensemble mean temperature and precipitation change ($\Delta\bar{x}$) was computed for each dataset, and various measures were used to identify regions of intermodel consensus. The investigation of agreement between models focused on precipitation. Many studies of precipitation projections assess model agreement in the direction of change, but there has been a recent emphasis on providing information about magnitude and signal-to-noise (Tebaldi et al. 2011; Kaye et al. 2012; Power et al. 2012; Collins et al. 2013; McSweeney and Jones 2013). One solution is to show areas with intermodel agreement on the direction of change, but to also highlight regions where models agree that there is no significant change; thus distinguishing between a lack of agreement and a lack of signal (McSweeney and Jones 2013). This approach has been applied here: maps of ensemble mean precipitation change have been provided with masks to indicate the percentage of models which show positive change, and the proportion of models with a significant signal according to the Mann Whitney U test (as described in section 3.2). In addition, the ensemble means were tested to establish whether their wetting or drying response is significant relative to variation between models; using a paired test of difference between historical (x_1) and future (x_2) climatologies. Information about direction and magnitude is incorporated in this test, as change in the ensemble mean is only significant if the models agree on the direction of change, and exhibit anomalies which are sufficiently different from zero.

Again, a non-parametric test was used, as the intermodel distribution of precipitation climatologies cannot be assumed to be normal. The Wilcoxon signed-rank test was applied (following Wilks 2006).

3.4.2 Quantifying intermodel variation

The ensemble variance (s^2) was calculated to quantify variation between modelled changes, on a grid-point by grid-point basis, as follows:

$$s^2 = \frac{\sum_1^p (\Delta x - \Delta \bar{x})^2}{p}$$

where p is the number of models. The range of modelled changes was also analysed using regional area-averages: the range, interquartile range, and median were visualised using box and whisker plots (Wilks 2006) for each ensemble.

3.4.3 Comparison between ensembles

In general dominant responses are identified for each ensemble (using the mean, proportion of models with positive or significant change, and Wilcoxon signed rank test), and variation between models is quantified for each dataset (using the variance, and box and whisker plots), and the results are presented together to allow

for comparison between ensembles. The difference between ensembles has not been computed directly or tested for significance. Each dataset has different characteristics: a different number of members, different scenarios, and in some cases different types of models and experiments. All of these factors make quantitative comparison difficult. The exception is the dataset of global and regional models: PRECIS-GCM and PRECIS-RCM, which together contain five pairs of global and regional models. The difference between their projections has been computed. It has not been tested for significance due to the small sample size. Instead the proportion of pairs which agree in the direction of difference between GCM and RCM was calculated.

3.5 Investigating sources of intermodel variation

Deriving modes of variability is a useful first step towards understanding the sources of variation between models. Empirical Orthogonal Function (EOF) analysis was employed to this end. EOF analysis, Principal Component Analysis (PCA), and eigenvector analysis are all similar techniques which have been widely used in climatology to isolate areas which vary together over time (e.g. Lough 1986), and have also been utilised to detect spatial patterns of variability between models (Sanderson et al. 2008a, b; Sexton et al. 2012). These tools are useful for data reduction, potentially enabling the majority of the total variability within a dataset to be represented by a collection of orthogonal variables. They produce EOFs, also known as principal components, eigenvectors, or loadings, which are spatial patterns of variability; and corresponding PC scores, also known as eigenvector scores, which

quantify the amplitude of the EOF in each timestep or model. Each EOF is also assigned an eigenvalue that can be used to calculate the fraction of total variance which it explains (Yarnal 1993). The first EOF extracts a maximum amount of variance from the input data, and the second EOF extracts a maximum from the remaining variance, etc. Usually no more than 10 EOFs are used. For a mathematical treatment of PCA see Joliffe (2002).

Here EOF analysis was computed from covariance matrices of grid-boxes versus ensemble members (similar to Sanderson et al. 2008b) for the large PPE of 280 members (AS-PPE). The resulting EOFs represent the major spatial patterns of intermodel variability across the model ensemble, and the PC scores illustrate the amplitude of the EOF in each ensemble member. There are many decisions to be made in conducting EOF analysis (see Yarnal 1993) and it remains a controversial technique. To ensure that the modes of intermodel variability identified using the EOF analysis were present in the model ensemble, various sensitivity tests were conducted. The computation was repeated with correlation rather than covariance matrices, and both unrotated and rotated EOFs were analysed. The importance of rotation is discussed by Richman (1986). The model versions with high and low PC scores were examined to verify that their anomaly from the ensemble mean matched the spatial pattern of the EOF. The North Test (North et al. 1982) was also applied to establish whether the EOFs were independent and non-degenerate. To apply this test, the sampling error of each eigenvalue ($\delta\lambda$) is computed as follows:

$$\delta\lambda \approx \lambda\left(\sqrt{\frac{2}{N}}\right)$$

where λ is the eigenvalue, and N is the number of simulations. EOFs are considered truncated if $\delta\lambda$ is comparable to the spacing of neighbouring eigenvalues, which can be easily established by plotting the eigenvalues for each EOF with error bars based on $\delta\lambda$ (e.g. Sanderson et al. 2008b).

Having identified modes of intermodel variability, the controls on these modes were investigated using correlation and composite analysis. In the large PPE it is possible to correlate the amplitude of any EOF with the values of a given perturbed parameter across the ensemble. The resulting relationship gives an indication of whether this parameter has any influence on the spatial pattern of variability in question. Sexton et al. (2012) have previously conducted multivariate eigenvector analysis on AS-PPE, and found a correlation between the first eigenvector and the heat convergences which are prescribed for each model (see section 2.1.2), suggesting that it might also be useful to correlate the PC scores with other model characteristics. As with any correlation it is important to interpret the results cautiously: causation cannot be inferred. In this case a significant correlation with one parameter could conceal the influence a second, related, parameter; as some parameter values are correlated across the ensemble (Sexton 2011, *pers. comm.*)

Composite analysis was also employed. Composites are averages of specific conditions, which can be used to find out more about those conditions, through examination of consistency of the data making up the composite, and through comparison between one composite and another contrasting composite (Yarnal 1993). This technique has been widely used in climatology, often to compare wet and dry years (e.g. Hastenrath 2000; Camberlin et al. 2001; Balas et al. 2007). Here composites of models with high and low PC scores for EOFs of interest were created to investigate dynamics associated with these spatial patterns. Composites of models with high and low values for each of the 31 perturbed parameters were also computed (similarly to Clark et al. 2010), and the resulting maps were examined: if the composite map and an EOF have a similar spatial pattern, it might give an indication that the associated parameter has an influence on the EOF.

3.6 Deducing mechanisms for precipitation change

Atmospheric dynamics were investigated in connection with selected regional precipitation responses. Given the diversity of climate systems across the continent (see section 1.2.1) such analysis is regionally contingent, and will be explained in the relevant chapters. However, there are various common elements to the methodology.

The first is the focus on atmospheric circulation. Horizontal moisture fluxes ($q\vec{V}$) are a helpful tool in diagnosing changes in precipitation, given the strong link

between water vapour provision and rainfall generation, and have been used in previous studies to explain seasonal variability (Suzuki 2010; Pokam et al. 2011) and long term change (Shongwe et al. 2009). qV is calculated frequently in this thesis (wind*specific humidity), alongside moisture divergence (following Haltiner and Williams 1980). Changes in vertical motion also exert a strong control on condensation, and ω is a key variable for investigation.

An important technique in unravelling the circulation changes associated with changes in precipitation is composite analysis, as described above. Composites of both dry and wet years and dry and wet models are employed to identify atmospheric dynamics associated with drying versus wetting responses. The size of the composite is somewhat arbitrary. In this case 10 years/models are included in each composite (following Hastenrath 2000). The 10 wettest years/models were averaged and differenced from the 10 driest years/models. The resulting "dry minus wet" maps give an indication of the dynamics associated with drying. The maps for dry and wet composites were also examined to check the symmetry of the composites (as in e.g. Camberlin et al. 2001). This is an important step, because if, for example, the wet years have a larger difference from the mean, the opposite dynamical anomalies might be falsely associated with a drying response. Another important test is whether the difference between the wet and dry composites is robust to variation between years/models. A Mann Whitney-U test was used (as described in section 3.2). A non-parametric test was chosen, as the distribution of precipitation between members of the composite is not necessarily normal.

4 Changes in African temperature and precipitation associated with degrees of global warming

Authorship Declaration

I did all of the analysis and writing for this paper. The rationale, methodology, interpretation of results, and structure of the paper were discussed with R. Washington, who also edited the text.

Changes in African temperature and precipitation associated with degrees of global warming

R. JAMES AND R. WASHINGTON

Climate Research Lab, Oxford University Centre for the Environment, South Parks Road, Oxford OX1 3QY, UK

Climatic Change, **117** (4) 859-872 doi:10.1007/s10584-012-0581-7 2013

Received 30 April 2012; Accepted 27 August 2012; Published online 15 September 2012

Abstract

For almost two decades, politicians have been negotiating temperature limits to which anthropogenic global warming should be restricted, and 2°C has emerged as benchmark for danger. However, there has been a lack of scientific research into the implications of such a change for African climate. This study aims to provide information for mitigation debates; through an examination of temperature and precipitation changes in Africa associated with 1°C, 2°C, 3°C, and 4°C of global warming. Data from Global Climate Models show little significant precipitation change at 1°C, then larger anomalies at 2°C which are strengthened and extended at 3°C and 4°C, including a wet signal in East Africa, and dry signals in Southern Africa, the Guinea Coast, and the west of the Sahel. Some of the models project changes with potential for severe societal implications. Despite the uncertainty attached to these projections, they highlight risks associated with 2°C and beyond. Using these findings as a framework for impact assessment and evaluation, further research has the potential to uncover the implications of global warming for African regions.

4.1 Introduction

Political debates on whether to limit global mean temperature change (ΔT_g) to 1.5°C or 2°C have limited scientific backing in the context of African climate. The majority of climate projection research has presented the impacts of anthropogenic interference in time-slices, for instance 2075-2100 (e.g. Giannini et al. 2008). Using these studies, policy-makers can develop adaptation strategies for specific decades, but cannot determine what level of global warming might be dangerous from a regional perspective. Important questions remain unanswered. Will changes be amplified as ΔT_g increases? Will the rate of change allow for incremental adaptation, or involve non-linear transformations which require early mitigation to avoid? By examining projections at specific levels of ΔT_g, this study will begin to confront these questions.

There is an additional, scientific, justification for taking this approach. In a time-slice, models have consistent greenhouse gas (GHG) concentrations but inconsistent ΔT_g, due to variation in climate sensitivity and feedbacks. GHGs have been shown to influence precipitation directly (Allen and Ingram 2002), but this effect is smaller than their indirect influence via global temperature (Andrews et al. 2010). Comparing models with consistent ΔT_g might develop understanding of the important radiative impact of temperature on precipitation.

Research into climate changes associated with ΔT_g has begun, showing that some changes projected at 2°C would have serious implications (e.g. Kaplan and New 2006), and there are larger shifts at 4°C (e.g. Zelazowski et al. 2011). However, these studies have rarely allowed for thorough assessments of difference between ΔT_g

intervals: either focusing on one level of warming (e.g. May 2008), or assuming change will be linear (e.g. Zelazowski et al. 2011). Furthermore, whilst the importance of vulnerable regions has been highlighted, the implications of ΔT_g have not been investigated for African climate.

Many African regions are prone to large interannual precipitation variability, which has substantial human impacts, in part due to high dependence on rain-fed agriculture, which in many cases is already limited by a lack of precipitation. There have been efforts to investigate how African climate will change in future, including several continent-wide studies (Hulme et al. 2001; Christensen et al. 2007; Giannini et al. 2008). The models project a decrease (increase) in precipitation in much of the subtropics (tropics). Research into specific regions has revealed trends for which there are substantial intermodel agreement, including a wet signal in East Africa (Shongwe et al. 2011), and a dry signal in Southern Africa (Shongwe et al. 2009). The Sahel has a more uncertain future (Biasutti and Giannini 2006), and other regions have received little research attention (Todd and Washington 2004). For all of Africa, there is relative uncertainty in future climate, due to under-researched and complex systems which are poorly understood and inadequately modelled in comparison to the mid-latitudes (Cook and Vizy 2006).

The present study proposes to re-evaluate the implications of climate change for precipitation across the African continent, by isolating changes at specific levels of ΔT_g. The paper will first outline the Global Climate Model (GCM) data employed and the tools for analysis. The results section will present the temperature and precipitation projections at 1°C, 2°C, 3°C and 4°C of ΔT_g. Then the implications

of these results will be discussed, including the lessons for mitigation debates. In the fifth section, potential effects of global warming on precipitation mechanisms will be explored, and conclusions will follow.

4.2 Data and Methods

4.2.1 GCM data

Monthly data were selected from the World Climate Research Programme (WCRP)'s Coupled Model Intercomparison Project phase 3 (CMIP3) multi-model dataset, documented by Meehl et al. (2007b) (Table 2.3). Data were interpolated to 1x1° spatial resolution. The models were run with the 20C3M scenario, which incorporates historical forcings; and two SRES scenarios: A2 and A1B, in which GHGs are increased to 2100. In A1B, some models were run in longer integrations in which GHGs are held at the same concentration from 2100 to 2200 and beyond. One realisation was used for each model in each scenario. The longest integrations available were selected.

Model projections of tropical precipitation are highly uncertain, owing to difficulties in representing convective systems and a lack of detailed observations (Randall et al. 2007). Previous studies have used assessments of model similarity and agreement with observations in model selection and weighting schemes, leading to contrasting conclusions for some regions, including the Sahel (Cook and Vizy 2006; Lau et al. 2006). In this study, data from all available models were employed, and the models were weighted equally in the calculation of the ensemble mean.

4.2.2 Deriving global mean temperature change

Annual ΔT_g time-series were constructed for each model in each scenario. Temperature data were weighted to correct grid-boxes to equal area; and spatially averaged annual global means were calculated. 20c3m data for 1985-99 were then averaged to create a reference climatology, and each year in A2 and A1B was differenced from this baseline (as described in section 3.2). The analysis was also repeated with a 1955-69 start point (see Figure 4.S1, 4.S2).

The ΔT_g time-series were smoothed using 15 year running means. For each model, the date at which the resulting time-series crossed 1°C, 2°C, 3°C, 4°C, and 5°C of ΔT_g was extracted (Table 4.S1) and defined as the median of a 15 year period, to be used to analyse local temperature and precipitation change. The 15 year sample length was designed to eliminate interannual variability. Ensemble mean climatologies were computed for A2 and A1B using the maximum number of models available in both scenarios: 19 at 1°C and 2°C, and 12 at 3°C; as well as the 6 models available at 4°C in A1B (see Table 4.S1). None of the models reached 4°C in time to take a 15 year sample when run in A2. One model reached 5°C in A1B, and projections from this model are provided online (Figure 4.S3, 4.S4), alongside ensemble means using all available models run in A1B.

4.2.3 Measuring local changes associated with ΔT_g

Having acquired samples corresponding to 1°C, 2°C, 3°C, 4°C, and 5°C ΔT_g, the temperature and precipitation anomalies and proportional changes relative to

the climatology were calculated for each available model and the ensemble mean, on a grid-point by grid-point basis (as described in section 3.2). These statistics were computed for the annual mean and 8 seasons, DJF, MAM, JJA, SON, JFM, AMJ, JAS, and OND (denoted by the initial letter of each month); since precipitation seasonality in Africa is regionally specific.

The percentage of models with positive anomalies was calculated on a grid-point by grid-point basis to illustrate model agreement on the direction of change. Statistical significance tests of difference between the baseline and each of the 15 year sample climatologies (at 1°C, 2°C, 3°C, 4°C, and 5°C) were undertaken for each model and the ensemble mean, at a confidence level of 0.95, also on a grid-point by grid-point basis. The Mann-Whitney *U* test was used, as precipitation has a skewed distribution in many arid regions and the test makes no assumptions about distribution. Due to the small sample size (15 years), the direct method was applied. The percentage of models with significant change was computed to identify grid-points where there is agreement on a lack of signal.

4.2.4 Regional area-averaging

Sub-regions were chosen for further analysis (Table 4.S2), and area weighted area-averages of temperature and precipitation climatologies were calculated for each model and the ensemble mean. These were used to compute anomalies and proportional changes, which were tested for significance in the same manner as above except on a regional basis.

4.3 Results

4.3.1 Time of a 1°C, 2°C, 3°C, and 4°C global warming

All of the models project increasing global temperatures in both A2 and A1B (Figure 4.1). For the same GHG scenario, different models show different rates of warming, leading to variation in year at which the models exceed specific ΔT_g thresholds (Table 4.S1). For example, the timing of a 2°C warming has a range of 2056-2083 in A2 and 2040-2116 in A1B.

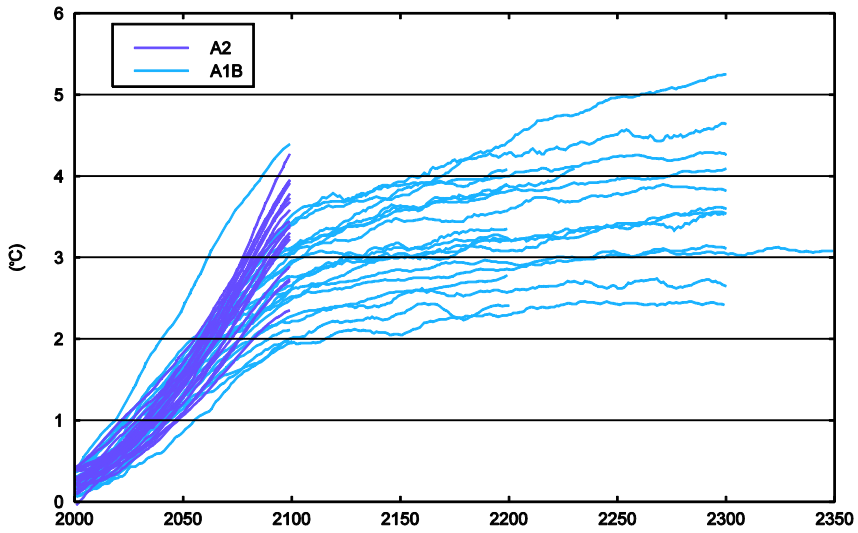

Figure 4.1 Global annual mean temperature anomalies (°C) relative to 1985-99 in 19 models run in A2, and 24 models run in A1B.

4.3.2 African temperature change

African temperatures are projected to rise with ΔT_g. Most of the continent warms more than the global average. The ensemble mean annual mean temperature change for Africa is 1.1°C at 1°C, 2.3°C at 2°C, 3.4°C at 3°C, and 4.3°C and 4°C in A1B, an approximately linear increase which is similar for A2. The highest anomalies are found in arid subtropical regions, particularly surrounding the Angolan and Saharan heat lows. Figure 4.2 shows how this varies seasonally. Other seasons, JFM, AMJ, JAS, and OND (not shown) are similar to DJF, MAM, JJA, and SON, respectively. The most pronounced warming occurs in JJA, when the ensemble mean for Africa in A2 (A1B) is 3.6°C (3.5°C) at 3°C ΔT_g, compared to 3.2°C (3.1°C) in DJF. This is particularly anomalous in the northern hemisphere subtropics: in JJA there is an increase of 5.3°C averaged 20-30°N at 4°C ΔT_g in A1B. These spatial and seasonal patterns are qualitatively consistent between A2 and A1B, and from model to model.

Figure 4.2 Ensemble mean seasonal temperature anomalies associated with global warming, in A2 (first 3 columns), and A1B (last 4 columns). ➢

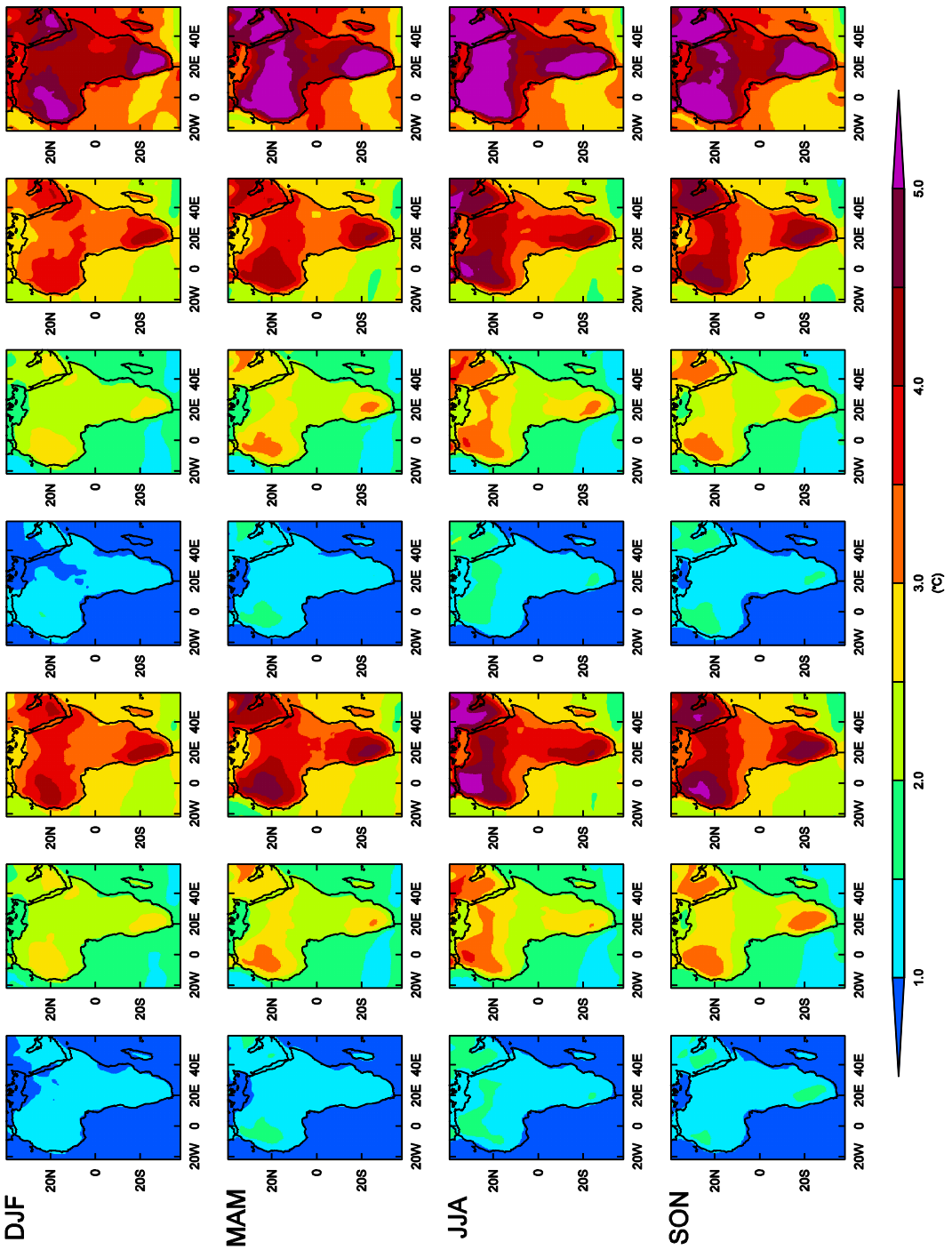
1°C
2°C
3°C
1°C
2°C
3°C
4°C
DJF
MAM
JJA
SON
20N
0
20S
20W 0 20E 40E
1.0
2.0
3.0
4.0
5.0
(°C)

4.3.3 African precipitation change

The precipitation projections exhibit more spatial, seasonal, and intermodel variability than projections for temperature, and there are some distinctions between A2 and A1B. The differences between 1°C, 2°C, 3°C, and 4°C are also more complex (Figure 4.3, 4.4). At 1°C there is model agreement for a lack of significance across much of the continent (shown in grey). At 2°C many more regions exhibit statistically significant anomalies, in some cases with model agreement on the direction of change. The progression from 2°C to 3°C is matched mainly in the magnitude of these regional changes. The models which reach 4°C in A1B show a further strengthening and extension of precipitation changes, with some new anomalies; although this is in part due to a different number of models being averaged (Figure 4.S5 and 4.S6 show the mean of these models at 1°C-3°C).

Figure 4.3 Ensemble mean seasonal precipitation anomalies (mm day^{-1}) associated with global warming, in A2 (first 3 columns) and A1B (last 4 columns). Grid-points where <66% of models agree on the direction of change are masked in white, and grid-points where >80% of models show no significant change are shown in grey. Stippling shows grid-points where >80% of models agree on the direction of change. ➢

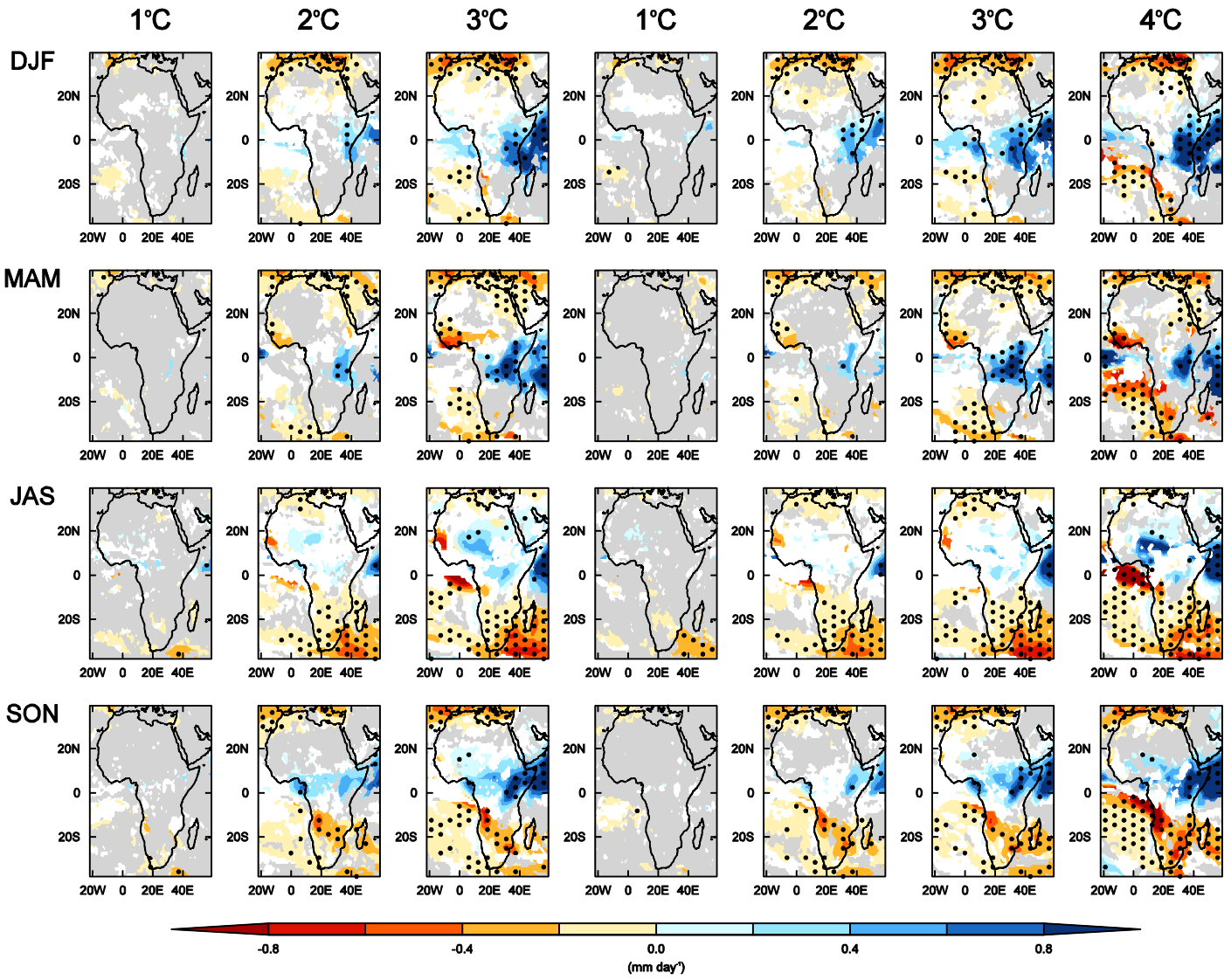
1°C
2°C
3°C
1°C
2°C
3°C
4°C
DJF
MAM
JAS
SON
20N
0
20S
20W 0 20E 40E
-0.8
-0.4
0.0
0.4
0.8
(mm day⁻¹)

Some regions experience consistent precipitation change in all seasons, for example the Mediterranean where there is strong drying from 2°C. In most other regions there is marked seasonal variation. In DJF the most prominent signal is moistening in East Africa. This constitutes a large proportional change in South Sudan, Ethiopia, and Somalia, where DJF is mostly a dry season, and a smaller ratio further south where the anomalies extend towards the climatological maximum (Figure 4.S7). In MAM, there is also an increase in precipitation in East Africa. This is orientated further south than during DJF in most models, and at 3°C extends into central Africa to the south of the equator. The opposite trend is shown at the Guinea Coast during this season: on average a 10% (5%) decrease at 3°C in the A2 (A1B) ensemble mean.

In JAS projections for much of tropical and North Africa are characterised by a lack of agreement between models, particularly at 2°C (as shown by the large areas in white in Figure 4.3 and 4.4). Some individual models produce contrasting futures, for example GFDL-CM2.0 experiences large amplitude drying throughout west Africa from 2°C, and ECHO-G projects extensive moistening from 3°C (not shown). Many other models and the ensemble means share a dry signal in west Sahel and a wet signal further east, although this has more model agreement in A2 than A1B. The sensitivity of this trend to the choice of baseline was tested, due to the prevalence of interdecadal variability in this region. Changes relative to 1955-69 also show a dry west and wet central Sahel, in both scenarios (Figure 4.S1, 4.S2).

Figure 4.4 as Figure 4.3 but for proportional change relative to 1985-99 (%). ➢

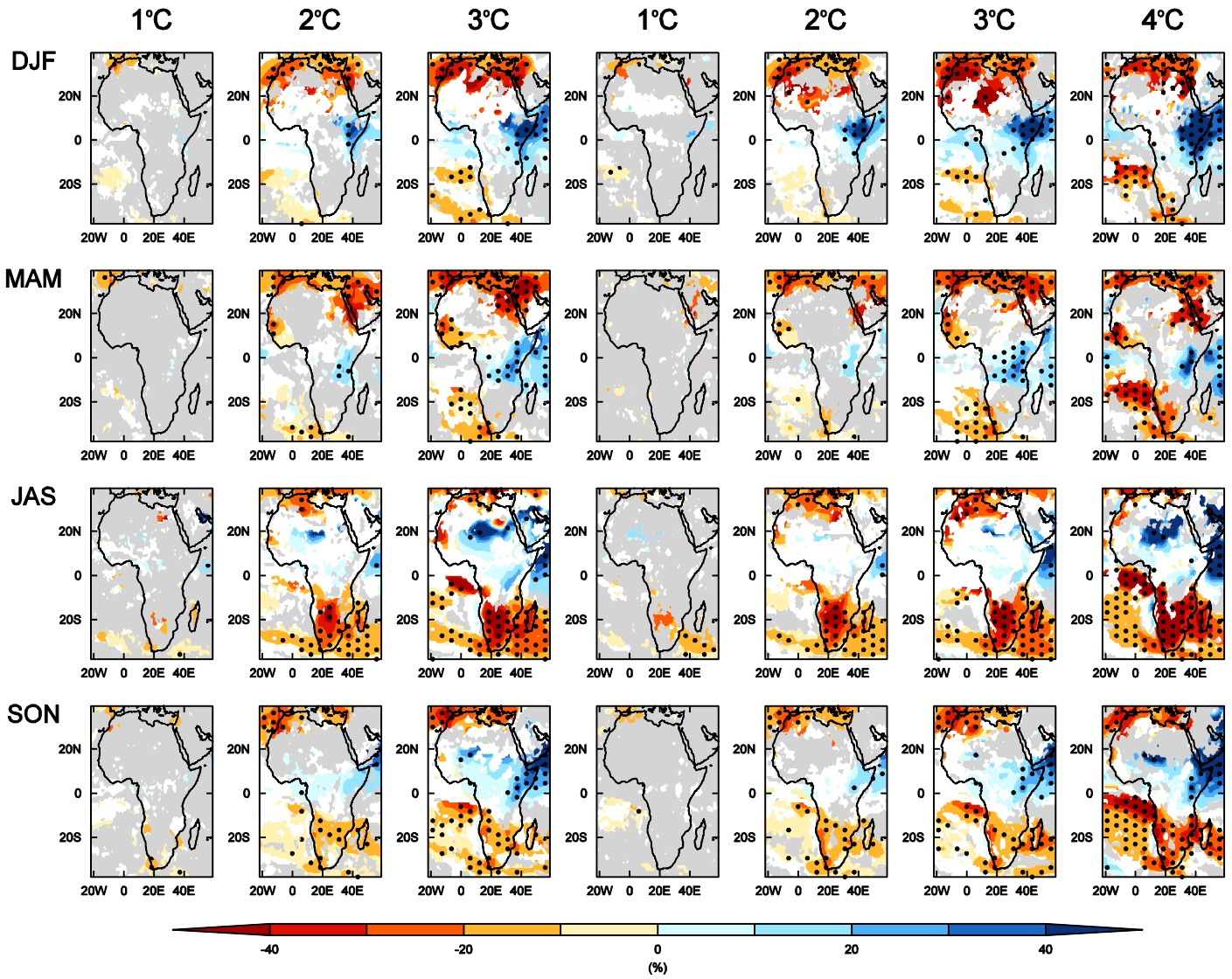
1°C
2°C
3°C
1°C
2°C
3°C
4°C
DJF
MAM
JAS
SON
20N
0
20S
20W 0 20E 40E
-40
-20
0
20
40
(%)

In southern Africa, over 80% of models show a dry signal for South Africa, Botswana, Zimbabwe, and Madagascar by 2°C during JAS. Relative to the low climatological precipitation this is a large proportional change (25% (24%) in the regionally averaged ensemble mean by 3°C in A2 (A1B)), but anomalies are relatively small (-0.2mm day^{-1} in A2 and A1B). Projections for JJA are similar to JAS (not shown), and the dry signal in southern Africa continues into SON, when anomalies are largest over Angola. In some models the negative changes extend towards the equator, into the south of the Congo basin. The north of the convective zone mainly shows the opposite trend in this season: an increase in precipitation, which forms an approximately zonal band around 0-5°N at 2°C in A2 and 3°C in A1B. As in DJF and MAM, the wet signal is much more pronounced over east Africa than central Africa, particularly at 3°C and 4°C.

4.4 Implications of Projected Changes

Climate change is widely recognised as one of the prime challenges facing Africa, and the continent is often cited as the hardest hit by potential transformations (Boko et al. 2007). Scientific rigour underpinning climate assessments does not match the strength of such claims, most notably in connection with what might be considered dangerous levels of warming. Whereas almost all projection work focuses on time-slices in the 21st century, mitigation debates are geared around degrees of global change for which there is a dearth of corresponding information in the case of African climate.

The projected changes in global temperature over time (Figure 4.1) illustrate that approaches based on time-slices conflate and therefore conceal differences between temperature intervals. As has been previously illustrated by Joshi et al (2011), there are a range of years at which the models reach 2°C and other ΔT_g intervals. Equally, for the same level of GHG forcing, models project different ΔT_g, due to variation in feedbacks (Bony et al. 2006), and forcings (Kiehl 2007). The time-averaged ΔT_g for 2085-99 ranges from 2.3-3.9°C in A2 and 1.8-4.2°C in A1B, so precipitation changes averaged across this time-slice give little information about the impact of 2°C or 3°C or 4°C. As a result, a time-slice approach is at odds with and inappropriate for mitigation debates as they are currently posed.

The analysis employed here, of climate change in Africa as a function of degrees of warming, can deliver more evidence about the implications of ΔT_g. Note that the changes identified are relative to 1985-99, whereas policy documents refer to temperature increase above preindustrial levels. Projections using an alternative baseline chosen to represent a period prior to the detection of anthropogenic influence (1955-69) have similar patterns but a slightly larger magnitude at 1°C (Figure 4.S1, 4.S2). The results presented here (for 1985-99) can therefore be considered a conservative estimate of changes associated with anthropogenic warming. These results reveal a heterogeneous spatial structure of associated climate responses. Moreover, where the same magnitude of precipitation response occurs in different regions, it is likely to have quite different consequences. The implications thus need to be assessed separately for each region.

In East Africa, OND precipitation is projected to increase by 3% (3%) at 1°C, 7% (8%) at 2°C, and 14% (13%) at 3°C in the A2 (A1B) ensemble mean (Table 4.1). In the 20th century, anomalously wet seasons have been associated with higher agricultural yields, but also flooding. For example, high precipitation October 1997 to January 1998 caused floods which led to loss of life, damage to infrastructure, and an outbreak of Rift Valley Fever (Conway et al. 2005). This was associated with a 40% precipitation increase in OND relative to 1985-99 (in NCEP-NCAR reanalysis, not shown). Ensemble mean changes projected are much smaller, even at 4°C (16%), but these are for 15 year climatologies, which preclude interannual variability. In a study of future East African precipitation, Shongwe et al. (2011) found an 8-21% shift in the mean was associated with an increase in the intensity of 10 year wettest seasons, suggesting that the mean change at 2°C, 3°C or 4°C might be accompanied by wetter extremes. Furthermore, high rainfall events are expected to intensify in general in response to global warming (Christensen et al. 2007). Some individual models show substantial changes in the 15 year mean. The model with the largest wet signal, MIROC3.2(medres) shows a 43% (62%) increase at 3°C in A2 (A1B) and a 68% increase at 4°C (Figure 4.5). If this model's 3°C or 4°C scenario were realised the region would have more precipitation in an average short rains season than in the extreme 1997 season.

In Southern Africa, the largest proportional changes are in JAS, when there is a decrease in the ensemble mean of 19% at 2°C, and 31% at 4°C (Table 4.1). However, this is a very dry season for this region, and most models overestimate precipitation in the Southern Hemisphere mid-latitude storm tracks during this season

(Neelin et al. 2006), meaning this trend should be interpreted cautiously without further work into the associated dynamics and impacts. A dry signal is also projected for southern Africa during SON, when the ensemble mean shows a 17mm (21mm) or 10% (12%) reduction by 2°C in A2 (A1B). In individual models this change is as high as 24% for 2°C and 33% for 3°C (GFDL-CM2.0 in A2). This suggests a delay in onset of the precipitation season (Shongwe et al. 2009) with possible implications for agriculture, such as a decrease in the growing season for maize. Little significant change is projected for the summer precipitation season itself in most models. However, Kay and Washington (2008) find more extreme wet and dry summers in HadCM3, a model which shows no significant change in the JFM mean at 2°C or 3°C (not shown). It is therefore difficult to decipher the implications from mean precipitation alone, particularly for JFM.

The multi-decadal Sahel drought in the 1970s-80s had particularly large social implications. Projections for the Sahel show little model agreement when zonally averaged, but there is some consensus for a drying at the west coast in JAS. Several previous studies have revealed this signal (e.g. Christensen et al. 2007), but it has only recently been highlighted (Fontaine et al. 2011). In the ensemble mean, the change is much smaller than the 40% reduction in rainfall associated with the 20th century drought (Held et al. 2005): at 12% (8%) for a 3°C warming in A2 (A1B). However, three models show more than 20% drying at 3°C (in A2 and A1B). Such changes might have serious ramifications for food security, especially given the reliance of local economic systems on rainfed agriculture (Biasutti et al. 2009).

Table 4.1 Area-averaged precipitation change for A2 and A1B, for selected regions and seasons. The values given for the anomaly (mm season^{-1}) and proportional change relative to 1985-99 (%) refer to the ensemble mean. Significant changes are highlighted in grey. Model agreement refers to the number of models which show the same direction of change as the ensemble mean, with the number of significant models to show the same direction of change in brackets.

		Anomaly (mm season^{-1})							Proportional Change (%)							Model Agreement						
		A2			A1B				A2			A1B				A2			A1B			
Region	**Season**	**1°C**	**2°C**	**3°C**	**1°C**	**2°C**	**3°C**	**4°C**	**1°C**	**2°C**	**3°C**	**1°C**	**2°C**	**3°C**	**4°C**	**1°C**	**2°C**	**3°C**	**1°C**	**2°C**	**3°C**	**4°C**
Angola	SON	-14	-25	-33	-11	-28	-32	-59	-6	-10	-15	-5	-12	-14	-24	12(4)	14(6)	10(7)	11(3)	17(7)	10(7)	6(7)
Central African Republic	MAM	8	10	30	-1	16	39	15	2	2	6	0	3	8	3	15(0)	14(3)	9(4)	8(0)	15(14)	11(10)	5(10)
Central African Republic	SON	1	6	9	2	-2	11	2	0	1	2	0	0	2	0	9(2)	12(3)	5(5)	11(14)	8(3)	6(9)	2(9)
Congo Basin	MAM	1	2	-3	-1	7	8	-3	0	0	-1	0	2	2	-1	10(0)	10(3)	6(2)	9(0)	12(15)	7(10)	3(1)
Congo Basin	SON	6	20	27	6	8	29	28	1	4	6	1	2	6	5	13(0)	15(7)	9(8)	13(14)	13(15)	9(10)	4(10)
East Africa	DJF	14	27	50	15	37	55	82	4	7	13	4	10	15	24	13(3)	15(7)	11(9)	13(15)	15(15)	11(12)	6(12)
East Africa	MAM	15	34	56	14	28	56	52	4	10	17	4	8	17	17	13(3)	16(9)	10(9)	14(14)	14(17)	11(11)	5(11)
East Africa	OND	13	28	56	12	31	50	63	3	7	14	3	8	13	16	12(2)	18(8)	11(9)	13(15)	17(16)	11(11)	5(11)
Guinea Coast	MAM	-11	-15	-36	-8	-17	-20	-43	-3	-4	-10	-2	-4	-5	-11	12(2)	16(4)	10(7)	14(0)	13(5)	9(5)	6(5)
Mediterranean	Annual	-5	-9	-12	-5	-10	-13	-14	-12	-21	-28	-12	-23	-31	-26	18(7)	18(15)	11(9)	18(6)	18(15)	12(10)	6(10)
Mozambique	SON	-10	-18	-21	-9	-18	-23	-30	-7	-12	-15	-6	-12	-17	-24	14(4)	17(8)	10(5)	13(3)	17(9)	12(4)	6(4)
Sahel	JAS	2	2	4	9	-2	3	21	1	1	1	3	-1	1	7	13(1)	14(4)	7(4)	14(14)	11(4)	7(8)	3(8)
West Sahel	JAS	-4	-16	-36	2	-12	-26	-23	-1	-5	-12	1	-4	-8	-7	9(4)	13(3)	8(5)	9(14)	13(5)	8(6)	4(6)
Central Sahel	JAS	6	16	35	13	7	25	54	3	6	14	5	3	10	19	13(3)	14(6)	9(5)	15(15)	12(14)	8(9)	4(9)
Southern Africa	JAS	-6	-12	-15	-7	-12	-14	-18	-9	-19	-25	-11	-19	-24	-31	15(6)	19(9)	12(8)	16(6)	18(13)	12(10)	6(10)
Southern Africa	SON	-11	-17	-21	-9	-21	-21	-34	-6	-10	-13	-5	-12	-13	-21	16(0)	16(8)	10(8)	14(1)	19(9)	11(6)	6(6)

The projections generally indicate that there will be greater consequences at higher degrees of warming. Some models project very large changes at 2°C, 3°C, and 4°C. These outliers cannot be rejected by default, as previous studies have shown that some reproduce observations well, for example GFDL-CM2.0 shows a large dry signal for the Sahel and also has one of the best 20th century hindcasts (Held et al. 2005).

Mapping regional climate change as a function of ΔT_g is a necessary but not sufficient step if dangerous climate change is to be assessed. An obvious next step is to consider the impacts of the associated climate on health, agriculture and water. This requires attention to measures of precipitation change which are most relevant to each sector. For example rainfed agriculture in Southern Africa is dependent on the onset, length, and dry spells within the growing season (Mupangwa et al. 2011). Research on the mechanisms behind precipitation responses would also be useful in diagnosing the effect on the climate system: does African climate shift into a new state at 2°C or 4°C? A thorough investigation of atmospheric processes is left for later work, but changes in mechanisms inferred from precipitation trends will be explored in the next section.

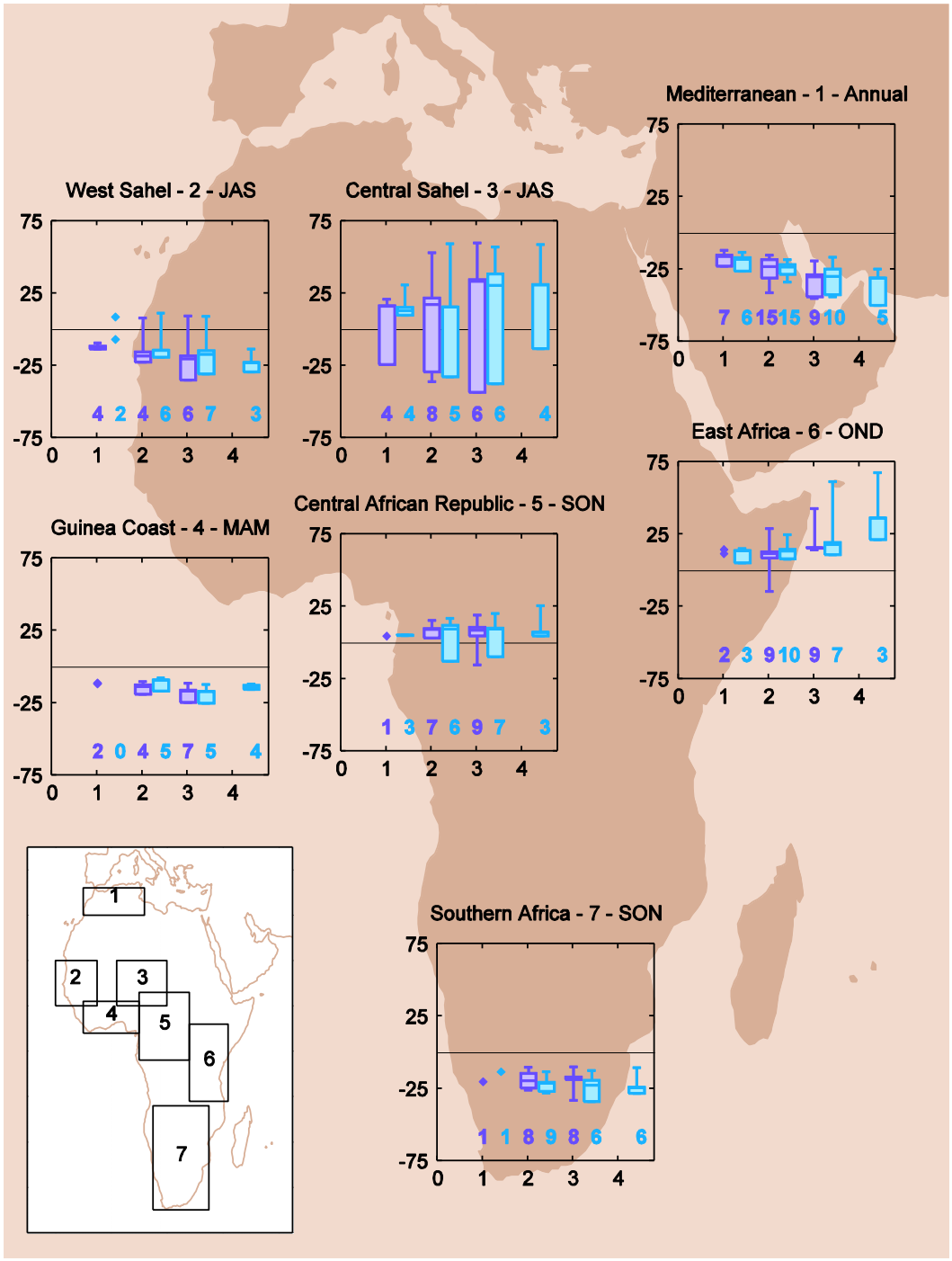

Figure 4.5 Proportional precipitation change relative to 1985-1999 (%) associated with global warming, for selected regions and seasons, in A2 (purple) and A1B (blue). Only models with significant change are included, the number of which is indicated below each boxplot. Where fewer than 3 models show significant change, boxplots are replaced with points to represent each individual model.

4.5 Potential Changes in Precipitation Mechanisms

On a large scale, the model projections suggest an evolution towards wetter tropical regions and dryer subtropical regions, in agreement with previous research for Africa (e.g. Giannini et al. 2008) and the global tropics (e.g. Allan et al. 2010). Robust trends in keeping with this include dry signals in many parts of the Mediterranean from 1°C ΔT_g. This is consistent with the "rich-get-richer mechanism", whereby moisture increases associated with higher tropospheric temperatures reduce gross moist stability, enhancing convection and precipitation in convective regions, whilst stability increases in subsidence regions (e.g. Chou and Neelin 2004). This tendency is helpful in explaining why temperature projections, in this study as in previous research (Figure 4.2 and Christensen et al. 2007), show greater change in the subtropics, as positive tropical rainfall anomalies might dampen surface temperature increases through cloud cover and/or soil moisture feedbacks. This has the potential to decouple local temperature from ΔT_g.

If this "rich get richer" response were the only impact of global warming, the pattern of precipitation anomalies could be expected to match the observed 20th century climatology (Figure 4.S7), with the amplitude of anomalies gradually increasing from 1°C to 4°C, but with those anomalies spatially anchored in the regions of current rainfall receipt. Figure 4.3 and 4.4 illustrate that this is not the case. This could be partly because the modelled climatologies contain biases, which might produce "wet-get-wetter" (and "dry-get-drier") responses in regions which are not wet (or dry) in the observed climatology. This would seem to be the case in the west

of the Sahel, where many models show a dry bias and also a dry signal associated with global warming. However, this is not the case for the other robust changes identified, for example East Africa has a dry bias but a wet signal associated with warming in MAM. Furthermore, we should not expect all changes to be governed by the "rich-get-richer" mechanism, as previous literature has demonstrated many other thermodynamic and dynamic influences on precipitation which can result from anthropogenic forcing (e.g. Held and Soden 2006; Chou et al. 2009). The interaction and relative importance of such mechanisms must be diagnosed on a case by case basis.

Central Africa, the core convective region, might be expected to see the greatest precipitation enhancement due to the "rich get richer" mechanism, however projected changes here are small, particularly in comparison to East Africa. Shongwe et al. (2011) suggest that the strong wetting of East Africa in OND is associated with changes in the Indian Ocean Dipole, which alter the Walker circulation, weakening subsidence over the western Indian Ocean. At the same time, most models show a decrease in ascent over Central Africa. Vecchi and Soden (2007) show annual mean upward (downward) anomalies in vertical velocity over East (Central and West) Africa, associated with a widespread weakening of tropical circulation.

The potential delay in the rainfall season in Southern Africa during austral spring also deserves further attention, particularly as other studies have found evidence for delayed precipitation seasons in observations for many parts of Africa (Kniveton et al. 2009), and in projections for West Africa (e.g. Biasutti and Sobel 2009). This delay is not visible in the projections for the Sahel presented in Figure 4.3

due to the seasonal timescale, but monthly projections for many CMIP3 models reveal that the enhancement of precip in central Sahel witnessed here occurs at the end of the rainfall season (Monerie et al. 2012b).

There are various potential mechanisms to explain why delayed tropical precipitation seasons might be a general phenomenon induces by global warming. Chou et al. (2007) suggest that longer dry seasons might be expected as part of the "rich get richer" mechanism. Seth et al. (2011) find a decrease in spring convection in many monsoon regions, including West and Southern Africa, due to increased stability and reduced surface moisture resulting from a more intense dry season. In contrast, Biasutti and Sobel (2009) ascribe the projected late onset of the West African Monsoon (WAM) to a delay in the seasonal cycle of SSTs. Under normal conditions, the maximum northern hemisphere SSTs occur in August, but with global warming models show a later peak in temperature, likely due to northern hemisphere sea ice loss. As well as influencing the WAM, this could be responsible for a large scale shift in the annual cycle of precipitation globally. This would not only explain drying in Southern Africa during SON, but also negative anomalies at the Guinea Coast in MAM from 2°C. Both of these changes occur at the leading edge of tropical convection, suggesting a delay in its migration. This hypothesis is further supported by the fact that the projected tropical precipitation enhancement in SON is further north than in MAM despite the symmetry of these transition seasons in the modelled climatology (Figure 4.S7) and in observations (Waliser and Gautier 1993).

A delay in the annual cycle of tropical convection would constitute a major modification of the atmospheric circulation, and the apparent link to sea ice opens up

the possibility of nonlinearity, as accelerated sea ice loss is projected for the Arctic (Meehl et al. 2007a). It is unclear whether the models have the ability to adequately represent such teleconnections. GCMs simulate 20th century precipitation well when forced with observed SSTs, but do not always capture interannual SST variability (e.g. Hoerling et al. 2006). Biasutti and Sobel (2009) show that there is little variation between models in the projected change in the global annual cycle of SSTs, but more research is needed to assess the plausibility of this mechanism, particularly given the potential implications of such a change at 2°C of global warming.

4.6 Summary and Conclusions

GCM data have been employed to investigate temperature and precipitation changes associated with 1°C, 2°C, 3°C, and 4°C of global warming in Africa. Temperatures are projected to rise more than the global average, particularly in arid regions. Precipitation projections show more variation between models in the amplitude and direction of change, but in all models precipitation changes are enhanced as global temperature increases, and the degree of response is regionally specific. At 1°C no significant change is projected for most parts of Africa, except for a dry signal in the Mediterranean, and a wet signal in East Africa in many models. At 2°C these trends are strengthened, and many other regions experience robust changes, including Southern Africa and the Guinea Coast which show dry signals in SON and MAM respectively. In the Sahel there is a drying at the west coast. At 3°C and 4°C these anomalies are strengthened and extended. The projected changes imply a delay

in precipitation seasons at 2°C and beyond, possibly associated with changing SSTs and sea ice loss. This would constitute a major shift in teleconnections, which warrants further investigation.

The magnitude of change projected by some models at 2°C, 3°C, and 4°C would likely have large societal implications, including for East Africa and the Sahel. Despite the uncertainty attached to the projections, they suggest that there are risks associated with these levels of global warming. More research is needed to investigate extremes, variability, and impacts associated with the mean precipitation projections presented here as well as the different climate sensitivities of the models. This study provides a framework for such analysis.

Acknowledgements

The authors would like to thank Gil Lizcano for technical support, and acknowledge the modelling groups, the Program for Climate Model Diagnosis and Intercomparison, and the WCRP's Working Group on Coupled Modelling for their roles in making available the CMIP3 multi-model dataset. Support of this dataset is provided by the Office of Science, U.S. Department of Energy.

Supplementary Information: Chapter 4

Table 4.S1 Medians of 15 year periods selected for climatologies, to represent ΔT_g increases relative to 1985-99, for A2 and A1B. Samples which were included in the ensemble means in the paper are highlighted in grey.

Model[a]	A2			A1B				
	1°C	2°C	3°C	1°C	2°C	3°C	4°C	5°C
BCCR-BCM2.0	2043	2070	2091	2042	2068			
CGCM3.1 (T47)	2036	2066	2089	2035	2077	2238		
CGCM3.1 (T63)				2026	2056	2093	2273	
CNRM-CM3	2037	2062	2082	2032	2065	2138		
CSIRO-Mk3.0	2047	2076		2055	2099			
CSIRO-Mk3.5	2032	2061	2083	2030	2062	2094	2169	2261
GFDL-CM2.0	2034	2063	2086	2033	2063	2105		
GFDL-CM2.1	2039	2070		2035	2068	2142		
GISS-AOM				2044				
GISS-EH				2041	2090			
GISS-ER	2038	2072		2037	2082			
FGOALS-g1.0				2038	2070	2129		
INGV-SXG	2035	2067	2092	2034	2067			
INM-CM3.0	2027	2058	2084	2022	2060	2123		
IPSL-CM4	2033	2061	2081	2029	2059	2088		
MIROC3.2(hires)				2019	2040	2062	2087	
MIROC3.2(medres)	2029	2059	2080	2027	2057	2086	2198	
ECHO-G	2038	2065	2089	2036	2064	2104		
ECHAM5/MPI-OM	2042	2065	2083	2038	2061	2086	2155	
MRI-CGCM2.3.2a	2047	2076		2041	2082			
CCSM3	2022	2056	2079	2023	2054	2221		
PCM	2048	2083		2042	2116			
UKMO-HadCM3	2037	2063	2085	2034	2063	2098		
UKMO-HadGEM1	2032	2058	2078	2033	2059	2085	2191	

[a]Naming conventions are taken from the IPCC www-pcmdi.llnl.gov/ipcc/model_documentation/ipcc_model_documentation.php

Table 4.S2 Co-ordinates of the domains selected for regional analysis.

Region	Co-ordinates	Season(s)
Angola	12-22°E; 6.5-19.5°S	SON
Central African Republic	10-28°E; 1.5°S-12.5°N	MAM; SON
Congo Basin	15-28°E; 9.5°S-4.5°N	MAM; SON
East Africa	28-42°E; 10.5°S-5.5°N	DJF; MAM; OND
Guinea Coast	10°W-10°E; 4.5°N-10.5°N	MAM
Mediterranean	10°W-12°E; 30.5-35.5°N	Annual
Mozambique	28-55°S; 12.5-26.5°S	SON
Sahel	18°W-20°E; 10.5-19.5°N	JAS
West Sahel	20°W-5°W; 10.5-19.5°N	JAS
Central Sahel	2-20°E; 10.5-19.5°N	JAS
Southern Africa	15-35°E; 12.5°S-34.5°S	JFM; JAS; SON

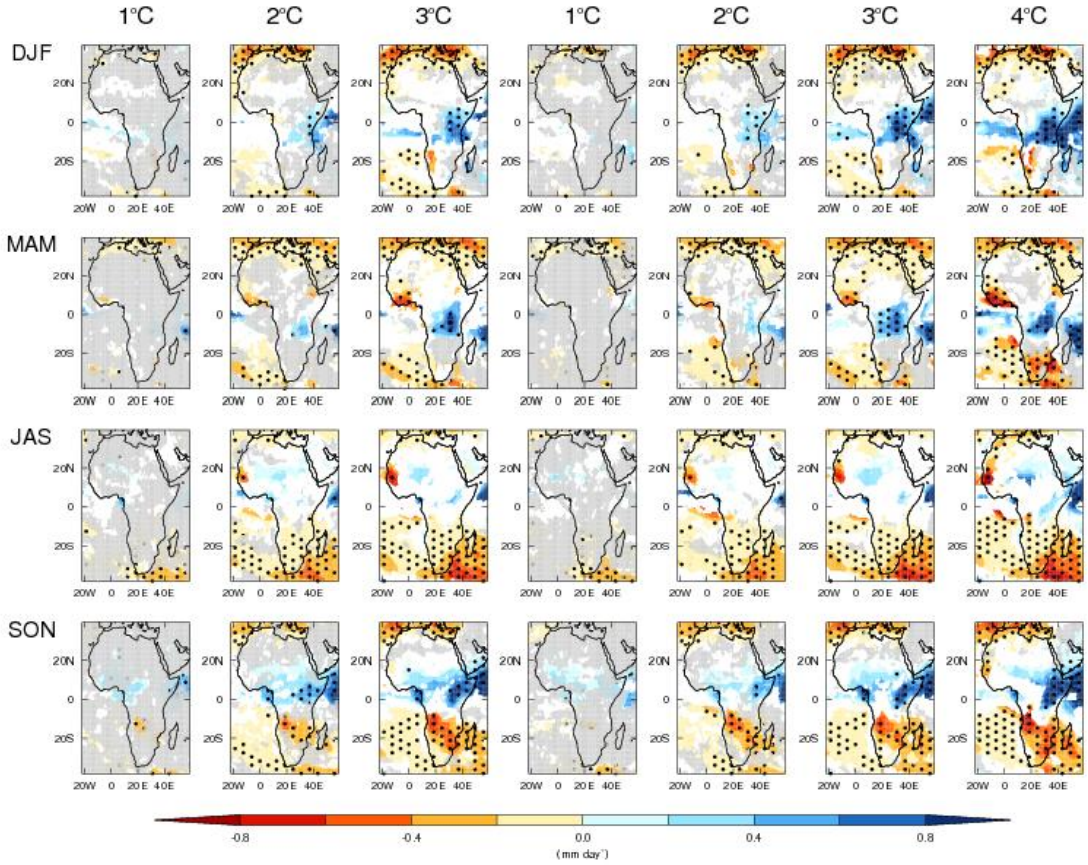

Figure 4.S1 as Figure 4.3 but for 5569 baseline. Ensemble mean seasonal precipitation anomalies (mm day^{-1}) associated with global warming, in A2 (first 3 columns) and A1B (last 4 columns). Gridboxes where <66% of models agree on the direction of change are masked in white, and gridboxes where >80% of models show no significant change are shown in grey. Stippling shows grid-points where >80% of models agree on the direction of change. From 1-3°C only models which are available in both ensembles are included in the ensemble mean. At 4°C all models available in A1B (9) are included in the mean.

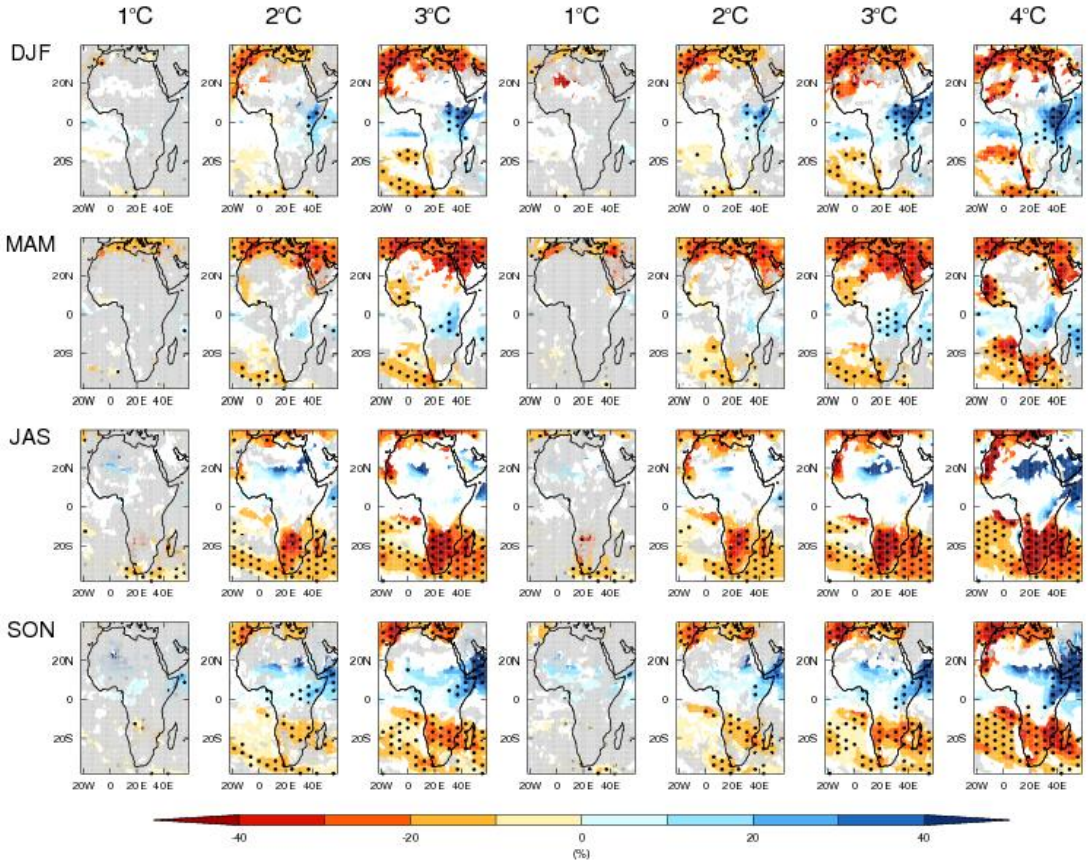

Figure 4.S2 as Figure 4.S1 but for proportional change (%) relative to 1955-69.

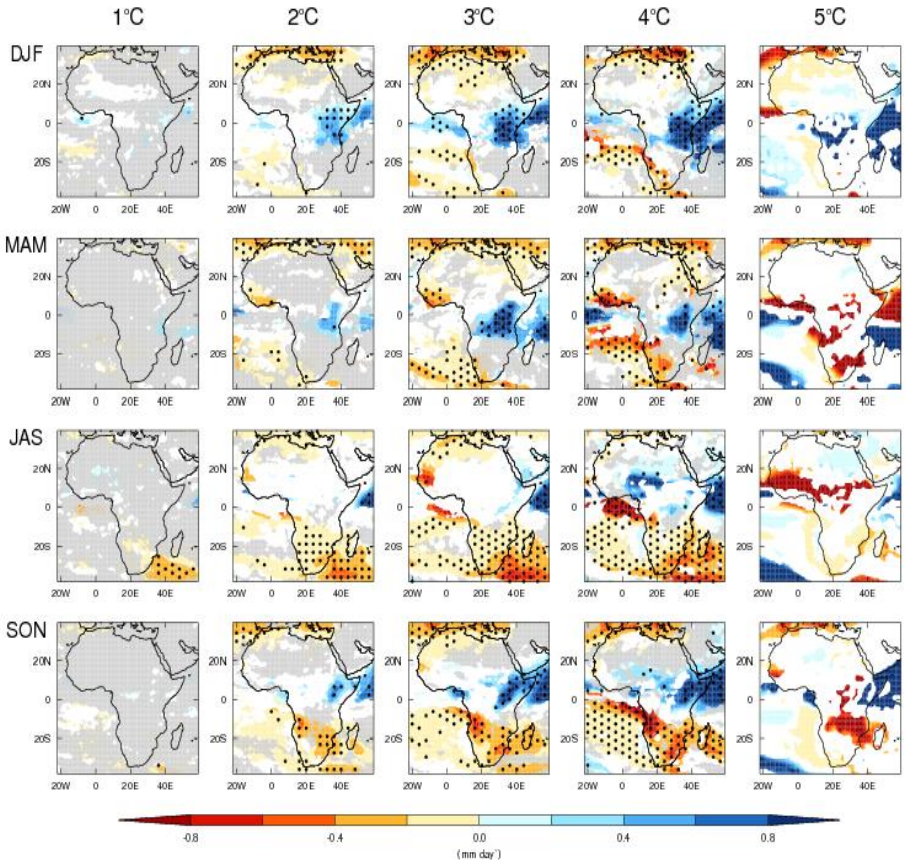

Figure 4.S3 Ensemble mean seasonal precipitation anomalies (mm day^{-1}) associated with global warming for all available models in A1B (24 at 1°C, 23 at 2°C, 16 at 3°C, 6 at 4°C, 1 at 5°C). Grid-points where <66% of models agree on the direction of change are masked in white, and grid-points where >80% of models show no significant change are shown in grey. Stippling shows grid-points where >80% of models agree on the direction of change. These masks are not applied at the 5°C level where only one model is used. In this case insignificant change has been masked in white.

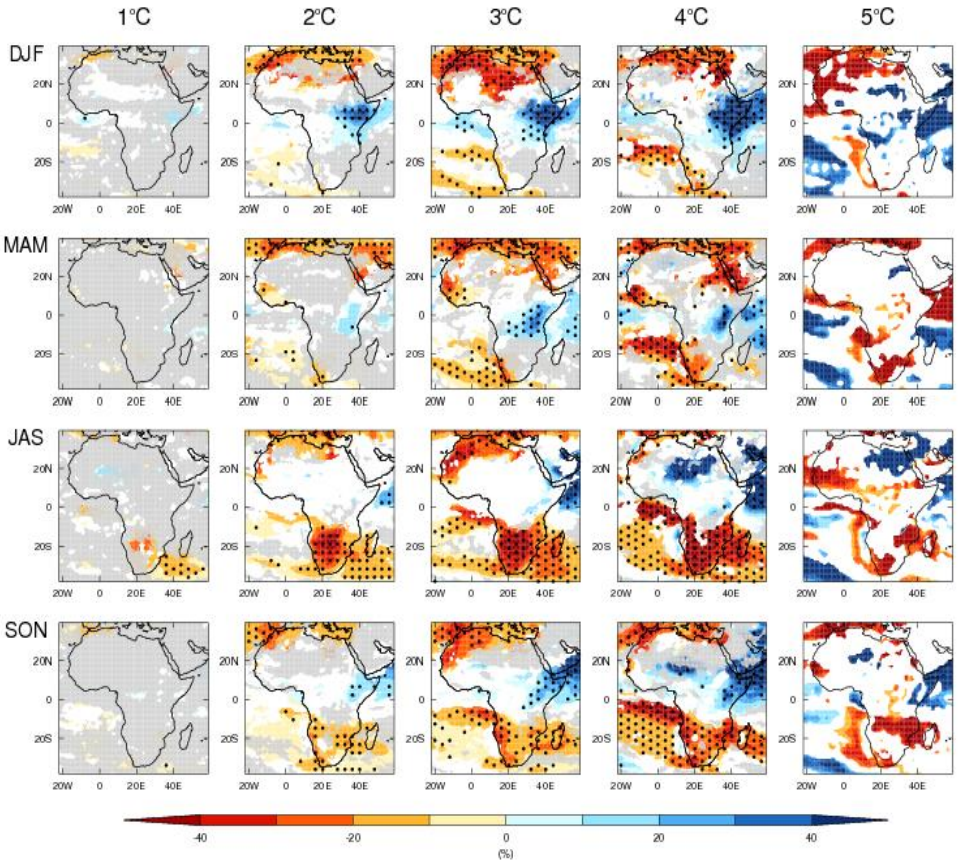

Figure 4.S4 as Figure 4.S3 but for proportional change (%) relative to 1985-99.

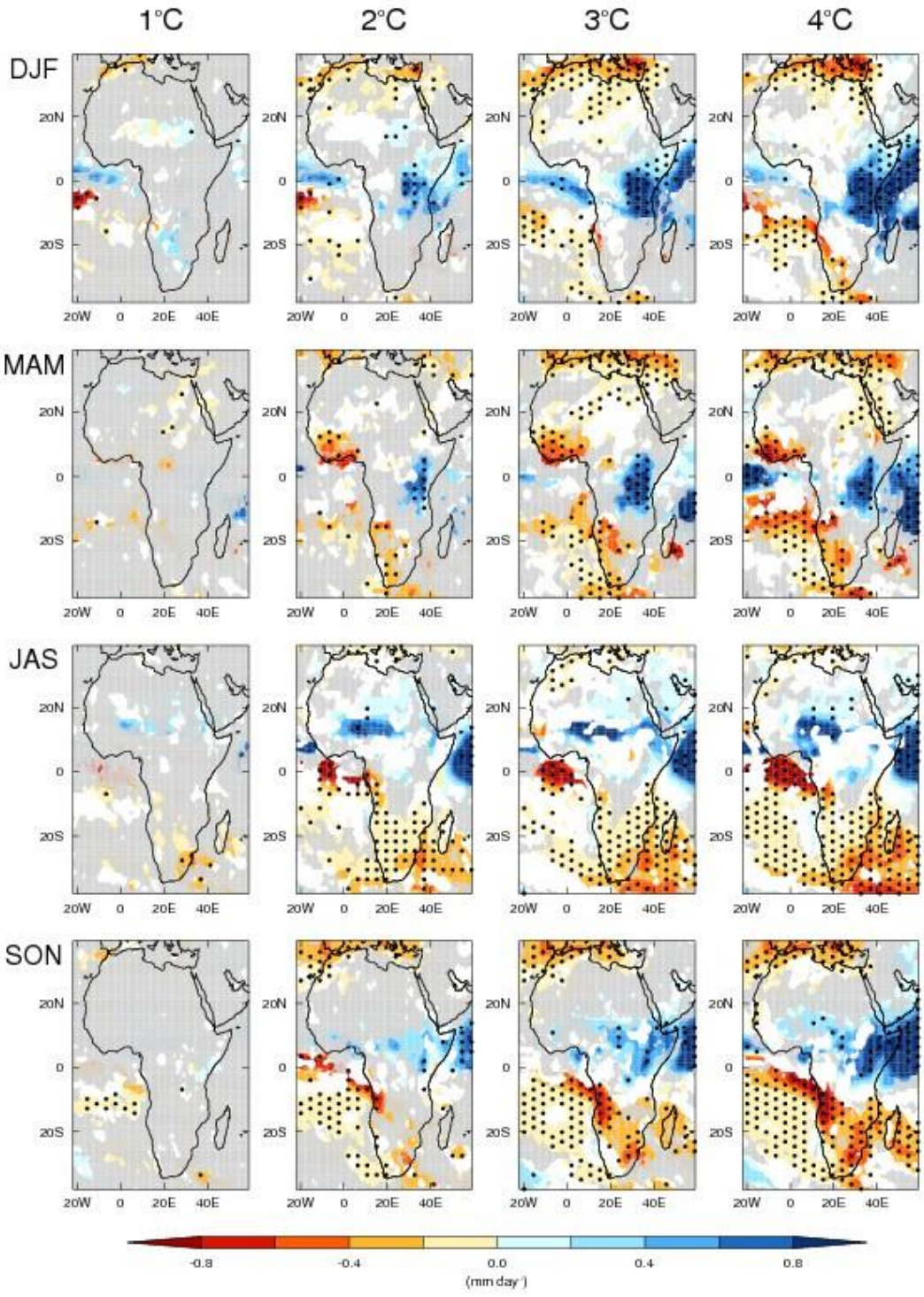

Figure 4.S5 Ensemble mean seasonal precipitation anomalies (mm day^{-1}) associated with global warming in A1B for only those models which reach 4°C in A1B. Grid-points where <66% of models agree on the direction of change are masked in white, and grid-points where >80% of models show no significant change are shown in grey. Stippling shows grid-points where >80% of models agree on the direction of change.

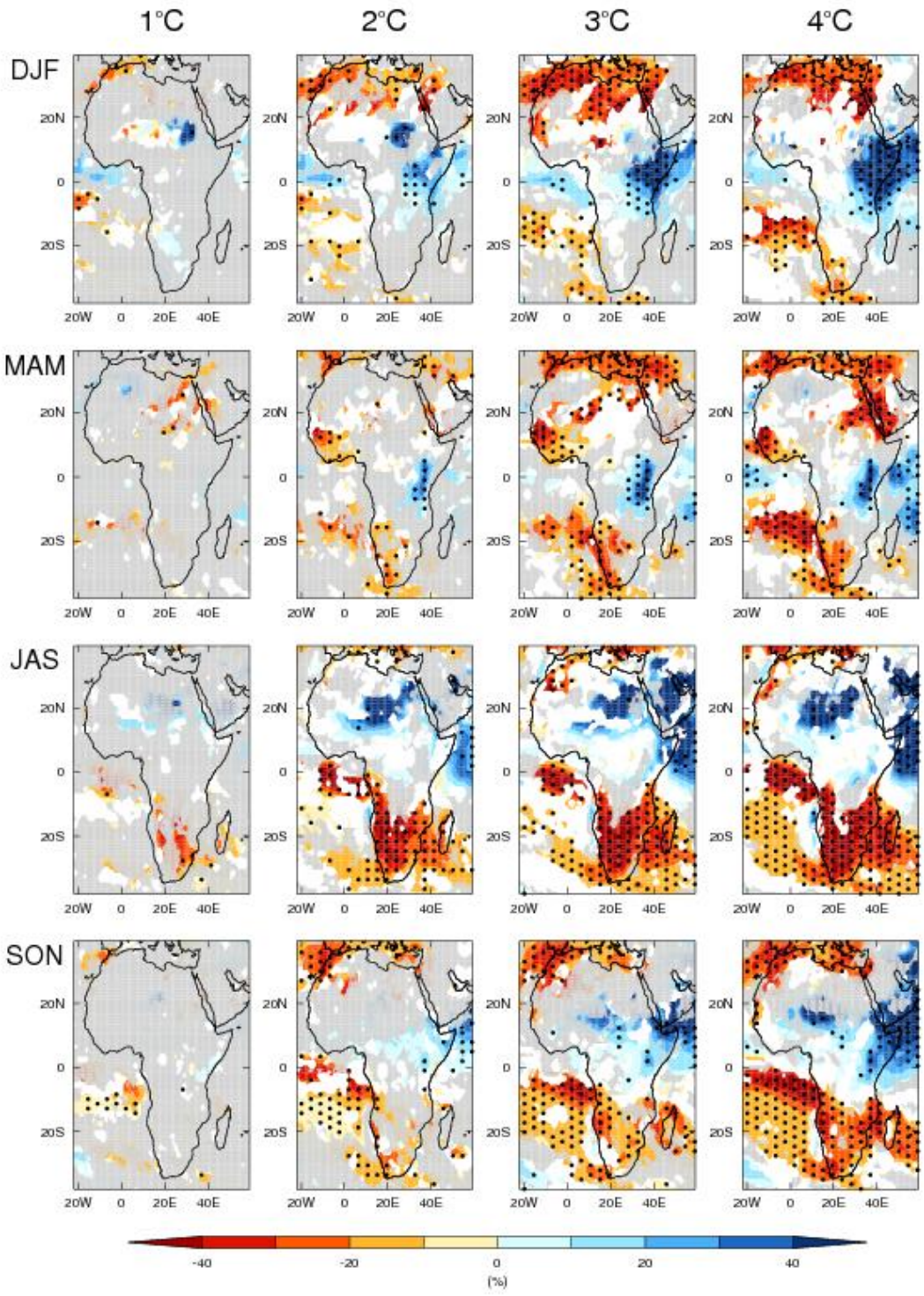

Figure 4.S6 as Figure 4.S5 but for proportional change relative to 1985-99.

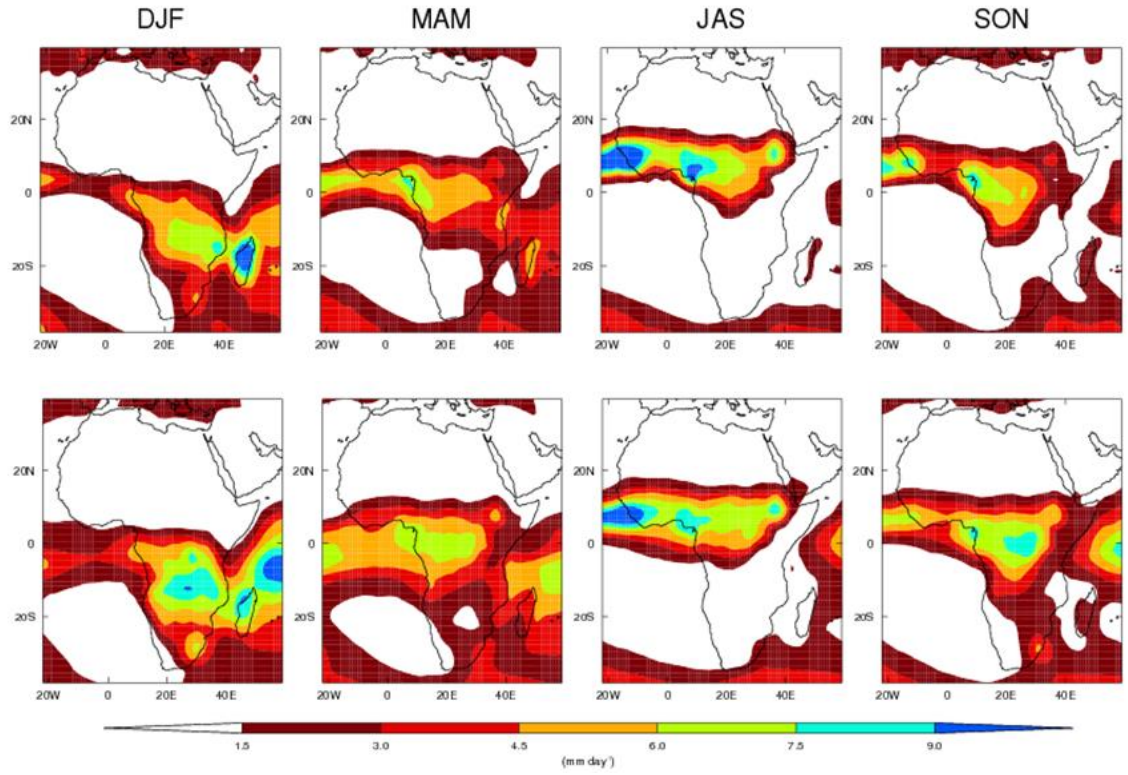

Figure 4.S7 GPCP (top) and CMIP3 20c3m ensemble mean (bottom) seasonal precipitation for 1985-99 for the 4 seasons used in change plots. The modelled climatology is the mean of the 19 models available in both scenarios.

5 African climate change uncertainty in perturbed physics ensembles: implications of warming to 4°C and beyond

Authorship Declaration

I conducted all of the analysis and did all of the writing for this paper. D.P. Rowell contributed to the planning through discussions on the methodology, particularly in connection with the regression of global temperature against local precipitation, and comparison between ensembles. He also gave useful advice on handling of the datasets based on previous experience, and helped to extract and prepare the data for analysis. R. Washington was involved with selecting the perturbed physics ensembles, and planning the methodology, especially how to extract samples at each degree of global warming, and how to constrain the ensembles. Both R. Washington and D.P. Rowell contributed to interpretation of the findings, and their comments were helpful in restructuring the manuscript.

African climate change uncertainty in perturbed physics ensembles: implications of warming to 4°C and beyond

R. JAMES AND R. WASHINGTON

Climate Research Lab, Oxford University Centre for the Environment, South Parks Road, Oxford OX1 3QY, UK

D.P. ROWELL

Met Office Hadley Centre, FitzRoy Road, Exeter EX1 3PB, UK

Submitted to: *Journal of Climate* (6th August 2013)

Abstract

Understanding the potential implications of global warming for regional climate is valuable for both mitigation and adaptation. The majority of existing climate change research has used medium emissions scenarios and collections of model experiments from the Coupled Model Intercomparison Project (CMIP). This leaves two important questions unanswered: how would regional climates evolve under higher emissions scenarios and higher degrees of global warming? And, are there plausible futures which are not represented by the models in CMIP? In this paper, two perturbed physics ensembles (PPEs) are used to address these issues with reference to African precipitation. Examination of experiments with large greenhouse gas forcing shows that changes in African precipitation are enhanced gradually with global temperature, even to 4°C and beyond, although there may be nonlinearities which are not incorporated here due to limited model complexity. The range of projections from the PPEs is compared to CMIP3 revealing regional differences. This is partly the result of implausible model versions, but the ensemble can be justifiably constrained due to its size and systematic nature; highlighting an additional advantage over CMIP. After applying constraints, the PPEs still show changes which are outside the range of CMIP3, most prominently strong dry signals in west equatorial Africa and the Sahel, implying that CMIP3 may underestimate risks for these regions. Analysis of African precipitation changes therefore demonstrates that regional assessments which rely on multi-model ensembles like CMIP3 overlook uncertainties associated with model parameterisations and pronounced warming. More systematic approaches are needed for conservative estimates of danger.

Keywords: regional climate change, global warming, perturbed physics, Africa, precipitation

5.1 Introduction

Research into the implications of greenhouse gas emissions for vulnerable regions has the potential to inform adaptation and mitigation. Climate projections presented as a function of global mean temperature increase (ΔT_g) are particularly important given the focus on 2°C as a benchmark for danger in international mitigation debates (e.g. UNFCCC 2011). This was previously highlighted in Chapter 4, which presents local precipitation changes at 1°C, 2°C, 3°C, and 4°C ΔT_g for Africa, a continent highly vulnerable to changes in water availability (Boko et al. 2007). However, Chapter 4, like the majority of existing climate projection research, is based on data from CMIP3. This has two fundamental limitations. Using CMIP3 it is not possible to directly investigate warming beyond 4°C; and it is difficult to evaluate modelling uncertainty.

Understanding the connotations of 4°C ΔT_g and beyond is imperative for mitigation. The costs and benefits of a 2°C target can only be appreciated with reference to the consequences of unmitigated warming, which is increasingly likely to exceed 4°C as anthropogenic emissions continue to rise. If mitigation is unsuccessful, research into higher degrees of warming could also provide information for adaptation. Several conferences have focused attention on 4°C and beyond (e.g. Oxford in 2009, Melbourne in 2011), but much of the subsequent research has relied on pattern scaling techniques (e.g. Thornton et al. 2011), assuming a linear relationship between ΔT_g and local climate. Experts suggest that the response to warming may be nonlinear, and there could be tipping points in the earth system, which are more likely to be reached at higher global temperatures (Kriegler and Hall

2009). Projections at 4°C and beyond are not widely available, however. In CMIP3, the combination of emissions scenarios and model sensitivity do not generate warming >3°C in most models. Its successor, CMIP5, provides greater potential to explore large anthropogenic forcing (Hurrell et al. 2011). Several PPEs also contain runs which exceed 4°C; and have additional advantages over CMIP.

CMIP3 and CMIP5 are multi-model ensembles (MMEs): "ensembles of opportunity" which result from organised experiments at many international modelling centres. Each model has been created separately using different resolutions and parameterisation schemes; and has been tested extensively (Collins 2007). Many regional climate assessments have used MMEs to investigate future climate change (e.g. Giannini et al. 2008; Chapter 4), in recognition of the importance of consulting multiple models given the large uncertainties involved; particularly for precipitation for which different models project diverging responses in many tropical regions. However, using MMEs to illustrate the range of possible futures is problematic. It is difficult to evaluate whether any of the projections within this range are implausible; and there may be other plausible futures which are not represented, as each model is designed to fit twentieth century conditions, and different models often share data and algorithms (Allen and Ingram 2002). PPEs explore uncertainty more systematically, by running many versions of the same base model with different parameters. This makes it easier to evaluate individual model versions, and to investigate whether differences in model physics produce different responses to global warming. PPEs developed by the Met Office Hadley Centre (MOHC, Murphy et al. 2007) and climateprediction.net (Stainforth et al. 2005) capture much of the uncertainty of MMEs (Webb et al. 2006; Rowell 2012) and enlarge the range of

projections for some variables (Stainforth et al. 2005; Fung et al. 2011; McSweeney et al. 2012).

The present study aims to re-evaluate the implications of global warming for African precipitation, using two MOHC PPEs to investigate the development of change to 4°C and beyond and examine the extent to which parameter perturbations broaden the range of potential futures from CMIP3. A smaller PPE of coupled models run in a high emissions scenario is used to explore higher degrees of warming and make quantitative comparisons to CMIP3; whilst a much larger ensemble of slab models enables analysis of the variability in local precipitation responses to anthropogenic forcing resulting from a wide range of parameter combinations, and the extent to which specific parameter values produce unrealistic simulations. These datasets are outlined in more detail in the next section, followed by a description of the tools used to explore projections in each. In section 5.4, local precipitation projections at 1°C to 6°C ΔT_g are presented. Then checks for implausible signals in the largest ensemble are described, before projections from both PPEs are compared to CMIP3. The implications of these results are discussed with reference to research and policy, and conclusions follow.

5.2 Data

Three ensembles of Global Climate Models (GCMs) are used here: CMIP3 and two MOHC PPEs, one consisting of 280 slab models (AS-PPE) and the other 17 coupled models (AO-PPE).

5.2.1 CMIP3

Monthly data were selected from CMIP3 for all 19 models run with SRES A2 (see Table 4.1) and the same models run with historical forcings (20C3M). Data were interpolated to a 1x1° spatial resolution.

5.2.2 Atmosphere Slab Model PPE (AS-PPE)

AS-PPE is based on HadSM3, which has the same atmospheric and land surface physics as HadCM3 (one of the coupled models in CMIP3), but with a 50m mixed layer or "slab" ocean. 31 atmospheric and land surface parameters were perturbed to create 280 model versions (Barnett et al. 2006). Each ensemble member was run in two equilibrium experiments forced by preindustrial and doubled CO_2 ($2xCO_2$). The runs continue for 20 years beyond equilibrium and 20 year monthly means from this period were the basis for analysis. These data have a spatial resolution of 2.5° latitude and 3.75° longitude.

5.2.3 Atmosphere Ocean Model PPE (AO-PPE)

The base model for AO-PPE is HadCM3: the same as in CMIP3 except with flux adjustments and an interactive sulphur cycle. HadCM3 has an atmospheric resolution matching HadSM3, coupled to a fully dynamical ocean. Due to the greater computational expense it was not possible to run all 280 atmospheric configurations from AS-PPE with the coupled model; therefore 17 versions were chosen (Collins et

al. 2011). Monthly data were selected from transient experiments: a control run with preindustrial forcings, and the high emissions scenario SRES A1FI (Betts et al. 2011). For the control a 20 year reference period was selected 40 years into the run to avoid spin up issues.

5.3 Methods

Changes in precipitation associated with global warming were calculated across the datasets. The AS-PPE experiments have a fixed level of anthropogenic forcing ($2xCO_2$), and climate sensitivity and local precipitation responses to $2xCO_2$ were computed for each ensemble member. CMIP3 and AO-PPE are run in transient scenarios, with increasing global temperature over time, allowing local changes to be analysed as a function of global temperature: in the case of AO-PPE up to 6°C due to the high emissions scenario.

5.3.1 Deriving global mean temperature change (ΔT_g)

For each member of AS-PPE, the global mean temperature change associated with $2xCO_2$, or climate sensitivity, was derived from 20 year annual mean 1.5m temperature data. Data were first weighted by grid-box area.

For the transient ensembles (AO-PPE and CMIP3), local precipitation change was analysed at 1°C intervals of ΔT_g. To find the time of each ΔT_g interval, ΔT_g time-series were created for each model as follows. Area-weighted global means

of annual mean temperature data (1.5m for AO-PPE, near surface for CMIP3) were calculated for control (preindustrial for AO-PPE, twentieth century for CMIP3) and forced (A1FI for AO-PPE, A2 for CMIP3) time-series. Each year in the twenty-first century was differenced from a 15 year control climatology. 1985-99 was used for CMIP3, which differs from the preindustrial reference referred to in policy, but previous work shows results are robust to changes in the baseline (Chapter 4).

The ΔT_g time-series were smoothed using polynomial regression (all r^2 values >0.97) and the year each 1°C interval of ΔT_g was reached was extracted and defined as the median of a 15 year period, to be used to analyse local precipitation change. The 15 year sample length was designed to eliminate interannual variability and to dampen multi-decadal variability. The number of ΔT_g levels available varies between models, and is a maximum of 6°C for AO-PPE and 3°C for CMIP3 (see Table 5.S1).

5.3.2 Local changes in precipitation

Precipitation anomalies associated with anthropogenic forcing ($2xCO_2$ for AS-PPE; ΔT_g samples for AO-PPE and CMIP3) were calculated on a model grid-point by grid-point basis for each ensemble member, for the annual mean and 8 seasons, DJF, MAM, JJA, SON, JFM, AMJ, JAS, and OND (denoted by the initial letter of each month), since precipitation seasonality in Africa is regionally specific. Gridded anomalies were tested at a significance level of 5% using non parametric tests, as precipitation has a skewed distribution in many arid regions. For all three

datasets a Wilcoxon signed-rank test was used (following Wilks 2006) to establish whether the ensemble shows significant positive or negative change distinct from variation between models. The control and forced climatologies for each ensemble formed pairs in the sample.

For CMIP3 and AO-PPE the Mann Whitney U test was also employed to test whether individual models show significant change relative to interannual variability. The direct method was applied due to the small sample size (15 years): for each year in the control, the number of years in the forced time period with a smaller value is counted, and the sum of these counts becomes the U statistic (U_1). This is repeated for the forced time period to get U_2, and the smaller of U_1 and U_2 is compared to the critical value. This test was not applied to AS-PPE as interannual data were not readily available.

5.4 Evolution of regional changes with 1-6°C global warming

AO-PPE models were run in a high emissions scenario, and some reach 4°C and beyond in the twenty-first century. By investigating changes from 1°C to 6°C in this ensemble, the extent to which a group of coupled models shows gradual or nonlinear change in African precipitation with higher degrees of global warming is examined here for the first time. Changes at 1.5°C are also presented due to the consideration of this level in policy (UNFCCC 2011).

Precipitation projections exhibit spatial, seasonal, natural, and intermodel variability. Here we show four seasons of relevance to regional precipitation, and present an overview of the most dominant responses in AO-PPE (Figure 5.1), by displaying the ensemble mean, but only where there is intermodel agreement in the direction of change, and not for grid-points where there is a lack of signal relative to interannual variability (shown in grey) or a lack of consensus as to whether conditions would be wetter or drier (shown in white). This is not designed to provide information about risks associated with each degree of warming, as the magnitude of response varies substantially between models, some of which illustrate the risk of considerably larger responses. Furthermore, the significance test used here is conservative given the small sample size (15 years), therefore even where all models show a lack of signal, there might still be changes which would be measured to be significant were a longer time period to be used. So rather than allowing for risk assessment, the figure is intended to illustrate how precipitation patterns develop on average as global temperature increases. Note that the ensemble mean is calculated using the models available at each degree of ΔT_g (see Table 5.S1), meaning some differences between ΔT_g intervals are due to the inclusion of different models rather than change in global temperature, but we emphasise that the development of local change with ΔT_g in individual models has also been considered (not shown).

Figure 5.1 Ensemble mean seasonal precipitation anomalies (mm day^{-1}) associated with 1°C, 1.5°C, 2°C, 3°C, 4°C, 5°C, and 6°C ΔT_g in AO-PPE. Grid-points where <66% of models agree on the direction of change are masked in white, and grid-points where >80% of models agree on the direction of change are stippled. Grid-points where >80% of models show no significant change are shown in grey. ➢

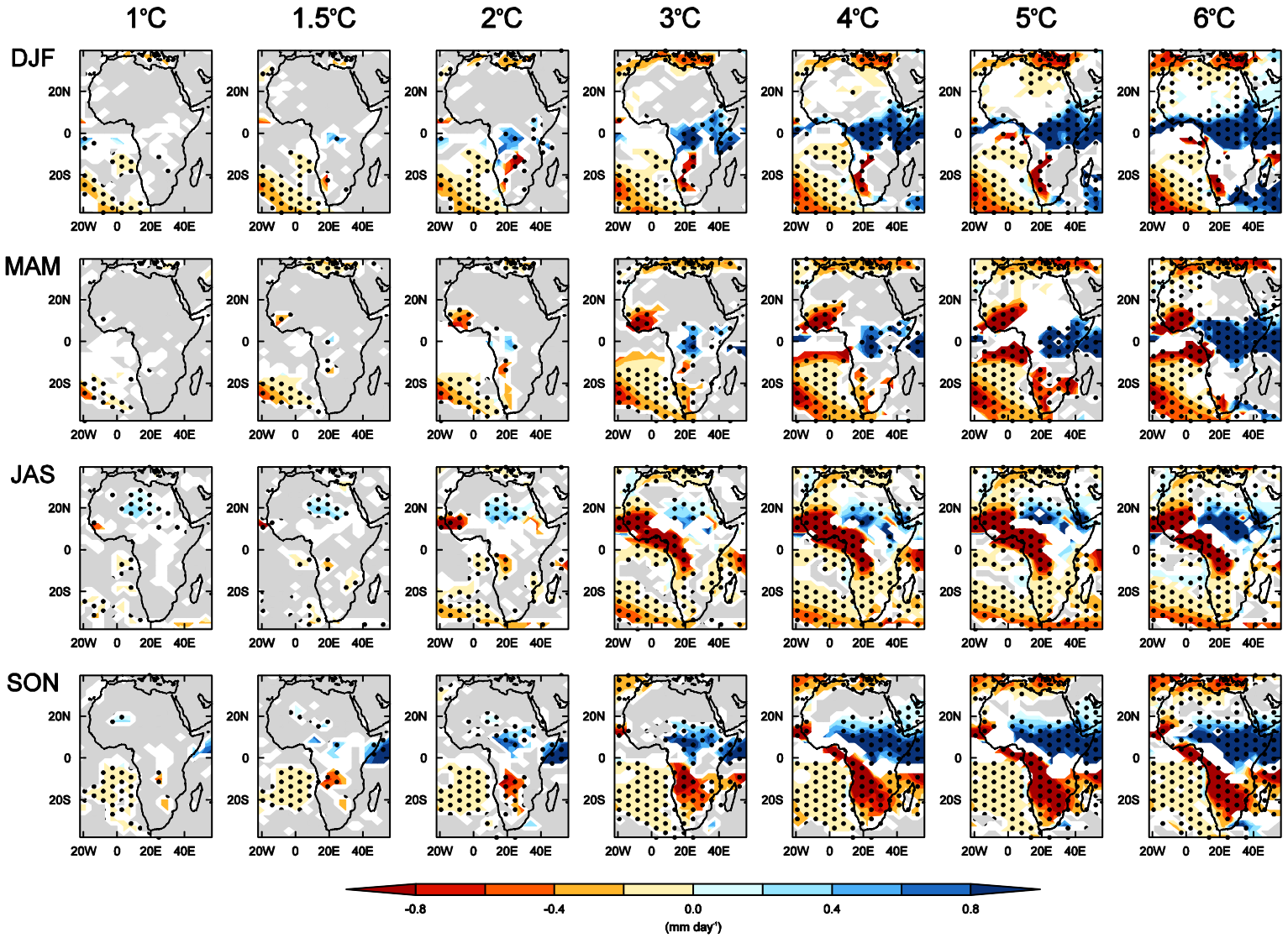
1°C
1.5°C
2°C
3°C
4°C
5°C
6°C
DJF
MAM
JAS
SON
20N
0
20S
20W
0
20E
40E
-0.8
-0.4
0.0
0.4
0.8
(mm day⁻¹)

At 1°C ΔT_g, most models experience a lack of significant change (shown in grey) across much of the African landmass. This does not imply that changes at 1°C are unimportant, for example there may be shifts in extremes. Rather it demonstrates the lack of change in the seasonal mean, in contrast to higher degrees of warming. At 1.5°C there are significant decreases in seasonal mean precipitation of >10% in parts of southern and West Africa. At 2°C these anomalies are strengthened and extended, and there are additional changes in Central Africa. By 3°C the ensemble mean shows drying throughout much of western Africa during JAS: >20% in the Sahel and the Congo Basin. In SON, negative anomalies stretch across most of southern Africa, meridionally opposed to a band of positive anomalies to the north of the equator, which extends into East Africa, implying a strengthening of the Short Rains and an increased likelihood of flooding.

At 4°C and beyond there are some new signals, particularly wetting at the Guinea Coast during DJF, but the main transformation from 3°C to 6°C is an increase in the spatial coverage of the anomalies and their amplitude. Southern Africa provides a typical example: the ensemble average drying during SON is >10% at 3°C and >40% at 6°C. Individual models also show approximately linear amplification of precipitation change with ΔT_g. AO-PPE therefore suggests gradual enhancement of local precipitation changes with global warming: the main difference between ΔT_g intervals is in the strength and extent of anomalies, rather than in the direction or rate of change.

5.5 Comparing projections from PPEs with CMIP3

AO-PPE and AS-PPE have been created by running the same base model multiple times with different parameter values. They explore uncertainty, and can be used to test the range of projections produced using CMIP3. The two PPEs contribute to this evaluation differently. AO-PPE consists of coupled models run in transient experiments, as in CMIP3, allowing for quantitative comparison of the range of projections. However, AO-PPE has relatively few members, meaning there is also value in making a qualitative comparison with the slab model equilibrium experiments from AS-PPE. This is a much larger ensemble, allowing for investigation of the influence of a greater number of parameter combinations on the range of precipitation projections, but also the extent to which the simulations which produce this range are reliable. Before comparing projections from all three ensembles we investigate variability within AS-PPE to determine whether any ensemble members should be judged as implausible and hence eliminated.

5.5.1 Applying constraints to a large PPE

The 280 members of AS-PPE were produced through perturbations of 31 parameters. This means there are many model versions and the differences between them are well understood, allowing for modes of variability to be identified and reasons for this variability to be diagnosed. This is particularly important given that the last of the three stages of development for AS-PPE (Murphy et al. 2004; Webb et

al. 2006; Rougier et al. 2009) was intended to explore parameter space rather than produce realistic climates. The ensemble was previously constrained by Sexton et al. (2012), who produce probabilistic projections using a multivariate Bayesian framework which combines information from AS-PPE, CMIP3, and observations. Here we opt for a simpler approach, which focuses on African precipitation, and allows for a more specific understanding of the causes of variability. This is informed by and is complementary to Sexton et al.'s framework.

Empirical orthogonal functions (EOFs) were calculated to identify dominant modes of variability, in terms of precipitation, and also separately for temperature at 1.5m due to the strong control on precipitation. The analysis was conducted for the global tropics (40°N to 40°S) to assess African variability in a large scale context; and for both climatologies and anomalies associated with $2xCO_2$, to identify variability in the background climate and in the response to anthropogenic forcing. The EOFs were computed from covariance matrices of grid-boxes versus ensemble members (similar to Sanderson et al. 2008b). The resulting EOFs represent the major spatial patterns of intermodel variability across AS-PPE, and principal components (PCs) illustrating the amplitude of the EOF in each ensemble member.

Several of the EOFs revealed large differences between model versions over Africa, in terms of precipitation climatologies, and temperature and precipitation changes associated with $2xCO_2$. The relationship between the strength of the corresponding PCs and different components of the model physics was investigated across the 280 model versions to diagnose the causes of intermodel variability and to establish whether this likely results from limitations in our understanding of climate

modelling or from identifiable model errors; and therefore whether the ensemble can be constrained based on existing knowledge.

5.5.1.1 Constraint based on precipitation climatologies

The first mode of variability in precipitation climatologies (EOF1, Figure 5.2a) shows a strong contrast between land and ocean. This pattern is also evident when the EOFs are rotated using varimax rotation, and the North test (North et al. 1982) suggests it is an independent mode. It continues to dominate variability after CO_2 doubling. Land-ocean contrast is therefore a pervasive signal in the dataset. Model versions with the largest positive amplitudes for EOF1 have dry continents and wet oceans relative to the ensemble mean, with precipitation <1000 mm $year^{-1}$ throughout the African continent. Despite uncertainty in precipitation climatologies for some African regions (Chapter 8), it seems clear that this is too dry, for example, African rainforests require approximately 1500 mm $year^{-1}$ (Malhi et al. 2009).

A composite of ensemble members with dry continents and wet oceans (high PC1) was investigated further to identify reasons for this pattern. These models belong to the third part of the ensemble (Figure 5.2b): intended to explore interactions between parameterisations rather than produce realistic models (Collins et al. 2011). They are also the same model versions which Sexton et al. (2012) found to dominate variability in AS-PPE when eigenvector analysis was conducted using 12 variables and multiple seasons. The amplitude of the first eigenvector from their analysis is negatively correlated with PC1 (r^2 = 0.88). Sexton et al. (2012) found this mode to be controlled by heat convergences: the heat sources which are added to slab

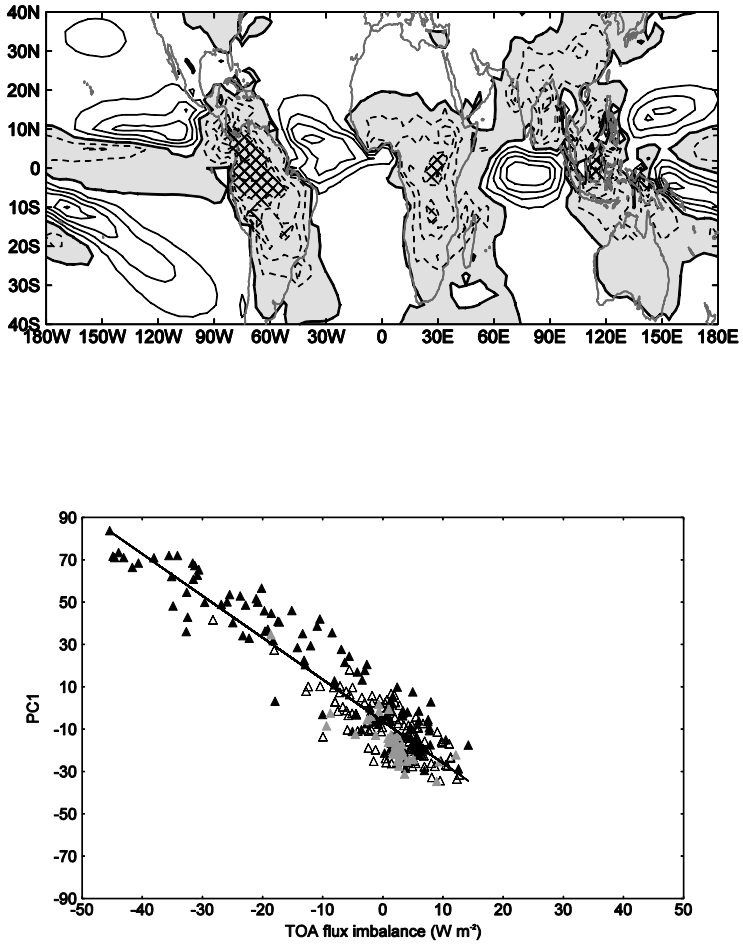

Figure 5.2 A map of EOF1 for the AS-PPE control annual mean precipitation climatologies (top), and the relationship between the amplitude of this mode and TOA flux imbalance (bottom). The EOF has been weighted in order to give a correlation score (r) as the EOF loadings, where $r=100(u/\sqrt{v})$, u is the eigenvector and v is the eigenvalue. The thicker black contour represents 0 with other contours at intervals of 0.05. Areas with positive (negative) values are distinguished by solid (dashed) contours and a white (grey) background. Cross hatching indicates values of $r < -0.15$. In (b) the different triangles represent the first (light grey), second (grey outline), and third (black), stages in which the ensemble was created.

oceans to simulate heat transport and correct for top of atmosphere (TOA) flux imbalances. Different heat convergences are calculated for each model version during calibration (Collins et al. 2011). Here we find that models with dry continents and wet oceans (large PC1 values) have a large negative TOA flux imbalance (meaning there is more outgoing than incoming radiation), and positive heat convergences. There is a strong correlation between TOA flux imbalance and PC1 across the ensemble (r^2 = 0.86, Figure 5.2b).

This can be understood physically. The negative radiative imbalance will have a cooling effect over land, but over the oceans it is offset by the heat convergence. Due to the tendency towards a constant ratio of temperature change over land and ocean (e.g. Joshi et al. 2007), heat will be transported from ocean to land, with associated changes in circulation (Lambert et al. 2011). The heat added to the oceans promotes evaporation, precipitation, and convection, whilst there is anomalous subsidence and drying over land. The precipitation climatology is therefore unrealistic, and a constraint was applied to the ensemble to remove the 140 model versions with TOA imbalances >5 W m^{-2}, corresponding to the estimated observational uncertainty in this value (Collins et al. 2011; Rowlands et al. 2012).

5.5.1.2 Constraint based on changes associated with 2xCO2

Of the modes of variability in changes associated with $2xCO_2$, EOF2 for precipitation change (Figure 5.3a) and EOF3 for temperature change (Figure 5.3b) have the clearest signals over Africa, most prominently the Congo Basin. The patterns persist when the EOFs are rotated, and are shown to be independent using the North

Test. Model versions with large amplitudes for these modes project strong drying and warming over this rainforest region, as well as in Amazonia. These ensemble members were explored further to assess the plausibility of this potentially dangerous response. Analysis of the difference in parameter values between ensemble members with high and low PC values revealed that models with a pronounced warming and drying response in the Congo have low entrainment coefficients, meaning there is little mixing of air with the surrounding environment in convective plumes. Composites of model versions with entrainment coefficients <2 show a similar response (Figure 5.3c, d).

Previous work has shown low entrainment to be unrealistic (Rodwell and Palmer 2007), and Sexton et al. (2012)'s analysis based on observational constraints reveals that the likely range is much smaller than the expert specified range used in the design of AS-PPE. Following their probability estimates, we remove ensemble members with entrainment coefficients <2 and >4, leaving a subensemble of 112. This constraint greatly reduces variability between model versions in terms of temperature and precipitation change associated with $2xCO_2$, particularly over the Congo Basin (Figure 5.4). There is still variability between members of the subensemble, however we did not find any other implausible signals, and therefore this group of model versions will be used to make comparisons with AO-PPE and CMIP3. AO-PPE also contains 4 model versions with entrainment coefficients >4 and these have been removed for the remainder of the analysis, leaving 13 members. Note that Figure 5.1 is very similar when produced using only these model versions (not shown).

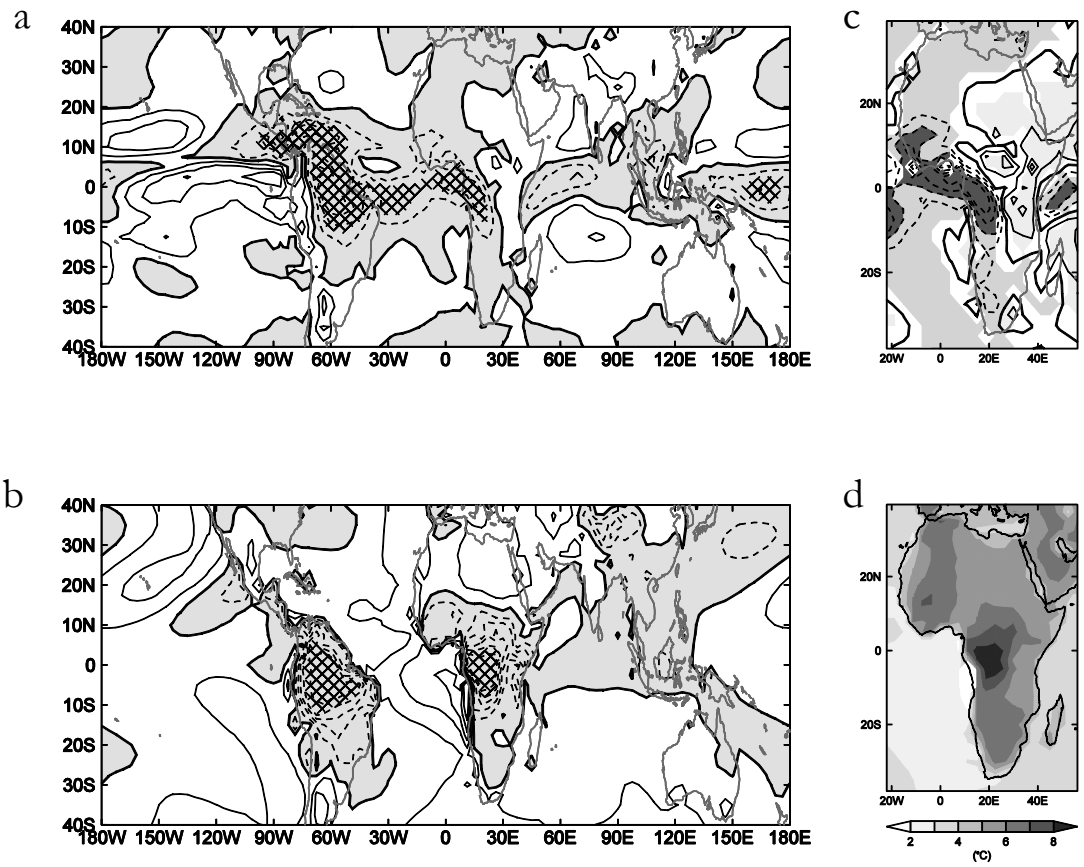

Figure 5.3 Maps of EOF2 for precipitation change (a) and EOF3 for temperature change (b) for AS-PPE. Maps of annual mean precipitation (c) and temperature (d) anomalies associated with $2xCO_2$ for composites of all model versions with entrainment coefficients <2. In all except (d) the thick black contour represents 0. In (a) contours are at intervals of 0.2 and areas with positive (negative) values of *r* are distinguished by dashed (solid) contours and a grey (white) background. Cross hatching indicates values of $r > 0.3$. In (b) contours are at intervals of 0.2 and positive (negative) values are distinguished by solid (dashed) contours and a white (grey) background. Cross hatching indicates values of $r < -0.8$. In (c) contours are at intervals of 0.4 mm day^{-1} and wetting (drying) regions are distinguished by solid (dashed) contours. Here shading is used to show gridboxes with locally significant change (5% level), and this is light grey (medium grey) for areas of wetting (drying). The darker grey shading indicates drying >-0.8 mm day^{-1}. In (d) grey shading shows the magnitude of warming (°C) for all gridboxes that experience significant change (5% level).

5.5.2 Comparing constrained PPEs with CMIP3

The AS-PPE and AO-PPE subensembles and are now compared with CMIP3 to assess whether systematic parameter perturbations produce precipitation projections which are not represented by the CMIP3 "ensemble of opportunity". The most important comparison is in the range of projected futures, however this is difficult to display on a continental scale, and therefore we first present ensemble mean projections, to give an overview of the dominant responses to global warming in each dataset, and to provide a context for comparing the ranges of projections, which is then done on a regional basis.

Figure 5.4 Maps of intermodel variance in annual precipitation (top row) and temperature (bottom row) change associated with $2xCO_2$ for all models in AS-PPE, AS-PPE models with TOA flux imbalance <5 W m^{-2}, AS-PPE models with entrainment between 2 and 4, and AS-PPE models with TOA flux imbalance <5 W m^{-2} and entrainment between 2 and 4. ➢

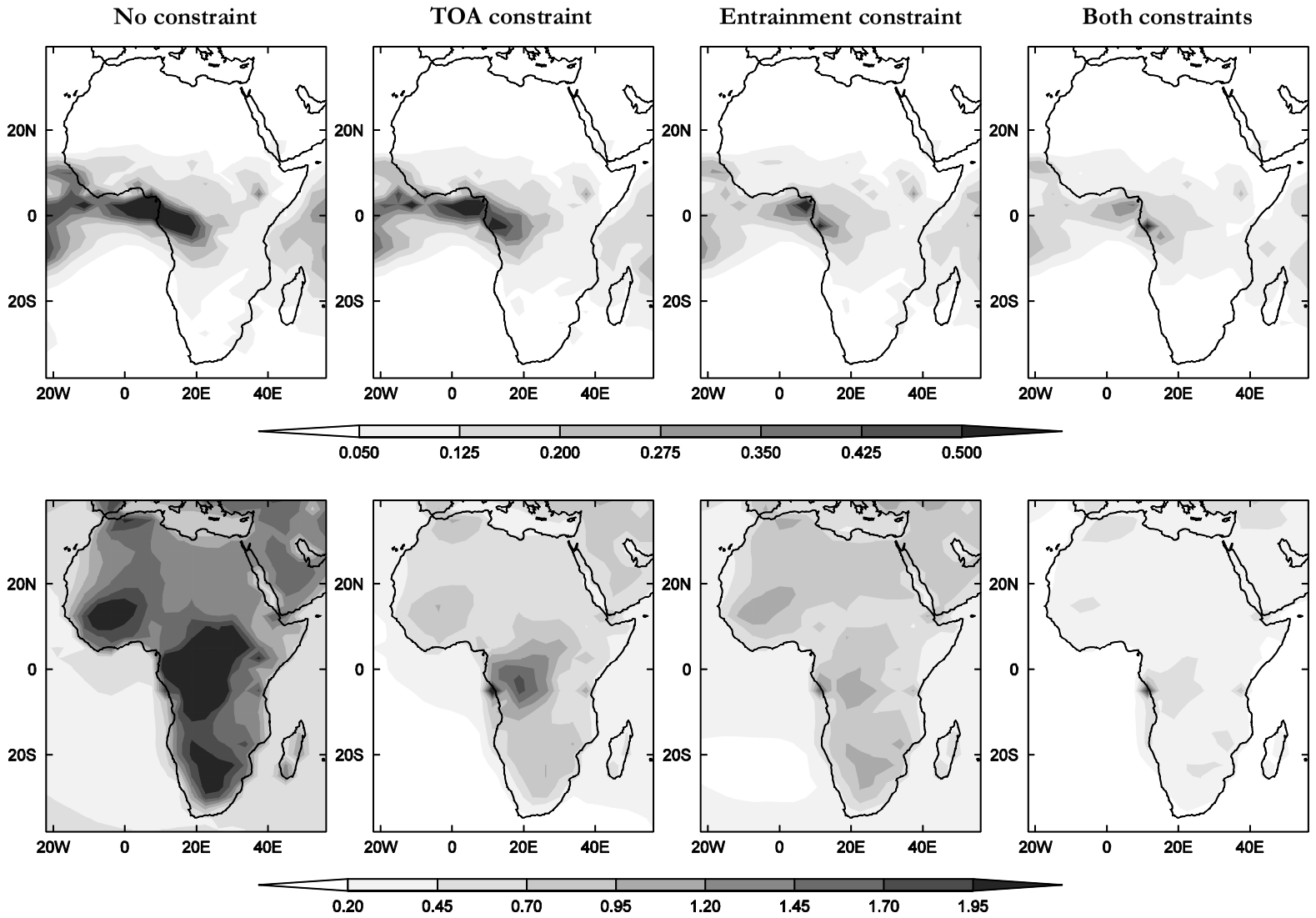
No constraint
TOA constraint
Entrainment constraint
Both constraints
20N
0
20S
20W
0
20E
40E
0.050
0.125
0.200
0.275
0.350
0.425
0.500
0.20
0.45
0.70
0.95
1.20
1.45
1.70
1.95

5.5.2.1 Differences in ensemble mean response

Figure 5.5 shows dominant precipitation responses in each ensemble. For AS-PPE these are ensemble mean anomalies associated with $2xCO_2$, for grid-points where change is significant relative to variation between ensemble members. For AO-PPE and CMIP3 the rate of change in local precipitation per °C of global warming is presented. This was calculated by linearly regressing local precipitation anomalies against global temperature (ΔT_g) using ordinary least squares. The slope of the regression line (m) represents local change per °C of ΔT_g, where data points are overlapping 20 year time periods: global temperature anomalies and local precipitation anomalies associated with 2000-2019, 2010-2029, etc., relative to control climatologies (20 year preindustrial for AO-PPE, 1980-99 for CMIP3). The baseline was not included as a data point, meaning the results are insensitive to the reference climatology, allowing for direct comparison between AO-PPE and CMIP3. For each model, the significance of the slope was tested for difference from zero using a t-test, following Wilks (2006), at a significance level of 5%. The figures show the ensemble mean slope. The percentage of models with a significant slope was calculated for each grid-box, and areas where the models agree on a lack of significance are shown in grey. The percentage of positive slopes was also computed, and areas where the models disagree in the direction of change are shown in white.

Using Figure 5.5 it is possible to make a qualitative comparison of the main wetting and drying responses across all three datasets and a quantitative comparison between the rates of change associated with warming in AO-PPE and CMIP3. The most consistent precipitation signals across all three datasets are the wet response in

East Africa and drying in southern Africa during SON. There are some responses in the PPEs which are not shared by CMIP3, notably a wet signal in the Congo Basin in DJF and large scale moistening of north east Africa during JAS.

The AO-PPE ensemble mean generally shows more precipitation change per °C of global warming than CMIP3. This is evident from the methodology used for Figure 5.5, and is corroborated by projections extracted at 1°C, 2°C, 3°C, and 4°C for AO-PPE (Figure 5.1) and CMIP3 (Figure 4.3). The difference in magnitude is clearest in western Africa, particularly in parts of the Congo Basin and west Sahel during JAS, where drying is more extensive and more enhanced in AO-PPE, at >15% per °C in places.

These differences in the ensemble mean could be due to greater intermodel agreement in AO-PPE. We might expect more consensus between perturbed versions of one base model (HadCM3) than for models with different physics, and Figure 5.5 indicates that there are more grid-points for AO-PPE than CMIP3 for which >80% of models agree in the direction of precipitation change. AO-PPE models may also be more sensitive to warming, as HadCM3 shows large changes per °C ΔT_g relative to other CMIP3 models. The larger response in the ensemble mean is therefore likely to be a combination of greater model consensus and greater sensitivity. A more important issue than the difference in ensemble mean projections is whether any of the individual perturbed model versions show changes outside the range of CMIP3, and this can be established by examining the range of projections from each ensemble on a regional basis.

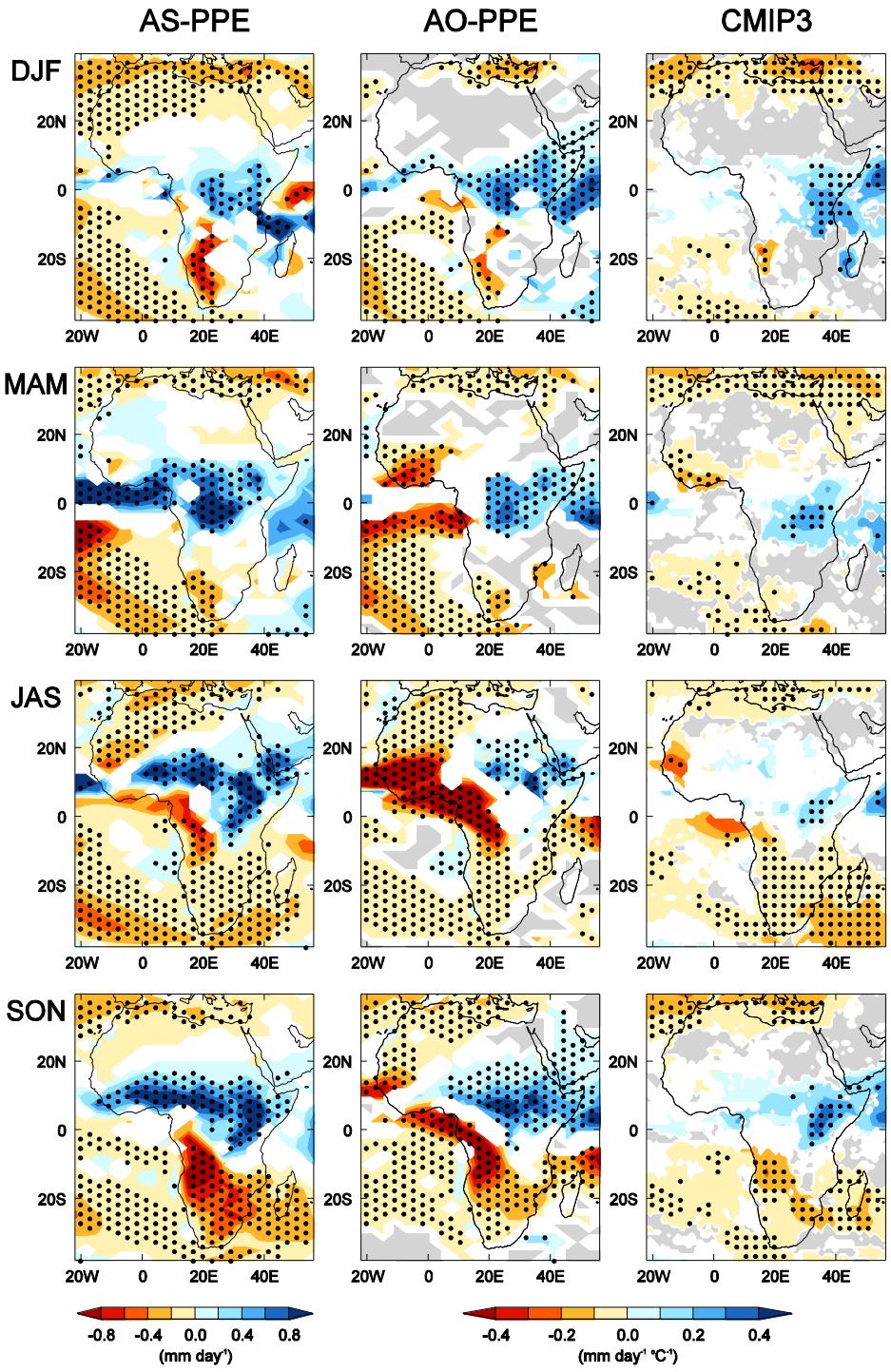

Figure 5.5 Maps of ensemble mean precipitation response. For AS-PPE (subensemble) seasonal mean anomalies associated with 2xCO2 (mm day^{-1}). Locally insignificant (5% level) anomalies are masked in white. For AO-PPE (subensemble) and CMIP3, seasonal mean precipitation anomalies (mm day^{-1}) per °C. White indicates <66% model agreement on direction of change, grey >66% model agreement on no significance. For all ensembles stippling indicates >80% model agreement on direction of change.

5.5.2.2 Differences in the range of projections

Area-averages of precipitation changes relative to control climatologies (%) are shown in Figure 5.6, for regions and seasons which have previously been identified as experiencing relatively robust projections in CMIP3 (East Africa, the Mediterranean, Southern Africa, Angola, West and Central Sahel; Christensen et al. 2007; Chapter 4), and/or show a contrast between the ensembles in Figure 5.5 (Congo Basin in DJF, West Equatorial Africa and West and Central Sahel in JAS). For each AS-PPE model regional change associated with $2xCO_2$ is plotted against climate sensitivity. For AO-PPE and CMIP3 the range of modelled changes is shown at specific ΔT_g intervals (1°C, 2°C, 3°C, etc), extracted using the methodology described in section 5.3.1. It is not possible to directly compare magnitudes across all three datasets. The figure gives an impression of the level of agreement in the direction of change for all three ensembles, and allows for direct comparison of the amplitude of precipitation responses in AO-PPE and CMIP3.

In terms of the direction of change, many signals are shared by the majority of models in all three ensembles. The most consistent responses are the dry signals in the Mediterranean and Southern Africa. However some regions show important contrasts between the datasets. In West Sahel, most coupled models show drying after 2°C, whereas in the slab models there is no agreement on the direction of change. In East Africa during MAM, there is more consensus for a wet response in AO-PPE and CMIP3 than AS-PPE. In Central Sahel, all members of the AS-PPE subensemble project wetter conditions or approximately no change, in contrast to CMIP3 which contains at least one model with a strong drying response.

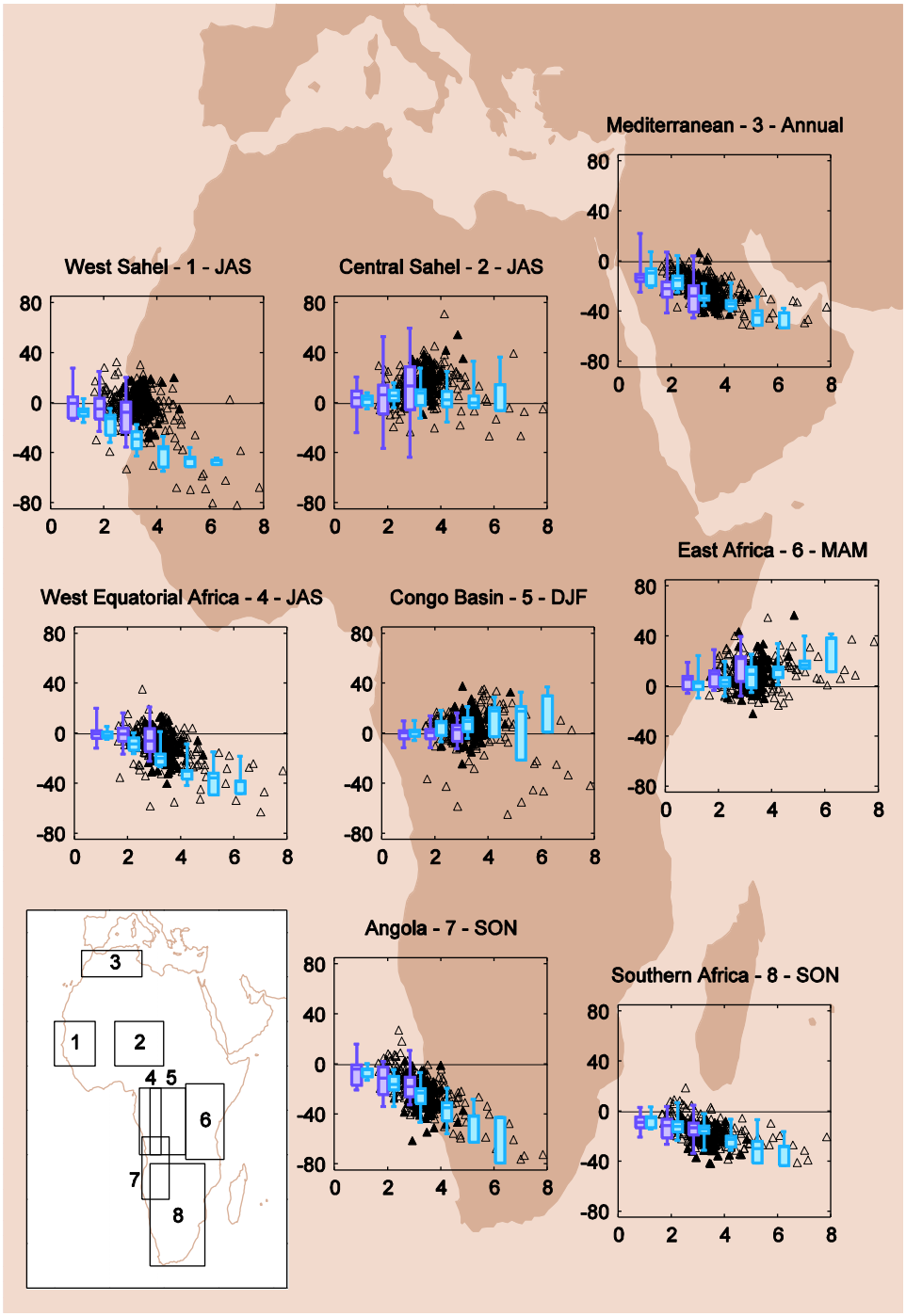

Figure 5.6 Regional precipitation change (%) associated with 2xCO_2 in AS-PPE (triangles), and ΔT_g levels for AO-PPE (subensemble) and CMIP3 (blue and purple boxplots respectively: minimum, lower quartile, median, upper quartile, maximum). For AS-PPE models included in subensemble are shown as filled triangles, and other models as outlined triangles. Regional coordinates are specified in supplemental material, Table 5.S2.

Differences in the magnitude of change can be measured between AO-PPE and CMIP3. Which ensemble contains the most extreme projections varies regionally. In East Africa during MAM CMIP3 includes models which have a larger wet signal per °C ΔT_g. The wettest CMIP3 model, MIROC3.2(medres), has a similar response at 3°C (40%) to the wettest AO-PPE model at 6°C (42%). This model also shows large change relative to AO-PPE in OND (not shown). AO-PPE has more extreme projections in western Africa: confirming that the stronger ensemble mean response noted in section 5.2.1 is the result of greater agreement between models in the direction of change and also larger model projections relative to CMIP3. In West Equatorial Africa, the driest CMIP3 projection is 22% at 3°C, and several AO-PPE models exhibit greater drying at 3°C and beyond. In Angola, AO-PPE models are outside the range of CMIP3, and in West Sahel the difference is clearest: from 2°C many AO-PPE runs produce dry signals with greater amplitude than any of the CMIP3 models.

Note that the contrasts between AO-PPE and CMIP3 might be partly due to natural variability and different scenarios and as opposed to model uncertainty. Comparisons of the same CMIP3 models run in A1B and A2 do show differences of the same order of magnitude in many regions (see Figure 5.S1); however in western Africa at 2°C and 3°C many AO-PPE models are dryer than CMIP3 run in both A1B and A2, confirming that perturbing the physics of HadCM3 has produced changes outside the range of CMIP3.

5.6 Discussion

In this paper PPEs have been used to address two questions which are often neglected in regional climate change assessments: how would regional precipitation evolve under higher degrees of global warming? And, are there plausible futures which are not represented by the models in CMIP? The analysis demonstrates that coupled models produce gradual responses to ΔT_g even at higher degrees of warming, that PPEs provide opportunities for constraining the range of projections, and that there are differences in the range of projections between CMIP3 and the PPEs. Here we discuss the extent to which these findings have connotations for adaptation and mitigation decisions, and the lessons for future climate change assessments, for Africa and beyond.

5.6.1 Gradual response to rising global temperatures

AO-PPE models project approximately linear local precipitation change with ΔT_g, suggesting that as global temperature increases, there will be progressive and unidirectional change in local climate away from preindustrial conditions. The models show no sign that global warming will lead tipping points to be reached, even at higher degrees of warming.

This suggests that, in principal, pattern scaling approaches (used by e.g. Thornton et al. 2011) could be employed to investigate different degrees of warming, although some existing techniques would not capture the spatial extension of anomalies with warming which is illustrated in Figure 6.1. There are also potential

implications for policy. Since larger changes in climate would bring greater challenges for society, the projections could provide evidence to support early mitigation of CO_2 emissions, but also gradual adaptation, as there do not appear to be trend reversals or accelerating rates of change relative to global temperature. For example, the 1.5°C and 2°C targets, due to be reviewed by the UNFCCC by 2015 (UNFCCC 2011), show quantitatively but not qualitatively different responses in the AO-PPE projections, and so it is difficult to distinguish between them without impacts assessment. There may be sudden changes in extreme precipitation, nonlinear evaporation responses, or thresholds in systems influenced by mean precipitation change, but there are no dramatic changes in seasonal temperature or precipitation which might support the selection of a particular ΔT_g level as a benchmark for danger. It is possible that our analysis obscures step changes, as have been identified through statistical analysis of observations and model projections for southeastern Australia (Jones 2012); however, the methodology used here is sufficient to show that there appear to be no trend reversals or large accelerations in the rate of change.

It would be useful to test these results against different scenarios, as Good et al. (2012) find nonlinear precipitation trends in HadCM3 in 4xCO_2 experiments. We must also interrogate how well HadCM3 and other coupled models are able to simulate the response to rising global temperatures. Many struggle to capture multi-decadal variability (Lau et al. 2006) and the influence of sulphate aerosols, which might be associated with trend reversals in regional precipitation, particularly in the Sahel (Ackerley et al. 2011). It is also unclear whether models can simulate climatic conditions associated with much higher greenhouse gases. GCMs may become less reliable as they are pushed further from today's conditions; just as they often struggle

to reproduce paleo-climatic states (Braconnot et al. 2007). Models of this generation may lack the resolution and complexity to represent nonlinearities or tipping points in the earth system, which are more likely to occur as global temperatures are increased (Lenton et al. 2008). Expert elicitation suggests that there is >56% probability of crossing at least one tipping point if warming exceeds 4°C (Kriegler and Hall 2009), for example rapid melting of the Greenland Ice Sheet, which could conceivably impact inter-hemispheric Atlantic sea surface temperature gradients known to influence the West African Monsoon (WAM) (e.g. Folland et al. 1986; Mohino et al. 2011). Yet many studies of twenty-first century changes in the WAM (e.g. Held et al. 2005) are based on GCMs which, like HadCM3, do not include interactive ice sheets (Lenton 2011b).

The projections based on AO-PPE therefore provide insufficient evidence on their own to understand the implications of higher degrees of warming for African climate, which remain largely unknown. Regional climate change assessments should acknowledge the degree of uncertainty surrounding pronounced warming and the potential for nonlinear change, as this could affect decisions surrounding mitigation, for example when evaluating the consequences of exceeding 2°C, and adaptation, as it is unclear how strategies based on medium term scenarios would cope at 4°C and beyond.

5.6.2 Ability to constrain a large PPE

The ability to constrain AS-PPE (as described in section 5.5.2) is a key outcome given the widely recognised importance of sub-selecting models for regional climate change assessments. GCM projections diverge substantially, particularly in terms of precipitation (Hoerling et al. 2006). Since it is impossible to validate their future simulations, a range of models must be considered, but it might not be wise to include all available models in this range, as some are likely to be better than others. Furthermore, regional downscaling and impacts assessment studies are usually restricted in the number of GCM simulations they can incorporate due to computational cost. Selecting models is therefore important for pragmatic as well as scientific reasons, but there is no consistent approach for this in the case of MMEs. Previous attempts to constrain CMIP3 have led to contrasting conclusions, for example for the Sahel (Cook and Vizy 2006; Lau et al. 2006). Members of a MME differ from each other in myriad ways, meaning it is not possible to diagnose reasons for differences between them. The models with the best fit to historical observations can be selected, but we cannot determine the reasons for their superior hindcasts and therefore it is difficult to assess whether these models will produce a more reliable response to warming.

In a PPE, the differences between each model version are small and well understood, and therefore the reasons for different modelled responses can be detected, particularly where there are a large number of members. Here, the parameter controlling a strong drying and warming response in the Congo Basin in AS-PPE was diagnosed by investigating the association between this response and

each of the 31 parameters which is varied within the ensemble. Based on previous research about this parameter, a constraint could then be applied consistently across the ensemble. Such an approach would not have been possible with a MME. Although the models in CMIP3 are optimised to fit twentieth century conditions, meaning there might be less intermodel variability than for AS-PPE, which has been designed to explore parameter space; CMIP3 may still contain implausible models, but these are difficult to identify and remove because the ensemble has not been designed systematically. Large PPEs are easier to constrain, and therefore present greater opportunity to understand the range of plausible futures for African precipitation. Previous studies have used Bayesian statistics to produce probabilistic projections from PPEs (Sexton et al. 2012). Whilst the approach used here is less comprehensive, it demonstrates the potential for simple justifiable constraints.

5.6.3 Projections outside the CMIP3 range

As well as the difficulty in evaluating whether any of the futures projected by MMEs are plausible, there is also the high likelihood that there are alternative plausible futures which are not represented. MMEs like CMIP3 are not designed to explore uncertainties in our understanding of physical processes, and therefore in theory they will underestimate uncertainty in responses to global warming. In this study PPEs are used to assess whether this is true in practice, in the case of African temperature and precipitation. The results show qualitative and quantitative differences between projections from each of the PPEs and CMIP3. Both PPEs project changes which are not represented by CMIP3, indicating that this MME does

not provide the most conservative envelope with which to make adaptation and mitigation decisions.

The differences are clearest in West Sahel. Many CMIP3 models show drying in this region in response to anthropogenic forcing (Figure 4.5; Monerie et al. 2012b), and the largest projections at 2°C (-22%), and 3°C (-35%) would likely be dangerous. The GFDL models show extensive dry signals and have often been perceived to represent a worst case scenario (Cook and Vizy 2006; Held and Soden 2006). Here it is shown that members of AO-PPE project even greater drying in West Sahel: the median for 3°C is -28%. The three model versions which exceed 6°C (due to large positive feedback mechanisms and the high emissions scenario) project >40% decreases in precipitation in West Sahel, which is the same magnitude as the change associated with the long term drought in the 1970s (Held and Soden 2006). AO-PPE therefore presents larger risks than CMIP3. Debates about which degree of global warming constitutes dangerous anthropogenic interference for this region might reach different conclusions depending on which ensemble is used.

The projections from AS-PPE for West Sahel add a further complication: whilst AO-PPE and CMIP3 models largely agree that precipitation would decrease, AS-PPE members are split between wet and dry futures. This undermines the consensus in CMIP3, and brings into question any adaptation measures for this region which might assume dryer conditions: planners would need to prepare for a wider range of possible futures if they were to incorporate uncertainty from all three ensembles. Of course, it may be possible to reduce this range by applying further constraints to the dataset, but until further research into mechanisms associated with

the modelled responses is conducted, it is difficult to assess which projections are more likely.

This paper therefore adds evidence to assertions that adaptation and mitigation decisions should not be based on CMIP3 alone. The newest collection of coupled models, CMIP5, is also likely to underestimate uncertainty. Existing research suggests little change in model spread from CMIP3 to CMIP5 in terms of temperature and precipitation (Knutti and Sedlacek 2012). The range of projections from these MMEs should not be viewed as the error bar for the range of potential outcomes from anthropogenic forcing. There is a wider range of uncertainty, and there is potential for this to be investigated systematically, for example through super-ensembles with multiple base models run in PPEs.

5.7 Summary and Conclusions

Investigating the potential influence of global warming on regional climate systems could provide valuable information for mitigation and adaptation. However, most existing climate change research has relied on CMIP3, which was not designed to consider higher degrees of global warming or to explore modelling uncertainty systematically. In this study two PPEs were employed to address these two issues: to examine the extent to which the implications of global warming for African precipitation deduced from these ensembles might be different from those inferred from CMIP3, and to evaluate whether PPEs can provide additional information about uncertainties associated with anthropogenic forcing.

To investigate changes to 4°C and beyond, projections from a coupled PPE (AO-PPE) run in a high emission scenario were presented for 1°C to 6°C ΔT_g. Precipitation anomalies at 2°C and 3°C, notably drying in southern Africa during SON and western Africa during JAS, are amplified and extended at 4°C and beyond. This amplification is approximately linear: there is no sign of tipping points being reached. This implies that early mitigation would be beneficial; but also suggests potential for gradual adaptation. However the models used may not be capable of representing climatic conditions under such different global mean temperatures, and do not provide potential to explore nonlinearities which are thought to be more likely under high anthropogenic forcing. Therefore further research is needed to test this finding, and the uncertainties associated with higher degrees of warming should be highlighted in regional climate change assessments.

AO-PPE and a larger ensemble of 280 slab models (AS-PPE) were also used to test the range of projections for Africa from CMIP3. First variability within AS-PPE was explored to eliminate implausible model versions. This revealed that the most dominant signal associated with $2xCO_2$ was not the result of warming but perturbations: many of the model versions have a negative TOA flux imbalance, creating a land-sea contrast in precipitation fields. These models were removed, alongside ensemble members with implausible entrainment coefficients, here found to be associated with high amplitude drying and heating of the Congo Basin. The application of these constraints was facilitated by the size and systematic nature of the ensemble, suggesting greater potential for model evaluation in PPEs relative to MMEs like CMIP3.

After applying the constraints, there are still differences between the PPEs and CMIP3. In the western Sahel many members of AS-PPE project wetter futures, undermining the consensus on drying in CMIP3, whilst AO-PPE models exhibit large negative anomalies: 4 ensemble members show more drying at 2°C than the drier of the GFDL models (-22%), previously perceived to represent the most extreme scenario (e.g. Cook and Vizy 2006). Therefore, CMIP3 does not present the most conservative envelope from the perspective of adaptation and mitigation: the inferred risks of global warming are different depending on which ensemble is employed.

Investigation of African precipitation projections from PPEs therefore suggests that there are deficiencies in the existing climate modelling infrastructure for impact assessment. Regional climate change assessments based only on CMIP3 overlook uncertainties associated with higher degrees of warming and parametric uncertainty. Coupled GCMs do not show tipping points in response to warming, but may lack the complexity to represent the feedbacks involved. MMEs such as CMIP3 and CMIP5 present a range of futures; yet this may contain implausible projections whilst also excluding other plausible responses. These issues should be emphasised if projections are to be used to inform policy without overconfidence. PPEs provide the opportunity to better understand uncertainties and produce a more defensible range of possible futures.

Acknowledgements

We acknowledge technical support from Gil Lizcano, and helpful discussions with Myles Allen, William Ingram, and David Sexton. The work undertaken by DPR is part of the output from a project funded by the UK Department for International Development (DFID) for the benefit of developing countries. The views expressed are not necessarily those of DFID. This study used MOHC data produced through work supported by the UK Joint 'Department for Energy and Climate Change' (DECC), 'Department for Environment, Food and Rural Affairs' (Defra) MOHC Climate Programme (GA01101). We also acknowledge the modelling groups, the Program for Climate Model Diagnosis and Intercomparison, and the WCRP's Working Group on Coupled Modelling for their roles in making available the CMIP3 multi-model dataset. Support of this dataset is provided by the Office of Science, U.S. Department of Energy.

Supplementary Information: Chapter 5

Table 5.S1 Number of models at each ΔT_g interval.

	n	1°C	1.5°C	2°C	3°C	4°C	5°C	6°C
AO-PPE	17	14	17	17	17	13	8	3
with constraint	13	10	13	13	13	10	7	3
CMIP3	19	19	19	19	14	-	-	-

Table 5.S2 Co-ordinates of the domains selected for regional analysis.

Region	Co-ordinates[a]
Angola	12-22°E; 6-20°S
Congo Basin	15-28°E; 10°S-5°N
West Equatorial Africa	11-19°E; 10°S-5°N
East Africa	28-42°E; 11°S-6°N
Mediterranean	10°W-12°E; 30-36°N
West Sahel	20°W-5°W; 10-20°N
Central Sahel	2-20°E; 10-20°N
Southern Africa	15-35°E; 12°S-35°S

[a]These dimensions were selected from the data. The resulting dimensions vary between ensembles depending on model resolution.

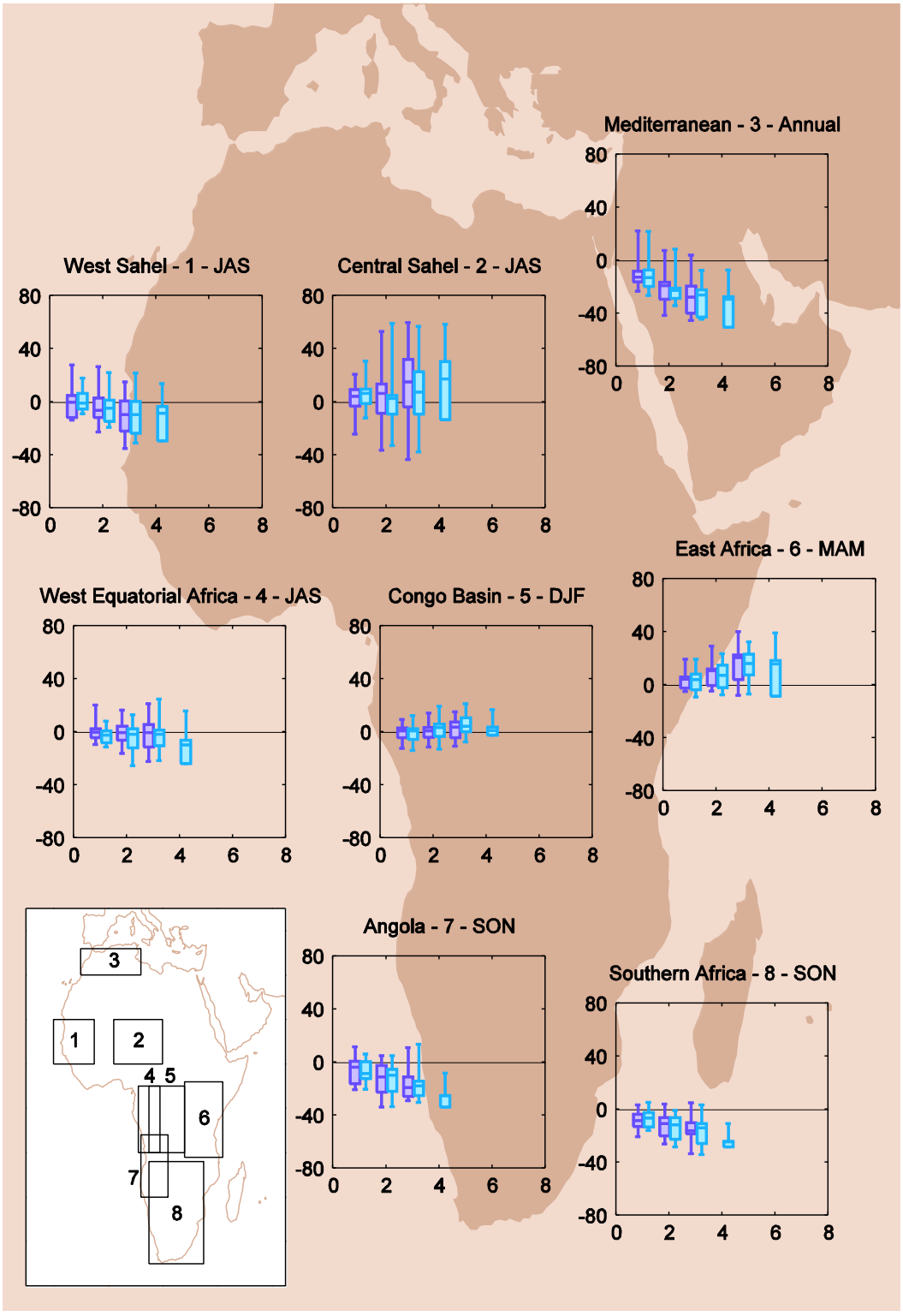

Figure 5.S1 Regional precipitation change relative to 1985-99 (%) associated with degrees of global warming in CMIP3 run in A2 (purple) and A1B (blue). The axes have been drawn to match Figure 5.6.

6 African climate change in global and regional models: a comparison of precipitation responses to global warming

Authorship Declaration

I did the analysis for this paper and wrote the text. R. Washington helped plan the analysis, and gave advice on the methodology for investigating atmospheric dynamics. He was involved in interpreting the findings. R. Jones also gave comments on the findings. Both R. Washington and R. Jones commented on a draft of the paper.

African climate change in global and regional models: a comparison of precipitation responses to global warming

R. JAMES AND R. WASHINGTON

Climate Research Lab, Oxford University Centre for the Environment, South Parks Road, Oxford OX1 3QY, UK

R. JONES

Met Office Hadley Centre, FitzRoy Road, Exeter EX1 3PB, UK

Submitted to: *Climate Dynamics* (21st September 2013)

Abstract

There is currently a worldwide effort to produce detailed climate projections using Regional Climate Models (RCMs), particularly over Africa. An important step in knowing the value of RCM data is to compare their output with Global Climate Models (GCMs), on which climate change assessments have largely been based. In this study five GCMs and RCMs are used to investigate whether the implications of global warming for African precipitation are different if inferred from RCMs versus GCMs. In West Africa both ensembles show a drying response to global warming but this is consistently larger in the GCMs. Circulation changes are analysed to investigate why the drying occurs and why it is more enhanced in global models. In both ensembles, precipitation decline is associated with anomalous subsidence in the upper atmosphere, and may be amplified by large warming in the heat low region, with potential links to the African Easterly Jet and the West African Monsoon. The changes in atmospheric dynamics represent a distinct mode which occurs during dry years in twentieth century simulations, and dominates in response to global warming. The mode is not found in association with dry years in reanalysis data. This does not inspire confidence in the GCMs' response to warming, and, as the RCMs show a similar but more muted response, their projections are no more trustworthy in this case. This study therefore highlights that comparison to GCMs is important before local scale data from RCMs can be assumed to be more useful for adaptation and mitigation.

Keywords: precipitation, West Africa, regional modelling, climate change projections, global warming

6.1 Introduction

Africa is widely recognised as highly vulnerable to changes in precipitation (e.g. Boko et al. 2007). Research into the potential implications of anthropogenic greenhouse gas emissions for African climate is therefore important: to provide information for adaptation, and also mitigation, allowing assessments of the level of interference which should be avoided to prevent dangerous climate change. Mitigation debates have often sought a global temperature threshold to which warming should be restricted, therefore examining the connotations of specific degrees of global mean temperature increase (ΔT_g) for African climate is particularly valuable from a political perspective.

The majority of previous work to investigate changes in African precipitation associated with increasing greenhouse gases (e.g. Christensen et al. 2007; Giannini et al. 2008) and global temperatures (Chapter 4) has been based on projections from Global Climate Models (GCMs). GCMs have coarse spatial resolution: each grid-point can represent several hundred kilometres. This may partly explain biases in modelled precipitation climatologies over Africa, and likely limits the models' capacity to respond reliably to global warming. For example, it is difficult to reproduce intense meridional precipitation gradients in the Sahel with large grid-spacing (Druyan et al. 2010; Patricola and Cook 2010), and many GCMs do not capture the boreal summer maximum over the Cameroon highlands (Cook and Vizy 2006) due to their poorly resolved topography. Inadequate representation of coastlines, regional water bodies, and land surface heterogeneity may also hamper the ability to model precipitation.

Another problem is that output from GCMs is at a scale which is generally too large to be used for impacts assessment and decision making. Whilst some state of the art GCMs have higher resolution, the grid-spacing is still 1° or greater in most CMIP5 (Coupled Model Intercomparison Project phase 5) simulations (Taylor et al. 2012a). Regional Climate Models (RCMs) allow experiments to be run at a higher resolution without incurring a prohibitive computational cost, providing the opportunity to produce projections at a scale which is more policy-relevant. This has been recognised in the international effort surrounding the Coordinated Regional Climate Downscaling Experiment (CORDEX), which is greatly increasing the number of twenty first century RCM projections available, particularly for Africa, which has been identified as a focus region (Giorgi et al. 2009; Jones et al. 2011; Hewitson et al. 2012).

It remains to be seen whether RCMs produce different, and more reliable, responses to warming than GCMs. Some RCMs run over Africa for the historical period, with reanalysis for boundary conditions, produce a closer fit to observations than their driving data, demonstrating the potential for added value over reanalysis (Nikulin et al. 2012; Kim et al. 2013). When historical GCM simulations are used as boundary conditions, RCMs can correct some but not all of the systematic biases (Laprise et al. 2013), and may also introduce their own biases (Mariotti et al. 2011). Analyses of twenty-first century projections also reveal differences between RCMs and their driving GCMs (Paeth et al. 2011; Diallo et al. 2012; Laprise et al. 2013), but in this case it is more problematic to establish which is more reliable. Mariotti et al. (2011) and Sylla et al. (2012) infer that RegCM3 produces more trustworthy

projections than its driving GCM (ECHAM5) over West Africa, since it is better able to incorporate soil moisture feedbacks and topography. Further work is needed to assess other RCMs. This might be challenging using CORDEX, which is a matrix of GCM and RCM experiments from different modelling centres. RCMs have different physics from one another and from their driving GCMs making it difficult to diagnose distinctions between them.

This study aims to assess the extent to which the implications of global warming for African precipitation are different if inferred from regional versus global models, by analysing projections from an ensemble of five RCMs and GCMs produced by the Met Office Hadley Centre (MOHC) (Buontempo et al. 2013). These simulations are not only some of the first century-long experiments run over the CORDEX Africa domain, but also present a unique opportunity to examine the influence of regional modelling on responses to global warming. The five model versions differ from each other only in small parameter perturbations to the driving GCM, meaning it is possible to make inferences about the difference between the GCM and RCM based on consistency between the ensemble members.

The model dataset is described in the next section, followed by a brief description of the methodology for presenting projections associated with degrees of global warming. Then precipitation responses in the RCMs and GCMs are compared, to assess how far there are important distinctions. The atmospheric dynamics associated with the most noteworthy regional signals are then examined, to investigate possible mechanisms for precipitation change, and identify any difference in circulation between GCMs and RCMs. Next composites of wet and dry years from

the historical period will be used to compare dynamics associated with interannual precipitation anomalies in models and reanalyses. This analysis is designed to assess the confidence in dynamical responses in the GCMs and RCMs, with the potential to improve understanding of future risks for African climate, and to inform judgements of whether RCMs should be considered the preferred tool to produce climate change scenarios for decision making. The implications of the findings for African precipitation and for regional modelling will therefore be discussed before a summary is given in the final section.

6.2 Model data

The MOHC ensemble of five RCM simulations (Buontempo et al. 2013) was produced using HadRM3P (Jones et al. 2004): the same model used for the PRECIS Regional Climate Modelling System. It was run over the CORDEX Africa domain (Giorgi et al. 2009) at a grid-spacing of 50km, with 19 vertical levels, and the land surface scheme MOSES 2.2 (Met Office Surface Exchange Scheme version 2).

The boundary conditions were provided from five versions of the coupled GCM HadCM3, forced with historical emissions and SRES A1B from 1949 to 2100. HadCM3 has an atmospheric grid-spacing of 2.5° latitude and 3.75° longitude, and 19 vertical levels. Each of the five versions has slightly different atmospheric and land surface parameter values. The five ensemble members were selected from a larger perturbed physics ensemble of seventeen members (Collins et al. 2011) using a methodology outlined in McSweeney et al. (2012) and applied to Africa by

Buontempo et al. (2013), to eliminate model versions with a poor simulation of key features of African climate, and select a sub-set from the remaining members which captures the range of African temperature and precipitation projections. One of the versions chosen has the standard parameterisations of HadCM3 (Pope et al. 2000), and is identical to the version which has been widely used as part of the Coupled Model Intercomparison Project phase 3 (CMIP3) except for an interactive sulphur cycle, and the addition of flux adjustments included at the sea-surface to ensure that baseline sea-surface temperatures (SSTs) and sea-ice are close to observed.

The core physics of the GCM and RCM is broadly similar. The RCM physics is based on the atmospheric component of HadCM3 (HadAM3), but with some structural changes to the representation of clouds, and other parameters optimised to deliver improved model performance over land regions when run as a global atmospheric model at double the standard atmospheric resolution of HadAM3/HadCM3. Details are provided in Jones et al. (2004). Whilst there are important physical differences between GCM and RCM, these are much smaller than for most of the GCM/RCM combinations in CORDEX.

6.3 Methods

For both the GCMs and RCMs local changes associated with specific degrees of global mean temperature increase (ΔT_g) were calculated following Chapter 4, and the difference between each RCM response and that of its driving GCM was computed.

6.3.1 Increments of global mean temperature (ΔT_g)

Annual ΔT_g time-series were constructed for each GCM. Temperature data were weighted by grid-box area, and spatially averaged annual global means were calculated. The years 1985-99 were then averaged to create a reference climatology, and each year in the twenty-first century was differenced from this baseline. The analysis was also repeated with a 1955–69 start point to ensure that the results are robust to interdecadal variability.

The ΔT_g time-series were smoothed using 15 year running means. For each GCM, the date at which the resulting time-series crossed 1°C, 2°C, 3°C, 4°C of ΔT_g was extracted and defined as the median of a 15 year period, to be used to analyse local climate change in both the GCM and its corresponding RCM. The 15 year sample length was designed to eliminate interannual variability. Ensemble mean climatologies were computed using the maximum number of models available at each ΔT_g level: 5 at 1°C and 2°C, 4 at 3°C, and 2 at 4°C.

6.3.2 Local changes associated with ΔT_g

Precipitation anomalies relative to the 1985-99 reference were calculated for each available GCM and RCM and the ensemble mean, on a grid-point by grid-point basis, for each of the 1°C, 2°C, 3°C, and 4°C ΔT_g increments. These statistics were computed for the annual mean and 8 seasons, DJF, MAM, JJA, SON, JFM, AMJ, JAS, and OND (denoted by the initial letter of each month); since precipitation seasonality in Africa is regionally specific. The same procedure was repeated for associated

variables: temperature (T), specific humidity (q), horizontal moisture flux (qV), vertical velocity (ω), sea level pressure (SLP), and cloud.

The percentage of models with positive anomalies was calculated on a grid-point by grid-point basis to illustrate model agreement on the direction of change. Statistical significance tests of difference between the baseline and each of the 15 year sample climatologies (at 1°C, 2°C, 3°C, and 4°C) were undertaken to establish whether changes are significant relative to interannual variability. The Mann-Whitney *U* test was applied to each model and the ensemble mean, at a significance level of 5%, also on a grid-point by grid-point basis. The non-parametric test was chosen as precipitation has a skewed distribution in many arid regions. The direct method was applied due to the small sample size (15 years): for each year in the control, the number of years in the forced time period with a smaller value is counted, and the sum of these counts becomes the U statistic (U_1). This is repeated for the forced time period to get U_2, and the smaller of U_1 and U_2 is compared to the critical value. The percentage of models with significant change was computed to identify grid-points where there is agreement on a lack of signal. For the RCMs these tests were also computed at the GCM grid-spacing to allow for fair comparison between GCM and RCM.

6.3.3 Difference between GCMs and RCMs

Each RCM response was interpolated to the GCM grid-spacing and then differenced from the corresponding GCM response. It was not possible to use a

statistical test to establish whether the difference between GCMs and RCMs is robust to variation between ensemble members due to the small sample size. Instead, the number of model pairs which agree in the direction of the difference between GCM and RCM is considered.

6.4 Precipitation projections from global and regional models

Precipitation projections at 1-4°C ΔT_g are presented in Figure 6.1(a,b) for four seasons of relevance to regional precipitation in Africa. To give an overview of the dominant responses in the GCMs and RCMs, the mean of all model versions at each degree of warming is displayed separately for the GCM and RCM ensembles, but only where there is consensus between ensemble members. Areas with a lack of significant change are highlighted in grey. Consistent differences between GCM and RCM projections are shown in Figure 6.1c. The figure complements projections provided for each model at the end of the 21st century in Buontempo et al. (2013).

On a continental scale there is broad agreement between the GCMs and RCMs on the development of precipitation change with global warming. At 1°C ΔT_g both the GCM and RCM ensembles suggest that many regions would not experience significant change in seasonal precipitation relative to interannual variability (shown in grey). The most prominent exceptions are southern Africa in MAM, where both ensembles show a moderate drying response (0-1 mm day^{-1}); and positive anomalies in East Africa during DJF and north central Africa in SON. As global temperature

rises, there are larger changes in precipitation. Both ensembles project drying in southern Africa in JAS and SON, and in western Africa during MAM and JAS. The largest wet signals in are in the Congo Basin, and in eastern Africa: from 3°C there is consensus in both ensembles for positive anomalies in north east Africa in JAS and the Horn of Africa in SON and DJF. The main development from 2°C to 4°C is an increase in the magnitude and spatial extent of these anomalies, as has been found for other GCMs (Chapter 4). As the anomalies grow, and significance emerges over larger areas, there is increased consensus between the ensembles in terms of the direction of change.

Figure 6.1 Projected changes in seasonal precipitation (mm day^{-1}) at 1°C, 2°C, 3°C, and 4°C ΔT_g for GCM (a) and RCM (b) ensemble means, and the difference (GCM-RCM) (c). In (a) and (b) grid-points where <75% (100%) of models agree on the direction of change are white (stippled), and grid-points where none of the models experience significant change (5% level) are grey. Analysis on RCMs was conducted at the GCM resolution (analysis at native resolution leads to the same findings). In (c) white (stippled) areas indicated that <75% (100%) of models agree in the direction of difference between GCM and RCM. ➢

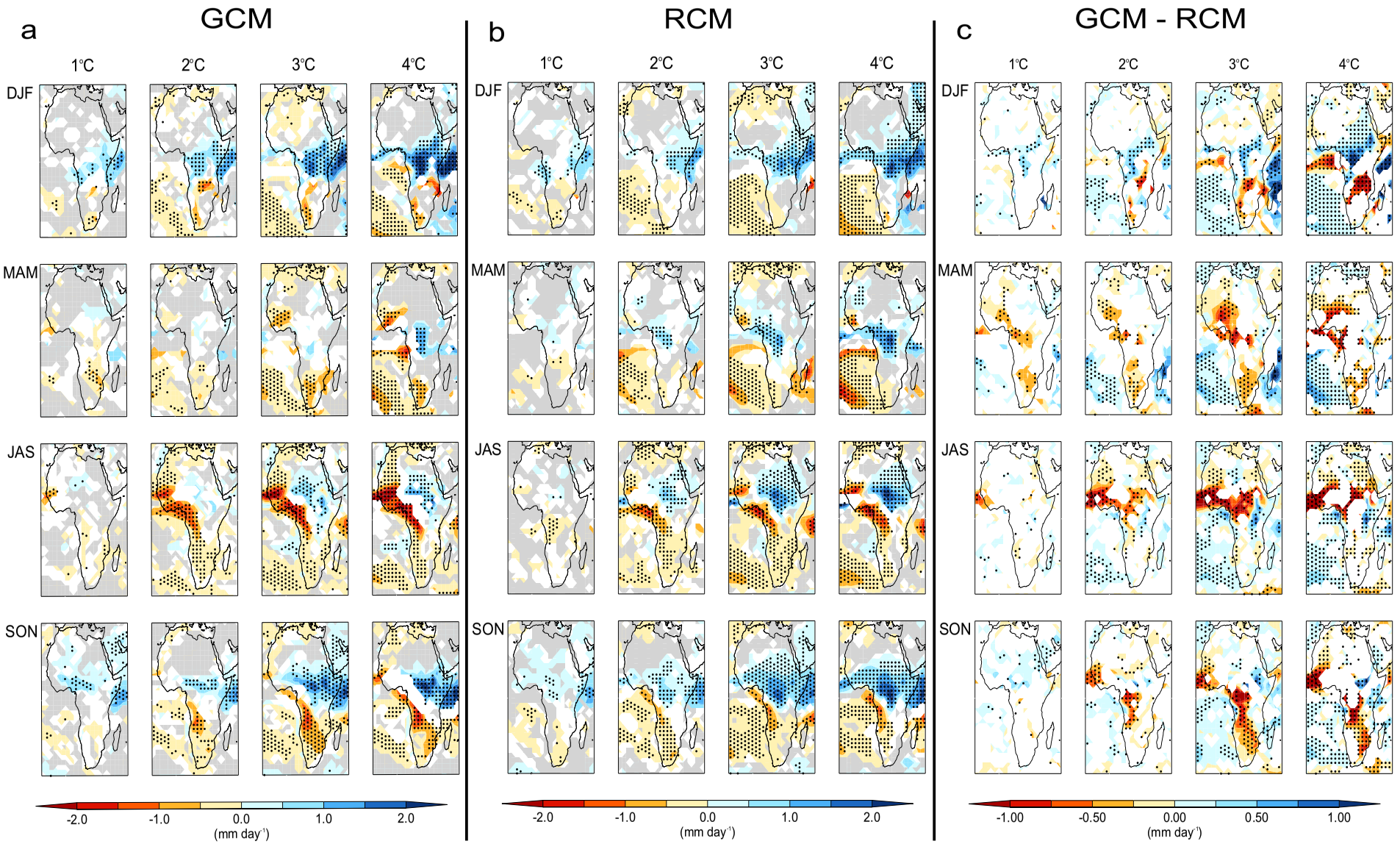
a
GCM
b
RCM
c
GCM - RCM
1°C
2°C
3°C
4°C
DJF
MAM
JAS
SON
-2.0
-1.0
0.0
1.0
2.0
(mm day-1)
-1.00
-0.50
0.00
0.50
1.00

There are however noteworthy distinctions between the GCMs and RCMs in terms of the magnitude, spatial extent, and level of agreement for regional signals. Many regions show consistent contrast between all five GCM and RCM pairs. The projected drying of southern Africa during SON, which has been reported in previous studies based on CMIP3, and may indicate a delay in the onset of the precipitation season (Shongwe et al. 2009; Chapter 4), is larger and more spatially extensive in the GCMs from 3°C: by >0.5 mm day^{-1} in places, as shown in Figure 6.1c. The GCMs also show more drying in this region during MAM. Another important contrast is in north east Africa during JAS, where both ensembles show a wetting response, but this is stronger in the RCM, at >2 mm day^{-1} in parts of Sudan from 3°C.

The most prominent contrast by far is in West Africa. During the monsoon season (JAS) the GCMs experience a strong drying in this region. At 1°C it is restricted to West Sahel and <1 mm day^{-1}, but by 2°C all five model versions show a dry signal in west Sahel, west Sahara, at the Guinea Coast, and in west equatorial Africa. For a 4°C warming this is >2 mm day^{-1} in many of these regions and there is also drying >1 mm day^{-1} in parts of western Africa during MAM and SON. Previous studies have found precipitation decline in west Sahel in CMIP3 and CMIP5 simulations (Monerie et al. 2012a; Chapter 4) and demonstrated that perturbed versions of HadCM3 produce greater drying than any of the CMIP3 models in West Sahel (Chapter 5), and the Congo Basin (Chapter 9). The RCMs also show negative anomalies associated with global warming, in West Sahel and west equatorial Africa during JAS, and to the west of the Guinea Coast in MAM. However, as illustrated in Figure 6.1c, the dry signal is weaker and less spatially extensive. In particular, the

RCMs show no significant change over a latitudinal band between the Guinea Coast region and the Sahel (approximately 8-10°N).

Figure 6.2 shows the range of GCM and RCM projections averaged over selected West African regions during JAS, providing further evidence that the difference is consistent between model versions. In West Equatorial Africa the magnitude of change and development of anomalies with global warming is similar for the GCMs and RCMs, but moving north into drier regions the difference is greater: at the Guinea Coast, and especially in West Sahel, where the GCMs show larger anomalies and a larger rate of change with global warming. In the Central Sahel most models show a wetting response and this is generally larger and more consistent in the RCMs.

Given the severity of impacts associated with multi-decadal drought in the Sahel during the twentieth century, there is a great deal of interest in understanding how the West African Monsoon (WAM) will be influenced by global warming. Precipitation decline could have serious connotations for food security, and projections of pronounced drying might therefore be an essential consideration for adaptation and mitigation decisions if deemed to be plausible. Understanding the drying responses in the GCMs and RCMs is therefore a high priority, and it is important to assess whether either can be deemed more realistic: the difference in the magnitude of the response is large (>1 mm day^{-1} from 2°C in the ensemble mean), particularly considering the aridity of the region. In the next section we examine changes in circulation associated with global warming, to try to understand why the

models show drying in west Sahel, and why this is larger in the GCMs than in the RCMs.

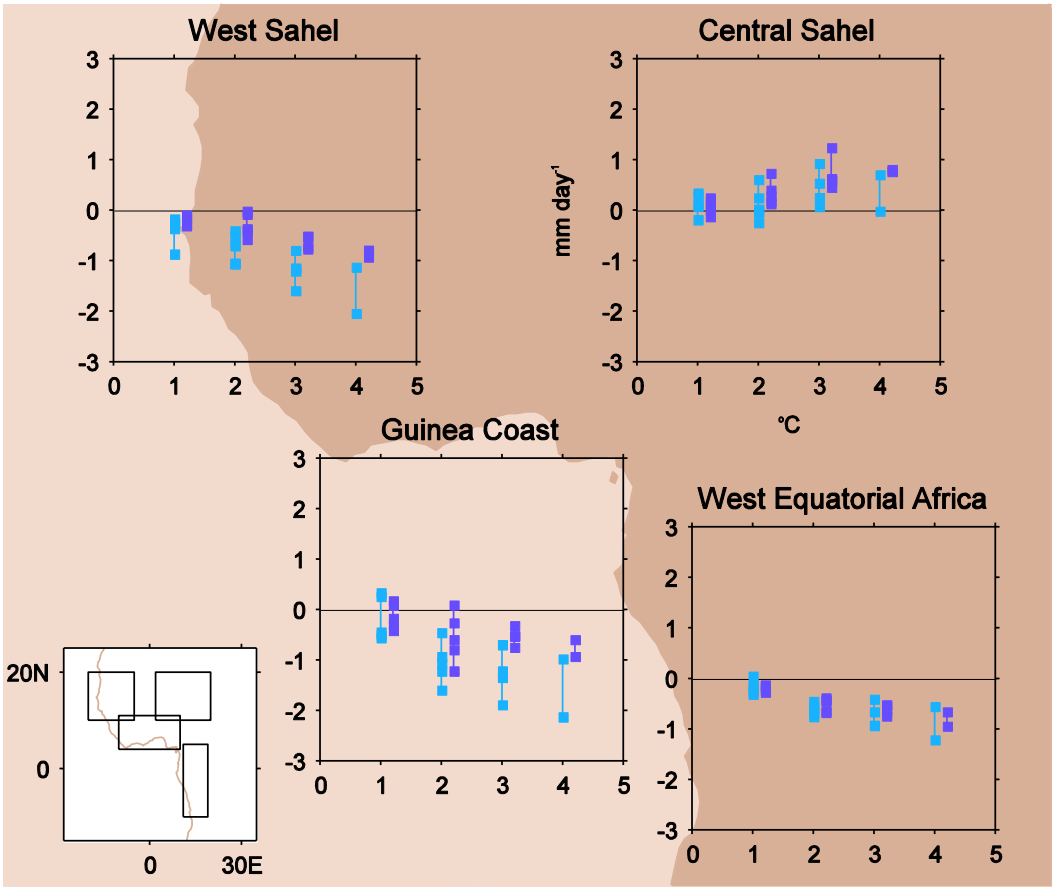

Figure 6.2 Projected changes in JAS precipitation (mm day^{-1}) at 1°C, 2°C, 3°C, and 4°C ΔT_g for selected West African regions, in GCMs (blue), and RCMs (purple). Coordinates are provided in Table 6.S1.

6.5 Modelled circulation changes associated with global warming

The meridional circulation in West Africa exerts an important influence on precipitation, therefore in order to infer mechanisms for drying in the GCMs and RCMs, cross sections of meridional wind (v) and vertical velocity (ω) are examined over the core region of negative precipitation anomalies. To give an insight into the spatial patterns of change, maps illustrating anomalies in key atmospheric variables across the African continent are also inspected.

6.5.1 Changes in meridional circulation

Figure 6.3 presents longitude-height cross sections of zonal mean wind circulation over West Africa (10°W to 0) during JAS for the GCM and RCM ensemble means. Plots for individual models are similar (not shown). In the twentieth century climatology, both the GCMs and the RCMs show monsoon inflow near the surface at the Guinea Coast (approximately 5°N), which penetrates to 20°N, and feeds deep convection across these latitudes, only constrained by the anticylonic circulation of the Saharan high which produces subsidence in the upper troposphere (200-500hPa) from 19°N in the GCM ensemble mean. This subsidence is more extensive in the RCMs, meaning convection is confined to slightly lower altitudes and latitudes. Both ensembles show southward flow at 250hPa over the Guinea Coast, and subsidence above the Gulf of Guinea.

As global temperature rises, the Saharan high migrates southwards in the GCMs, and to a slightly lesser extent in the RCMs. There is an increase in subsidence over the Sahara and northern Sahel. In both ensembles the monsoon circulation at the Guinea Coast moves north, allowing the subsidence over the Gulf of Guinea to spread to approximately 4°N, and reducing convection in the southern Sahel. This is clarified by anomaly plots at 1-4°C (Figure 6.4), which confirm that there are downward ω anomalies at all altitudes over the Guinea Coast and southern Sahel, and in the upper atmosphere further north. There is a corresponding weakening of the southward outflow from the Sahelian convection, at 250hPa, which may be associated with a reduction in the strength of Tropical Easterly Jet (TEJ). Near the surface, the monsoon flow is strengthened from 2°C, as is convection in the northern Sahel up to approximately 600hPa, at which height it meets anomalous subsidence from the strengthened Saharan high and is diverted southwards, reinforcing downward anomalies near 10°N.

Figure 6.3 Latitude-height cross sections of streamlines (v; -ω*100) averaged 10°W to 0 during JAS, for the GCM and RCM ensemble means, in the twentieth century reference period, and for the 15 year periods which correspond to 1-4°C ΔT_g. For clarity, the RCM is plotted at GCM resolution (equivalent figures at native resolution produce the same findings).

➢

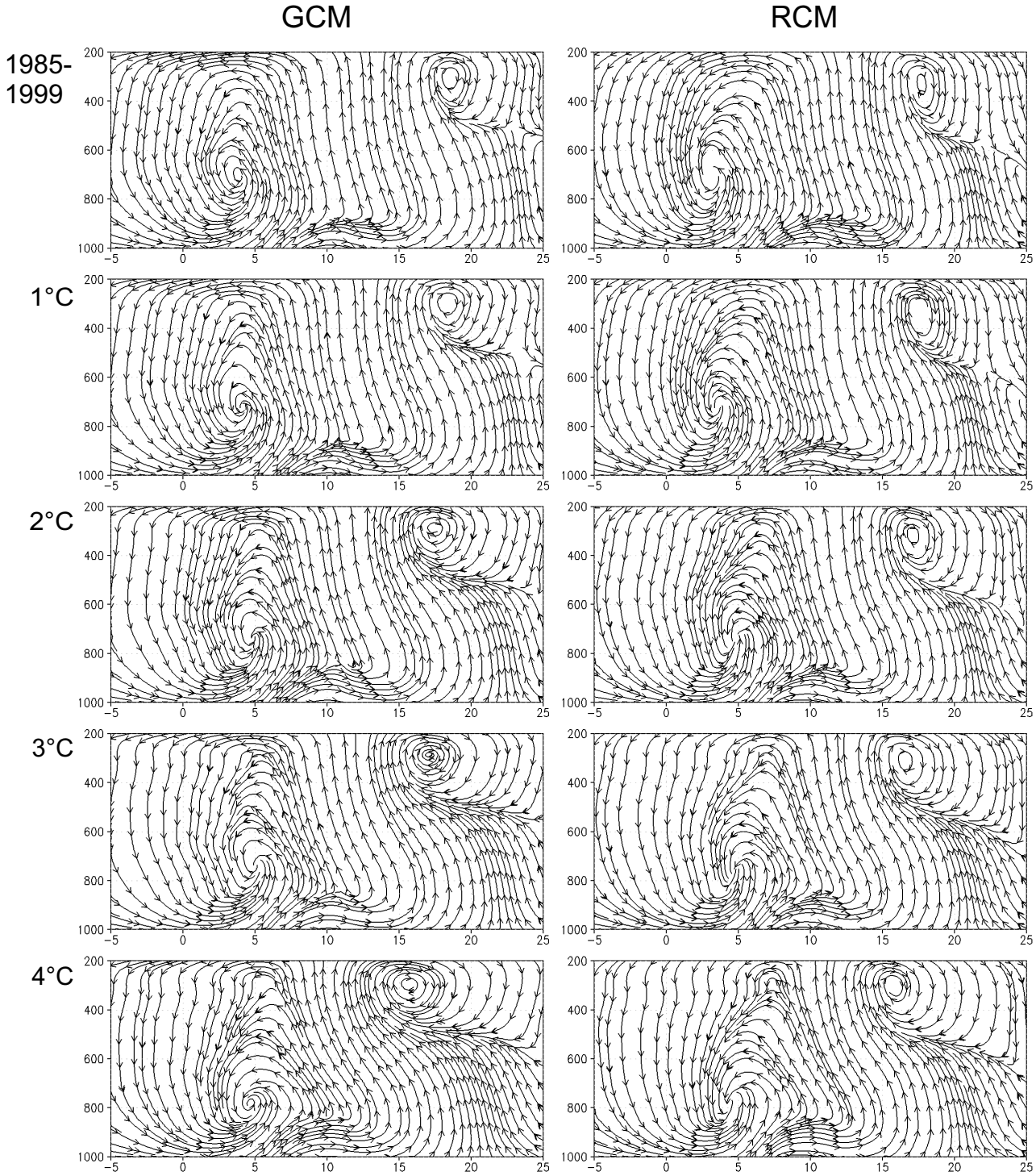
GCM
RCM
1985-1999
1°C
2°C
3°C
4°C
200
400
600
800
1000
−5
0
5
10
15
20
25

These dynamical changes develop progressively from 1 to 4°C and are remarkably similar between the GCMs and RCMs. The main difference between the ensembles is at 600hPa and 10°N, where both exhibit northerly flow but the RCMs do not show downward anomalies as in the GCMs. This may be responsible for the lack of significant precipitation decline in the RCMs at this latitude.

6.5.2 Spatial patterns of change

Responses to global warming across the African continent in the GCMs and RCMs are presented in Figure 6.5 for selected atmospheric variables in JAS. As in Figure 6.1 the ensemble means are shown but with masks to indicate regions where there is a lack of significance or lack of agreement between models. Maps of ω at 400hPa substantiate findings from Figure 6.4 of downward anomalies in the upper atmosphere. For each ensemble the spatial pattern of change closely matches the precipitation anomalies in Figure 6.1, with downward anomalies in West Sahel, the Guinea Coast, and the Congo Basin, of >1.8hPa s^{-1} at 4°C in both the GCM and RCM ensemble mean, but with a larger spatial extent in the global models. In north central Sahel both ensembles show smaller upward anomalies (approximately 0.8hPa s^{-1}) corresponding to the wet signal in Figure 6.1. These changes are amplified with global warming. This suggests a strong association between ω at 400hPa and simulated precipitation.

Figure 6.4 as Figure 6.3 but for anomalous streamlines at 1-4°C ΔT_g. Green shading indicates the percentage of models which show significant change (in either v or ω) of the same direction (5% level). ➢

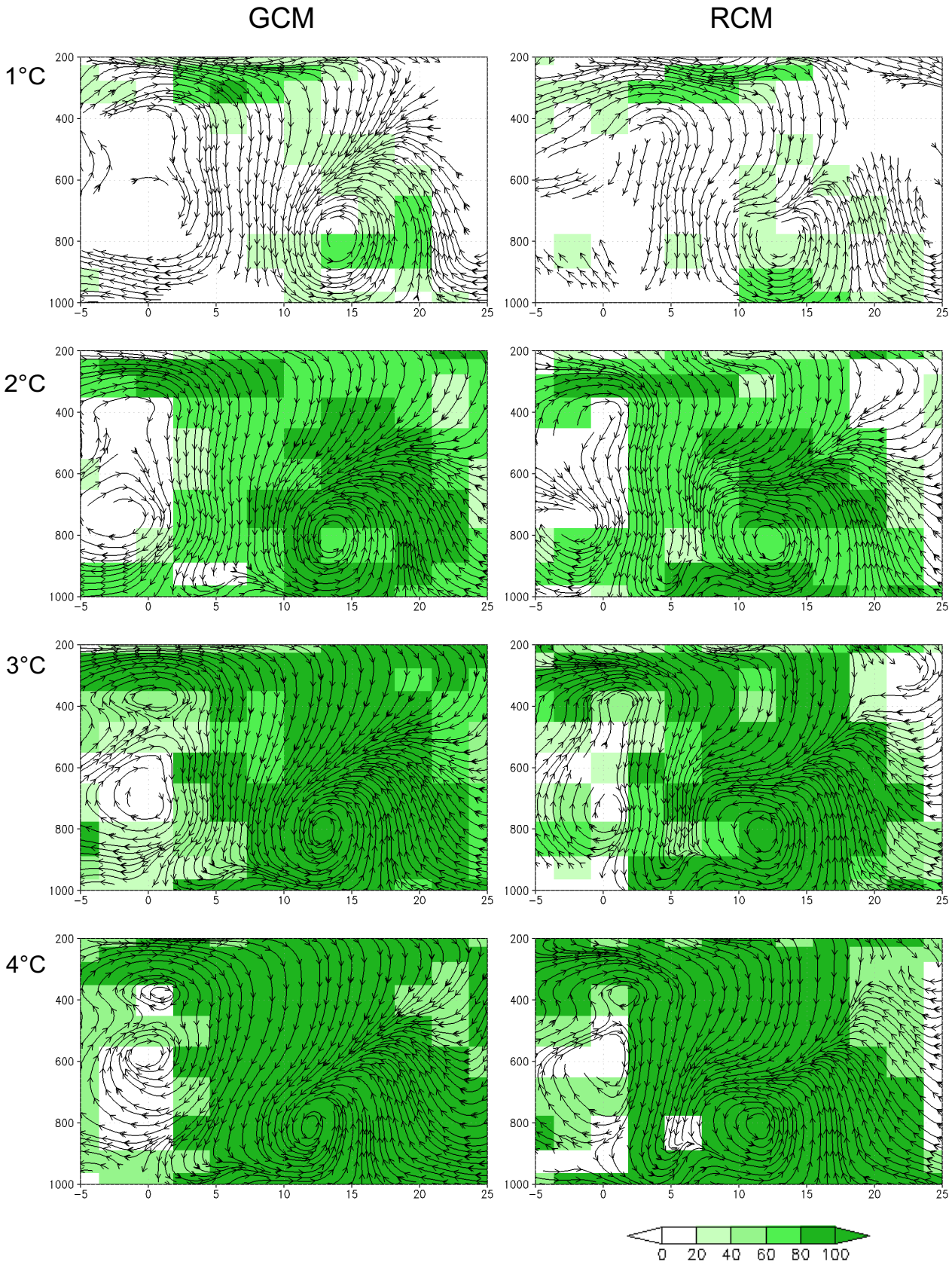
GCM
RCM
1°C
2°C
3°C
4°C
200
400
600
800
1000
−5
0
5
10
15
20
25
0
20
40
60
80
100

There are also downward anomalies at lower levels in the Congo Basin (to 700hPa) and the Guinea Coast (to 850hPa) (see Figure 6.S1), but in the north west Sahel the maps show an increase in convection in the low to mid troposphere, in keeping with Figure 6.4. This anomalous convection increases in amplitude and spatial extent with global warming, and has a stronger signal in the GCMs than the RCMs. The $q\vec{V}$ maps demonstrate that the increased northward wind flow noted in the meridional cross sections is part of a large scale amplification or northward shift of the monsoon, with an increase in moisture flux from the Atlantic and the Guinea Coast (where there is divergence) to the northern Sahel (where there is convergence). This moisture convergence is at approximately 18°N in west Sahel and slightly further north (22°N) in central and east Sahel in both ensembles.

Figure 6.5 Projected responses to global warming during JAS for ω at 400hPa and 850hPa (hPa s^{-1}), $q\vec{V}$ at 925hPa (kg kg^{-1} ms^{-1}) with contours of moisture divergence (kg kg^{-1} s^{-1}), q at 925hPa (kg kg^{-1}), and temperature at 1000hPa (°C); in GCM (a) and RCM (b) ensemble means, and the difference (GCM-RCM) (c). For all variables except $q\vec{V}$ significance and intermodel agreement is shown as in Figure 6.1. For $q\vec{V}$ and contours of divergence, in (a) and (b) white areas indicate that <75% models agree in the direction of change or all models show no significant change, and in (c) white areas indicated that <75% of models agree in the direction of difference between GCM and RCM. Analysis on RCMs was conducted at the GCM resolution (analysis at native resolution leads to the same findings). ➢

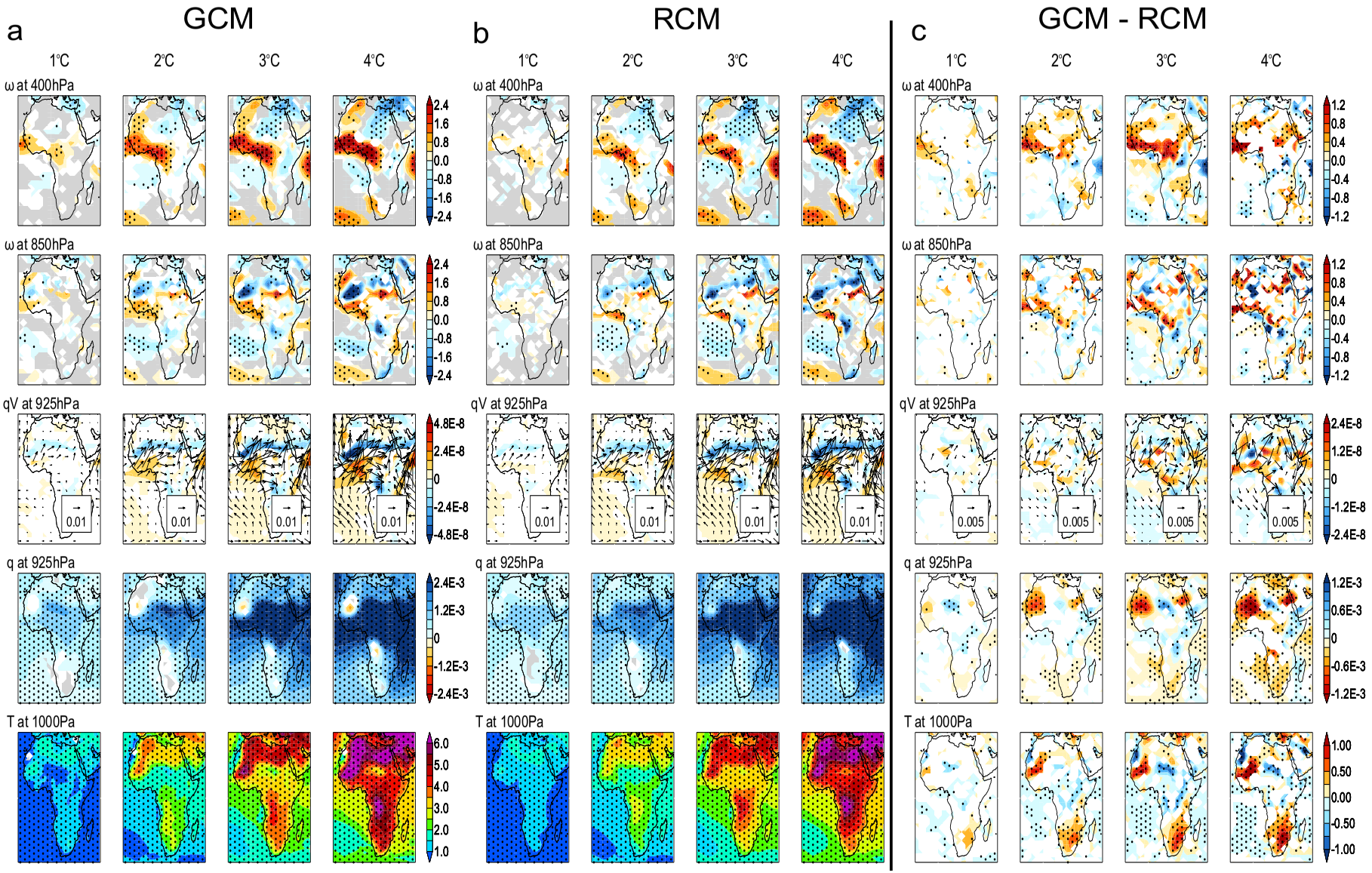
a
GCM
b
RCM
c
GCM - RCM
1°C
2°C
3°C
4°C
ω at 400hPa
ω at 850hPa
qV at 925hPa
q at 925hPa
T at 1000Pa
2.4
1.6
0.8
0.0
-0.8
-1.6
-2.4
4.8E-8
2.4E-8
0
-2.4E-8
-4.8E-8
0.01
2.4E-3
1.2E-3
-1.2E-3
-2.4E-3
6.0
5.0
4.0
3.0
2.0
1.0
1.2
0.8
0.4
0.0
-0.4
-1.2
0.005
1.2E-8
-1.2E-8
-2.4E-8
0.6E-3
-0.6E-3
-1.2E-3
1.00
0.50
0.00
-0.50
-1.00

6.5.3 Discussion

The GCM and RCM ensembles therefore show similar changes in horizontal and vertical circulation in response to global warming. So why might these atmospheric dynamics be associated with drying in West Africa, and why do the GCM and RCM project different magnitudes of precipitation change?

6.5.3.1 Hypothesised mechanisms for drying

The increase in moisture convergence and convection found near the surface of west Sahel may seem contradictory with the strong precipitation decline. Many previous studies have postulated that a strengthening of the WAM would be a plausible response to global warming, due to changes in inter-hemispheric SST gradients (e.g. Hoerling et al. 2006), an increase in the land-ocean temperature contrast (Haarsma et al. 2005), or a deepening of the Saharan Heat Low (SHL) (Biasutti et al. 2009). This is expected to lead to wetter conditions in the Sahel. The strengthening of the monsoon found in the GCMs and RCMs used here may be responsible for the wetting in central and east Sahel. It might also explain the drying at the Guinea Coast and the Congo Basin: the dipole between the Guinea Coast and the Sahel caused by a northward shift in the monsoon is well known (e.g. Vizy and Cook 2002), and some also relate precipitation in Central Africa to latitudinal changes in tropical convection (e.g. Tokinaga and Xie 2011).

In west Sahel, however, there is no corresponding increase in precipitation, but rather some of the largest negative anomalies experienced anywhere on the

continent. This is likely due to the ω changes aloft, which cap the anomalous uplift from the surface at approximately 500hPa; in contrast to central Sahel, where there are upward anomalies throughout the atmospheric column (Figure 6.S2). The increase in subsidence must be large enough to force a reduction in precipitation. q decreases near the surface of west Sahel (Figure 6.5) despite the anomalous moisture convergence and the general increase in atmospheric moisture content in response to global warming (e.g. Allen and Ingram 2002). This means that whilst there is anomalous convection in this region, this is not an increase in moist convection: lapse rates of potential temperature between the surface and 600hPa decrease with global warming (not shown) indicating that convection becomes drier.

The zonal contrast in ω anomalies, possibly remotely forced, therefore appears to explain the drying in west Sahel despite the increase in the monsoon. Previously many CMIP3 (Monerie et al. 2012b) and CMIP5 (Monerie et al. 2012a) models have also been shown to exhibit a strengthened monsoon flow, but precipitation decline in west Sahel in association with downward anomalies. It is even conceivable that drying of west Sahel could have feedback effects which strengthen the monsoon. Both GCMs and RCMs project an associated reduction in cloud (not shown) and large temperature anomalies at the surface of the west Sahel and west Sahara (>6°C for a 4°C global warming; Figure 6.5) relative to the rest of Africa and the surrounding oceans. SLP consequently decreases (not shown) suggesting a strengthening of the SHL, which could act to enhance the WAM. This possibility complicates the relationship between the heat low and precipitation presented by Biasutti et al (2009), who find that a stronger SHL leads to a wetter Sahel. The role of

the SHL may be contingent on the location of maximum warming, as implied by Vizy et al. (2013).

As well as influencing the monsoon, the heat low region has an influence on the African Easterly Jet (AEJ). As west Sahel becomes drier in the models, there is an increase in temperature, decrease in humidity, and decrease in pressure relative to the Guinea Coast. Strengthening and southward migration of these gradients (not shown), may be responsible for the increase and southward shift of the AEJ which is found in the qV anomalies at 700hPa and 600hPa (Figure 6.S3), and the southward anomalies at these levels in Figure 6.4. Many authors have linked changes in the AEJ to Sahel precipitation (e.g. Jenkins et al. 2005; Sylla et al. 2010): it may have a feedback effect via the influence on the African Easterly Waves (Nicholson and Grist 2003), and through moisture export to the Atlantic. So whilst the convection in northern Sahel may not be expected together with negative precipitation anomalies, it could in fact be a response to drying and pronounced warming, which may be associated with feedback effects via the WAM and/or AEJ.

6.5.3.2 Difference in dynamics between GCM and RCM

Figure 6.5c demonstrates that there are consistent differences in dynamics between the RCMs and the GCMs, but these are in the amplitude and spatial extent of the anomalies: the difference is in magnitude rather than in kind. The largest qualitative difference in the precipitation signal is at 8-10°N, where the GCMs show drying but the RCMs show no significant change, and this is explained by corresponding differences in the omega fields at 700-400hPa (Figure 6.S1) and

moisture divergence at 850hPa (Figure 6.S3). However, the GCMs also have a weaker precipitation response here relative to stronger drying in west Sahel and at the Guinea Coast, and so this also appears to be a difference in the spatial extension of the signal rather than a difference in mechanism.

The smaller precipitation anomalies in the RCMs are therefore not due to different atmospheric dynamics but a weaker version of the same mechanism. The similarity to the GCMs is an important finding in itself for regional modelling. The RCMs have optimised physics and a higher resolution than the GCMs and therefore would not necessarily be expected to reproduce the same dynamical response to anthropogenic forcing. The reason for the weaker circulation changes in the RCM is still unclear, but having identified a characteristic dynamical response which is common to both ensembles we can now investigate the reliability of this mode, and this may provide evidence with which to judge whether the GCM and RCM projections are realistic.

6.6 Dry year dynamics in models and reanalysis

It is impossible to validate atmospheric changes associated with global warming, so instead dry years in the models' twentieth century runs will be examined. If the modelled circulation anomalies during these dry years are similar to those associated with drying in response to global warming; the modelled dry years can be compared to dry years in reanalysis to assess the reliability of the response. Here the

GCM and RCM ensembles are presented alongside NCEP-NCAR reanalysis 1 (NCEP) (Kalnay et al. 1996) and ERA-interim (ERA-I) (Dee et al. 2011).

Composites of the 10 wettest and 10 driest years in West Sahel (20W-0; 10-20N, following (Hastenrath 2000)) were created from precipitation time-series for each model (1960-1999) and the two reanalysis datasets (1979-2009, due to availability of ERA-I). The difference between dry and wet composites (dry-wet) was calculated for a range of atmospheric variables, and tested for significance relative to variation between years using the Mann-Whitney U-test. For all datasets the tests were computed at native resolution, and at the GCM grid-spacing to allow for fair comparison.

The spatial signatures of the precipitation composites are presented in Figure 6.6 to provide a context for the investigation of atmospheric dynamics. During dry years in west Sahel the GCMs and RCMs also experience drying over parts of the west Sahara, the Guinea Coast, the west of the Congo Basin, and in most models, the central Sahel. This is very similar to the spatial pattern of change in their precipitation projections (Figure 6.1) (with the exception of central Sahel), suggesting that the composites are a useful means of appraising the dry signal associated with global warming. The precipitation maps for the reanalysis are different (Figure 6.6). The largest anomalies are in central Sahel, to the south of the Sahel, and in parts of central Africa, rather than in west Sahel. This suggests a difference in modes of interannual variability between the models and reanalysis, which is now explored further through meridional circulation anomalies and spatial patterns of change in selected atmospheric variables.

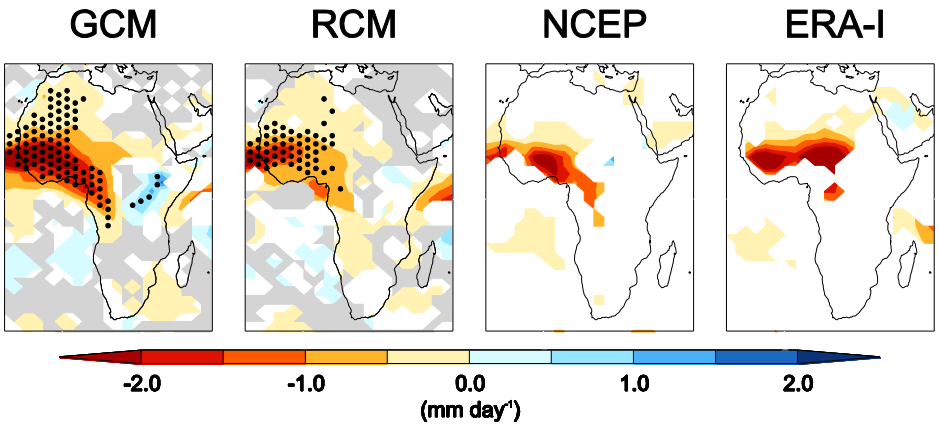

Figure 6.6 Dry minus wet composite JAS precipitation (mm day^{-1}) for GCM and RCM ensemble means, NCEP, and ERA-I. For reanalysis, only areas where the difference between dry and wet composites is significant relative to variation between years are shown (5% level). For model ensembles, areas where <4 (all 5) models agree in the direction of difference between dry and wet years are white (stippled), and grey indicates that all models show no significant difference between dry and wet composites relative to variation between years (5% level). All datasets have been analysed at GCM grid-spacing (analysis at native resolution leads to the same findings).

6.6.1 Meridional circulation anomalies

Before examining the dynamics associated with dry years, the long term mean circulation in each dataset is inspected (Figure 6.7). The model ensembles show almost identical flow as for the 1985-99 mean in Figure 6.3, described in section 6.5.1. Whilst they have a relatively good representation of the meridional circulation in comparison to some CMIP3 models (see Cook and Vizy 2006), there are important differences from the reanalyses.

In both the GCMs and the RCMs there is convection from approximately 5°N to the Sahara, with little to prevent uplift; whereas NCEP shows two distinct zones of convergence, with deep moist convection between 5 and 10°N, and a shallower region of dry convection associated with the thermal low in the southern Sahara. In between these two zones upward motion is restricted to higher levels (above approximately 600hPa) and the monsoon flow at the surface is vertically confined by southward and downward motion at 800hPa. The ERA-I plot is more similar to the models', but the equivalent figures at native resolution (Figure 6.S4) demonstrate that this dataset also shows convection to be restricted in the southern Sahel by southward flow at 700hPa.

Figure 6.7 Latitude-height cross sections of streamlines (v ; -ω*100) averaged 10°W to 0 during JAS, for the long term mean (1960-1999 for models, 1979-2009 for reanalysis), dry, wet, and dry minus wet composites; for GCM and RCM ensemble means, NCEP, and ERA-I. For the reanalysis the green shading on the dry-wet plots indicates significance difference between dry and wet composites (in either v or ω) relative to variation between years within the composites. For the model ensembles, the green shading indicates the percentage of models which show significant difference between dry and wet composites (in either v or ω) of the same direction (5% level). All datasets are plotted at the horizontal and vertical resolution of the GCM. Equivalent figures at native resolution are provided as Figure 6.S4.

➢

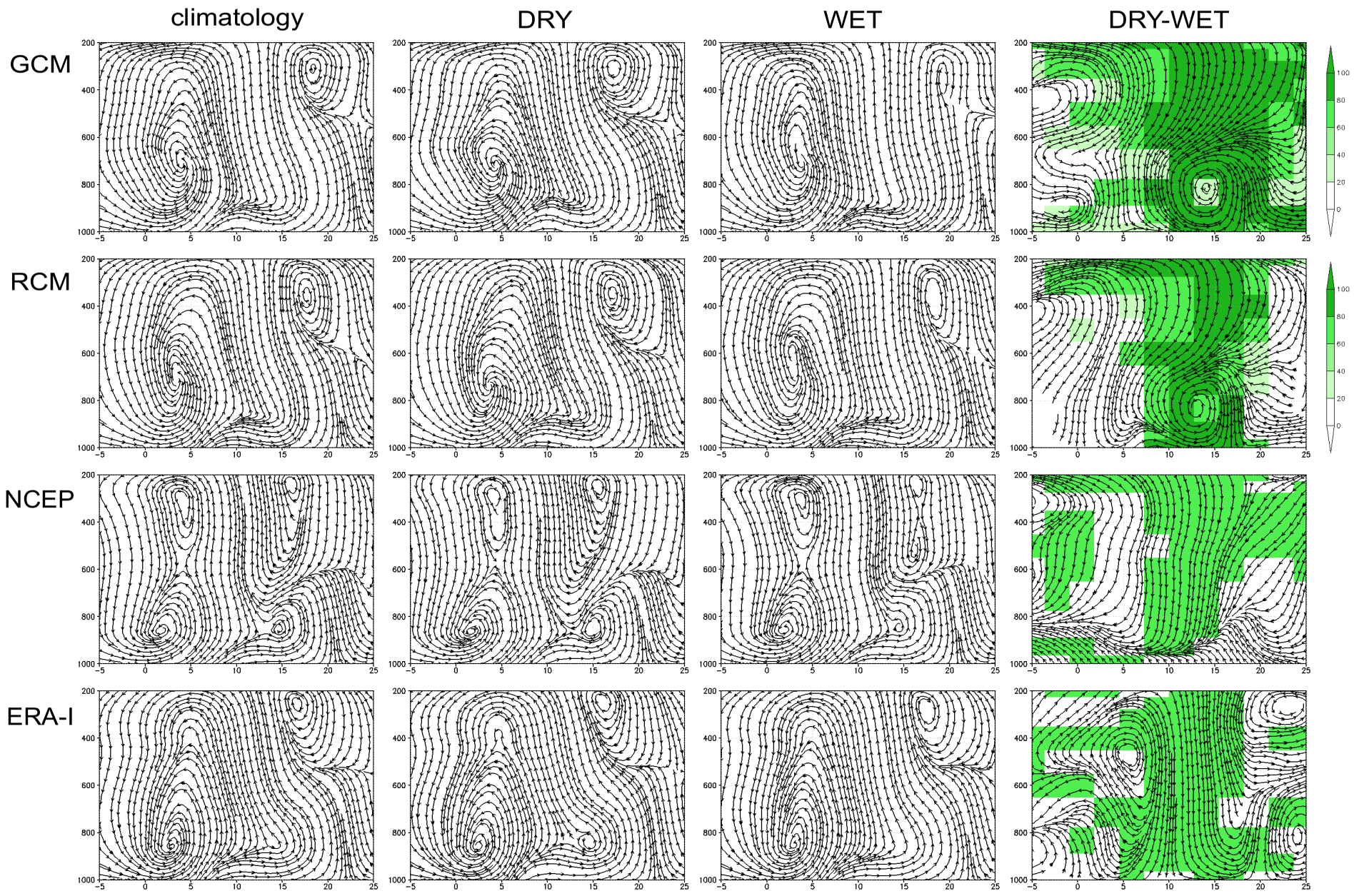
climatology
DRY
WET
DRY-WET
GCM
RCM
NCEP
ERA-I
200
400
600
800
1000
−5
0
5
10
15
20
25
100
80
60
40
20
0

In all datasets, the uplift in the Sahara is capped by subsidence from the Saharan high, but this occurs at lower levels and lower latitudes in the reanalyses relative to the RCMs and especially the GCMs; meaning the models are missing the southward outflow from the Saharan high at 600hPa which is associated with the AEJ. Note that there are also important differences between ERA-I and NCEP: prominently NCEP shows sinking air to 900hPa at 12°N which is not found in ERA-I.

Given the differences in background climatology we might also expect differences between datasets in the dynamics associated with dry and wet years. The model ensembles' response in dry years is very similar to their response to global warming: the dry-wet composites in Figure 6.7 correspond closely to the anomaly plots in Figure 6.4 (see Figure 6.S5 for a direct comparison). There are downward anomalies above 500hPa from 5°N to the Sahara, and there is the same anomalous overturning nearer the surface, with an increase in monsoon flow, uplift in northern Sahel, southward motion at 600hPa, and downward anomalies in southern Sahel.

The reanalyses show different dynamics from the models. The main distinction between dry and wet composites is in the amount of convection over the Sahel. The dry-wet composites show significant downward anomalies from just above the surface to 200hPa and from approximately 8-15°N in both NCEP and ERA-I. There are also differences between the reanalysis products. They each share some but not all of the features shown by the models. ERA-I, like the GCMs and RCMs, suggests that the Saharan high moves further south in dry years, and has significant upward anomalies near the surface of the northern Sahel/southern Sahara, although

these are further north than in the RCM. NCEP also has an increase in convection at the surface of the northern Sahel, but it is confined to lower levels (800hPa) than in the models and ERA-I (600hPa).

6.6.2 Spatial anomaly patterns

The meridional cross sections suggest that the GCMs and RCMs have similar dynamical responses to global warming as during twentieth century dry years. The spatial patterns of change in Figure 6.8 support this finding. As at 2-4°C ΔT_g, the anomalies associated with dry (minus wet) years include subsidence at 400hPa (>1.5 hPa s^{-1} over much of west Africa in the GCM and RCM ensemble means), and large warming near the surface of west Sahel (>2°C in the GCM mean). In both the GCMs and RCMs there is uplift in low levels of the northern Sahel, but also a decrease in q suggesting this is dryer convection than in wet years (which is confirmed by lapse rates of potential temperature; not shown). This dry convection meets the subsidence aloft and is diverted south, as shown in southward anomalies of qV at 600hPa, which are associated with large scale moisture divergence in West Africa (Figure 6.S8), and subsidence over the Guinea Coast.

Near the surface there is moisture flux from southern to northern West Africa and moisture convergence in northern Sahel. However, this is not associated with a large scale increase in the monsoon as in response to global warming. In fact, qV anomalies at 925hPa in the Atlantic suggest a weakening of the monsoon. This may explain the different sign of anomalies in the central Sahel. Another differences

in qV between the dry-wet composites and the anomalies at 1-4°C is in the low level westerlies (LLWs) from the Atlantic at 850hPa (Figure 6.S3, 6.S9), which decrease (increase) in dry years (future). The composites therefore imply that decreases in LLWs and a reduction in the monsoon are associated with drying, as would be expected from previous literature (e.g. Nicholson 2009; Sylla et al. 2010), but this does not fit with the models' response to global warming. It could be that other drivers, for example subsidence in the upper troposphere, are sufficient to cause drying in the future simulation *despite* increases in the WAM and LLWs. Or it might be that the drying in future, when combined with global warming, leads to a larger magnitude temperature increase in west Sahel and North Africa, and the increased land-sea contrast *forces* an increase in the WAM and LLWs.

Figure 6.8 Dry minus wet JAS composites for ω at 400hPa and 850hPa (hPa s^{-1}), qV at 925hPa (kg kg^{-1} ms^{-1}) with contours of moisture divergence (kg kg^{-1} s^{-1}), q at 925hPa (kg kg^{-1}), and temperature at 1000hPa (°C), for GCM and RCM ensemble means, NCEP, and ERA-I. For all variables except qV for models, significance and intermodel agreement is shown as in Figure 6. For qV and contours of divergence in models, white areas indicate <4/5 models agree in the direction of difference between composites or all models show no significant difference. The same figure with no significance testing is provided in Figure 6.S6, and dry and wet composites are provided in Figure 6.S7. All datasets have been analysed at GCM resolution (analysis at native resolution leads to the same findings). ➢

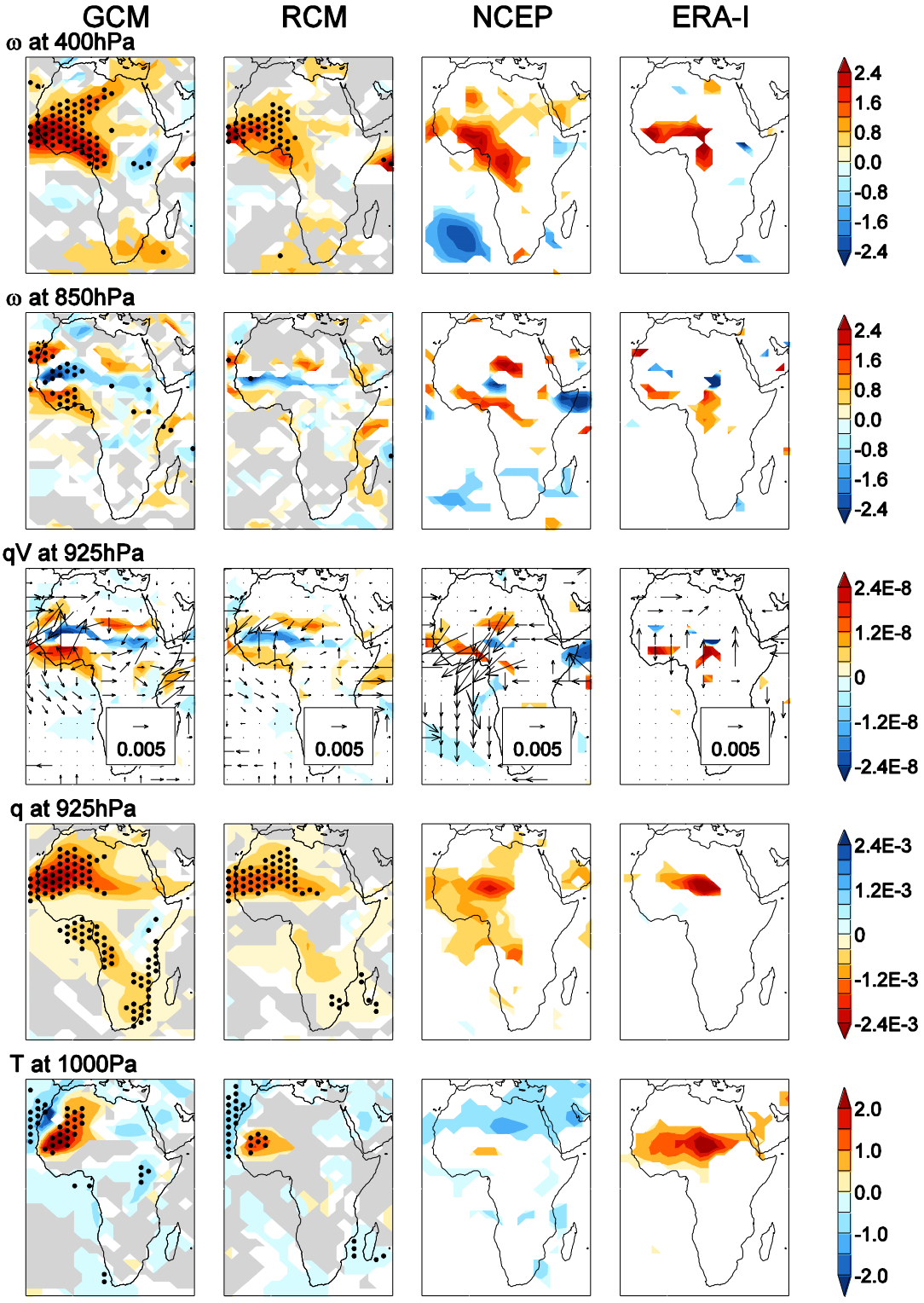
GCM
RCM
NCEP
ERA-I
ω at 400hPa
2.4
1.6
0.8
0.0
-0.8
-1.6
-2.4
ω at 850hPa
2.4
1.6
0.8
0.0
-0.8
-1.6
-2.4
qV at 925hPa
0.005
0.005
0.005
0.005
2.4E-8
1.2E-8
0
-1.2E-8
-2.4E-8
q at 925hPa
2.4E-3
1.2E-3
0
-1.2E-3
-2.4E-3
T at 1000Pa
2.0
1.0
0.0
-1.0
-2.0

There are thus some aspects of the dynamics associated with global warming which cannot be appraised based on the composites. The circulation anomalies nevertheless show sufficient similarity between composite and future simulation to imply that the main responses associated with drying are consistent. And whilst some of these are shared by the reanalysis, other elements are distinct. All of the datasets show close correspondence between precipitation anomalies and ω at 600-400hPa (Figure 6.8, 6.S8). There are also easterly anomalies in all datasets near the Guinea coast at 700-600hPa (Figure 6.S9), implying a strengthening of the AEJ; and, as noted from the meridional cross sections, both NCEP and ERA-I show some upward anomalies at 850hPa in the Sahel, possibly representing a more muted version of the stronger increase in convection in the models. Both of these changes are likely responses to rather than causes of drying, but, as discussed in section 6.5.3, may have feedback effects. Given the much larger amplitude in the models (particularly the GCMs), any feedback effects would be exaggerated in comparison to the reanalyses.

The magnitude of drying in the reanalyses would not seem to be derived from feedbacks but from larger forcings. In NCEP there are large $q\vec{V}$ anomalies at 925hPa which show north easterly moisture flux from the central Sahel to the Atlantic, indicating a weakening of the WAM which is not matched by the models or ERA-I. And, in both NCEP and ERA-I there would appear to be strong connection with ω in the lower troposphere over west Sahel (seen in Figure 6.7 at 850hPa and Figure 6.S8 at other levels), which is not shown by the models. Correlations between ω at 700hPa and precipitation suggest that this is a strong relationship in both NCEP and ERA-I (r=-0.9 and -0.8 respectively), but not in the GCMs or RCMs. Hastenrath

(2000) also finds that dry years in NCEP are associated with anomalous subsidence throughout the atmospheric column.

6.6.3 Discussion

In summary, whilst there are some differences between modelled dry years and the modelled response to global warming, there appears to be a common mode, with the largest precipitation anomalies in west Sahel, downward anomalies in the upper troposphere, and possible feedback effects linked to a strong warming of the heat low region. This is remarkably consistent in character between the GCM and RCM ensembles, the main difference being in the magnitude of precipitation and associated circulation anomalies, which is substantially larger in the GCM, both in twentieth century dry years, and in response to global warming. The reanalyses have some points of similarity with the modelled mode, suggesting that the atmospheric dynamics in the model are not necessarily implausible; but the differences are sufficient to show that the mode is not found in the reanalyses: NCEP and ERA-I do not have a dominant response in west Sahel, and appear to have additional forcings during dry years. Although there is uncertainty in the understanding of West African climate dynamics, and differences between NCEP and ERA-I, these are not as large as the differences with the models. It is therefore possible to conclude that the GCM and RCM show a circulation mode which is not found in reanalyses. So what does this tell us about how West African precipitation might respond to global warming? And what are the lessons for regional modelling?

6.6.3.1 Implications for West Africa

Previous research has shown that many GCMs project dry signals in west Sahel (Monerie et al. 2012a, b; Chapter 4), but that the drying in versions of HadCM3 is of a particularly high amplitude and spatial extent, stretching to the Guinea Coast and the Congo Basin (Chapter 5). The findings from the present study cast doubt on this high magnitude response. It is not possible to definitively identify the drivers of precipitation decline based only on analysis of transient simulations, therefore further experimentation would be necessary to establish that the circulation mode characterised here is responsible for the dry signal. If this is shown to be the case, it may be possible to constrain the range of precipitation projections which is used for impacts assessment over West Africa, to exclude the models which show this mode. Examination of atmospheric dynamics in other GCMs and RCMs, to investigate whether they show dry signals for the same or for different reasons, would be another step towards producing a defensible range of possible futures for decision making. Therefore further work is required to understand the implications of global warming for West Africa, but these findings bring the higher risk drying projections into question. This does not necessarily imply that wetter futures are more likely, although a recent analysis by Vizy et al. (2013), designed to provide reliable projections, did produce a wetter future for the Sahel.

6.6.3.2 Implications for regional modelling

The consistent difference in the amplitude of both precipitation and circulation anomalies between the GCMs and the RCMs is worthy of note, and reinforces previous work which shows contrasting projections based on individual pairs of RCMs and driving GCMs (e.g. Mariotti et al. 2011). However, given that the models have similar mechanisms which are not found in reanalyses, it is certainly not possible to suggest that either the (larger) GCM or (smaller) RCM response is more realistic.

In fact, the similarity between GCM and RCM is probably the more interesting result from the perspective of regional modelling, implying limited added value from higher resolution and optimised physics in this case. This could be because the boundary conditions have such a large control on the regional model as to ensure comparable dynamics, however previous research suggests that RCMs are relatively autonomous from their driving GCMs (Patricola and Cook 2010), and this is likely to be the case here given the large size of the CORDEX Africa domain. Furthermore, not all RCMs project drying in west Sahel when forced with HadCM3 (Diallo et al. 2012). It is more probable that the consistency in the dynamical response found here is due to the related physics in the GCMs and RCMs used in this study. Parameters from HadCM3 have been optimised for HadRM3P (as described in Jones et al. 2004), but relative to other GCM/RCM pairs in CORDEX the basic physics is still very alike. Druyan et al. (2010) find a similar climatology in HadAM3 and HadRM3P over West Africa, even when different boundary conditions are used to force the regional model, implying that the physics favour a certain circulation

regardless of boundary conditions or resolution. It may be that if the resolution was increased further there would be an improvement. The 50km horizontal grid-spacing is still coarse relative to the scale of convective processes governing tropical precipitation (see Marsham et al. 2013); and the vertical resolution may inhibit the models' ability to incorporate the complex Saharan boundary layer (see Messager et al. 2010). The findings therefore highlight that added value from RCMs at 50km should not be assumed: improvements in physics and higher resolution might be necessary to produce more reliable projections.

6.7 Summary and Conclusions

Investigating the potential implications of global warming for African precipitation is important for both mitigation and adaptation. The majority of regional climate change assessments to date have been based on GCMs, which are not able to provide local scale information. Understandably, there is a great deal of interest in using RCMs to produce downscaled climate projections for decision making. However, there has been little previous work to assess the reliability of RCM projections, and an improvement over GCMs is yet to be demonstrated.

Here we use an ensemble of five MOHC GCMs and RCMs to examine the extent to which the implications of global warming for African precipitation inferred from RCMs is different from that of GCMs. The precipitation projections are broadly similar in terms of the direction of change, but there are some important differences in the magnitude and spatial extent of the anomalies. The distinction between the

ensembles is by no means restricted to the grid-spacing of their output. More detailed RCM projections should not therefore be adopted without first comparing them to GCMs.

The largest contrast between the ensembles is in West Africa, where all models show a drying response, but this is consistently larger in the GCMs than the RCMs (by >1 mm day^{-1} from 2°C). This region is very vulnerable to shifts in precipitation, and so it is important to understand the extent to which a drying response is plausible, and whether the GCM or RCM projection can be deemed more realistic, since the difference between them would require a different level of adaptation or mitigation. Atmospheric dynamics associated with the dry signal are analysed in order to investigate why there is drying and why it is larger in the GCMs.

In both ensembles drying is associated with anomalous subsidence at 400hPa, possibly amplified by a large warming of the surface (>6°C for a 4°C global warming) in west Sahel and the west Sahara in response to negative precipitation anomalies. This warming may be responsible for increases in dry convection in northern Sahel and a strengthening of the heat low, with potential feedbacks on the monsoon and the AEJ. The reason for the larger precipitation decline in the GCMs relative to the RCMs would appear to be the difference in the magnitude and not the nature of the circulation changes.

To assess the reliability of this dynamical response, dry years from the models' twentieth century simulation are examined, revealing many similar circulation changes to those associated with global warming, and thus allowing an appraisal of the future response based on comparison with dry years in NCEP and ERA-I

reanalysis. Whilst some features are shared between reanalyses and the models, the GCMs and RCMs appear to have a distinct mode focused on west Sahel which is not found in the reanalyses. This casts doubt on the dynamical changes in both the GCMs and the RCMs. Comparison of precipitation mechanisms over West Africa therefore suggests that RCMs at 50km do not necessarily produce more reliable projections than their driving GCMs.

Acknowledgements

The GCM data used in this study were produced through work supported by the UK Joint 'Department for Energy and Climate Change' (DECC), 'Department for Environment, Food and Rural Affairs' (Defra) MOHC Climate Programme (GA01101). The RCM experiments were generated by the PRECIS team at the MOHC. The authors would like to thank Carlo Buontempo, Karina Williams, and David Sexton for assistance with data access. We also acknowledge NOAA/OAR/ESRL PSD and ECMWF for making available the NCEP and ERA-I datasets.

Supplementary Information: Chapter 6

Table 6.S1 Coordinates of the regional domains in Figure 6.2.

Region	Co-ordinates[a]
West Sahel	20°W-5°W; 10-20°N
Central Sahel	2-20°E; 10-20°N
Guinea Coast	10°W-10°E; 4-11°N
West Equatorial Africa	11-19°E; 10°S-5°N

[a]These dimensions were selected from the data. The resulting dimensions vary between GCM and RCM depending on model resolution.

Figure 6.S1 Projected ω responses (hPa s^{-1}) to global warming during JAS, at 925hPa-400hPa: in GCM (a) and RCM (b) ensemble means, and the difference (GCM-RCM) (c). Intermodel agreement is shown as in Figure 1 and Figure 5. Analysis on RCMs was conducted at the GCM resolution (analysis at native resolution leads to the same findings). ➢

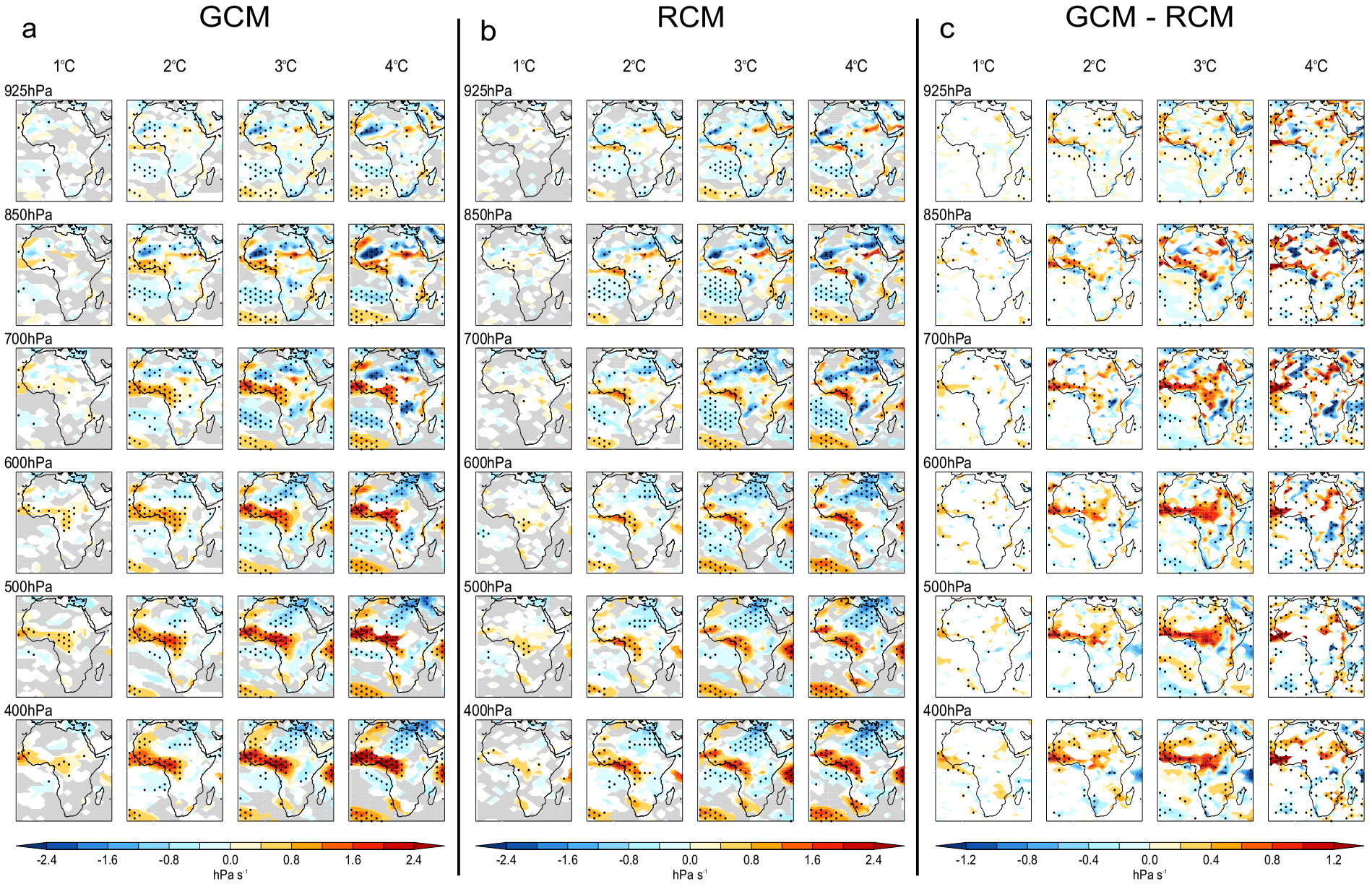
a
GCM
b
RCM
c
GCM - RCM
1°C
2°C
3°C
4°C
925hPa
850hPa
700hPa
600hPa
500hPa
400hPa
-2.4
-1.6
-0.8
0.0
0.8
1.6
2.4
hPa s-1
-1.2
-0.8
-0.4
0.0
0.4
0.8
1.2
hPa s-1

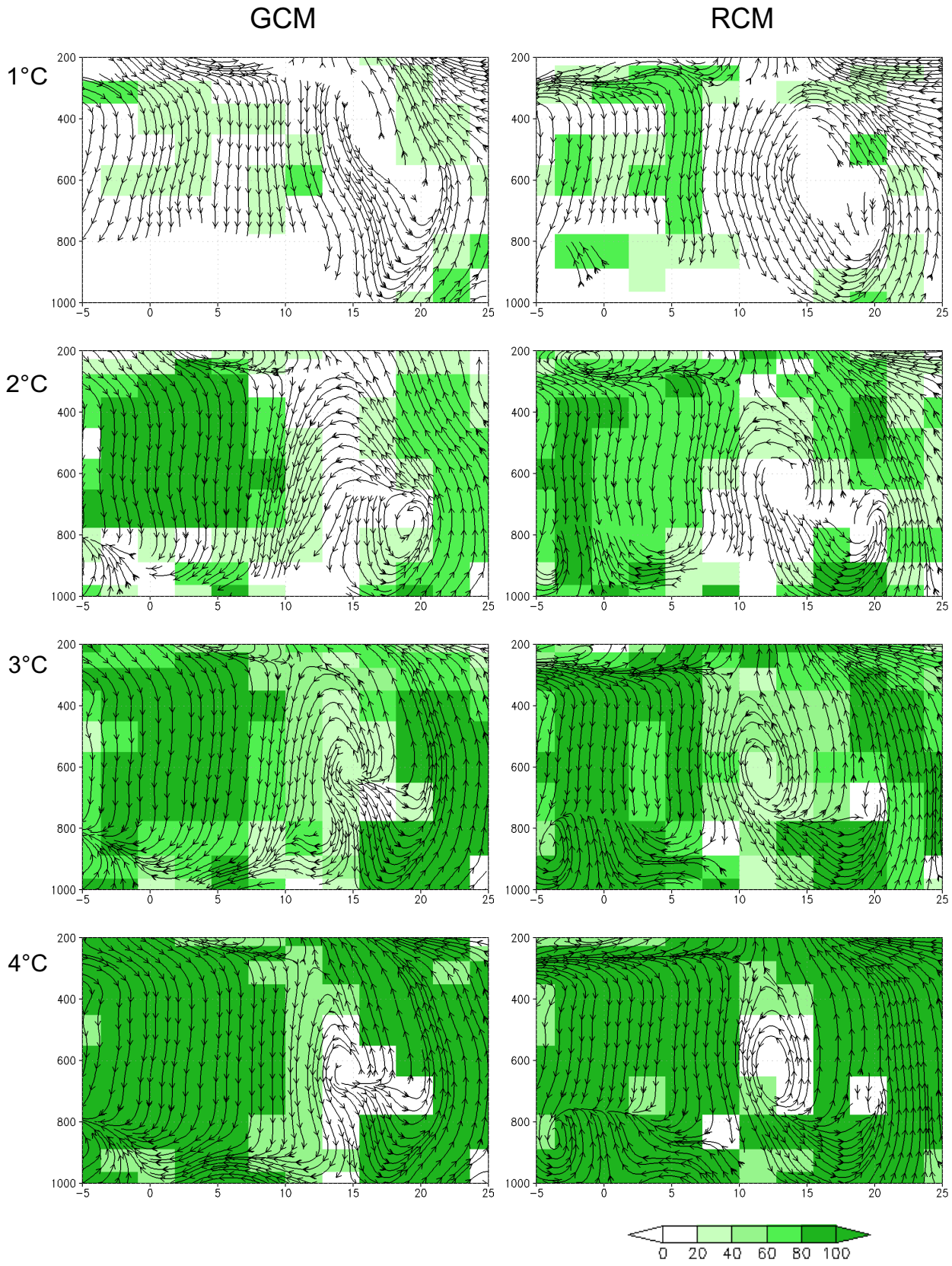

Figure 6.S2 as Figure 6.4 but for 10°E-20°E.

Figure 6.S3 Projected $q\vec{V}$ responses (kg kg^{-1} ms^{-1}) to global warming during JAS, with contours of divergence (kg kg^{-1} s^{-1}), at 925hPa-600hPa: in GCM (a) and RCM (b) ensemble means, and the difference (GCM-RCM) (c). Intermodel agreement is shown as for $q\vec{V}$ in Figure 6.5. Analysis on RCMs was conducted at the GCM resolution (analysis at native resolution leads to the same findings). ➢

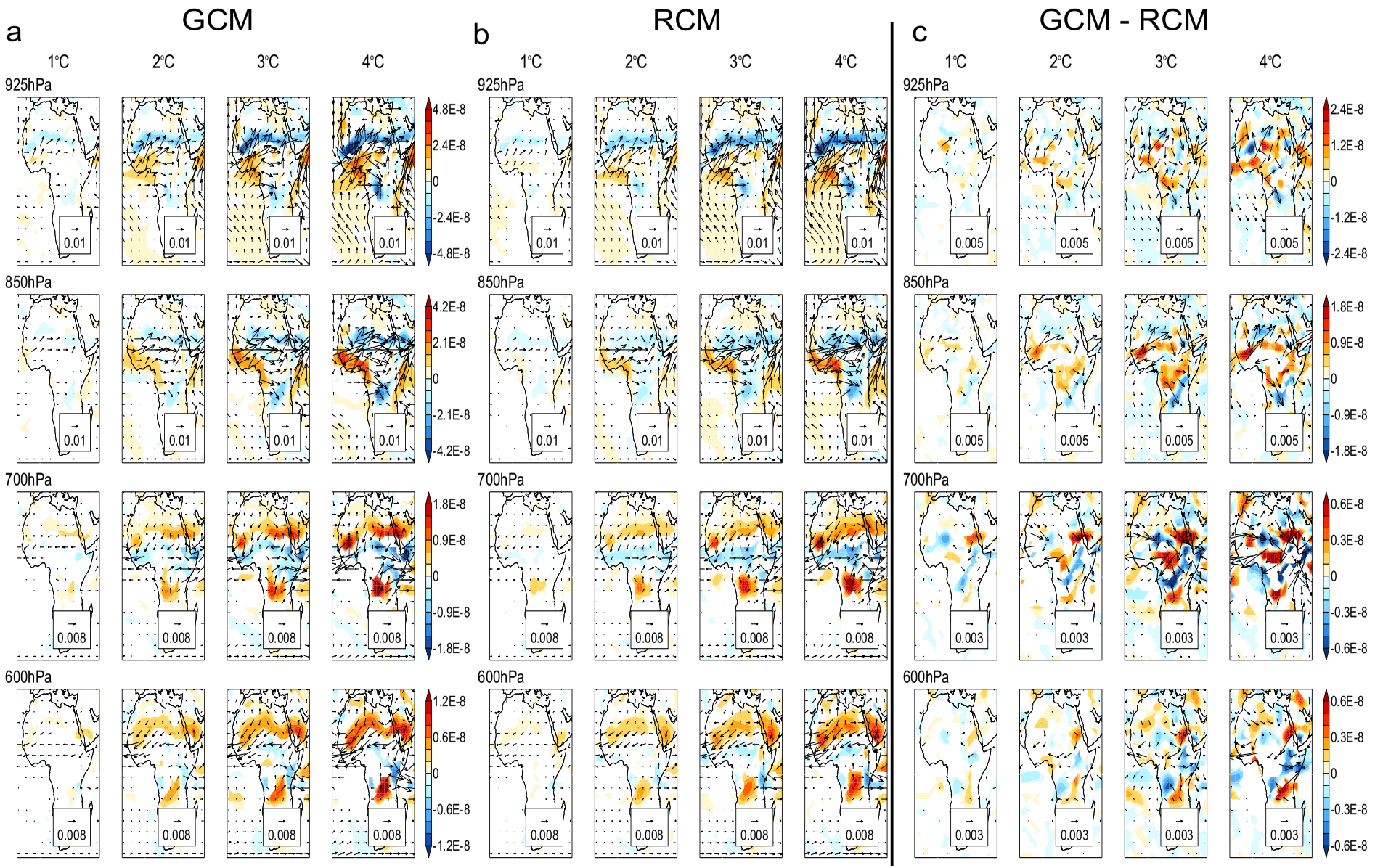
a
GCM
b
RCM
c
GCM - RCM
1℃
2℃
3℃
4℃
925hPa
850hPa
700hPa
600hPa
0.01
0.005
0.008
0.003
4.8E-8
2.4E-8
0
-2.4E-8
-4.8E-8
4.2E-8
2.1E-8
-2.1E-8
-4.2E-8
1.8E-8
0.9E-8
-0.9E-8
-1.8E-8
1.2E-8
0.6E-8
-0.6E-8
-1.2E-8
2.4E-8
1.2E-8
-1.2E-8
-2.4E-8
0.6E-8
0.3E-8
-0.3E-8
-0.6E-8

Figure 6.S4 as Figure 6.7 but with the native horizontal and vertical resolution for each dataset. GCM and NCEP have 2.5° latitude spacing and 10 vertical levels to 200hPa, RCM has 0.44° latitude spacing at 10 vertical levels. ERA-I has 0.75° latitude spacing and 23 vertical levels to 200hPa. ➢

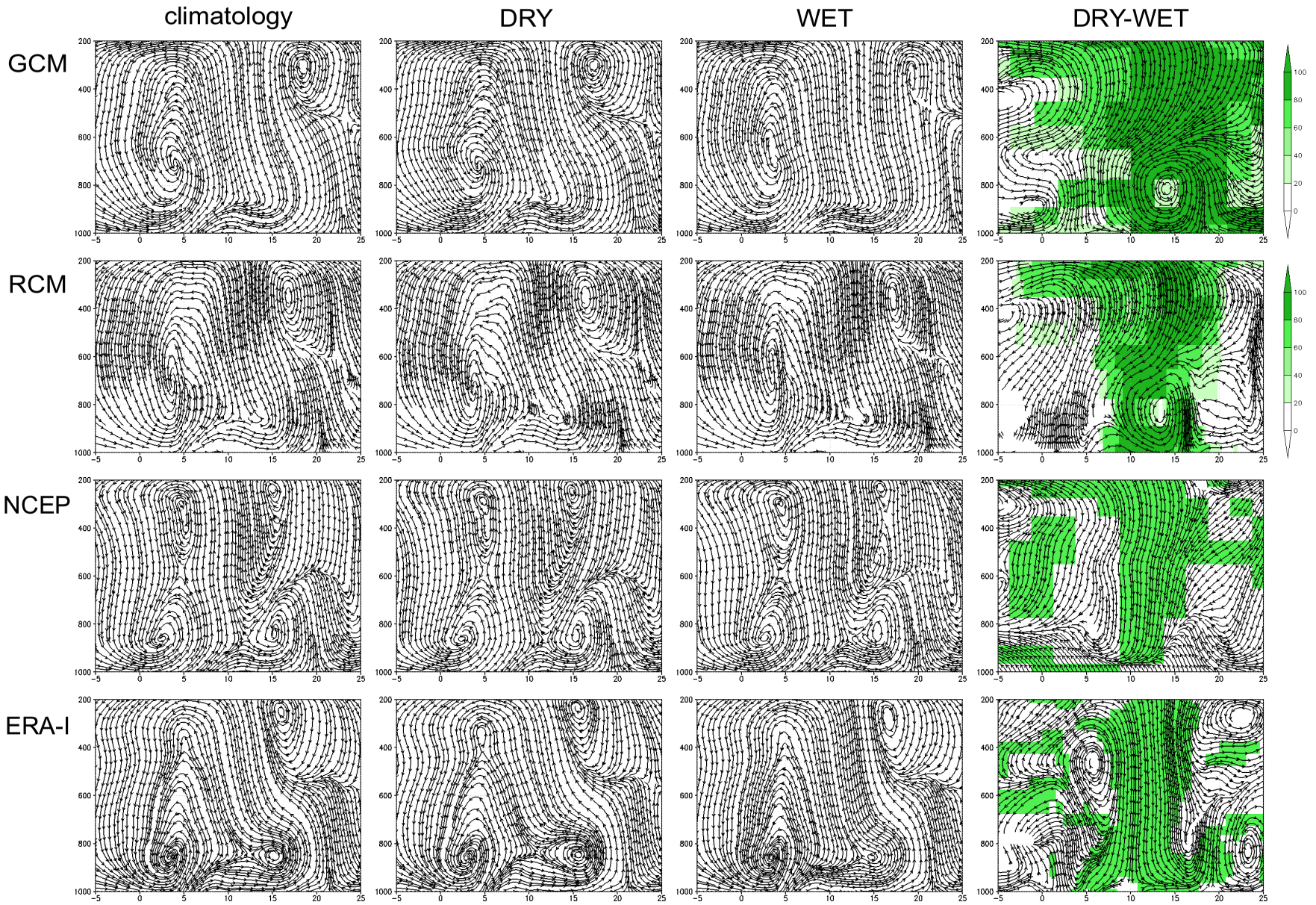
climatology
DRY
WET
DRY-WET
GCM
RCM
NCEP
ERA-I
200
400
600
800
1000
−5
0
5
10
15
20
25
100
80
60
40
20
0

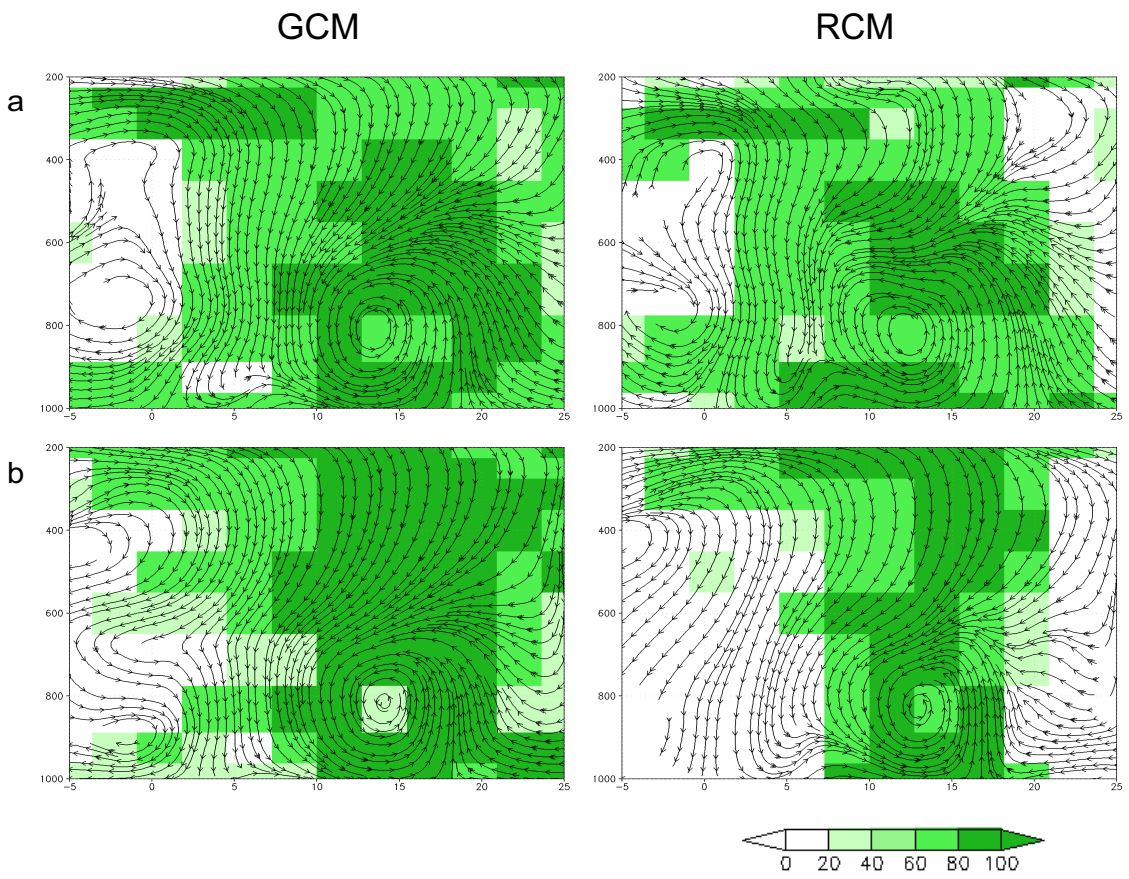

Figure 6.S5 Latitude-height cross sections of anomalous streamlines (*v*; -ω*100) averaged 10°W to 0 during JAS for the GCM and RCM ensemble means, associated with a 2°C global warming (a), and for dry minus wet years from twentieth century simulations (b). These are the same plots found in Figure 6.4 and Figure 6.7, but are provided together here to aide comparison. The green shading indicates the percentage of models which show significant change (in either *v* or ω) of the same direction (5% level). In (a) this significance is of change associated with global warming relative to interannual variability. In (b) this significance is of difference between dry and wet composites relative to variation between years within the composite

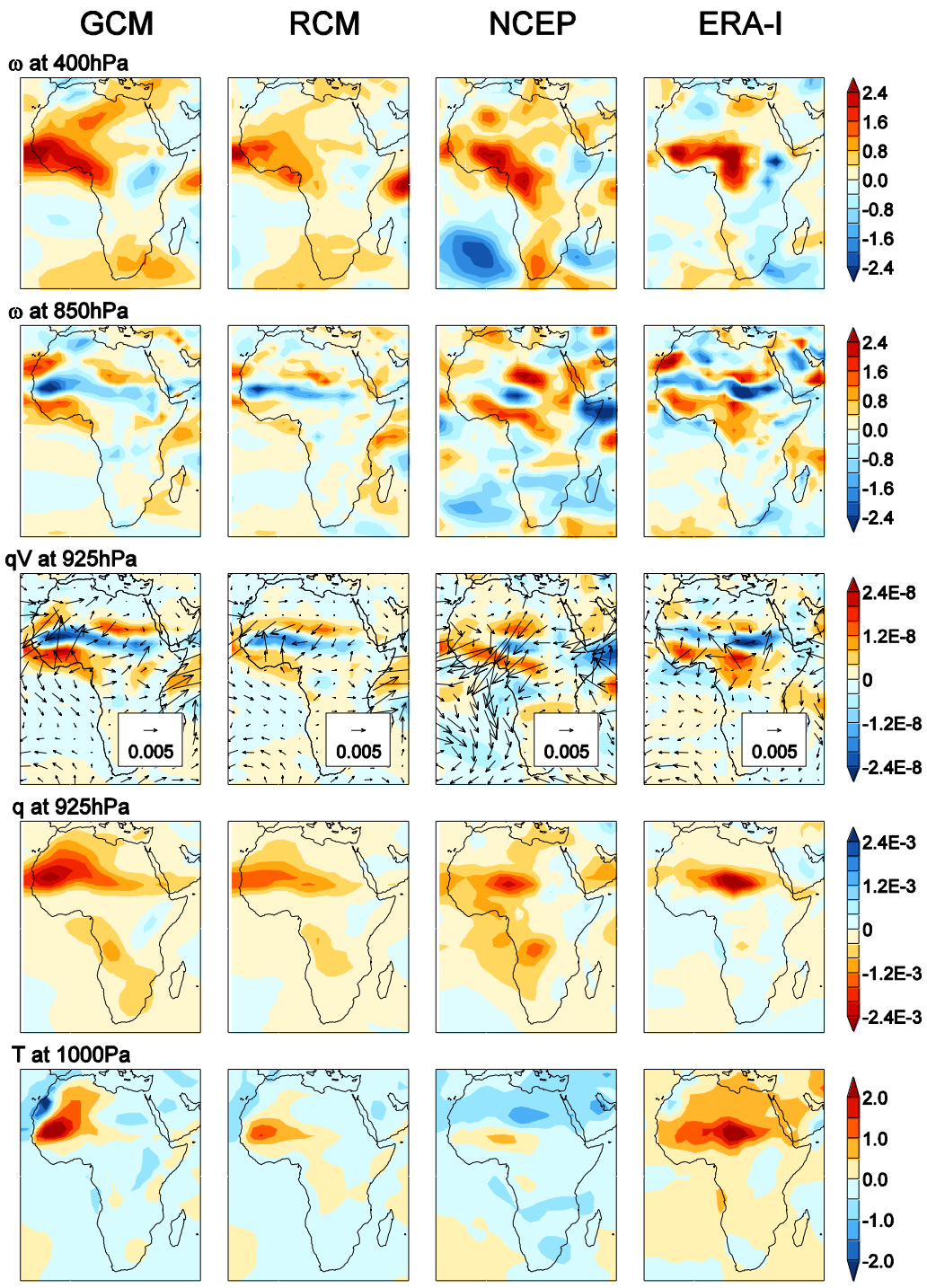

Figure 6.S6 as Figure 6.7 but without significance testing.

Figure 6.S7 Dry and wet JAS composites as anomalies from the long term mean, for the same datasets and variables as in Figure 6.7 ➢

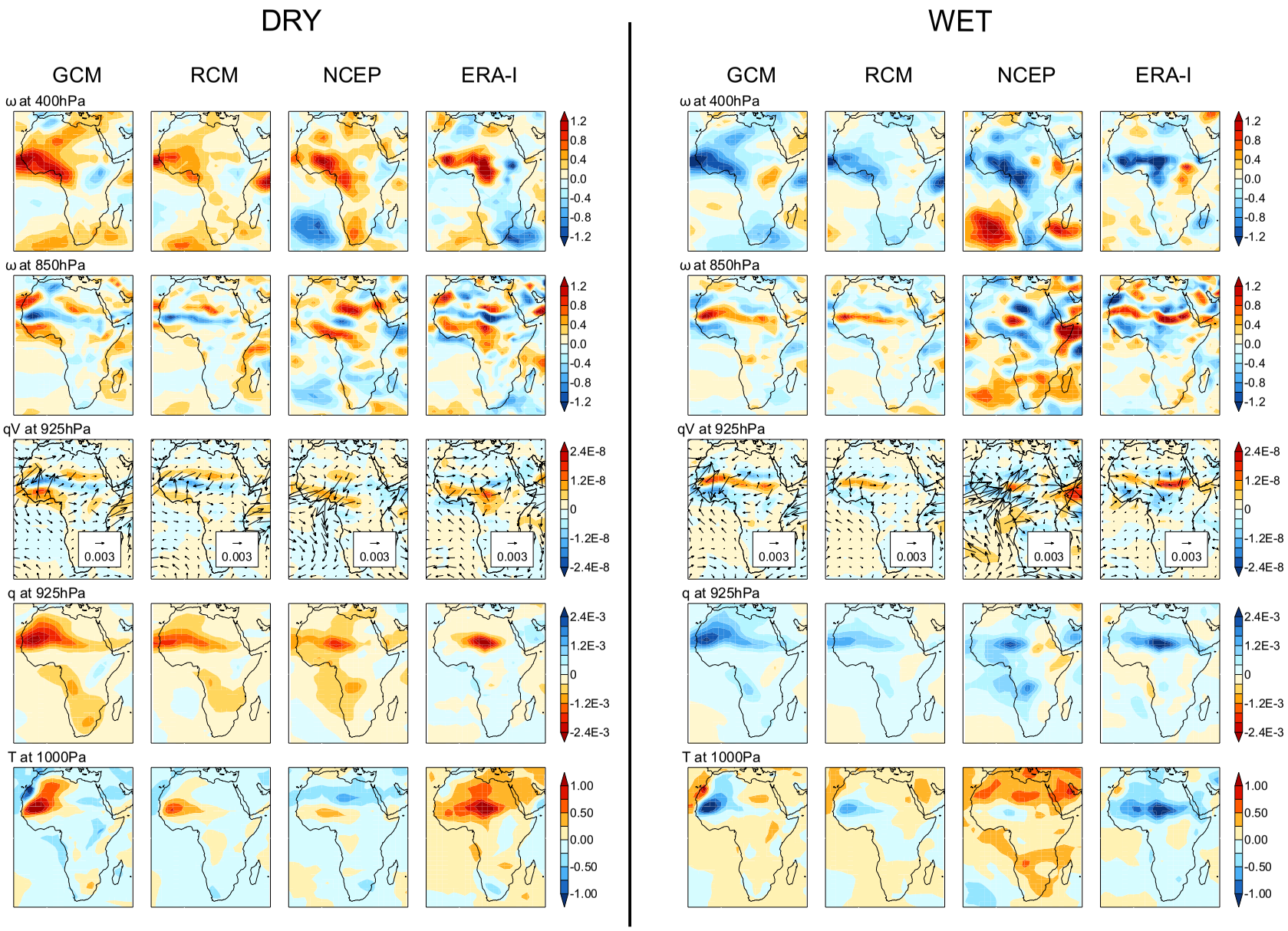
DRY
WET
GCM
RCM
NCEP
ERA-I
ω at 400hPa
ω at 850hPa
qV at 925hPa
q at 925hPa
T at 1000Pa
1.2
0.8
0.4
0.0
-0.4
-0.8
-1.2
2.4E-8
1.2E-8
0
-1.2E-8
-2.4E-8
2.4E-3
1.2E-3
-1.2E-3
-2.4E-3
1.00
0.50
0.00
-0.50
-1.00
0.003

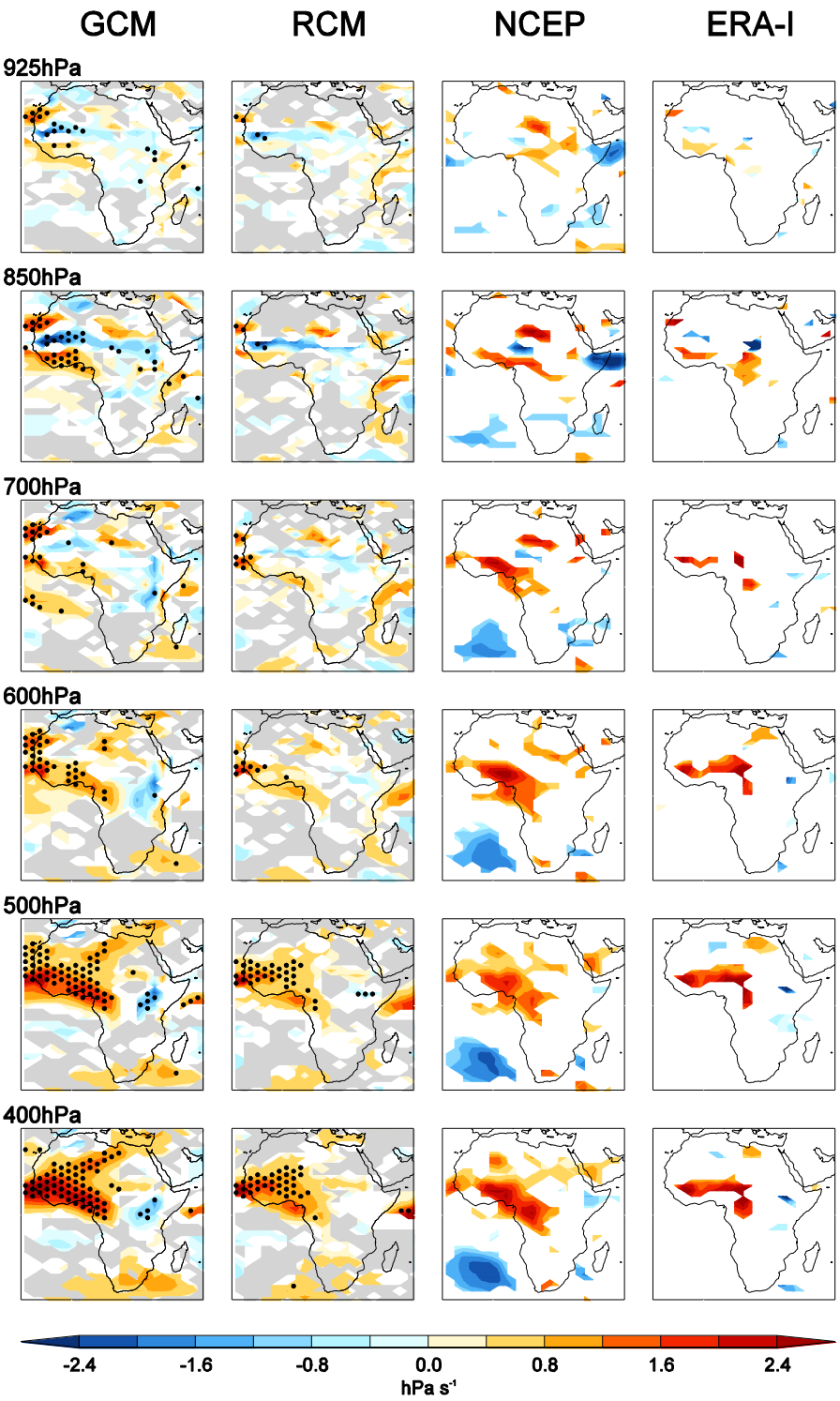

Figure 6.S8 Dry minus wet JAS composites for ω (hPa s^{-1}) at 925hPa-400hPa, for GCM and RCM ensemble means, NCEP, and ERA-I. Significance and intermodel agreement is shown as in Figure 6.8. All datasets have been analysed at GCM resolution (analysis at native resolution leads to the same findings).

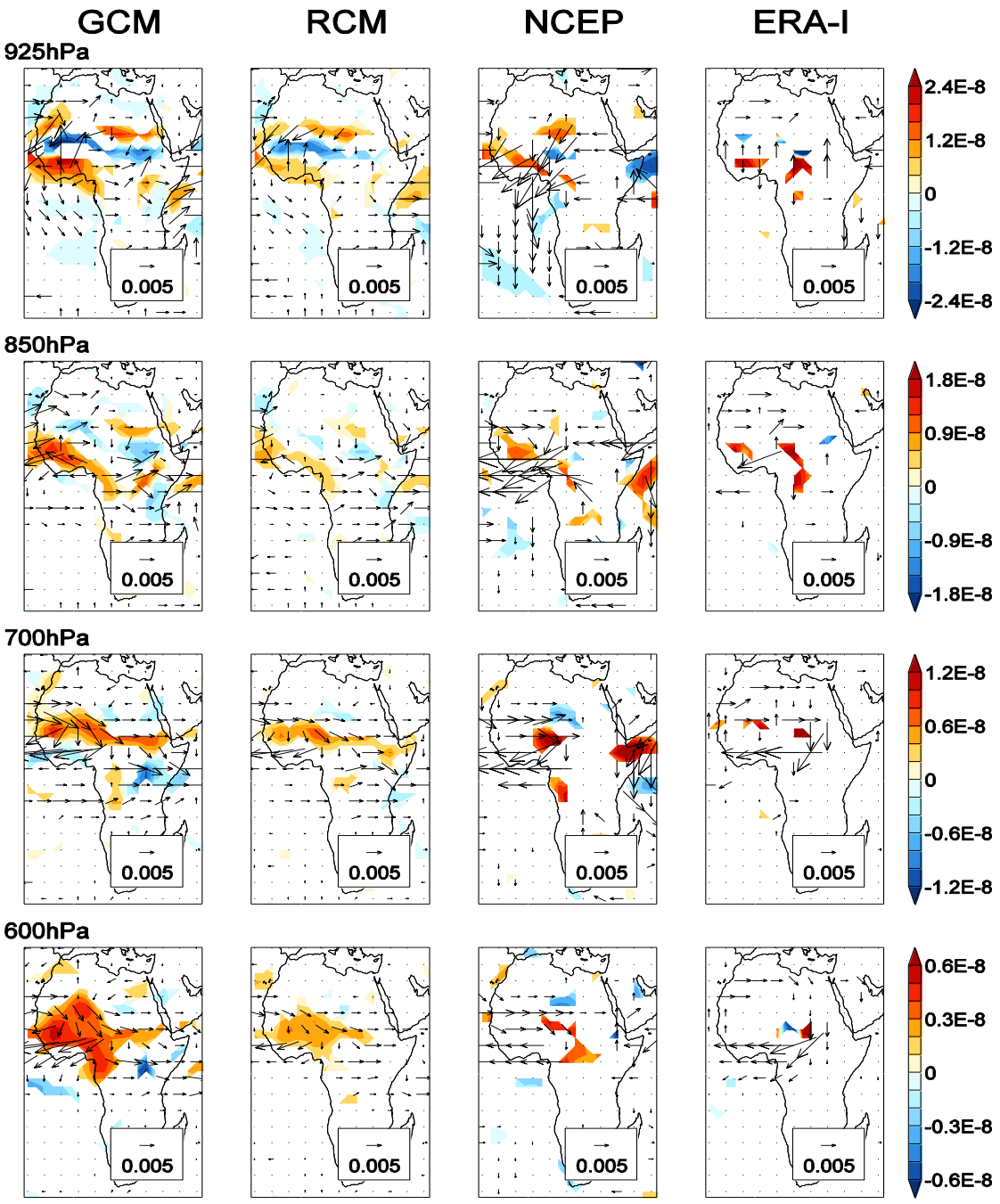

Figure 6.S9 Dry minus wet JAS composites for qV (kg kg^{-1} ms^{-1}) with contours of divergence (kg kg^{-1} s^{-1}), at 925hPa-600hPa, for GCM and RCM ensemble means, NCEP, and ERA-I. Significance and intermodel agreement is shown as for qV in Figure 6.8. All datasets have been analysed at GCM resolution (analysis at native resolution leads to the same findings).

7 Introduction to the Congo Basin case study

7.1 Introduction

In Chapters 4, 5, and 6, changes in African climate at 1°C, 2°C, 3°C, 4°C ΔT_g and beyond were inspected from three datasets in turn. The next section of the thesis is an investigation of the implications of global warming for the climate of the Congo Basin. The present chapter will first offer a short discussion of the results from the thesis so far, clarifying the motivation for a regional case study; before presenting a review of existing work which might inform understanding of potential future change in the Congo Basin. The aims and objectives of the case study will then be summarised.

7.2 Rationale

The aim of the thesis is to identify and interrogate changes in African temperature and precipitation associated with degrees of anthropogenic global warming in climate model experiments. It is intended to examine what the models show, in terms of change at 1°C, 2°C, 3°C, etc.; but also to start interpreting and appraising these projections, with the hope of providing insights about the extent to which existing climate model data constitute a trustworthy evidence base to understand the risks associated with global warming.

After examining pan-African projections from CMIP3, PPEs, and RCMs, the thesis has uncovered the evolution of change with global warming in many model experiments (a total of 70 transient runs). The analysis shows that as global

temperature rises, local temperature and precipitation anomalies, including wet signals in East Africa and the central Sahel, and dry signals in west Sahel and southern Africa, increase in amplitude and spatial extent. The development of change with global warming is gradual: in connection with more moderate anthropogenic forcing (1°C to 3°C), and at higher degrees of warming (4°C and beyond; Chapter 5). The range of projections at each ΔT_g level for different African regions has been defined (see Figure 4.5, 5.6, 6.2). These outputs have the potential to provide a basis for impacts assessment to compare 2°C with other ΔT_g increments. But should these data be used to support policy decisions?

Assessing the credibility of the climate model projections is a crucial but challenging task. The analysis in Chapters 5 and 6 makes a small contribution towards an appraisal of the evidence base. Comparison of the range of projections from CMIP3, PPEs, and RCMs, reveals that the implications of global warming for African climate are different depending on which dataset is consulted: whether MME or PPE, GCM or RCM. The finding that PPEs show large anomalies which are not represented by CMIP3 (including for west equatorial Africa and west Sahel), and that RCMs modify the range of projections from their driving GCMs (most notably in west Sahel and southern Africa), demonstrates the importance of consulting multiple sources of evidence for regional climate change assessment. The contrast between datasets also suggests that further experiments might be required in order to provide a basis for conservative estimates of danger at each degree of global warming. These experiments might include PPEs with different base models and RCMs run at higher resolution (as emphasised in sections 5.6.3 and 6.6.3.2; and discussed further in

Chapter 10). The finding of an approximately linear relationship between global temperature and local climate change also has important implications for the level of confidence in the model projections. It implies that the models used here do not experience tipping points even at higher degrees of warming, emphasising the need for further research to assess the whether the models can incorporate nonlinearities in the earth system (see section 5.6.3). Finally, the results of the composite analysis of atmospheric dynamics in Chapter 6 cast doubt on the projected drying of west Sahel, which suggests the need for more mechanistic investigation to assess the credibility of projected changes from other models and in other regions.

The motivation for this thesis was the lack of research into the implications of specific degrees of global warming for African climate. After investigating projections from three datasets, it is now much clearer what the models show, but the analysis also highlights the limitations of the existing model outputs in terms of their ability to characterise uncertainty in the local climatic response to each degree of ΔT_g.

In the interim there is a demand for information about how global warming will influence regional climates in Africa: political decisions are unlikely to wait for developments in climate modelling infrastructure. The UNFCCC review of long term mitigation goals is the most relevant example in this case: new evidence will be considered until 2015 (UNFCCC 2013). Scientists can either decide that uncertainties are too great to make an appraisal within this timeframe, and allow political debates to continue with limited scientific backing; or provide an assessment of the current state of the evidence. The role of this case study is to explore the extent to which it is possible to deliver useful information from climate models in the presence of large

uncertainty, and to expose the difficulties in making an assessment of the implications of global warming given incomplete evidence, by examining model projections for one region and considering approaches for judging the credibility of these data.

There are many parts of Africa for which a case study would be beneficial. The Congo Basin is just one example, but it is also a very important one. As highlighted in section 1.4, this region epitomises the dilemma faced by the continent as a whole: the consequences of climate change could be globally significant, but the limited previous research and scarcity of observational data inhibit understanding of the potential implications of global warming. It is particularly interesting to shift the focus to the Congo Basin following the analysis of the West Africa in the previous chapter. The Sahel has received the most research attention of any African region (see section 1.2.1). In Chapter 6, it was possible to deliver an appraisal of the confidence in the modelled responses. For the Congo Basin, one of the most neglected regions on the continent, is it possible to find out anything about the implications of global warming?

7.3 Existing Research

Before describing the analysis, existing research which might provide insights into the possible response of Central African climate to anthropogenic global warming will be reviewed. This work includes relevant previous literature as well as results from Chapters 4-6.

7.3.1 Previous literature

The Congo Basin is one of the largest convective regions on the planet (Webster 1981) with annual rainfall >1200 mm year^{-1} from approximately 8°N to 8°S (based on CRU data, Figure 1.1), and substantial precipitation throughout the year. Its main rainfall seasons are in MAM (146 mm month^{-1}) and OND (160 mm month^{-1}), with drier seasons in JAS (73 mm month^{-1}) and DJF (123 mm month^{-1}) (Todd and Washington 2004; see also Figure 1.2). These precipitation totals are, however, uncertain given the lack of long term rain gauge records for the region (e.g. McCollum et al. 2000; Camberlin et al. 2001; Todd and Washington 2004; Conway et al. 2009). River flow records provide an alternative data source to study climate variability in the region (Todd and Washington 2004), but the stability of the rainfall-runoff relationship is difficult to establish without more precipitation data (Conway et al. 2009). There are also limited observational data with which to describe the atmospheric circulation, and most studies into controls on precipitation in west equatorial Africa are based on a single reanalysis dataset (e.g. Nicholson and Grist 2003 and Pokam et al. 2011 using NCEP; Suzuki 2011 using ERA-40). The findings of individual papers might therefore be interpreted cautiously.

Taken together recent work suggests that although the movement of the Inter-Tropical Convergence Zone (ITCZ) has an influence in Central Africa (Suzuki 2011), the generation of precipitation is much more complex than through local scale convection driven by the migration of maximum insolation. Approximately 70% of rainfall is organised into Mesoscale Convective Systems (MCSs) (Nicholson and Grist 2003; Jackson et al. 2009), and the precipitation climatology is more heterogeneous

than for most other African regions (Balas et al. 2007), with an important role for topography (Jackson et al. 2009; Vondou et al. 2010). There is considerable asymmetry between the dry seasons, with more cloud in JJA than DJF (Gond et al. 2013), which can be explained in terms of the contrasting horizontal moisture fluxes during these seasons. In boreal winter the Congo Basin is fed by northerly Harmattan winds from the dry Sahara, whilst during JJA, and to a greater extent SON, much of the moisture is supplied by Low Level Westerlies (LLWs) from the Atlantic Ocean at 850hPa (Pokam et al. 2011).

Interannual variability in Congo Basin precipitation is related to change in the LLWs (Pokam et al. 2011), as well as to the AEJ, TEJ, and possibly a southern hemisphere equivalent of the AEJ referred to as "AEJ-S" by Nicholson and Grist (2003). There is likely an important influence from regional SSTs, including the Atlantic cold tongue (Tokinaga and Xie 2011), and the Benguela current (Balas et al. 2007). Nicholson (2010) suggests that there is a Benguela Jet which might control the climate of coastal regions. The Congo Basin has further been found to have teleconnections to Ethiopia and south Sudan (Williams et al. 2011), Atlantic SSTs, and ENSO (Nicholson and Entekhabi 1986; Camberlin et al. 2001; Malhi and Wright 2004; Todd and Washington 2004; Giannini et al. 2008). Recent studies (Balas et al. 2007; Nicholson and Dezfuli 2013; Dezfuli and Nicholson 2013) demonstrate complexity within Central Africa, whereby different locations and seasons have different, and in places opposite, teleconnections to global SSTs.

Research into the general response of tropical regions to anthropogenic global warming (see section 1.2.1) may therefore be insufficient to understand

potential future changes in the Congo Basin. Whilst the "rich-get-richer mechanism" might induce an increase in precipitation in the core of the convective region (Chou and Neelin 2004), or there might be a decrease in updrafts due to the weakening of tropical circulation (Vecchi and Soden 2007); any number of SST anomalies or shifts in regional dynamics could complicate these local thermodynamic responses.

It is unclear whether global warming has led to a change in Central African climate over the twentieth and early twenty-first centuries. Aguilar et al. (2009) studied station data over western central Africa, Guinea Conarkry, and Zimbabwe from 1955-2006; and found significant warming which was largest in Central Africa. Some studies have also noted an observed drying trend in the Congo Basin (Malhi and Wright 2004; Aguilar et al. 2009; Fisher et al. 2013); whilst other authors find that the region experienced some negative precipitation anomalies coincident with the 1970s drought in the Sahel (Servat et al. 1999; Conway et al. 2009), and a recovery from 1995 (Jury 2013).

Previous research into future change in the Congo Basin is limited. Africa-wide projection studies show warming throughout the continent, which is larger in subtropical regions than at the equator (Hulme et al. 2001; Figure 1.3). In terms of precipitation, the CMIP3 ensemble mean shows a modest wetting, but there is substantial spread between the CMIP3 models (Christensen et al. 2007; Giannini et al. 2008; Christensen et al. 2013) as well as RCMs (Paeth et al. 2011). Cook and Vizy (2012) provide a more in depth analysis of change in the Congo Basin using projections from WRF. They find wetting from January to May, associated with an increase in low level moisture transport from the Atlantic Ocean and East Africa; but

a dry signal in JAS, and in the south of the Congo Basin during SON, linked to a wider drying of southern Africa (see section 1.2.1). A recent study published by the Climate Service Center (CSC 2013; Haensler et al. 2013) has made a substantial addition to the literature through analysis of 77 simulations over Central Africa, from CMIP3, CMIP5, and two RCMs. Haensler et al. (2013) conclude that climate change is unlikely to lead to an increase in water scarcity in the region, but there may be an intensification of heavy rainfall events, and more frequent dry spells.

7.3.2 New findings

The first three papers from this thesis deliver an important contribution to existing investigation of modelled responses to global warming in the Congo Basin, including analysis of change in all seasons, and from 350 simulations, including PPEs. The most striking signal identified is in the subset of AS-PPE models which show extreme warming (>8°C) and drying (>1mm day^{-1} in the annual mean) of the region in response to $2xCO_2$. However, these model versions have low entrainment coefficients (<2) which are not considered plausible (see section 5.5.1.2). After applying constraints to the ensemble, the remaining models show more moderate signals.

In DJF the Hadley Centre PPEs experience a wetting response to global warming, but there is no agreement in CMIP3. During MAM most models also show positive precipitation anomalies, which are widespread in AS-PPE and PRECIS-RCM, but restricted to the east of the basin in AO-PPE and CMIP3. The wetting could be a

rich-get-richer response, although in CMIP3 it is weak (<0.2 mm day^{-1} °C^{-1} in the ensemble mean) compared to the larger wetting of East Africa (>0.2 mm day^{-1} °C^{-1}). This spatial pattern might suggest a change in zonal overturning, as noted in Chapter 4, with reduced uplift in the core convective region of the Congo Basin, and upward anomalies over the climatologically drier East Africa.

In SON the majority of models also show wetter futures in Central Africa, but there is additionally some drying in the south west of the Congo Basin. The dry signal might be linked to the widespread negative anomalies over southern Africa during this season; various hypotheses for which have already been discussed. It could indicate a delay in the seasonal migration of precipitation (section 4.5), or an eastwards shift in the SICZ which simultaneously acts to decrease precipitation in southern Africa and increase precipitation in East Africa (section 1.2.1; Cook and Vizy 2012). However, the negative anomalies in SON may also be related to the pattern of change during JAS, when all ensembles show a dry signal in west equatorial Africa. This drying is much more widespread and of a greater magnitude in the Hadley Centre PPEs (>0.4 mm day^{-1} °C^{-1} in AO-PPE mean) than CMIP3 (<0.2 mm day^{-1} °C^{-1}) (Figure 5.5).

In Chapter 6 atmospheric dynamics associated with global warming are investigated using PRECIS-GCM and PRECIS-RCM in an attempt to understand mechanisms for the drying response during JAS. The focus of the analysis is on west Sahel, but the results may also shed light on the negative anomalies in the Congo Basin, as there is a reduction in precipitation throughout much of western Africa in these models. The precipitation decline is associated with downward ω anomalies at

400hPa, and an anomalous overturning circulation nearer the surface, characterised by: southerly monsoon flow from the Gulf of Guinea to approximately 20°N, dry convection at low levels in the northern Sahel, southward moisture flux at 600hPa, and subsidence over the Guinea Coast and Congo Basin (700hPa-400hPa) (see Figure 6.4). The implied northward shift in the monsoon may be partly responsible for the response over the Congo Basin, increasing precipitation in the central Sahel whilst it decreases nearer the equator, as has also be suggested by Cook and Vizy (2012) to describe projections from WRF.

The credibility of the response over west Sahel is examined using composites of wet and dry years from the twentieth century run, which are compared to wet and dry years from NCEP and ERA-I. The composites reveal that the circulation mode associated with global warming is similar to the mode found in dry years in the models, but is not found in reanalysis. This finding casts doubt on the modelled drying response over west Sahel in the PRECIS ensembles, but also in AO-PPE given the consistency of the circulation response between versions of HadCM3. However, it is not clear to what extent the circulation mode is linked to change beyond west Sahel. Therefore, Chapter 6 does not provide sufficient evidence to understand, or to dismiss, the drying in the west of the Congo Basin, which warrants more focused investigation. It does seem clear that the dry signal is linked to downward anomalies at 400hPa, and so it would be useful to examine potential reasons for this change in ω; whether it is part of a general weakening of circulation (Vecchi and Soden 2007), a response to remote SST forcing, or another mechanism.

Whilst the first section of the thesis has therefore developed the understanding of model projections for the Congo Basin, the results also underline the importance of further research. The dry signal in west equatorial Africa during JAS is of particular concern, potentially bringing into question Haensler et al.'s (2013) conclusion that water scarcity is unlikely to increase in future, and motivating additional work to investigate the potential influence of the projected change for the Congo Basin, and to explore mechanisms for the drying.

7.4 Aims and objectives

The case study is an investigation of the implications of global warming for the climate of the Congo Basin. The aim is to identify how Central African climate evolves with increasing global temperature in model experiments, but also to interrogate projected changes, contributing towards an assessment of their credibility. The case study is an opportunity to review available data sources for one region, and to explore the extent to which it is possible to deliver useful information from climate models. The value of model projections is particularly controversial in the case of the Congo Basin given the paucity of gauge data for model evaluation. Previous projection studies over Africa have omitted this region (e.g. Shongwe et al. 2009), and there has been little attempt to validate model hindcasts (except CSC 2013). Here a different approach is taken. Rather than bypassing the Congo Basin assuming that uncertainty is too large, that evidence which is obtainable is reviewed.

The first step is to question the extent of observational uncertainty. Many satellite and reanalysis products are now available over the Congo Basin, and by measuring the variation between these datasets against variation between GCMs, it will be possible to determine the potential for evaluation. Whilst it has been noted (section 1.2.3) that comparison of models with observations is insufficient to determine the validity of their projections, it is fundamental for understanding their weaknesses.

It may also be possible to evaluate precipitation climatologies based on moisture flux. If models with different representations of precipitation have different atmospheric circulation, the models with a less trustworthy circulation could be excluded. However, this assessment requires an understanding of the regional climate dynamics which is not necessarily in place. Chapter 6 demonstrated the potential difficulty in assessing modelled processes given variation between reanalysis products. In the case of West Africa, NCEP and ERA-I were sufficiently consistent, and sufficiently different from the models, to conclude that the modelled circulation mode is not found in reanalysis. Previous research has not yet investigated whether reanalysis products show common dynamics over the Congo Basin: the majority of studies are based on one dataset (see section 7.2). It is therefore important to compare circulation between data products, and here two of the most commonly used reanalyses (NCEP and ERA-I) will be examined.

The analysis of climatological precipitation and associated circulation will give a context for presenting model projections. Changes in the climate of the Congo Basin have already been inspected in Chapters 4-6. The regional case study enables

these projections to be re-examined, with a focus on metrics which are impacts relevant. One of the key issues with reference to mitigation debates is the impact of climate change on humid tropical forests (see section 1.4). The case study will therefore seek to identify changes in indices of relevance to African rainforests, and examine how these anomalies evolve with global warming.

The first three papers show that the models employed in this thesis project progressive change with global warming, in terms of seasonal mean temperature and precipitation. The development of change from 1°C to 2°C to 3°C and beyond is therefore not a dominant focus in the case study, although the extent to which local change remains to be approximately linear for indices of relevance to Congo Basin rainforests will be examined, and the rate of change with global warming presented.

To investigate consistency in the model projections, data from different model ensembles will be compared. The results from Chapter 5 highlight the importance of including both MMEs and PPEs, and both CMIP3 and the MOHC PPEs will be examined here, although the members of the PPEs which were identified as less trustworthy in Chapter 5 will be removed. Chapter 6 demonstrated a difference between RCMs and GCMs: the RCM projections for the Congo Basin are wetter than the GCMs' in MAM and SON, but drier in DJF. Further comparison of GCM and RCM projections over the Congo Basin would make a useful addition to the case study but will not be covered during this thesis. Instead, to better understand the potential value in RCMs relative to GCMs, precipitation climatologies from a GCM and physically consistent RCM run at two different resolutions are presented. This may clarify results from Chapter 6 in terms of the cause of difference between

GCM and RCM. Finally, the case study will also seek to interpret and begin to appraise projected changes through analysis of atmospheric dynamics.

The research questions for each chapter are summarised below.

Chapter 8: Congo Basin climatologies

Chapter 8 presents precipitation and moisture flux climatologies from a range of satellite, reanalysis, and model datasets over the Congo Basin to assess the extent of the observational uncertainty.

- How large is the range of climatological precipitation from eight satellite and reanalysis datasets? How does this compare to the range from CMIP3 and CMIP5 models? What are the consequences for model evaluation?
- Are there important differences in precipitation climatologies between physically consistent GCMs and RCMs? Does a change in the resolution of an RCM simulation generate important differences in the precipitation climatology?
- Can contrasting precipitation climatologies be explained by differences in regional circulation?
- Are moisture flux climatologies consistent between reanalysis datasets? What are the consequences for model evaluation based on the representation of atmospheric circulation?

Chapter 9: Congo Basin projections

In Chapter 9, changes in the climate of African rainforests associated with global warming are presented from CMIP3 and the MOHC PPEs.

- What changes of relevance to rainforests are projected for the Congo Basin?
- How does the climate of the Congo Basin evolve with global warming?
- Do parameter perturbations modify the range of projected futures?
- What changes in atmospheric dynamics are associated with precipitation responses to global warming?

8 Congo Basin rainfall climatology: can we believe the climate models?

Authorship Declaration

This paper was designed and written by R. Washington. I conducted the analysis for all of the figures included in the paper as well as much of the supporting analysis which can be found in the supplementary material. This work was directed by R. Washington. H. Pearce performed analysis of daily data which could not be included in the final version of the paper due to the space restrictions of the journal. W. Pokam also participated in data analysis which could not be included in the final paper, and his previous work informed the investigation of moisture flux over the Congo Basin. W. Moufouma-Okia contributed analysis of RCMs, which is described in section 8.3.3 and illustrated in the supplementary material. All authors were involved in editing the drafts.

Congo Basin rainfall climatology: can we believe the climate models?

R. WASHINGTON, R. JAMES, AND H. PEARCE

Climate Research Lab, Oxford University Centre for the Environment, South Parks Road, Oxford OX1 3QY, UK

W. POKAM

Laboratory for Environmental Modelling and Atmospheric Physics, Department of Physics, University of Yaounde, Yaounde, Cameroon

W. MOUFOUMA-OKIA

Met Office Hadley Centre, FitzRoy Road, Exeter EX1 3PB, UK

Philosophical transactions of the Royal Society of London. Series B, Biological sciences **368** (1625) 20120296. doi:10.1098/rstb.2012.0296 2013

Published 22 July 2013

Abstract

The Congo Basin is one of three key convective regions on the planet which, during the transition seasons, dominates global tropical rainfall. There is little agreement as to the distribution and quantity of rainfall across the basin with datasets differing by an order of magnitude in some seasons. The location of maximum rainfall is in the far eastern sector of the basin in some datasets but the far western edge of the basin in others during March to May. There is no consistent pattern to this rainfall distribution in satellite or model datasets. Resolving these differences is difficult without ground-based data. Moisture flux nevertheless emerges as a useful variable with which to study these differences. Climate models with weak (strong) or even divergent moisture flux over the basin are dry (wet). The paper suggests an approach, via a targeted field campaign, for generating useful climate information with which to confront rainfall products and climate models.

Keywords: Congo rainfall, climatology, moisture flux, CMIP5

8.1 Introduction

The Congo Basin is one of the three core regions of convection in the global tropics, the other two being the Maritime continent of the tropical West Pacific and Eastern Indian Oceans and the Amazon basin (Webster 1981). Together, these regions drive large-scale tropical circulation. Congo Basin latent heating from convection exceeds 120 W m^{-2} (Jury et al. 2009), second only to the Maritime continent. The basin is also the region of highest lightning strike frequency on the planet. Congo River discharge to the ocean exceeds 60 000 $m^3 s^{-1}$ seasonally with a mean annual flow of 40 000 $m^3 s^{-1}$, contributing roughly 3.5 mm yr^{-1} to global sea level (Beighley et al. 2011). In the transition seasons, the Congo Basin dominates the global tropical rainfall distribution. Rainfall amounts and dry season climate characteristics over the Congo Basin are also sufficient to support one of the world's largest tropical humid forests (Zelazowski et al. 2011). The Congo Basin's role in the planetary circulation and the earth system is undisputed.

The Maritime continent, as the most spatially extensive region of tropical convection and the core of the Walker circulation, has unsurprisingly been widely studied (Mitchell et al. 1992; Wang et al. 2003). Similarly, the Amazon has long been the focus of attention in both theoretical and observational studies, with the latter being underpinned by major field programmes such as the Large-Scale Biosphere Atmosphere Experiment in Amazonia (LBA 1996) and more recent programmes such as the South American Biomass Burning Analysis (SAMBBA). Within Africa, knowledge of the climate system is concentrated in three areas. The multi-decadal Sahel drought dominates the African climate science research focus while study of the

West African Monsoon culminated in the largest ever land-based climate experiment, AMMA (Redelsperger et al. 2006). In southern African, multi-decadal and interannual rainfall characteristics have resulted in a legacy of both observational and modelling efforts, while East Africa, with its unusually high potential predictability on seasonal timescales, particularly in October to December, emerges as the third most studied region (Washington et al. 2006). The Congo climate regime, on the other hand, is the most understudied climate regime in Africa (Washington et al. 2006) and the most under researched large-scale convective region in the global tropics.

A key reason for the paucity of work on the Congo, notwithstanding its global importance, is the dearth of available climate observations from the region, particularly during the satellite data era. Only three meteorological stations from the Democratic Republic of Congo, for example, reported to the Global Telecommunication System in 2013. There was a dramatic decline in the number of rain gauges from more than 50 gauges between 1950 and 1980, following the work on collating the available record (Nicholson et al. 1988), to fewer than 10 over the 20 year period to 2010 (Figure 8.1). As a result, analyses of African rainfall based on gauge data have generally excluded the Congo Basin even though recent satellite-based studies show the region to capture the leading mode of Africa-wide rainfall (Jury and Mpeta 2009). To compensate for the lack of observed climate data, studies have tended to adopt proxies such as streamflow to represent rainfall quantities (Todd and Washington 2004) or satellite altimetry to evaluate water resources and climate (Lee et al. 2011).

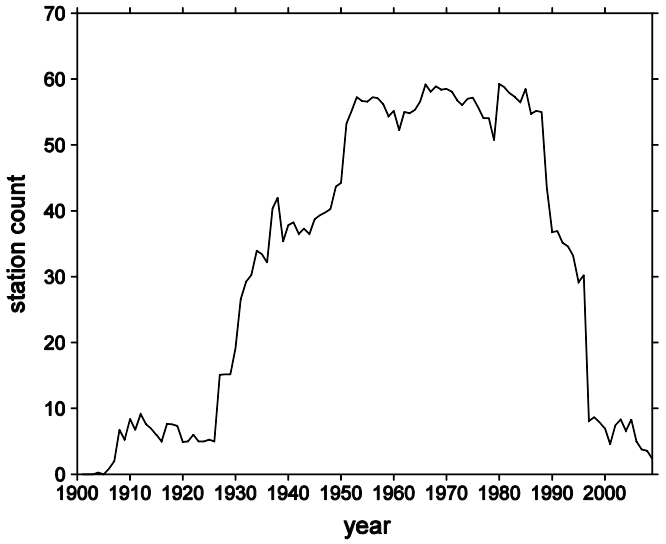

Figure 8.1 Number of rain gauges per year over the region 5°S-5°N, 12.5-30°E in the CRU 0.5° rainfall dataset. See box in Figure 8.3a for domain.

Given the importance of the Congo, several recent studies have probed the vulnerability of the region to climate change (Vizy and Cook 2012; Chapter 9) and the nature and controls on climate variability (Jackson et al. 2009; Jury et al. 2009; Pokam et al. 2011; Nicholson and Dezfuli 2013). These studies necessarily rely heavily on satellite data, numerical model products such as the reanalyses and/or coupled climate models. The relative performance of these tools over the Congo region is difficult to assess and compare because individual studies of the climate system tend to depend heavily on one type of data source without comparison across data products. Given that satellite rainfall products alone differ by a factor of 2–3 (Balas et al. 2007) and up to 2000 mm per annum in absolute terms (Beighley et al. 2011), a basic assessment of

the climatology of the Congo as represented by a variety of frequently used key products is much needed. The aims of this paper are therefore to:

- assess the rainfall climatology in two key rainfall seasons in rainfall datasets and as simulated in reanalysis and coupled climate models,
- evaluate the role of spatial model resolution in simulated Congo rainfall, and
- compare the basic state of moisture flux in reanalysis data and historical coupled model runs.

Section 8.2 outlines the data, 8.3 the rainfall climatologies and 8.4 the moisture flux regime. The final section is a summary of the results.

8.2 Data

This section outlines the data products used in this analysis. Years used for each dataset are defined in the relevant results section.

The following rainfall data have been used: standard monthly satellite-based products from CMAP (Climate Prediction Centre Merged Analysis of Precipitation) (Xie and Arkin 1997) and Global Precipitation Climatology Project (GPCP) (Adler et al. 2003), both available at 2.5° spatial resolution, monthly 0.5° resolution rain gauge-based datasets from Climatic Research Unit (CRU) (Mitchell et al. 2004), monthly TAMSAT satellite derived data at 0.0375° spatial resolution (Tarnavsky et al. 2013), monthly CMORPH (CPC Morphing Technique) satellite derived data at 0.0727° spatial resolution (Joyce et al. 2004) and data from the Tropical Rainfall Monitoring Mission (TRMM) version 3B43V7 (Huffmann et al. 2007) available at 0.25° spatial resolution (see ftp://meso-a.gsfc.nasa.gov/pub/trmmdocs/3B42_3B43_doc.pdf).

CMAP rainfall rates are obtained from five satellite estimates (not including TRMM). Although gauge data are merged in TRMM and GPCP, its impact over the Congo Basin may be expected to be minimal given the paucity of gauge data there.

Reanalyses data include NCEP/NCAR (Kanamitsu et al. 2002), CFSR (Saha et al. 2010), ECMWF reanalysis products including ERA-40 (Uppala et al. 2005) and ERA-Interim (Dee et al. 2011). These are used to evaluate the circulation controls on rainfall and rainfall itself. Monthly data from Coupled Model Intercomparison Project 3 (CMIP3) (Meehl et al. 2007a) for 24 climate models forced with historical estimates of variables known to be important to climate (e.g. greenhouse gases, sulphates, ozone and halocarbons) during the twentieth century (20C3M) are used in part to evaluate the numerical models used in climate change assessments to date (Table 2.3). Since CMIP5 (http://cmip-pcmdi.llnl.gov/cmip5/index.html) will supersede CMIP3, this newly released set of climate model runs that will dominate analyses in forthcoming years is also inspected (see Table 2.4 for details). CMIP3 and CMIP5 model data were interpolated to a common grid of 1.9° × 1.9° resolution. Ensemble means of CMIP3 and CMIP5 have been calculated from the common grid with even weighting applied to all models.

8.3 Congo rainfall climatology

In this section, the rainfall climatology of NCEP, CSFR, ERA-40, ERA-Interim, TRMM, CMAP, TAMSAT, CMORPH, CMIP3 ensembles and CMIP5 ensembles are evaluated.

8.3.1 Annual cycle of rainfall

Long-term monthly rainfall means (1961–1990 in the case of NCEP, ERA-40, CMIP3 ensemble and CMIP5 ensemble and 1979–1990 for ERA-Interim, CSFR and CMAP, 1998–2011 for TRMM and TAMSAT and 2002–2011 for CMORPH) have been computed for data interpolated to 1.9° × 1.9° latitude–longitude resolution (Figure 8.2) over the largely forested sector of the Congo Basin, namely 5°S–5°N, 12.5–30°E (see box in Figure 8.3a) (Pokam et al. 2011). All data products correctly feature the well-known bimodal rainfall distribution for the Congo Basin with peak rainfall in the transition seasons of September to November (SON) and March to May (MAM). SON is wetter than MAM in all datasets apart from TAMSAT and TRMM. There is broad agreement in the phase of the peak rainfall months (April and October) with the exception of ERA-Interim where MAM rainfall peaks a month earlier than any dataset. Minimum rainfall in the June to August season (JJA) is reached in July in all but the TAMSAT and TRMM data which show a May and June minimum, respectively. The minimum in the JJA season is lower than the December to February dry season minimum in all datasets with the exception of three model members of the CMIP5 ensemble and TAMSAT. The phase of the annual rainfall cycle is therefore well captured by these rainfall datasets. As reported previously (Beighley et al. 2011), the problem with the Congo rainfall datasets lies in the spread of rainfall magnitudes. This spread is clear in Figure 8.2 and varies across the datasets by a factor greater than 2 in both the rainy and dry seasons. When individual model members of the CMIP5 ensemble are considered, the spread reaches an order of magnitude in the DJF dry season. The reanalyses datasets (ERA-Interim and ERA 40)

and CMORPH are the wettest across all months in the rainy season and some of the individual CMIP5 models together with TAMSAT are the driest of the datasets considered here. These disparities are very large when compared with other regions of the planet.

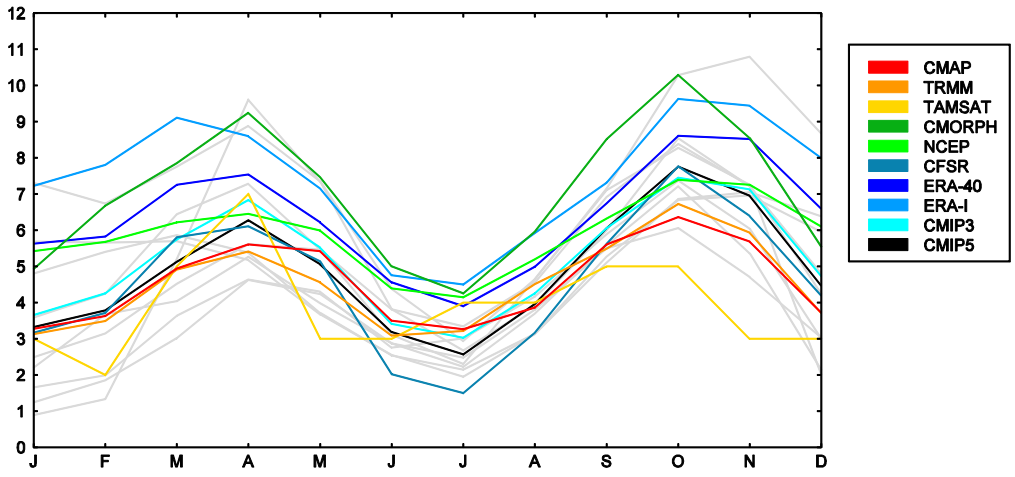

Figure 8.2 Long-term mean annual cycle of rainfall (mm d^{-1}) for Equatorial Central Africa over the region 5°S–5°N, 12.5–30°E for the following datasets: CMAP, TRMM, TAMSAT, CMORPH, NCEP, CSFR, ERA-40, ERA-Interim, ensemble mean of CMIP3 and CMIP5. Individual CMIP5 models are shown in grey. Years as defined in text.

8.3.2 Spatial distribution of rainfall

In MAM, all datasets capture the core convective regions of the Guinea coast, Congo Basin, Ethiopian highlands and the equatorial western Indian Ocean

(Figure 8.3). In some, such as CMAP, the rainfall distribution is zonally even, whereas others show a marked distinction between the Congo Basin and the Indian Ocean convective centres (e.g. NCEP and especially ERA-40, ERA-Interim, CMIP3 and CMIP5). In TAMSAT, the Congo Basin rainfall is dominant relative to other areas. The southwest to northeast orientation of the Congo Basin southern rainfall boundary is strongly represented in TRMM, CMORPH, NCEP, ERA-Interim and CMIP3 and CMIP5. Some products show a rainfall maximum in the western Congo (ERA-Interim, TRMM) while others an eastern Congo Basin maximum (e.g. NCEP, CMORPH and CMIP3). Individual CMIP5 models (Figure 8.S1) show a greater degree of spatial difference than that evident in Figure 8.3. Several models simulate a dry Congo Basin (e.g. MRI, GISS and HadGEM2) with others (CNRM, CSIRO, CanESM2, GISS) featuring a rainfall maxima over the equatorial Atlantic Ocean, most probably associated with the warm ocean eastern equatorial Atlantic bias of almost all CMIP5 coupled models (not shown).

Spatial agreement of rainfall distribution is generally higher in the rainfall datasets in SON (Figure 8.S2). All datasets show a coherent Congo Basin rainfall regime and a southwest to northeast orientation of the rainfall on the eastern side of the basin. A western basin maximum is evident in TRMM, CMAP, CFSR and NCEP while CMORPH and CMIP3 and CMIP5, the datasets used for climate projections, favour a maximum in the eastern Basin. Taken individually, the CMIP5 models in SON (Figure 8.S3), with the exception of CNRM and MPI, simulate a maximum over the Congo Basin. The diagonal eastern edge is evident in all models although the rainfall structure is latitudinally extensive in some (NorESM1, CSIRO). Four models place the rainfall maximum in the western Congo Basin and four in the east. A five

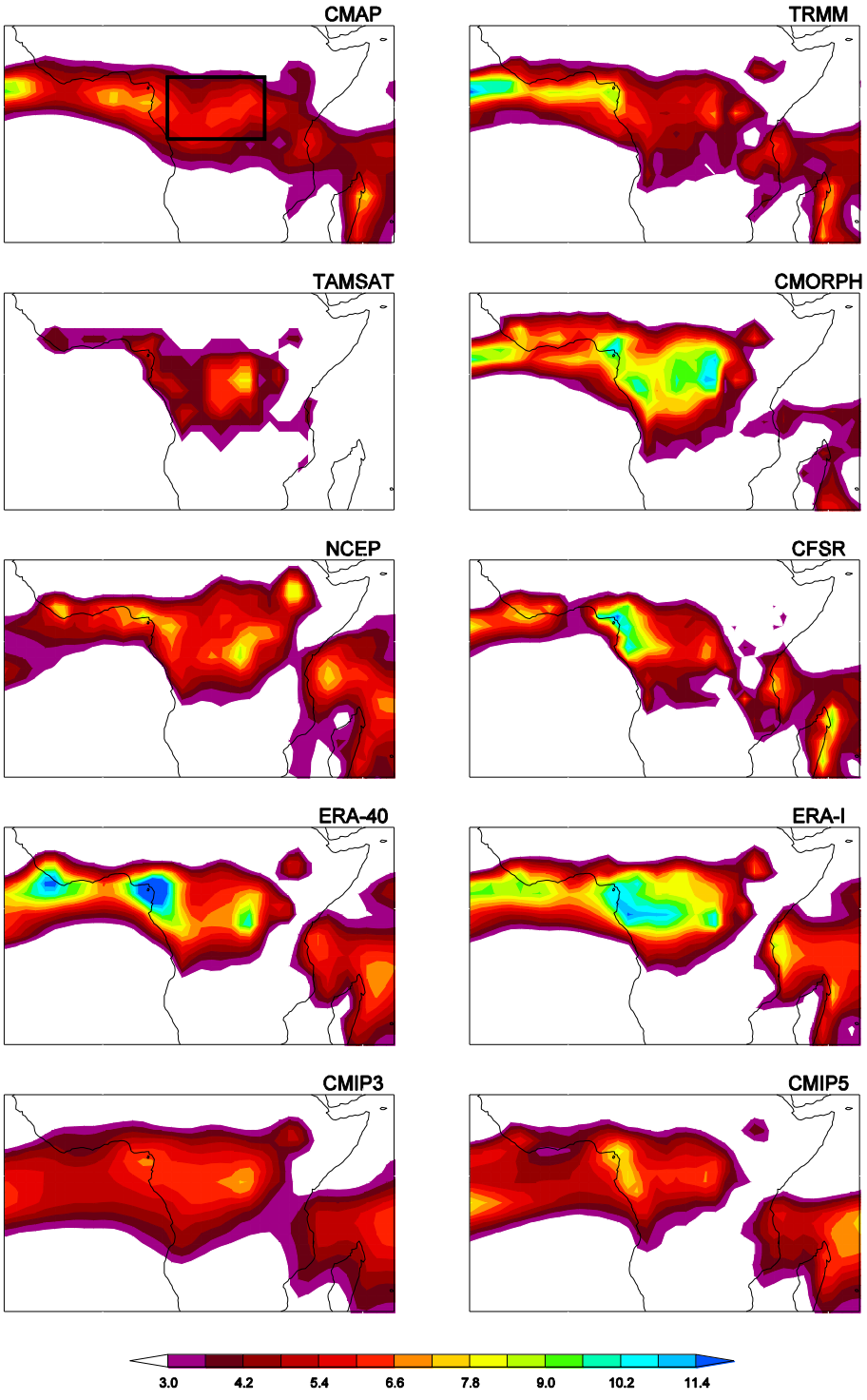

Figure 8.3 Rainfall climatologies (mm d^{-1}) during MAM for the following datasets: CMAP, TAMSAT, NCEP, ERA-40, ensemble mean of CMIP3, TRMM, CMORPH, CFSR, ERA-Interim, ensemble mean of CMIP5. Years as defined in text. Box in (a) plot corresponds to area-average used to derive data in Figures 8.1 and 8.2.

year climatology of mesoscale convective complexes based on analyses of TRMM data over the Congo Basin identified four spatial maxima which they relate in part to orography and associated circulation systems some of which collocate with the maxima discussed here (Jackson et al. 2009). Similarly, a study also using TRMM data, draws attention to the extreme spatial heterogeneity of interannual variability which maps on to the complex climatology (Nicholson and Dezfuli 2013). Diagnosing the controls on climate is made more uncertain by the extent of differences in the distribution of rainfall in these climatologies.

Differences among the rainfall totals for the datasets over the region 5° S–5° N, 12.5–30° E for MAM and SON (Figure 8.4) are demonstrably greater in SON where the driest dataset (TAMSAT) is some 50% of the wettest (CMORPH). Interestingly, the range of individual models in the CMIP3 ensemble spans the range of the non-numerical model products. The same is true for MAM although the differences among the data products are smaller in that season.

8.3.3 Regional models

Regional climate models (RCMs) are of growing importance as a source of detailed climate change projections partly because high spatial resolution (typically 50 km) allows the models to capture regional and local scale climate forcings (Giorgi et al. 2009), and associated potential improvements in model physical and dynamical formulations (e.g. representation of circulation controls on rainfall and land-surface feedbacks) compared with global climate models run at much coarser resolution

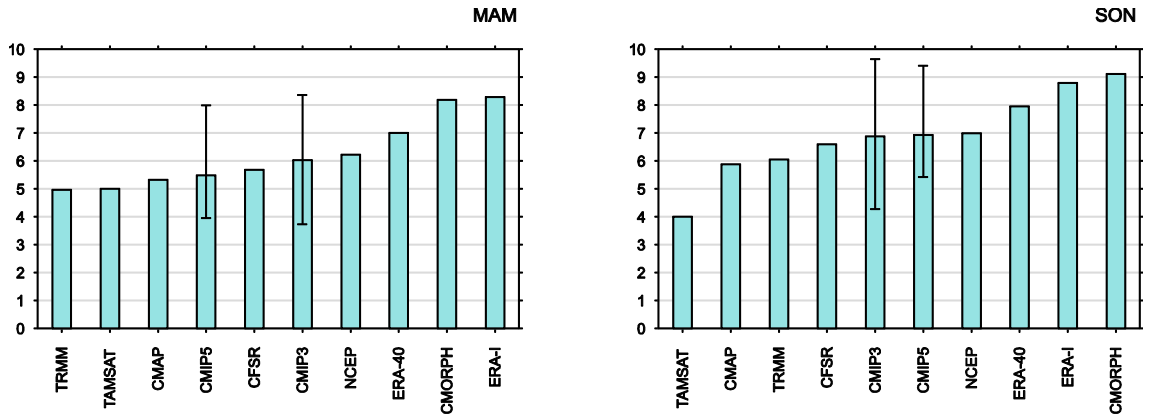

Figure 8.4 Rainfall climatologies for MAM and SON for the 10 datasets used in Figure 8.2.

(typically 250 km). The Coordinated Downscaling Experiment (CORDEX) (Giorgi et al. 2009), has Africa as its priority domain. The ensemble mean CORDEX simulations for the historical record (1989–2008) from 10 regional models run over Africa demonstrate that the regional models simulate the annual cycle reasonably well (Nikulin et al. 2012) although as with the CMIP simulations and the satellite derived and reanalysis datasets, the details of the annual cycle differ from model to model. Similarly, without the benefit of a gauge derived observed rainfall dataset at a resolution appropriate to the regional models, it would be difficult to confront the regional model climatologies definitively. Instead, the approach taken here is a comparative one. The Met Office Unified Model global atmospheric model GA3 is run continuously from 1982 to 2008 at 135 km horizontal resolution and the results are compared against that of the derived GA3 RCM, which is nested within quasi-observed atmospheric conditions from ERA-Interim reanalysis and run separately with two horizontal resolutions (135 and 50 km). The GA3 GCM RCM simulations

are forced with common observed daily oceanic boundary conditions and the results are assessed over the period 1996–2006. The advantage of this approach is the consistency in model physics across the global and regional models—which are unique to the Unified Model of the Met Office—an approach not possible in CORDEX framework.

The rainfall climatology of the model in all three configurations is wetter over the northern Congo than the comparative observed datasets in MAM (Figure 8.S4). The model Congo rainfall region is larger and more continuous than any of the observed datasets. In addition, the models are wetter in the eastern part of the basin west of the Great Lakes and in the far west of the basin. The general distribution of rainfall in the models is similar although at higher resolution (50 km) the eastern rainfall maximum is higher than either the coarser resolution regional model or the global model. At the same resolution (135 km), the global model is drier than the regional model. The difference between the global and regional model pertains to the forcing fields of the regional model (ERA-Interim). In SON (Figure 8.S5), the modelled rainfall over the Congo is again wetter than the observed datasets although the models produce a wetter eastern Congo and a drier western Congo compared with the observed. The eastern maximum in the model is least distinct in the global model and the finer resolution regional model but peaks in the coarser resolution regional model. It is important to note that these features fall into a particularly data sparse region with respect to gauge data. Even when using a physically consistent set of modelling tools, it is difficult to be precise about which resolution of regional model is better at simulating Congo rainfall although the differences resulting from

spatial resolution are even more pronounced when higher order statistical moments (variance, extremes, etc.) are analysed.

8.4 Moisture flux climatology

Differences between rainfall climatologies revealed in section 8.3 derive in part from the algorithms used to detect rainfall in the case of satellites and the parametrization schemes used in the case of reanalysis and coupled model simulations. Where observed gauge data are not available to constrain, confront or develop these tools, there is a tendency for the median representation of the rainfall climatology to be taken as the best estimate (Nikulin et al. 2012). There are seldom strong physical grounds for this decision. One way of evaluating the products without comparing rainfall itself, is to examine the underlying mechanisms closely associated with rainfall. Provision of water vapour through the moisture flux is one, albeit important, step in the process of rainfall generation. An advantage of evaluating moisture flux is that winds exert a strong control on the quantity and winds are generally better simulated in models than rainfall. If models are seen to diverge substantially in their moisture flux climatology, then reasons beyond different convective parametrization schemes could underlie the reasons for the divergent rainfall climatologies. For these reasons, moisture flux over the Congo Basin is evaluated in this section.

We start with the annual cycle of column stratified moisture flux convergence over the basin (Pokam et al. 2011) by representing this field along the meridional and zonal boundaries of the basin in three numerical datasets (Figure 8.S6).

Moisture convergence in MAM derives from upper level (850–300 hPa) meridional convergence resulting from the northern branch of the African Easterly Jet. The second maximum in SON is due to zonal moisture convergence from the Atlantic Ocean in the near-surface layer up to and including 850 hPa. Upper and lower layer net fluxes have opposite signs through most months pointing to Hadley and Walker-type circulations in the region. Reassuringly the three model products considered here (NCEP, ERA-Interim and CMIP5 ensemble) agree well in their basic structure and values of moisture flux through the Congo Basin boundaries although there are notable differences in the transition steepness and depth of the flow to and from the moist seasons. The differences in the net flux are larger between the two reanalysis products than between CMIP5 and ERA-Interim. Next, we consider the within basin details. To simplify the maps, we use 700 hPa for MAM (Figure 8.S7) and 850 hPa for SON (Figure 8.S8).

At 700 hPa in MAM, strong moisture flux divergence dominates west Africa and the Horn of Africa. Divergence over these regions is strongest in NCEP and ERA-Interim and substantially weaker in CMIP5. All three datasets show moisture flux convergence over the Congo Basin. The wettest of the three, ERA-Interim, features convergence furthest to the east of the basin while the driest in the east has the most bounded eastern interface between moisture convergence and divergence. These fields offer a simple insight into the differences in the model rainfall climatologies.

The SON moisture flux fields (Figure 8.S8) are more complex. Strong convergence in the north of the Congo Basin is separated from convergence into the

Angolan low by weak convergence across much of the basin itself in two datasets (ERA-Interim and CMIP5) but weak divergence in the case of NCEP. In all three, moisture flux is strongly convergent in the east of the basin. Best agreement between all three is the strongly divergent coast of East Africa—a region known to be anomalously dry for its latitude. As with MAM, there is a simple mapping between the strength of the moisture convergence in the Congo Basin and the model rainfall. The wetter models (ERA-Interim and CMIP5) feature convergence while the driest (NCEP) features divergence. These differences in the distribution of convergent moisture flux are even more stark in the case of individual CMIP5 models during MAM (not shown) and SON (Figure 8.S9) where five of the nine models have very weak or no convergence in the central basin. Taking the extremes in CMIP5 model rainfall, the driest model (Figure 8.5), CNRM in SON, features no moisture flux convergence in the core of the basin while moisture flux is convergent in the wettest, NorESM1, from 6° N, through the core of the basin, to south of 30° S. These results suggest that observations of moisture flux convergence are a promising field with which to confront the models.

8.5 Summary

The primacy of the Congo Basin in earth system dynamics is undisputed. The basin forms one of three major convective regions on the planet. During the transition seasons, this convection is larger than any other region in the global tropics. A dearth in observed meteorological data over the basin severely constrains progress with understanding the climate system. Satellite derived datasets differ by a factor of

at least 2 and, in absolute terms, by up to 2000 mm yr^{-1}. An order of magnitude separates rainfall simulated in some coupled models in the dry season and rainfall simulated in reanalyses datasets. There are fundamental ambiguities such as whether the western or eastern Congo Basin is wetter.

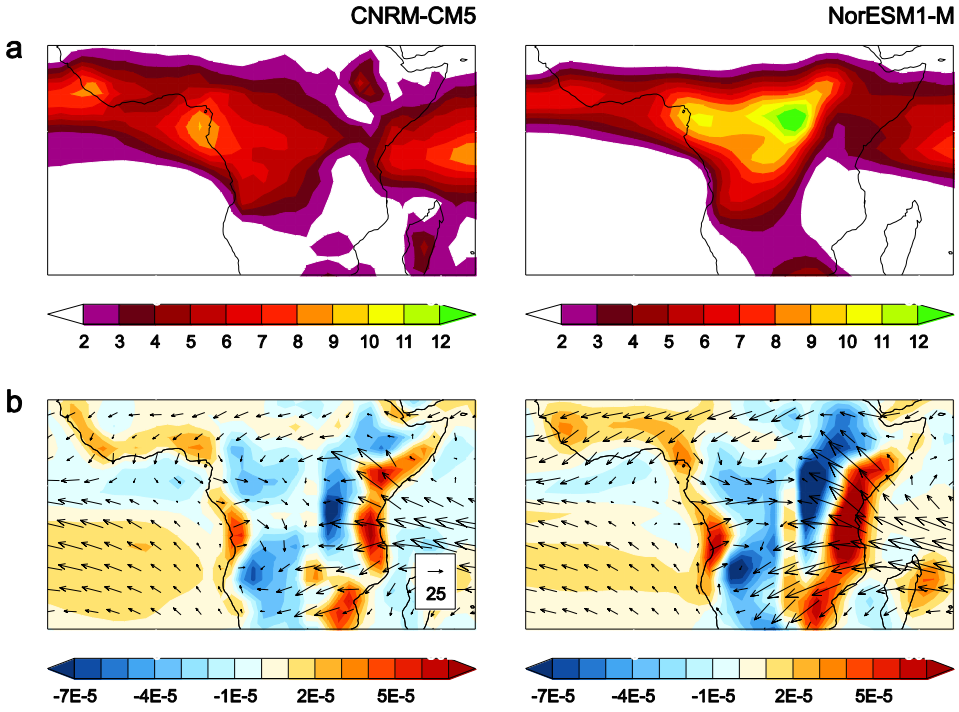

Figure 8.5 (a) Rainfall (mm d^{-1}) and (b) moisture flux at 850 hPa climatologies for the driest (CNRM-CM5) and wettest (NorESM1-M) models in SON. Units are mm d^{-1} in (a) and g $kg^{-1}m\ s^{-1}$ in (b) with contours of divergence (g $kg^{-1}\ s^{-1}$).

It turns out that moisture flux is a particularly useful quantity with which to compare model rainfall products since there is a simple mapping between the strength of the moisture convergence in the Congo Basin and model rainfall. Wet models

feature well-defined moisture flux convergence. Very dry models show moisture flux divergence. Long-term rain gauge-based monitoring over the basin is unlikely to be put in place in time to understand the dynamics of climate change. A different approach is therefore needed. What these results point to is the potential utility of short-period intensive observation campaigns which target atmospheric circulation, notably water vapour transport in concert with rainfall measurements. A short-term network of radiosonde stations over the Congo Basin in combination with weather radar and Aircraft Meteorological Data Relay (AMDAR) could provide the data to develop the tools, both from instruments on satellites and numerical models, much needed in climate research of the region. These data could be used to confront climate models and potentially establish which models are producing a realistic simulation of Congo rainfall. Without such steps, we are left to deal with the spectrum of possibilities of both current and future simulations of Congo rainfall. Given the importance of the basin, this is not a good position to be in.

Supplementary Information: Chapter 8

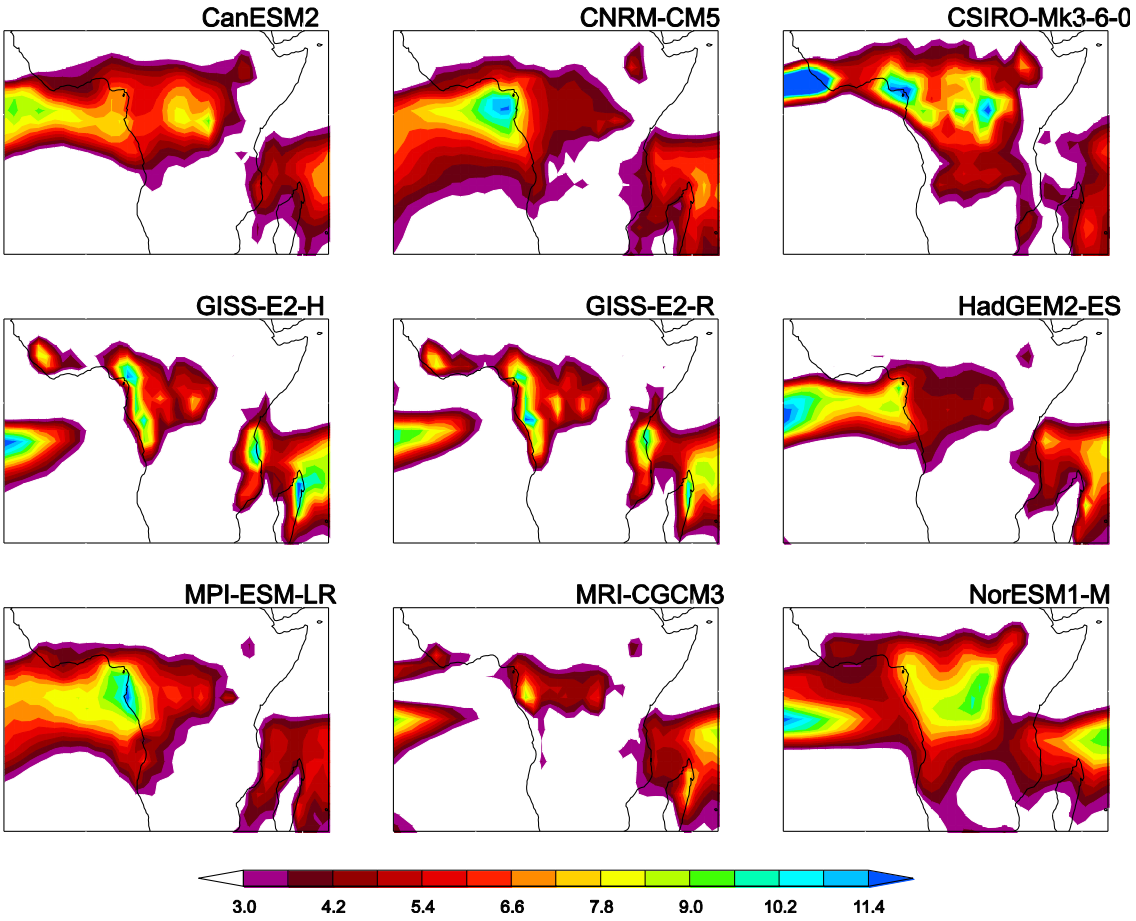

Figure 8.S1 Rainfall climatologies (mm day^{-1}) during MAM for 9 CMIP5 models.

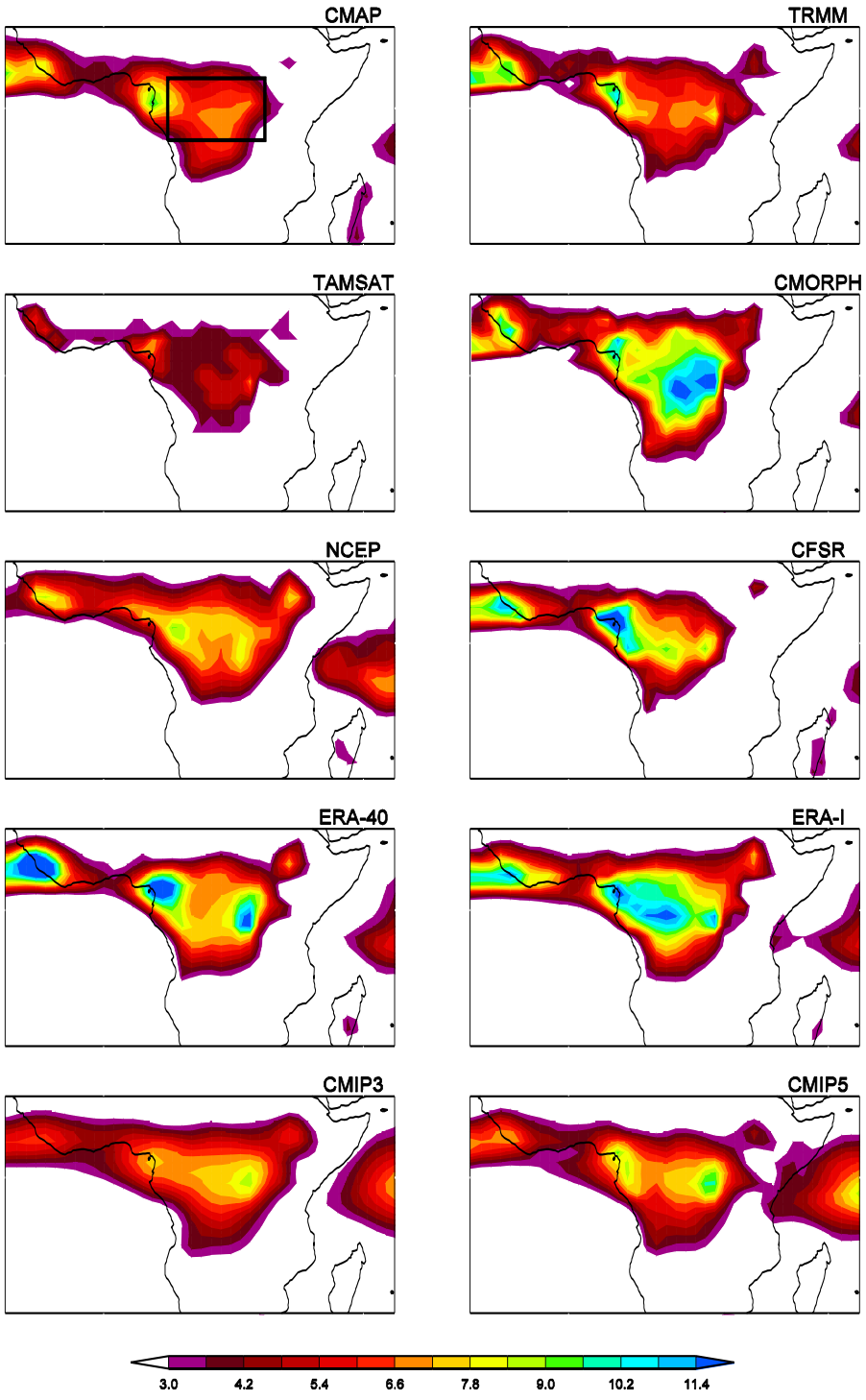

Figure 8.S2 Rainfall climatologies (mm day^{-1}) during SON for the following data sets: CMAP, TAMSAT, NCEP, ERA-40, ensemble mean of CMIP3, TRMM, CMORPH, CFSR, ERA-Interim, ensemble mean of CMIP5. Years as defined in text.

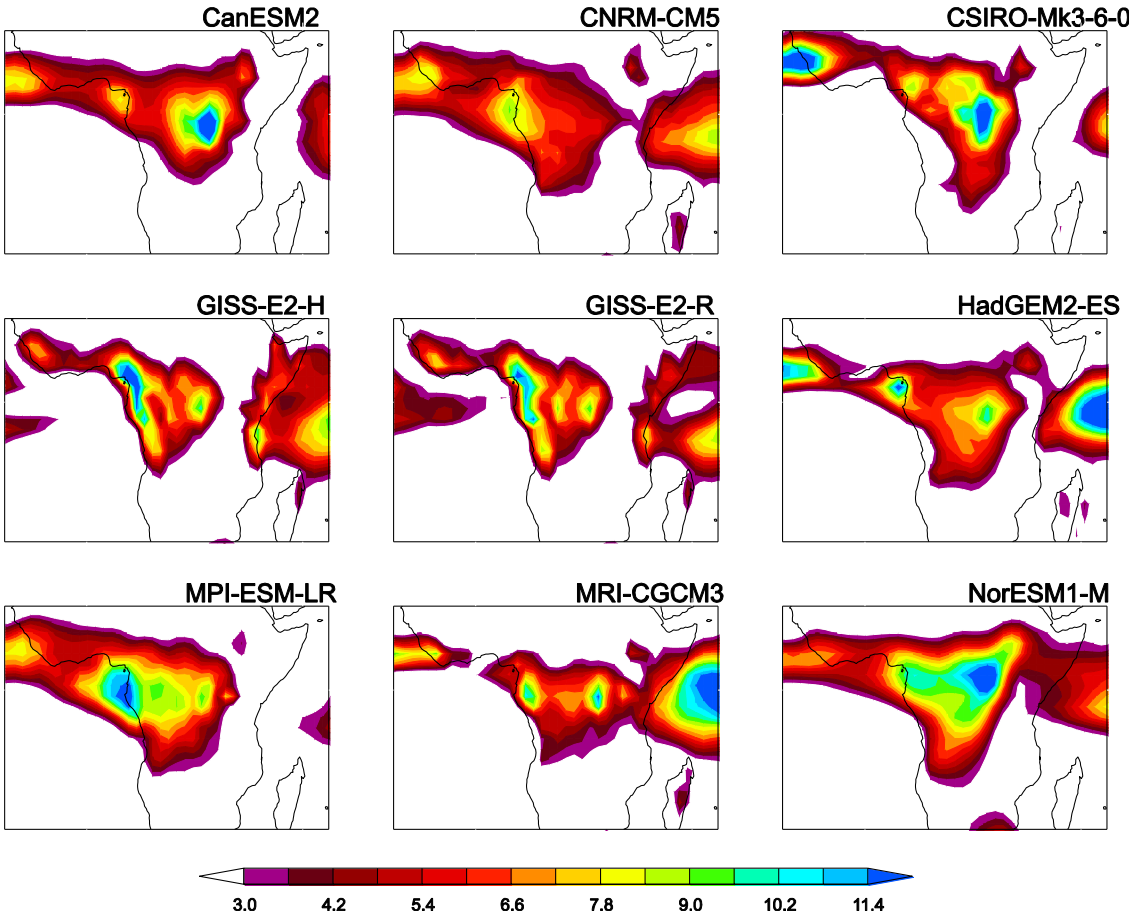

Figure 8.S3 Rainfall climatologies (mm day^{-1}) during SON for 9 CMIP5 models.

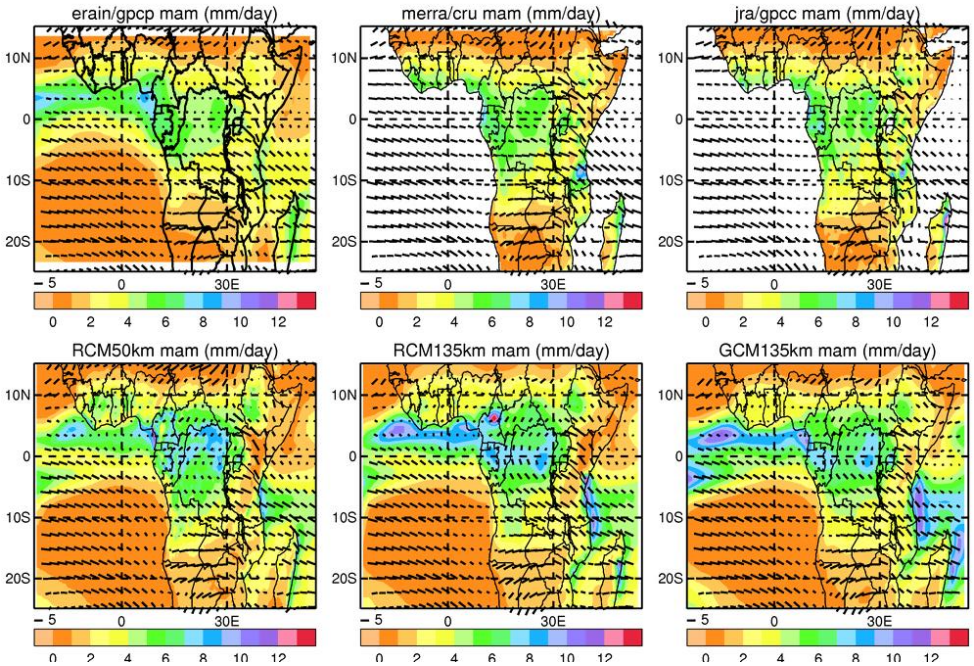

Figure 8.S4 MAM mean rainfall (mm day^{-1}) for 1990-2006. Top row, ERA-Interim (left), CRU (middle), GPCP (right), bottom row RCM at 50km (left), RCM at 135 km (middle) GCM at 135 km (right).

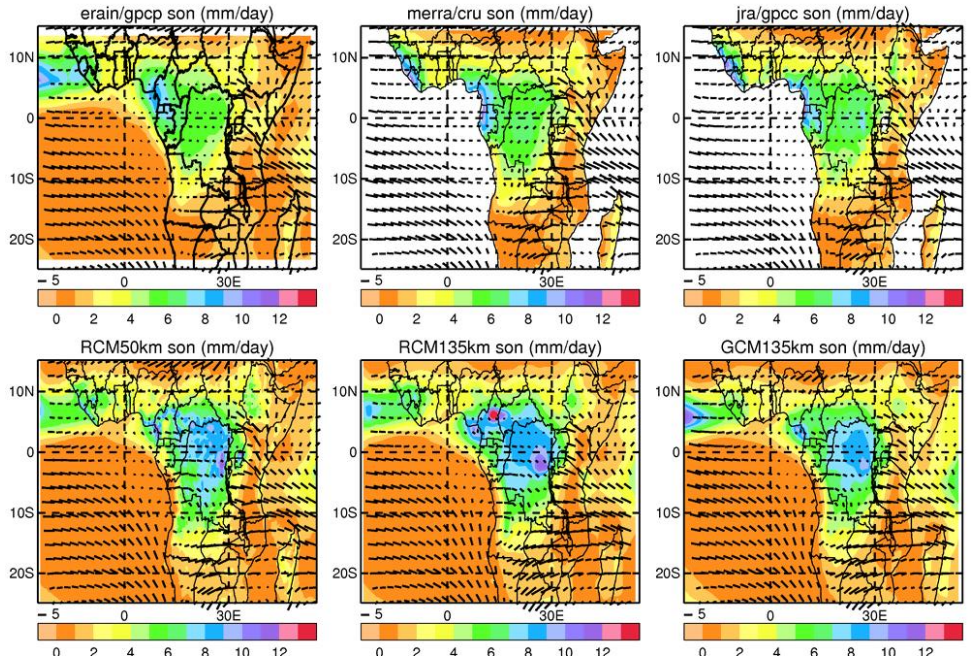

Figure 8.S5 SON mean rainfall (mm day^{-1}) for 1990-2006. Top row, ERA-Interim (left), CRU (middle), GPCP (right), bottom row RCM at 50km (left), RCM at 135 km (middle) GCM at 135 km (right).

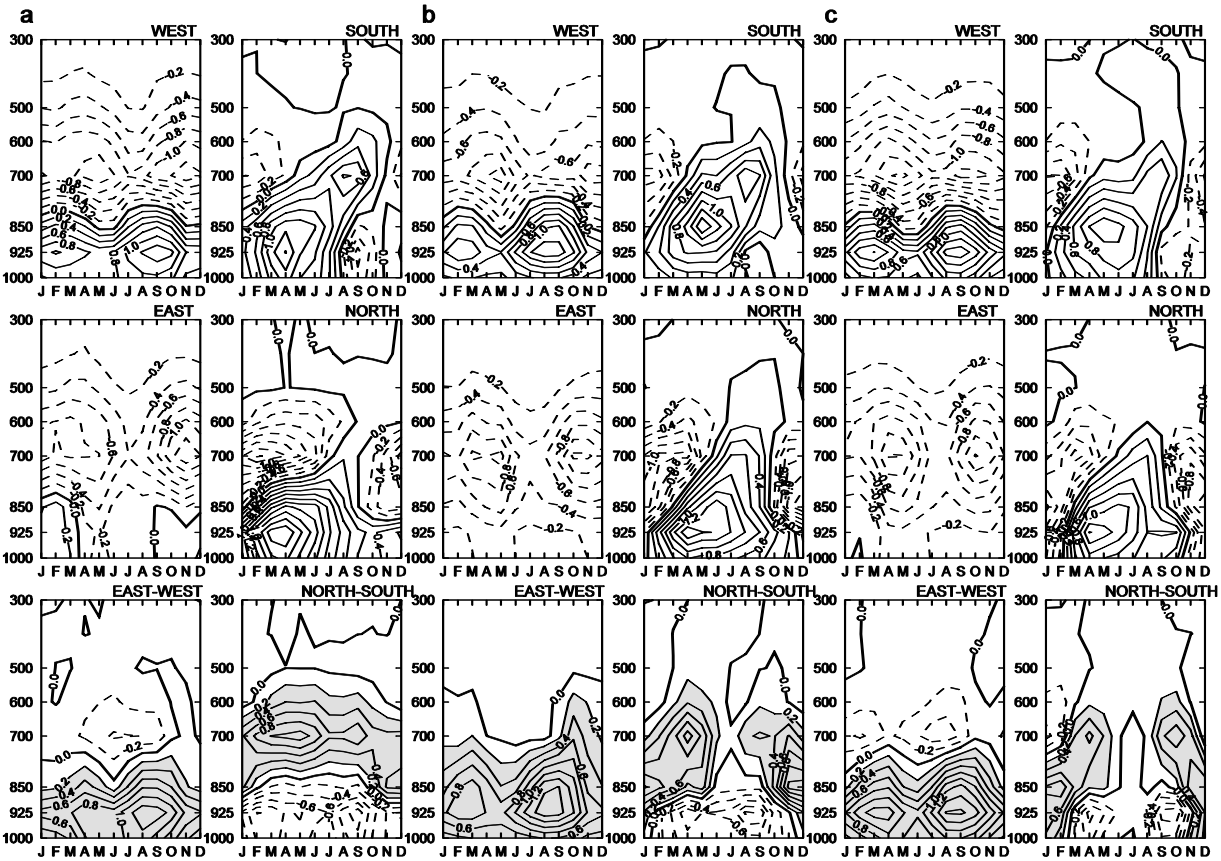

Figure 8.S6 Time height sections of water vapour fluxes (units: 10^{-3} Kg m^{-2} s^{-1}) through borders of Equatorial Central Africa, scaled by the surface area of the region: West (12°E), East (30°E), South (5°S), North (5°N), and net zonal (East minus West) and meridional (North minus South). Moisture convergence >0.2 x 10^{-3} Kg m^{-2} s^{-1} is shaded in grey. For NCEP (a), ERA-Interim (b) and the CMIP5 multi-model mean (c).

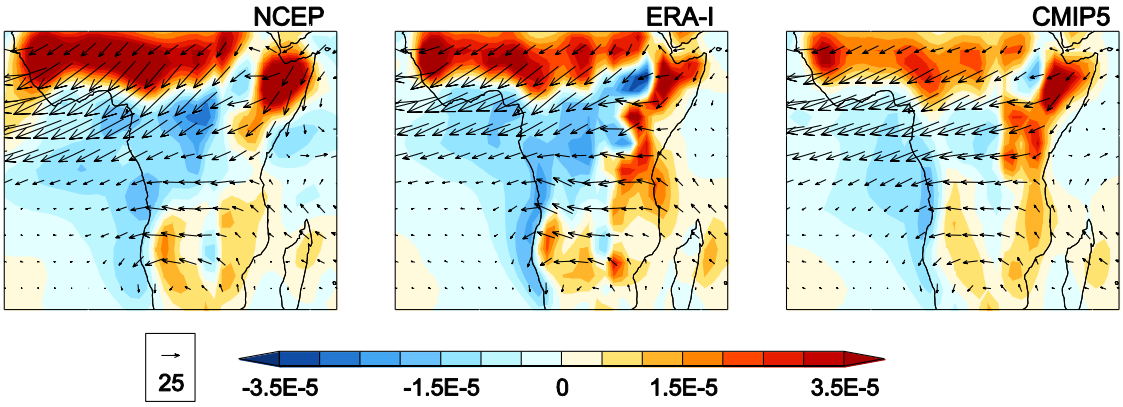

Figure 8.S7 Moisture flux climatologies (g kg^{-1} ms^{-1}) at 700hPa during MAM for NCEP, ERA-Interim and the CMIP5 multi-model mean, with contours of divergence (g kg^{-1} s^{-1}).

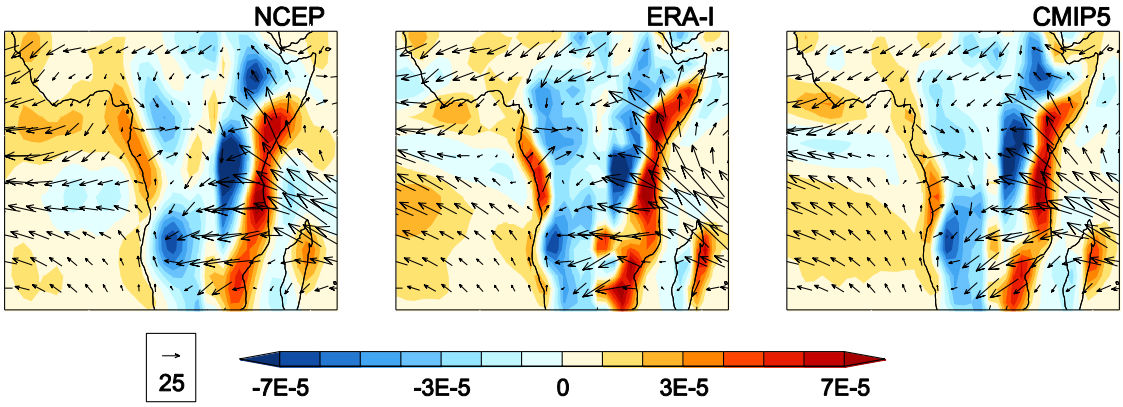

Figure 8.S8 Moisture flux climatologies (g kg^{-1} ms^{-1}) at 850hPa during SON for NCEP, ERA-Interim and the CMIP5 multi-model mean, with contours of divergence (g kg^{-1} s^{-1}).

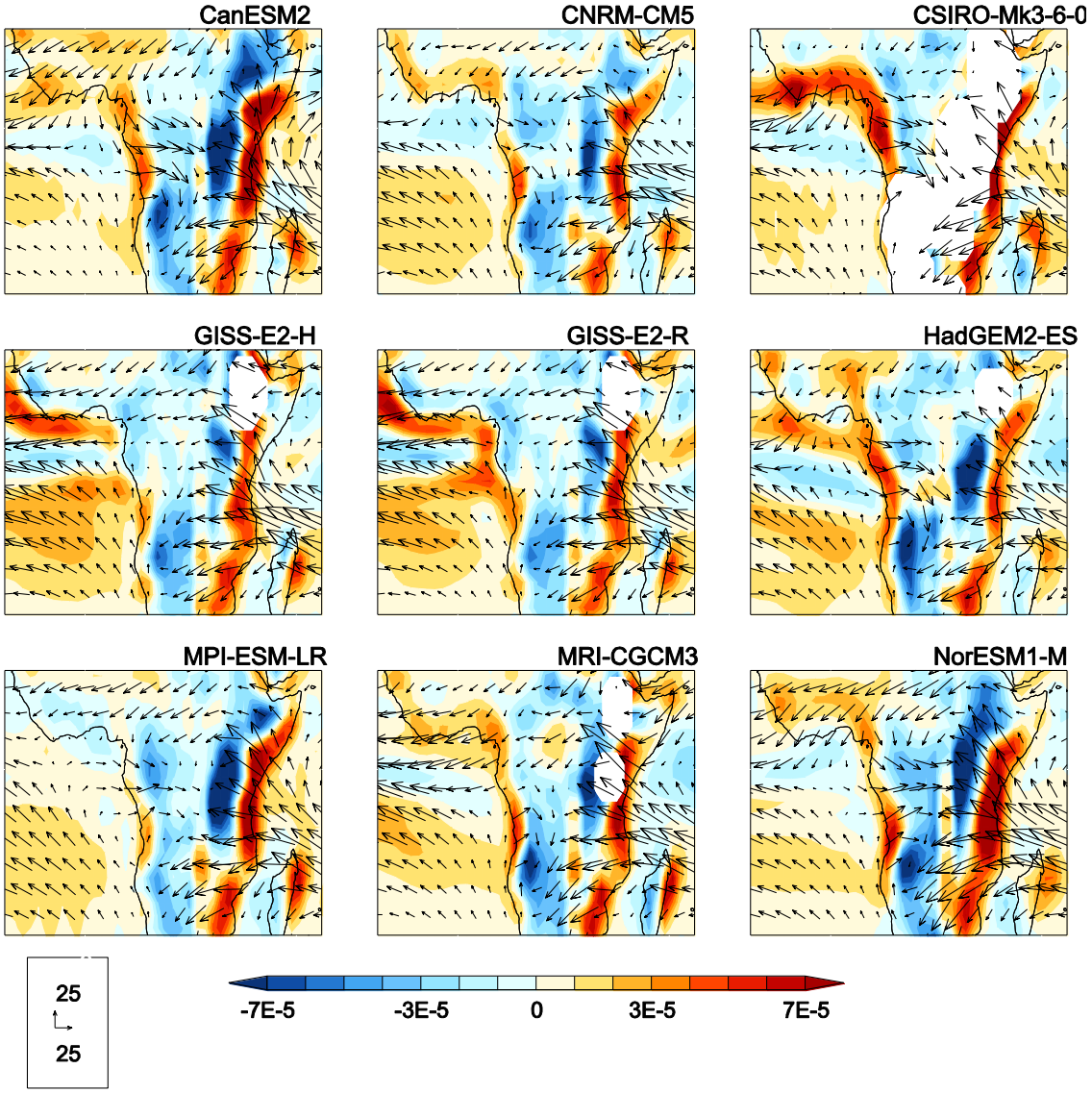

Figure 8.S9 Moisture flux climatologies (g kg^{-1} ms^{-1}) at 850hPa during SON for for 9 CMIP5 models, with contours of divergence (g kg^{-1} s^{-1}).

9 Implications of global warming for the climate of African rainforests

Authorship Declaration

I performed the analysis for this paper and did all of the writing. R. Washington was involved in planning the analysis, especially the investigation of atmospheric dynamics, and played an important role in helping to interpret the results and advising on the structure of the paper. As noted in Chapter 5, D. P. Rowell helped with accessing and pre-processing the perturbed physics ensemble data, and consulted on the regression of global temperature against local precipitation. He made a useful contribution towards revising the paper, particularly with respect to comparison between ensembles.

Implications of global warming for the climate of African rainforests

R. JAMES AND R. WASHINGTON

Climate Research Lab, Oxford University Centre for the Environment, South Parks Road, Oxford OX1 3QY, UK

D.P. ROWELL

Met Office Hadley Centre, FitzRoy Road, Exeter EX1 3PB, UK

Philosophical transactions of the Royal Society of London. Series B, Biological sciences **368** (1625) 20120298 doi:10.1098/rstb.2012.0298 2013

Published 22 July 2013

Abstract

African rainforests are likely to be vulnerable to changes in temperature and precipitation, yet there has been relatively little research to suggest how the regional climate might respond to global warming. This study presents projections of temperature and precipitation indices of relevance to African rainforests, using global climate model experiments to identify local change as a function of global temperature increase. A multi-model ensemble and two perturbed physics ensembles are used, one with over 100 members. In the east of the Congo Basin, most models (92%) show a wet signal, whereas in west equatorial Africa, the majority (73%) project an increase in dry season water deficits. This drying is amplified as global temperature increases, and in over half of coupled models by greater than 3% per °C of global warming. Analysis of atmospheric dynamics in a subset of models suggests that this could be partly because of a rearrangement of zonal circulation, with enhanced convection in the Indian Ocean and anomalous subsidence over west equatorial Africa, the Atlantic Ocean and, in some seasons, the Amazon Basin. Further research to assess the plausibility of this and other mechanisms is important, given the potential implications of drying in these rainforest regions.

Keywords: climate change, global warming, Central Africa, precipitation, projections, Indian Ocean

9.1 Introduction

Changes in local temperature and precipitation have the potential to affect African rainforests and have led to large ecological shifts on millennial timescales (Malhi and Wright 2004). Projecting the impact of anthropogenic interference on the climate of West and Central Africa is therefore important: to provide information for forest conservation and adaptation, and also for mitigation, allowing assessments of the level of anthropogenic forcing that should be avoided if rainforests are to be protected. International mitigation debates have often sought a global temperature threshold to which warming should be restricted, and 2°C has emerged as a benchmark for danger. Projections presented as a function of global mean temperature increase (ΔT_g) are therefore particularly valuable from a political perspective, and could inform judgements of whether 2°C is a safe limit for African rainforests.

Existing analysis of climate change projections for Central Africa is very limited, and studies of African futures have sometimes omitted this region owing to the lack of observational data for model validation (e.g. http://www.knmi.nl/africa_scenarios/). Projections for the global tropics suggest that convective regions will become wetter in response to global warming (Allan and Soden 2007) owing to an increase in atmospheric boundary layer moisture (Chou and Neelin 2004); but this will be partly offset by a weakening of tropical circulation (Vecchi and Soden 2008) and may be reversed locally by regional dynamics. The Intergovernmental Panel on Climate Change projections for Central Africa show small positive precipitation anomalies, based on data from the Coupled Model

Intercomparison Project phase 3 (CMIP3) (Christensen et al. 2007). However, during the late twentieth century some western African forest regions experienced a drying trend (Malhi and Wright 2004), and some climate models project drier futures at the Atlantic coast (Delire et al. 2008). Hence, there is considerable uncertainty about the direction of precipitation change resulting from anthropogenic forcing, and this further creates uncertainty about the magnitude of local warming, which is likely to be modified by precipitation through cloud cover and/or soil moisture feedbacks.

Several studies have used the CMIP3 models to investigate the implications of specific ΔT_g thresholds for African precipitation (Chapter 4) and the impact of these precipitation changes on the potential distribution of humid tropical forests (Zelazowski et al. 2011). These papers reveal that the increase in precipitation in Central Africa projected by many of the models is enhanced from 2°C to 3°C to 4°C of global warming, suggesting greater potential for rainforest expansion as global warming progresses. However, some models show drying in western regions, which could be associated with forest retreat, especially at 4°C. This is further complicated by projected increases in local temperature, which could allow rainforests to move into regions with higher elevations, but might also have an influence via changing rates of transpiration, photosynthesis and respiration.

The present study aims to explore trends in Central African temperature and precipitation associated with ΔT_g, adding to previous work by comparing CMIP3 with two perturbed physics ensembles (PPEs) developed by the Met Office Hadley Centre (MOHC). Indices of specific relevance to tropical rainforests are used, and the range of model projections is presented for regions of interest, including west

equatorial Africa where many models show a dry signal. Dynamics associated with contrasting precipitation responses in this region are examined as a first step to assessing the plausibility of a drying trend.

The model ensembles are described in section 9.2, followed by an outline of the methodology. Section 9.3 presents the regional climate projections, and 9.4 assesses global fields from a subset of models in order to evaluate the mechanisms associated with drying. The implications of projected changes are then discussed.

9.2 Material and methods

9.2.1 Data

9.2.1.1 Coupled Model Intercomparison Project phase 3

Monthly data were selected from CMIP3 (Meehl et al. 2007a) for all 19 models run in SRES A2 (see Table 2.3), and the same models run in 20C3M, which incorporates historical forcings, available at: http://esg.llnl.gov:8080/index.jsp. These data were interpolated to a 1° x 1° spatial resolution.

9.2.1.2 Atmospheric Slab model Perturbed Physics Ensemble

Atmospheric Slab model PPE (AS-PPE) consists of 280 versions of HadSM3, which has the same atmospheric and land surface physics as HadCM3 (one of the coupled models included in CMIP3), but with a 50 m thermodynamic mixed

layer or 'slab' ocean. Each model version was run in equilibrium experiments, with preindustrial and doubled CO_2 ($2xCO_2$). The runs continue for 20 years after equilibrium, and 20-year monthly means from this period were used for the analysis. These data have a spatial resolution of 2.5° latitude and 3.75° longitude, and 19 vertical levels.

Thirty-one atmospheric and land surface parameters were perturbed (Barnett et al. 2006), with the intention of sampling uncertainties rather than producing a match to observations. Model versions with large top of atmosphere flux imbalances (greater than 5 Wm^{-2}) and entrainment coefficients outside the likely range (less than 2 or greater than 4) (Sexton et al. 2012) were excluded from the analysis, leaving 112 members. Data are available via the British Atmospheric Data Centre (BADC) at http://tiny.cc/qump_oxford (http://tiny.cc/badc_access).

9.2.1.3 Atmospheric Ocean model Perturbed Physics Ensemble

Atmospheric Ocean model PPE (AO-PPE) consists of 17 versions of HadCM3. The 17 parameter combinations were chosen from the possible 280 explored in AS-PPE and then coupled to a dynamical ocean. Each model version was run in transient experiments: a 150-year control run with preindustrial (1860) forcings and SRES A1FI. For the preindustrial, a 20-year period was selected 40 years into the run, to avoid spin up issues.

One of the 17 versions has the standard parameterisations of HadCM3, and this version is identical to that included in CMIP3 except for the addition of flux

adjustments and an interactive sulphur cycle. Another version was chosen because it had the best simulation of present-day climate, and the other 15 were selected to span a range of climate sensitivities and parameter values (Collins et al. 2011). Four of the model versions have entrainment coefficients greater than 4, which is outside the likely range, and these are excluded from the analysis, leaving 13 members. Data are available via the BADC as above.

9.2.2 Methods

Changes in annual temperature, annual precipitation and maximum climatological water deficit ($MCWD_{100}$) were calculated, as these have been found to be good indicators of humid tropical forest extent (Zelazowski et al. 2011). Local changes were related to global mean temperature increase (ΔT_g). Area-averages were used to explore the range of model projections for regions with contrasting signals in the ensemble means.

The different ensembles were used for different stages of this analysis. CMIP3 and AO-PPE were used to evaluate local change as a function of ΔT_g, as these models were run in transient scenarios, with a change in anthropogenic forcing (and global temperature) over time. In AS-PPE, each model has a fixed level of anthropogenic forcing ($2xCO_2$); therefore, it is not possible to directly investigate the impact of changes in global temperature that arise from different levels of anthropogenic forcing. However, this ensemble has a larger number of members and was used to explore intermodel variability.

9.2.2.1 Maximum climatological water deficit

MCWD is calculated from monthly mean precipitation (*P*) and evapotranspiration (*ET*) (mm month^{-1}). The climatological water deficit (CWD) is computed for each month as follows. First, the month with the highest mean precipitation is identified and CWD for this month is set to 0, on the assumption that soil is saturated. For each month (*n*) that follows CWD is computed from the difference between precipitation and evapotranspiration, and the previous month's CWD:

$$CWD_n = CWD_{n-1} + P_n - ET_n$$

If $CWD_n > 0$, then CWD_n is set to 0. The MCWD is the most negative value of CWD:

$$MCWD = Min(CWD_1, CWD_2, \ldots, CWD_{12})$$

For multi-year periods the calculation is applied to long term monthly means. Here *ET* is set at 100 mm month^{-1}. Previous studies have used this approximation for calculating MCWD and shown skill in reproducing historical tropical vegetation distributions in Africa (Zelazowski et al. 2011). Changes in

$MCWD_{100}$ represent modifications in dry season water deficit due to precipitation change alone (assuming constant evaporation).

9.2.2.2 Rate of local change per °C of ΔT_g

For CMIP3 and AO-PPE, changes in temperature, precipitation, and $MCWD_{100}$ for each model grid-point were linearly regressed against global mean temperature increase (ΔT_g) using ordinary least squares and the slope of the regression line (m) used to represent local change in each index per °C of ΔT_g. The regression slope (m) was calculated separately for each model and the ensemble mean. The data points were overlapping 20 year time periods: area-weighted global mean temperature anomalies and local anomalies of temperature, precipitation, and $MCWD_{100}$ associated with 2000-2019, 2010-2029, etc. (Table 9.S1), relative to control climatologies (20 year preindustrial for AO-PPE, 1980-99 for CMIP3). The slope was tested for difference from zero using a t-test, following (Wilks 2006), at a significance level of 5%. The percentage of models with positive slopes was calculated on a grid-point by grid-point basis to illustrate model agreement on the direction of change; and the percentage of models with significant slopes was computed to show agreement on a lack of signal.

9.2.2.3 Regional change associated with ΔT_g

Area-weighted area-averages of temperature, precipitation, and $MCWD_{100}$ anomalies were calculated for regions identified as exhibiting contrasting trends in the

gridded ensemble mean projections: "West Equatorial Africa" (11-18°E; 10°S-5°N) and "Central Equatorial Africa" (23-32°E; 10°S-5°N). For AS-PPE the changes associated with $2xCO_2$ were used (based on 20 year means for the control and $2xCO_2$ scenarios). For CMIP3 and AO-PPE, changes associated with specific ΔT_g thresholds (1°C, 2°C, 3°C, etc.) were calculated.

In order to sample at each ΔT_g interval annual ΔT_g time-series were created for each model (Figure 9.S1), using a 15 year control climatology (preindustrial for AO-PPE, 1985-99 for CMIP3). These time-series were smoothed using polynomial regression, and then the date at which the regression line crossed 1°C intervals of ΔT_g was extracted and defined as the median of a 15 year sampling period (Table 9.S2). Anomalies of temperature, precipitation, and $MCWD_{100}$ were calculated by differencing these 15 year climatologies from control climatologies (preindustrial for AO-PPE, 1985-99 for CMIP3). Note that the number of ΔT_g levels available varies between models, and is a maximum of 6°C for AO-PPE and 3°C for CMIP3.

A statistical significance test of difference between the control and each ΔT_g interval was computed for each model to establish whether the response to warming is distinct from interannual variability. The Mann Whitney U test was chosen as precipitation is a skewed distribution in many arid regions and the test makes no assumptions about distribution. The direct method was applied due to the small sample size (15 years): for each year in the control, the number of years in the forced time period with a smaller value is counted, and the sum of these counts becomes the U statistic (U_1). This is repeated for the forced time period to get U_2, and the smaller of U_1 and U_2 is compared to the critical value. The significance level was set at 5%.

9.3 Projected trends in regional climate

The African tropics are projected to warm more than the global average in all three ensembles (Figure 9.1a; AS-PPE not shown). In CMIP3 the largest warming is in the subtropics, in contrast to AO-PPE, in which there is also pronounced heating (>1.4°C per °C of ΔT_g) in the south of Central Africa and in West Africa.

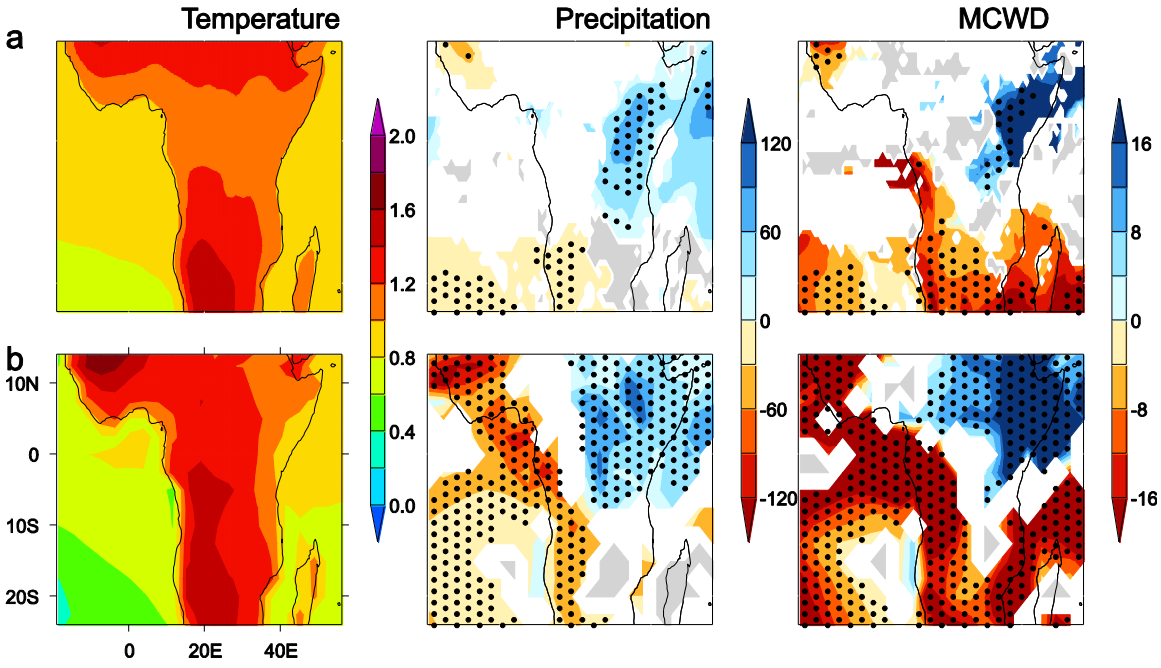

Figure 9.1 Maps of local ensemble mean change per °C of ΔT_g: annual temperature (°C per °C), annual precipitation (mm yr^{-1} per °C) and $MCWD_{100}$ (mm $month^{-1}$ per °C) in CMIP3 (a) and AO-PPE (b). For temperature, locally insignificant (5% level) anomalies are masked in white. For precipitation and $MCWD_{100}$, white indicates less than 66% model agreement on the direction of change, grey indicates more than 66% of models show no significant change and stippling indicates greater than 80% model agreement on the direction of change.

Precipitation changes demonstrate substantial variation between and within the ensembles (Figure 9.1b). In general AO-PPE projects larger changes per °C of ΔT_g than CMIP3. Both ensemble means show positive annual mean precipitation anomalies in East Africa, and negative anomalies in some western regions, with >80% model agreement in the direction of change. The dry signal is much more extensive and of a larger magnitude in AO-PPE, at >90 mm year^{-1} °C^{-1} in parts of West Africa and west equatorial Africa in the ensemble mean. Both ensembles show agreement for a lack of signal over parts of Mozambique and Madagascar.

The spatial distribution of $MCWD_{100}$ anomalies (Figure 9.1c) is similar to that of annual precipitation (Figure 9.1b): with most models projecting dry signals in western regions, and wet signals in the Horn of Africa. Relative to Figure 9.1b, negative anomalies occupy a larger proportion of the African tropics: including the south and west of the Congo Basin, where there is a negative anomaly >16 mm month^{-1} per °C of ΔT_g in the AO-PPE ensemble mean. This means there is intermodel agreement that dry seasons will intensify in regions where models agree that there will be no significant change averaged across the annual cycle (grey in Figure 9.1b), or disagree in the direction of mean change (white in Figure 9.1b). Therefore even where there is considerable uncertainty about how the wet and dry season changes will average, there is consensus that precipitation will be reduced during dry seasons.

The ensemble mean plots for both annual precipitation and $MCWD_{100}$ suggest a contrast in the precipitation signal between western and eastern equatorial regions. Area-averages of "West Equatorial Africa" and "Central Equatorial Africa"

(Figure 9.2) illustrate the spread of CMIP3 and AO-PPE model responses in each of these regions, and show how local changes develop as global temperature increases. Changes in AS-PPE associated with $2xCO_2$ are also shown. In Central Equatorial Africa most models show little change or a modest wet signal. At 4°C and beyond none of the models shows negative anomalies. In West Equatorial Africa there is a great deal of spread between members of AS-PPE in the direction and magnitude of change, although more models exhibit a dry signal than a wet signal. In the transient ensembles there is little significant change at 1°C, but from 2°C there is a progressive decrease in $MCWD_{100}$, and from 3°C this is >100 mm $month^{-1}$ in some versions of HadCM3. Note that the boxplots in Figure 9.2 are based on a different number of models at each ΔT_g interval, but that individual models also show progressive change as global temperature rises.

The projections of annual precipitation and $MCWD_{100}$ change presented here exhibit variation between models in terms of the direction, magnitude, and spatial pattern of change; but there is one signal which emerges from many different models within the core rainforest zone: a drying in West Equatorial Africa. There have been indications of such a signal in previous literature based on annual mean precipitation (Delire et al. 2008). When measured here as $MCWD_{100}$ the pattern shows consistency between models and the dry signal extends over a larger proportion of the Congo Basin. In the next section mechanisms associated with drying in this region are explored.

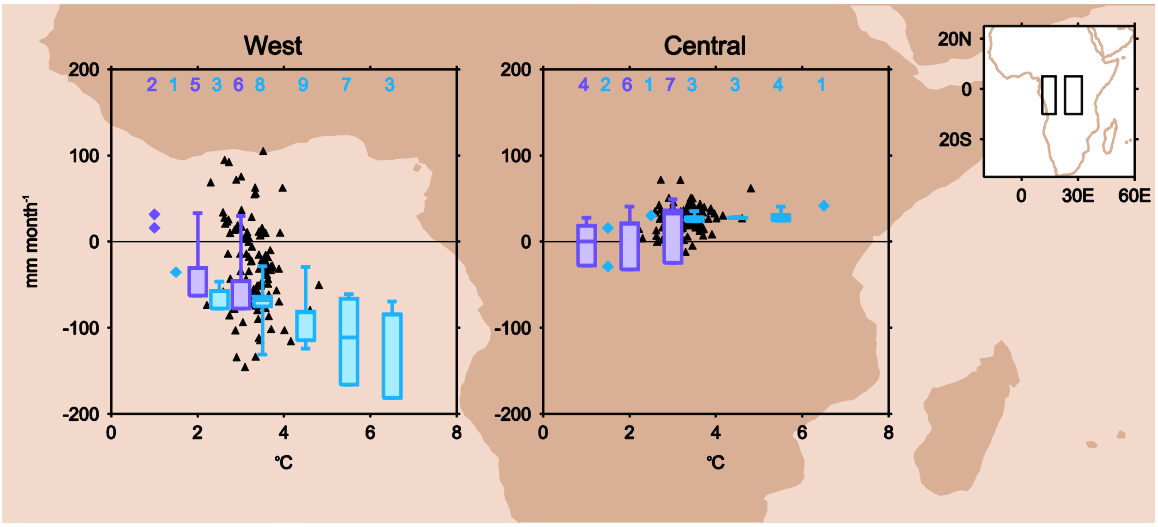

Figure 9.2 Regional $MCWD_{100}$ anomalies (mm month^{-1}) for 'west equatorial Africa' and 'central equatorial Africa'; associated with $2xCO_2$ in AS-PPE (triangles), and ΔT_g levels for CMIP3 and AO-PPE (purple and blue boxplots, respectively: minimum, lower quartile, median, upper quartile and maximum). Only models with significant change (5% level) are included in the boxplots, the number of which is indicated. Where fewer than three models show significant change, boxplots are replaced with points for individual models. Boxplots based on all models are shown for comparison in Figure 9.S2. Note that not all models are available at each ΔT_g interval. Alternative plots based on the regression slope for all models are shown in the electronic supplementary material, figure S3.

9.4 Dynamics associated with drying in west equatorial Africa

The majority of models project an increase in dry season water deficit in west equatorial Africa, but AS-PPE also includes some models which show a wet signal in response to CO_2 (Figure 9.2). The slab model ensemble therefore provides the opportunity to investigate mechanisms associated with regional precipitation decline, through a comparison of members which show wetting and drying. The models with the 10 most negative and 10 most positive $MCWD_{100}$ anomalies in West

Equatorial Africa were used to form a "dry" and a "wet" composite; and changes associated with $2xCO_2$ were explored for a range of atmospheric variables across the globe. Figure 9.3 displays the difference between the composites (dry – wet) in terms of precipitation, vertical velocity (ω), sea level pressure (SLP), sea surface temperature (SST), wind, horizontal moisture flux (qV), and divergence.

These plots are based on averages of each group of 10 models, but grid-points are only shown where the difference between the dry and wet models is robust to variation within each composite according to the Mann Whitney U test. This test for consistency is important, as models with a similar $MCWD_{100}$ response in "West Equatorial Africa" might have different regional precipitation signals and/or large scale dynamical responses. The grid-points with significance in Figure 9.3 represent signals which are shared by many models within the same composite, confirming that there are consistent differences between composites in regional precipitation response.

Models in the dry composite exhibit negative precipitation anomalies over this region in the annual mean and all four seasons: DJF, MAM, JJA, SON (denoted by the initial letter of each month); albeit with limited spatial extent in MAM. The strongest dry signal occurs during SON. The same models have wet anomalies in East Africa in all seasons. In contrast, the wet composite shows positive precipitation anomalies throughout equatorial Africa, with the largest wetting at the Atlantic coast during SON. This regional precipitation difference in SON is clear from Figure 9.3, and is matched by differences in ω, indicating that dry models experience a larger enhancement of subsidence over west equatorial Africa, and convection over East Africa.

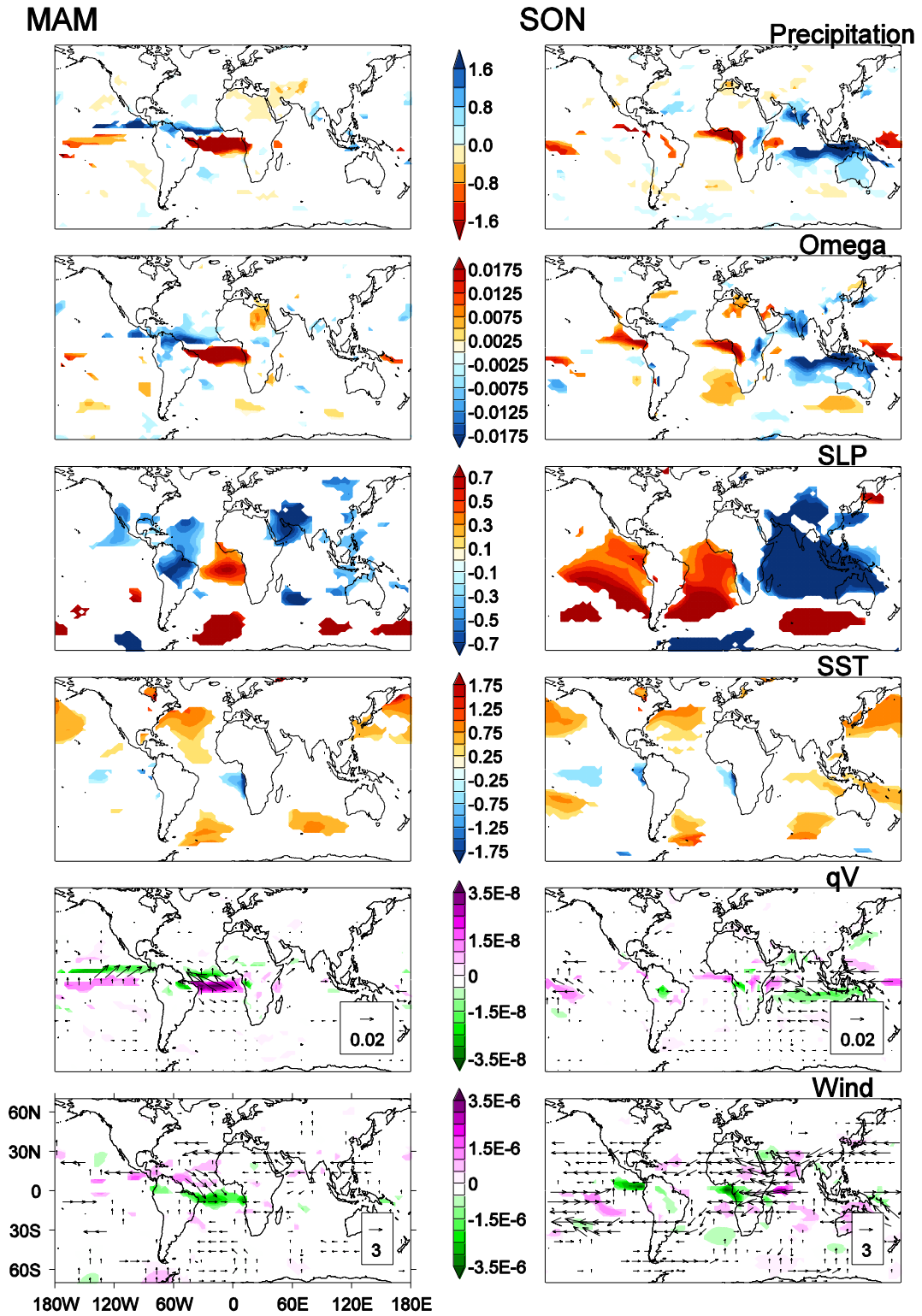

Figure 9.3 'Dry' minus 'wet' AS-PPE composite seasonal anomalies associated with 2xCO_2 for precipitation (mm day^{-1}), ω at 500 hPa (hPa s^{-1}), SLP (hPa), SST (°C), qV at 925 hPa (kg kg^{-1} ms^{-1}) with contours of moisture divergence (kg kg^{-1} s^{-1}) and wind vectors at 200 hPa (m s^{-1}) with contours of divergence (s^{-1}), for MAM and SON. Areas not significantly different from zero (5% level) are masked in white.

There are also consistent distinctions between the dry and wet composites beyond the African tropics, suggesting that changes in large scale dynamics may be at least partly responsible for the trends projected in this region. The tropical Atlantic and Indian Ocean could both be important.

9.4.1 Tropical Atlantic

The maps of difference in precipitation, ω at 500hPa, and qV at 925hPa (Figure 9.3) indicate that the precipitation reduction and downward anomalies in west equatorial Africa in the dry composite forms the eastern edge of a larger zonal band of subsiding air and moisture divergence at the surface which stretches across the Atlantic Ocean. To the north of this region of drying is a wet signal; suggesting a northward displacement of the Atlantic Inter-Tropical Convergence Zone (ITCZ). This is evident in all seasons (Figure 9.S4), but has the largest anomalies and is most zonally oriented during MAM. It might be explained by a meridional contrast in SLP and SST anomalies: with more warming in the North than South Atlantic Ocean. Relative to wet models and the ensemble mean, dry models show cooling and pressure increases in the Gulf of Guinea, suggesting a more pronounced Atlantic cold tongue. This has previously been associated with changes in the latitude of the ITCZ and, as a consequence, precipitation changes in western Africa (Tokinaga and Xie 2011).

There may also be a connection with South America. Hadley Centre models are known to dry the Amazon in response to global warming (Malhi et al. 2009), and

in AS-PPE the ensemble mean, wet, and dry composites all have negative precipitation change in this region; but the dry composite shows the largest reduction in precipitation. The anomalous subsidence which the dry models experience in the Atlantic Ocean throughout the year extends into the Amazon during DJF (Figure 9.S4). This adds an additional motivation for diagnosing the mechanisms in these models, as the same processes might dry both rainforest regions. The Amazon dieback has been attributed to an El Nino-like state in HadCM3 (Cox et al. 2004), and drying in Central Africa on interannual timescales has also been linked to El Nino (Balas et al. 2007); but there is no clear El Nino-like difference between dry and wet models.

9.4.2 Indian Ocean

There are also large differences between the composites in the Maritime Continent and eastern Indian Ocean, although these are only significant during SON (Figure 9.3). Dry models show much more moistening associated with $2xCO_2$, and this is accompanied by a larger warming of SSTs, a convergence of moisture and decrease in pressure at the surface, and upward ω anomalies; suggesting an augmentation and westward extension of the warm pool region.

Links between the Indian Ocean and African precipitation have been found in previous studies, with particular emphasis on East Africa and the Sahel. Idealized Indian Ocean warming experiments, designed to diagnose teleconnections with the Sahel in JAS, have also shown a strong drying response in west equatorial Africa

(Hoerling et al. 2006; Mohino et al. 2011). Hoerling et al. (2006) attribute this to anomalous zonal circulation with rising air over the Indian Ocean and subsiding air over western Africa.

The dry models used here show evidence of a shift in zonal circulation during SON, in terms of ω anomalies, and horizontal fluxes in the Indian Ocean: with westerly flow at 925hPa and easterly flow at 200hPa, as well as convergence in the upper atmosphere over west equatorial Africa and the Gulf of Guinea (Figure 9.3). The high SLP over the Atlantic Ocean could potentially be amplifying the strength of these anomalies, in keeping with Balas et al. (2007)'s suggestion that an opposition between Indian and Atlantic Ocean SSTs might cause an eastward shift in convection, drying western Africa and wetting eastern Africa. Perhaps it is this contrast between ocean basins which is key: the difference between Maritime Continent (75-130°E; 10°S-10°N) and Gulf of Guinea (5°W-8°N; 10°S-3°N) SLP anomalies calculated for the 112 models in AS-PPE is positively correlated with $MCWD_{100}$ anomalies in West Equatorial Africa; during SON ($r=0.61$) and the annual mean ($r=0.72$). The correlation with Maritime Continent anomalies alone is weaker.

9.4.3 Discussion

The composite analysis therefore implies that drying in west equatorial Africa is associated with a zonal SLP anomaly between the Gulf of Guinea and the Maritime Continent and a shift in zonal circulation. However, further research is necessary: to establish whether there is a causal connection, to investigate reasons why

the models might project differences between the Atlantic and Indian Oceans, and to examine the plausibility of the response.

Part of the explanation for the signal may lie in the preindustrial climatology. There are contrasts between the dry and wet composites before any doubling of CO_2, in both the Gulf of Guinea and the warm pool region (Figure 9.S5). This is likely to influence the response to greenhouse gases. For example, the dry models have more precipitation in the warm pool region during the preindustrial, so it is not surprising that they show greater enhancement of convection under $2xCO_2$, as wet regions are expected to become wetter in a warmer climate (Chou and Neelin 2004). Analysis of model biases in the preindustrial might therefore be a useful means for identifying implausible signals. In the case of the Maritime Continent, both the dry and wet composite have large biases relative to the observed climatology (GPCP), so it is not possible to suggest that either is more realistic on this basis.

Another way to investigate the mechanisms in the dry composite would be to establish whether the same zonal anomalies are associated with drying in west equatorial Africa in AO-PPE and CMIP3. The slab models do not have a dynamical ocean, so any change in SSTs and teleconnections are due to atmospheric forcing. It would be useful to examine whether there is evidence for a zonal shift in models with a fully coupled ocean-atmospheric system.

Additional mechanisms must also be investigated, as the zonal SLP contrast explains a maximum of 50% of the intermodel variability in the precipitation response (r^2 =0.5 in the annual mean). Other changes in large scale atmospheric dynamics, such as the north-south contrast in Atlantic Ocean SSTs, may be important. However,

previous work suggests that variation between modelled precipitation responses over tropical landmasses is associated more with uncertainties in the representation of direct local responses to greenhouse gases than with remote teleconnections to SSTs (Rowell 2012). For example, drying in west equatorial Africa might be associated with the representation of the land-sea contrast, which would influence the strength of low level westerlies during SON. Analysis using regional climate models might help to disentangle the role of local and remote influences.

Establishing whether spatially coherent drying of west equatorial Africa is a plausible or likely response is therefore beyond the scope of this paper. However, given that this signal is produced by many different models, and a potential mechanism for precipitation decline has been identified, the implications of such a change will now be examined.

9.5 Potential implications for African rainforests

African rainforests are already close to the hydrological limits of closed canopy forest (Lewis et al. 2009), and their resilience to increases in water stress is uncertain, particularly given that drier conditions would also heighten the risk of fire (Poulter et al. 2010). Drier periods in the last two to three millennia led some forests to become more open, more fire-prone, and less carbon-dense (Brncic et al. 2007). It is difficult to judge whether the magnitude of $MCWD_{100}$ change projected here would drive this scale of ecological change. The average $MCWD_{100}$ for humid tropical forests in Africa is approximately -300 mm $month^{-1}$ and regions with $MCWD_{100}$

below -400 mm month^{-1} are generally inhabited by other types of forest or savanna (Zelazowski et al. 2011). Therefore the order of magnitude of the anomalies projected by some AO-PPE models after 2°C of global warming could have a large impact: at 3°C one model exhibits a decrease >100 mm month^{-1}, and at 4°C three models project change of this amplitude.

These changes are averaged over 15 years, and do not provide any information about the magnitude or frequency of single drought years, which have been shown to exert a damaging influence on rainforests in Amazonia during the last decade (Phillips et al. 2009). A tentative analysis of AO-PPE precipitation trends during JJA, the season with the most drying, suggests that there is little modification in interannual variability with warming: the change in standard deviation is <0.09 per °C of warming in all models. Thus there is a shift in the mean with little to no change in variability, implying an increase in the intensity of dry years, which warrants further research.

Temperatures are also projected to increase, and in the AO-PPE ensemble mean this warming is >1.4°C per °C of ΔT_g in the south west of the Congo Basin (Figure 9.1a). The vulnerability of rainforests to higher temperatures is debated. Warming may have a direct effect on rainforest trees by inhibiting photosynthesis, but the thermal tolerances of most species are poorly understood, as is the extent to which the influence of temperature will be overridden by CO_2 enrichment (Corlett 2011). Higher temperatures would also have hydrological implications; enhancing transpiration through higher leaf-to-air vapour pressure deficits. This could potentially amplify the projected increase in dry season water stress, which has been calculated

here assuming fixed evapotranspiration. Though increasing CO_2 concentrations are expected to increase plant water use efficiency, decreasing transpiration, initial assessments indicate that the net impact of higher temperature and higher CO_2 will be an increase in evapotranspiration (Malhi et al. 2009).

The projected dry signal therefore represents a potential risk to rainforests in the west of the Congo Basin, but it is unclear how resilient the forests would be to this precipitation forcing, especially given interactions with changing temperature and CO_2. There is further uncertainty about how vegetation changes would feedback to regional climate, via modifications to surface roughness, albedo, and evapotranspiration. If precipitation decreases were large enough to cause a reduction in tree cover, there might be less evapotranspiration and more runoff into rivers, leading to lower precipitation rates. However, the models used here do not incorporate dynamic vegetation, with the result that vegetation cover, and therefore evapotranspiration levels, are maintained even under very low precipitation levels.

The precipitation projections presented here might therefore differ if the models included a dynamic vegetation model and more advanced land surface scheme, although it is not clear whether this would dampen or enhance the dry signal. Betts et al. (2004) find that dynamic vegetation in HadCM3 amplifies drying in Amazonia, but not in Congo Basin. The newest generation of global model experiments (CMIP5) includes several Earth System Models with dynamic vegetation, and existing research has largely found projections from CMIP5 to be similar to CMIP3 (Knutti and Sedlacek 2012; Monerie et al. 2012a). However there has been little work to date to

differentiate the influence of dynamic vegetation, and this represents an opportunity for further research.

9.6 Conclusions

Many climate models project increases in precipitation in East Africa and decreases in western Africa in response to global warming. In west equatorial Africa, some models show large increases in dry season water deficit at 2°C (up to 78 mm month^{-1}); with potentially dangerous implications for African rainforests. This is amplified at 4°C (up to 124 mm month^{-1}) and beyond (up to 180 mm month^{-1}), and is associated with pronounced local warming. In a subset of slab models, the dry signal in west equatorial Africa is found to be at the eastern edge of a large region of subsidence in the Atlantic Ocean. This may be associated with a northward shift of the Atlantic ITCZ, and/or a rearrangement of the zonal circulation during SON, with anomalous ascent over the Maritime Continent and Indian Ocean, and anomalous subsidence over western Africa and the Atlantic Ocean. In some seasons the subsidence extends to South America, suggesting that this could have an influence on both the Congo and Amazon rainforests. Further research to assess the validity, plausibility, and likelihood of these mechanisms is a priority. This should be accompanied by investigation into the potential interactions with other atmospheric and vegetation changes, which are highly uncertain, and could act to dampen or enhance the ecological risks implied by changes in precipitation.

Funding statement

The work undertaken by D.P.R. is part of the output from a project funded by the UK Department for International Development (DFID) for the benefit of developing countries. The views expressed are not necessarily those of DFID. The PPE datasets were produced through work supported by the UK Joint 'Department for Energy and Climate Change' (DECC), 'Department for Environment, Food and Rural Affairs' (Defra) MOHC Climate Programme (GA01101). The CMIP3 dataset was supported by the Office of Science, U.S. Department of Energy.

Acknowledgements

The authors would like to thank Gil Lizcano for technical support, and Yadvinder Malhi for useful discussions. We also acknowledge the modelling groups, the Program for Climate Model Diagnosis and Intercomparison and the WCRP's Working Group on Coupled Modelling for their roles in making available the CMIP3 multi-model dataset.

Supplementary Information: Chapter 9

Table 9.S1 Time periods used to construct regression coefficients for AO-PPE and CMIP3. The differences between the ensembles are due to data availability.

CMIP3	AO-PPE
-	2001-2020
2010-2029	2011-2030
2020-2039	2021-2040
2030-2049	2031-2050
2040-2059	2041-2060
2050-2069	2051-2070
2060-2079	2061-2080
2070-2089	2071-2090
2080-2099	2081-2100

Table 9.S2a Medians of 15-year periods selected for climatologies from CMIP3 models, to represent 1°C, 2°C, and 3°C ΔT_g increases relative to 1985-99.

Model[a]	**1°C**	**2°C**	**3°C**
BCCR-BCM2.0	2044	2071	2091
CGCM3.1 (T47)	2037	2066	2089
CCSM3.0	2037	2063	2083
CNRM-CM3	2046	2077	-
CSIRO-Mk3.0	2033	2061	2083
CSIRO-Mk3.5	2034	2063	2087
ECHAM5/MPI-OM	2040	2070	-
ECHO-G	2039	2073	-
GFDL-CM2.0	2036	2067	2092
GFDL-CM2.1	2026	2058	2085
GISS-ER	2033	2061	2082
INGV-SXG	2031	2059	2080
INM-CM3.0	2036	2067	2089
IPSL-CM4	2041	2065	2084
MIROC3.2(medres)	2047	2077	-
MRI-CGCM2.3.2a	2024	2055	2079
PCM	2048	2084	-
UKMO-HadCM3	2037	2064	2085
UKMO-HadGEM1	2032	2059	2078

[a]Naming conventions are taken from the IPCC www-pcmdi.llnl.gov/ipcc/model_documentation/ipcc_model_documentation.php

Table 9.S2b Medians of 15-year periods selected for climatologies from AO-PPE models, to represent 1°C, 2°C, 3°C, 4°C, 5°C, and 6°C ΔT_g increases relative to a 15 year preindustrial climatology.

Model	1°C	2°C	3°C	4°C	5°C	6°C
1[b]	2014	2041	2062	2081	-	-
2	2036	2063	2084	-	-	-
3	2032	2059	2081	-	-	-
4	2035	2060	2080	-	-	-
5	2022	2050	2071	2089	-	-
6	2013	2043	2064	2081	-	-
7	2015	2044	2064	2081	-	-
8	2011	2040	2060	2076	2090	-
9	2027	2051	2070	2086	-	-
10	2013	2041	2061	2078	2092	-
11	2007	2035	2054	2069	2083	-
12	-	2035	2054	2069	2081	2093
13	2011	2038	2057	2074	2089	-
14	-	2032	2050	2064	2077	2088
15	2012	2038	2056	2072	2085	-
16	-	2033	2052	2066	2079	2090
17	2051	2074	2093	-	-	-

[b]standard version of HadCM3

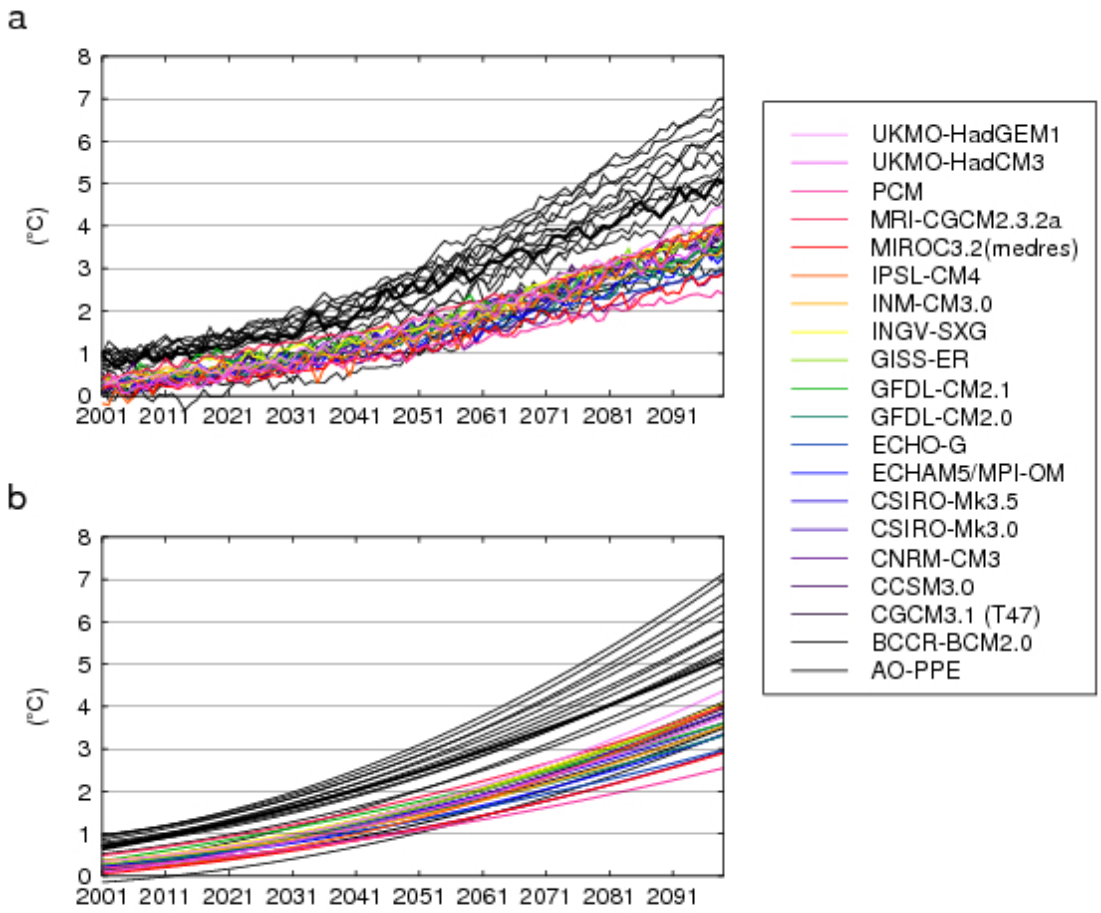

Figure 9.S1 Global annual mean temperature anomalies (°C) relative to control climatologies, for AO-PPE (all models in black, with a thicker line for the standard model), and CMIP3 (coloured) (a), and the same data smoothed using polynomial regression (b). Note that the model ensembles are run in different emissions scenarios and anomalies are calculated using different reference climatologies. AO-PPE is run in a higher emissions scenario (A1FI) than CMIP3 (A2), and anomalies are calculated using a preindustrial baseline (in contrast to the 1985-99 baseline used for CMIP3). This might explain why ΔT_g is higher in AO-PPE, although it could also be the case that the models are more sensitive to greenhouse gas forcing.

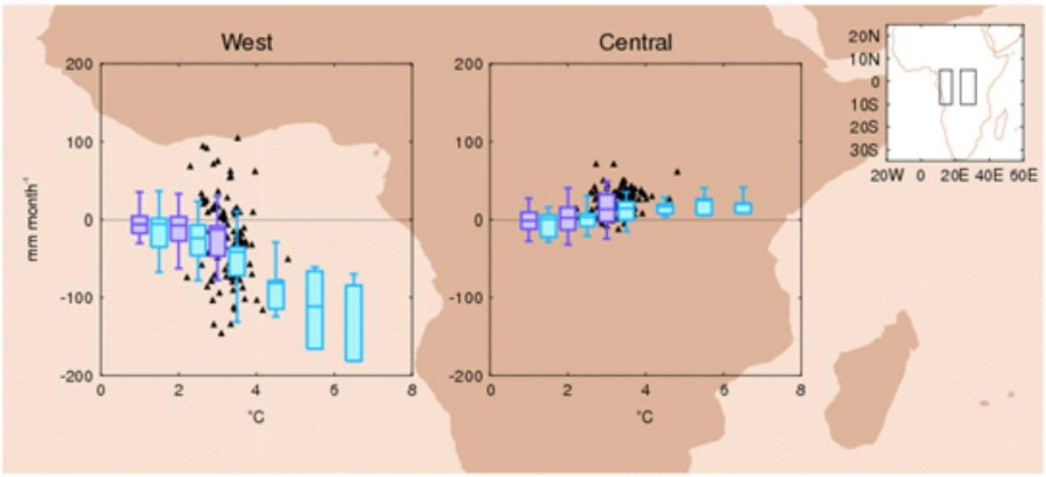

Figure 9.S2 as Figure 9.2 but showing all models in the boxplots.

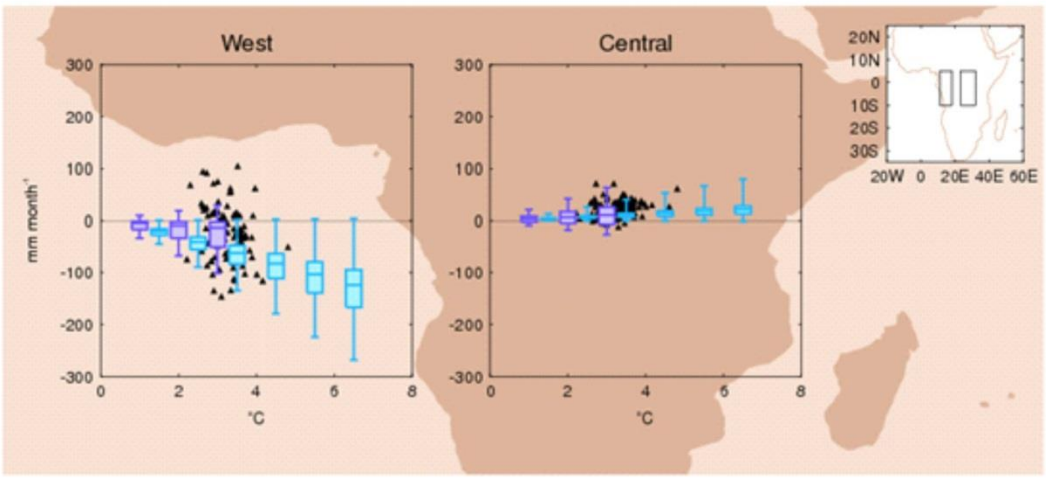

Figure 9.S3 as Figure 9.2 but here change at each ΔT_g in CMIP3 and AO-PPE is calculated based on the slope of the regression line between global temperature and regionally area-averaged precipitation (mm month^{-1} °C^{-1}), where datapoints are overlapping 20 year periods as used for Figure 9.1. Note that the axes are different to Figure 9.2.

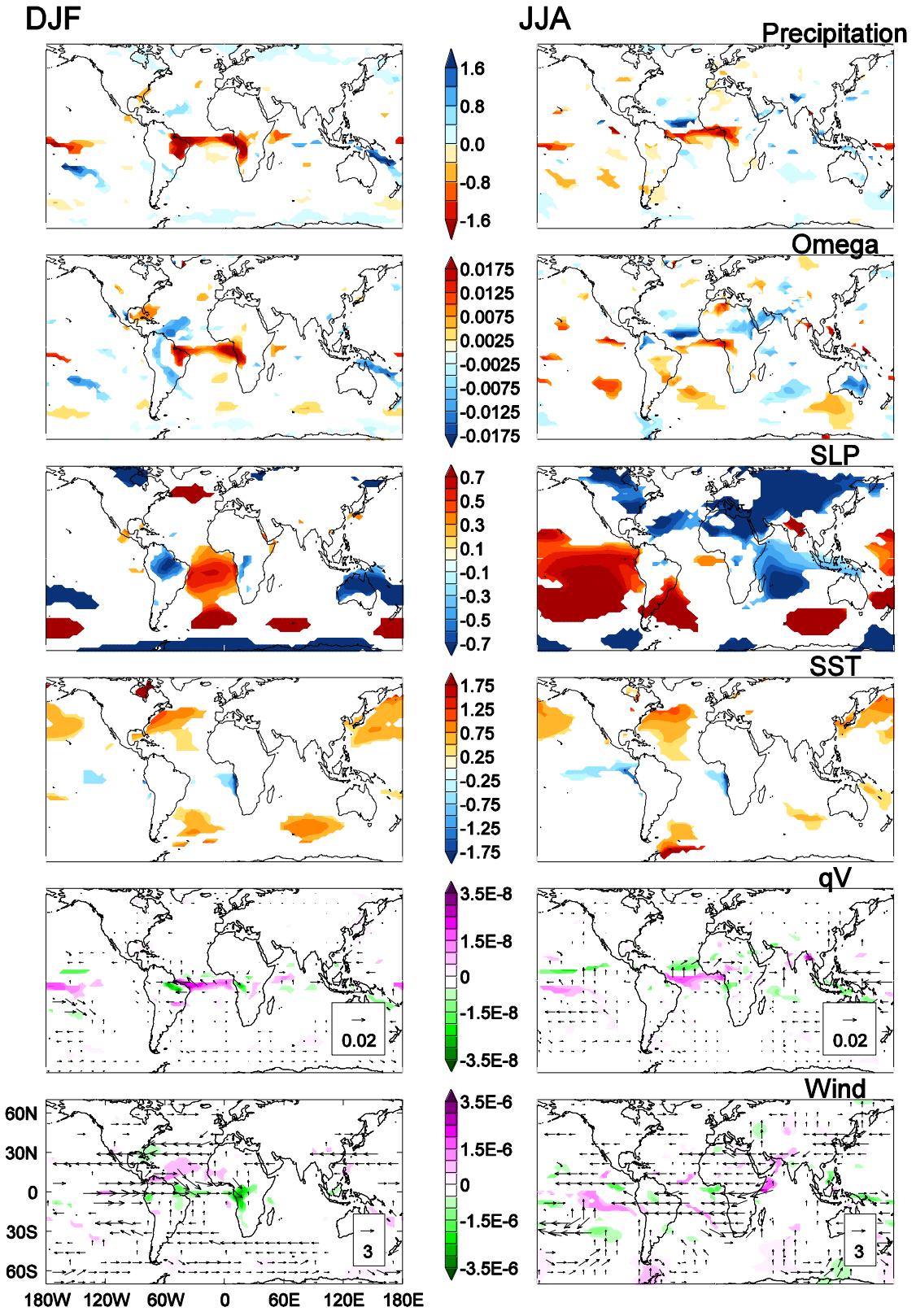

Figure 9.S4 as Figure 9.3 but for DJF and JJA.

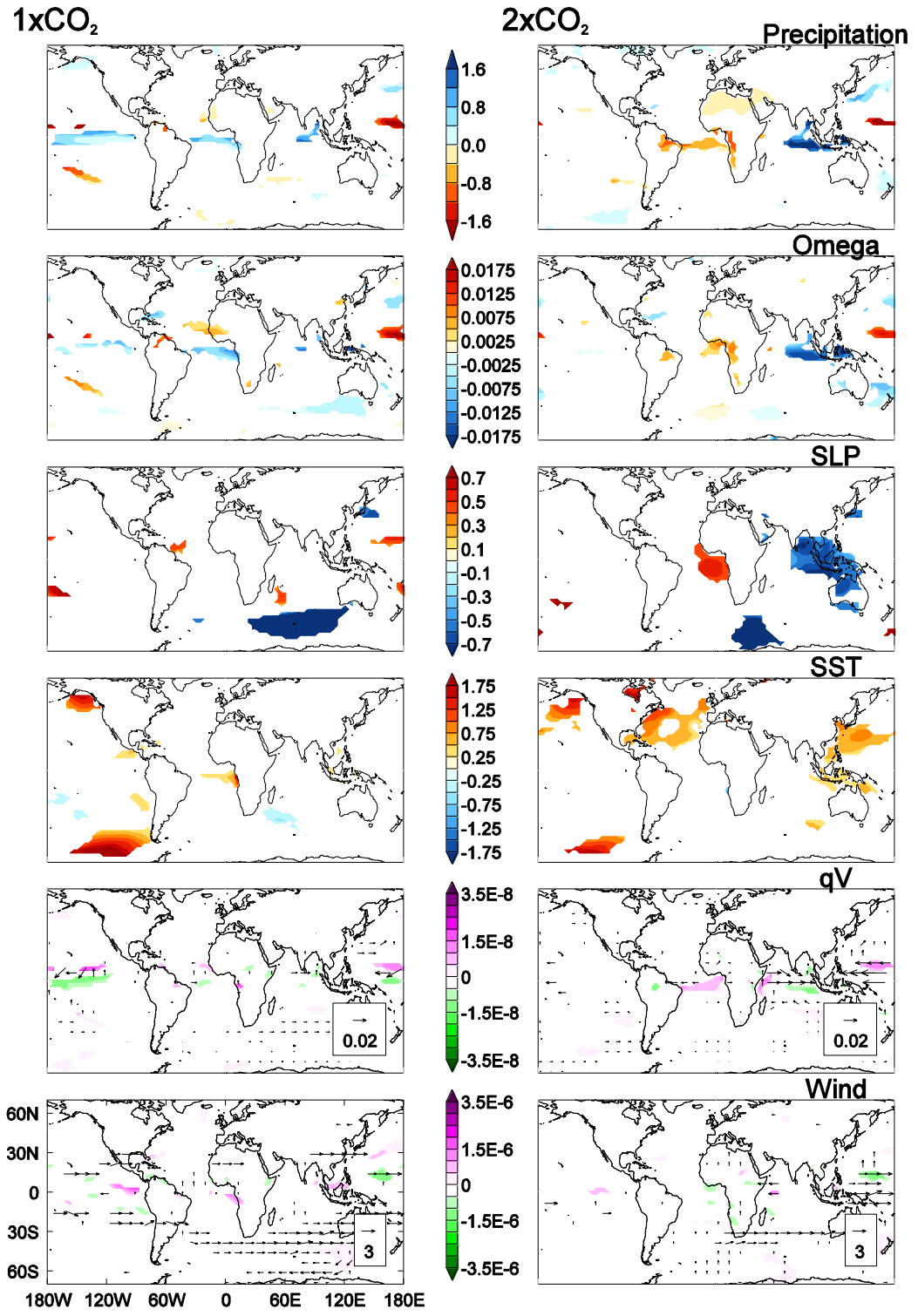

Figure 9.S5 'Dry' minus 'wet' AS-PPE composite annual mean climatologies for 1xCO_2 and 2xCO_2 for precipitation (mm day^{-1}), ω at 500hPa (hPa s^{-1}), SLP (Pa), SST (°C), qV at 925hPa (kg kg^{-1} ms^{-1}) with contours of moisture divergence (kg kg^{-1} s^{-1}), and wind vectors at 200hPa (m s^{-1}) with contours of divergence (s^{-1}). Areas not significantly different from zero (5% level) are masked in white.

10 Conclusions

10.1 Introduction

For over two decades, politicians have been negotiating the avoidance of dangerous anthropogenic interference in the climate system (UN 1992; UNFCCC 2013). Much of this debate has concerned how to limit global warming to 2°C, which is widely accepted as a benchmark for danger (Tol 2007; Randalls et al. 2010). However, there is a lack of scientific research which can be used to judge whether 2°C would be the most appropriate mitigation target from a regional perspective, particularly for Africa. Climate models offer the potential to investigate the influence of anthropogenic forcing on regional climate systems, but there has been very limited work using model data to identify changes associated with specific intervals of global mean temperature increase (ΔT_g) (see section 1.2.2).

The aim of this thesis is to investigate African temperature and precipitation anomalies at 1°C, 2°C, 3°C, 4°C ΔT_g and beyond, using data from climate model experiments with increasing GHGs. The output from the analysis could potentially provide scientific underpinning for political judgements about the suitability of 2°C as a mitigation goal. Yet if climate models are to be used for decision making, it is necessary to consider their credibility. The thesis make a contribution towards assessing the trustworthiness of the evidence base provided by climate models, by comparing results from different datasets, and exploring methods to better interpret and appraise modelled responses to global warming.

The present chapter will review findings from the analysis and offer conclusions. First a summary of the thesis is presented, which incorporates each of

the five papers in turn. Then the **knowledge gaps** highlighted in section 1.2 will be revisited, to clarify what has been revealed about *projected changes in African climate*, and the evolution of local temperature and precipitation anomalies with *degrees of global warming* in climate models. Lessons about the credibility of climate model experiments as an **evidence base** will then be considered. Finally the conclusions from the thesis will be summarised with an outlook for future research.

10.2 Summary of papers

The investigation has been arranged into two main sections. The first section was an analysis of pan-African projections from three datasets (Chapters 4-6). This was followed by an examination of the implications of global warming for the climate of a case study region: the Congo Basin (Chapters 7-9).

10.2.1 Pan-African Projections

The first step towards identifying how African climates evolve with global warming in climate models was to examine projections from the most widely used climate projection ensemble to date (Easterbrook 2012): the Coupled Model Intercomparison Project phase 3 (CMIP3), in **Chapter 4**. Analysis of this dataset was used to demonstrate that the approach based on ΔT_g intervals has the potential to deliver more useful information for mitigation debates than previous research using "time-slices". The paper also revealed for the first time that projected changes in

African climate are enhanced progressively with global temperature. For example, the wet signal in East Africa during OND is amplified from 1°C (3%) to 2°C (8%) to 3°C (13%) to 4°C (16%) ΔT_g in the ensemble mean. The range of projected changes identified from CMIP3 at 1-4°C (Figure 4.5) could potentially be used as input for impacts assessment to support decision making, however the CMIP3 models only allow for limited examination of uncertainties associated with global warming, which should be explored if the results are to be used for policy.

Two of the key uncertainties were addressed in **Chapter 5** using Perturbed Physics Ensembles (PPEs). The first issue is the potential for nonlinear change. CMIP3 models show progressive change to 3°C or 4°C ΔT_g, and it is not possible to establish whether this is because they project an approximately linear response to warming in general, or whether they would show trend reversals or tipping points but these require higher anthropogenic forcing. In Chapter 5 projections from 17 versions of HadCM3 (AO-PPE) run in a high emissions scenario (A1FI) were presented, showing an approximately linear evolution of change to 6°C, and demonstrating that tipping points are not reached, even at higher degrees of warming.

Chapter 5 also addressed uncertainty in the range of projections at each ΔT_g increment. CMIP3 is an "ensemble of opportunity" (Tebaldi and Knutti 2007; section 1.3.1) and is not designed to explore uncertainty in future climate change. PPEs were used to test the extent to which CMIP3 underestimates modelling uncertainty in practice, in the case of African precipitation. The PPEs were shown to exhibit a different range of futures to CMIP3, with the clearest contrast in western Africa. The dominant response in CMIP3 is precipitation decline, but members of AO-PPE show

drying which is larger than for any of the CMIP3 models (>35% in west Sahel), and a 280 member ensemble of slab models (AS-PPE) brings into question the apparent consensus on negative anomalies, since many model versions have a wetting response.

The results from Chapter 5 imply that the focus of current climate projection research overlooks uncertainties associated with global warming. In presenting projected changes from models which do not show tipping points, regional climate change assessments may not be incorporating the potential for nonlinear responses to GHG forcing. In focusing on data from Multi-Model Ensembles (MMEs) such as CMIP3 and CMIP5, projection studies do not provide the most conservative (cautious) envelope to support decision making, as systematic investigation of uncertainty can enlarge the range of futures. Further work to test the potential for nonlinear change using more complex models and to run PPEs using a range of base models might develop understanding of the risks associated with global warming.

Additional research using GCMs might therefore be considered a priority. However, the extent to which models with such low grid-spacing can produce trustworthy projections has been questioned (e.g. Smith 2012). The recent increase in RCM experiments over Africa offers the opportunity to test whether they produce different responses to global warming. In **Chapter 6** projections from an ensemble of five RCMs (PRECIS-RCM) were compared to their driving GCMs (PRECIS-GCM), exposing differences in regional precipitation anomalies. The largest distinction is in West Africa, where both GCMs and RCMs show drying, but this is at least 1mm day^{-1} greater in the GCM than RCM ensemble mean from 2°C. The precipitation decline

appears to be associated with regional circulation changes which are common to both ensembles, but more muted in the RCMs. The dynamical mode is however not found during dry years in NCEP and ERA-I, which casts doubt on the dry response to global warming in West Sahel. Thus there are differences between the GCM and RCM, but the RCM projections are not necessarily more credible.

The findings from Chapter 6 therefore demonstrate that data from RCMs should not automatically supersede GCM projections. Further work, possibly using higher resolution RCMs, would be useful to understand the role of grid-spacing on projection, and to assess the credibility of evidence based on GCMs versus RCMs.

Discussion

The results from the first three papers suggest that available climate model projections constitute a limited evidence base for investigating the risks associated with global warming. Yet there is a demand for relevant information about changes in African climate associated with ΔT_g intervals, to support decisions which cannot wait for scientific developments. Scientists face two options: to advise that there is too much uncertainty to project future changes in climate, or to provide an assessment of the current state of the evidence. In Chapters 7-9 the potential to assess the implications of global warming using available evidence was explored for a case study region: the Congo Basin.

10.2.2 Congo Basin Case Study

Rationale

By examining model projections, and pursuing approaches to assess confidence in these data, the case study provided an opportunity to explore the difficulties in making an assessment of the implications of global warming given incomplete evidence, and to test the extent to which the climate models can provide useful information. The Congo Basin is a fitting example due to the paucity of gauge data (e.g. McCollum et al. 2000) and limited knowledge of this region. The investigation of West Africa in Chapter 6 demonstrated the potential to develop process-based understanding of projected changes through analysis of atmospheric dynamics, with implications for the level of confidence in the response to warming. The Sahel has received the most research attention of any African region, including the largest ever land based climate experiment, AMMA (Redelsperger et al. 2006). For the Congo Basin, the antithesis of the Sahel in terms of African climate science, is it possible to find out anything about the implications of global warming?

Findings

The case study began with an appraisal of the level of observational uncertainty in the Congo Basin (**Chapter 8**). Precipitation climatologies were compared between 8 satellite and reanalysis data products, 24 CMIP3 models, and 9 CMIP5 models. The analysis revealed large discrepancies among satellite and reanalysis datasets (up to 5 mm day^{-1} in SON), inhibiting model evaluation. The

difference in models' precipitation climatologies was found to be partly explained by contrasts in horizontal moisture flux, and therefore examination of modelled circulation might be an alternative route to evaluation; however the moisture flux climatology in this region is poorly understood, with distinctions between NCEP and ERA-I. Therefore field campaigns are recommended in order to better assess models' credibility.

Model projections were presented in **Chapter 9**, as an additional source of evidence, albeit one which should be treated with caution given the uncertainty in observations demonstrated in the previous chapter. Data from both CMIP3 and the PPEs were used to examine change in temperature, precipitation and dry season water deficit (MCWD). The analysis revealed a strong and robust dry signal in the west of the Congo Basin in CMIP3 and AO-PPE, which is enhanced progressively with global warming. The magnitude of this change in the most sensitive models at 3°C and beyond (>100 mm month^{-1}) is equivalent to the difference between humid tropical forest and savannah, but some models (27%) show positive MCWD anomalies. Atmospheric dynamics associated with the drying in west equatorial Africa were investigated as a step towards process-based understanding of this signal. This analysis uncovered a potential change in zonal overturning linked to a contrast in surface pressure between the Indian and Atlantic Oceans.

Discussion

Having reviewed evidence from climate models experiments as well as satellite and reanalysis datasets what can be concluded about the implications of global warming for the climate of the Congo Basin? Many models project a gradual transition to dryer conditions in west equatorial Africa, leading to very large drying from 3°C in some cases, whilst other models show more moderate drying or wetting. These modelled responses could be used for impacts assessment to construct potential future scenarios and/or described to decision makers as potential risks to rainforests. However, it would also be vital to communicate that it is difficult to assess the credibility of these projections, and that there may be alternative futures not represented by the models, including the potential for more rapid changes.

The gradual evolution of change with global warming may not be trustworthy. This uncertainty was discussed in Chapter 5, but also further highlighted by Chapter 9. The case study emphasises the issue of nonlinearity, in revealing that precipitation anomalies in some models are likely large enough to generate a shift in the distribution of the tropical forests, the feedback effects of which cannot be incorporated in the models used here in the absence of dynamic vegetation (see section 9.5).

The limited capacity of the model projections to explore uncertainty in the range of possible futures at 1°C, 2°C, 3°C, 4°C, and beyond was established in Chapter 5 and 6, and confirmed in the case of the Congo Basin. The PPEs show changes in MCWD in west equatorial Africa which are not represented by CMIP3,

implying that systematic investigation of future climate using different base models might generate alternative plausible futures.

Those futures which are represented by the available models may not be trustworthy. Whilst some AS-PPE models have already been excluded, including ensemble members with the strongest drying responses over the Congo Basin associated with low entrainment coefficients (Chapter 5); there may other models with questionable projections in this region. The extent to which the models' have climatological biases is unknown, due to the observational uncertainty demonstrated in Chapter 8. In addition, all of the GCMs may struggle to produce plausible responses to warming given the coarse resolution. The Congo Basin has been demonstrated to exhibit spatial heterogeneity in precipitation variability (Balas et al. 2007) with a strong role for topography (Jackson et al. 2009; Vondou et al. 2011). The improved representation of extreme events at finer grid-spacing may also alter the response to anthropogenic forcing (Saeed et al. 2013). Analysis of the credibility of RCM versus GCM projections would therefore make a useful extension to this case study. Further work to assess the plausibility and likelihood of the shift in zonal overturning found in Chapter 9 would also be a sensible addition. However, the observational uncertainty in moisture flux climatologies demonstrated in Chapter 8 may inhibit appraisal of atmospheric dynamics.

The case study therefore substantiates the conclusions from Chapter 4-6; implying that impacts assessment for decision making should not be based on model output alone. In assessing the evidence for one region, the case study has confirmed issues identified from pan-African analysis, and highlighted additional concerns, in

demonstrating the limited capacity for evaluation of model biases, and emphasising the potential for vegetation feedbacks on climate.

10.3 Summary of projections: *How does African climate evolve with global warming in climate models?*

The summary of papers in the previous section outlines the progression of ideas in this thesis. The findings will now be discussed thematically and in more depth, first with regard to what the models show (section 10.3), and second considering the value of this information (section 10.4).

In revealing projected changes in African temperature and precipitation at 1°C, 2°C, 3°C, 4°C, and beyond, the thesis has made use of model data to address the two knowledge gaps highlighted in section 1.2 surrounding *future changes in African climate*, and *degrees of global warming*. The findings relevant to each are discussed below.

10.3.1 Future change in African climate

In analysing climate change projections across the African continent, in all seasons, and from three different datasets, this thesis makes a considerable contribution to previous literature on modelled responses to anthropogenic forcing over Africa. The majority of research attention to date has been focused on East Africa, southern Africa, and the Sahel. The thesis delivers new insights of relevance to

these regions, as well as findings for other regions which have been neglected to date. The Congo Basin was given specific attention, but inspection of precipitation anomalies across Africa (Figure 4.2-4, 5.5, 6.1) has additionally revealed consistent projections, for the Guinea Coast, Angola, and North-East Africa; and two large scale responses: a possible delay in the onset of precipitation seasons, and a contrast between western and eastern Africa. Temperature projections have also been examined.

East Africa

Previous work has shown that GCMs consistently project a wet signal in East Africa in both the long rains (MAM) and short rains (OND) seasons (Shongwe et al. 2011). However, some RCMs project dryer conditions during MAM (Cook and Vizy 2012; 2013), and the drying observed in recent decades (Lyon and DeWitt 2012) is expected to continue in future (Williams and Funk 2011; Williams et al. 2011). Analysis in Chapter 4 confirms the consensus on positive anomalies in CMIP3, and additionally demonstrates a wet signal in MOHC PPEs and RCMs, including in DJF. The wetting during this dry season has received less attention than other seasons in previous work, but is worthy of further investigation given the large absolute changes (>1 mm day^{-1} at 4°C in the PRECIS-GCM ensemble mean).

Southern Africa

Southern Africa has been found to experience drying in JJA and SON in CMIP3 models and RCM experiments (Christensen et al. 2007; Shongwe et al. 2009; Cook and Vizy 2012), possibly linked to a shift in the SICZ (Cook and Vizy 2012). The PPEs and RCMs investigated here also show a dry signal, including in western southern Africa during MAM (Figure 6.1). The negative anomalies are smaller in the RCMs than their corresponding GCMs, which represents an interesting topic for further analysis.

The Sahel

Many studies have sought to explain the apparent disagreement between CMIP3 models in the future precipitation response over the Sahel (e.g. Hoerling et al. 2005; Held et al. 2005; Biasutti et al. 2009; Druyan 2011). However, Fontaine et al. (2011) illustrate more consensus than previously noted, in terms of a drying in west Sahel and wetting in east Sahel. The results from Chapters 4-6 confirm that many models, including perturbed versions of HadCM3 and RCMs, also show a zonal contrast in precipitation anomalies. The drying in west Sahel has a particularly large amplitude and spatial extent in PRECIS-GCM. In Chapter 6 this signal is shown to be associated with an anomalous circulation mode, with downward ω anomalies at 400hPa, but also an increase in dry convection near the surface at ~20°N, and a strengthening of the monsoon. As noted in section 10.2, this circulation mode is not found not found in NCEP or ERA-I, which casts doubt on the precipitation decline

over west Sahel in the PRECIS-GCMs and RCMs, and also in AO-PPE given the similarity in the model physics. This finding contributes process-based understanding of the Hadley Centre model projections analysed here, and could be used to interpret and potentially constrain responses in other models, since many show drying and anomalous subsidence in the upper atmosphere over the same region (Monerie et al. 2012a, b).

The Congo Basin

The results of the Congo Basin case study are summarised in section 10.2. The dry signal found in the west of the basin, in terms of JAS precipitation and an increase in dry season water deficit, has not been emphasised in previous work, and possibly brings into question Haensler et al. (2013)'s conclusion that there is unlikely to be an increase in water scarcity in the region.

The Guinea Coast

All ensembles show some drying at the Guinea Coast during MAM, with the most intermodel agreement over southern Mali, Guinea, Liberia, and Sierra Leone. Whilst West Africa has received substantial research attention, the work has focused on the monsoon season (JAS), and to the author's knowledge this change in MAM has not been highlighted on the basis of CMIP3 models; although Cook and Vizy (2012) find a drying during May in WRF.

Angola

The projected drying of southern Africa during SON has been well documented (e.g. Shongwe et al. 2009), but there has been less emphasis on the fact that the largest anomalies (>0.8 mm day^{-1} in the AS-PPE mean) and most intermodel consensus are concentrated over Angola and the southern Democratic Republic of Congo (Figure 4.3, 5.5, 6.1). This region suffers from a lack of observations (Figure 1.5) and so appraisal of this trend is difficult, but it warrants further investigation.

North-East Africa

North East Africa was given little attention in Chapter 4, as the CMIP3 projections show limited model agreement, no significant change, or very small absolute changes over Egypt and Sudan (Figure 4.3). However, the Hadley Centre PPEs both experience wetting in this region during JAS (Figure 5.5), and this signal is particularly widespread and consistent between ensemble members in the RCMs (Figure 6.1; and highlighted in Buontempo et al. 2013). Near to the Mediterranean the absolute change is small (<1 mm day^{-1} in the ensemble mean), but the larger anomalies in the eastern Sahel (>1 mm day^{-1}) suggest that the signal deserves further research.

Delayed onset of precipitation seasons

Several of the signals found in CMIP3 suggest a delay in precipitation seasons, notably the drying of southern Africa in SON prior to the rainy season in DJFM, and the drying at the Guinea Coast during MAM. Both of these anomalies occur at the leading edge of the migration of tropical rainfall, which, as discussed in Chapter 4, might suggest a delay in the seasonal cycle of precipitation, possibly linked to the influence of global warming on the annual cycle of SSTs (Biasutti and Sobel 2009). The same pattern of precipitation change in MAM and SON is shared by the datasets which have been investigated since Chapter 4 (Figure 5.5, 6.1).

Zonally contrasting precipitation anomalies

As noted above, the distinction between drying in west Sahel and wetting in central Sahel has been found in previous literature (Fontaine et al. 2011), and all ensembles studied here. Projections for Central Africa also show drying in the west of the basin and wetting further east (Figure 9.1). In the Hadley Centre PPEs, the dry signal during JAS extends through much of western Africa, including the Guinea Coast and Angola (Figure 5.5, 6.1); whilst in eastern regions there are more moderate positive anomalies. During MAM and SON there are also signs of west/east distinctions. The pattern of change in CMIP3 with the strong increase in precipitation in dry East Africa, and the weaker increase or little change in the core convective region of Central Africa (see section 4.5) also represents a contrast between longitudes.

Many of these precipitation signals have been associated with a zonal contrast in ω anomalies, including the wet signal in East vs. Central Africa (Vecchi and Soden 2007; Shongwe et al. 2011), the dry signal in west vs. central Sahel (Figure 6.5; Monerie et al. 2012a, b), and the increase in dry season water deficits in west vs. east equatorial Africa (Figure 9.3). Whilst doubt has been cast on the circulation mode identified over west Sahel in Chapter 6, the results do not necessarily reject the role of upper atmosphere subsidence, which was also found in dry years in NCEP and ERA-I. Any further insights into drivers of change in ω at 400/500hPa might therefore be important in assessing the likelihood of these precipitation responses.

Several studies (Shongwe et al. 2011; Monerie et al. 2012a), and Chapter 9, suggest that the ω anomalies are associated with a shift in zonal circulation linked to warming of the Indian Ocean. The role of Indian Ocean SSTs would appear to be strong in GCMs: idealised warming experiments of the Indian Ocean show drying through much of western Africa (Hoerling et al. 2005; Mohino et al. 2011). The Indian Ocean is thought to have influenced observed precipitation trends in the Sahel (Giannini et al. 2003) and East Africa (Williams et al. 2011; Williams and Funk 2011). However, it is unclear whether GCMs are able to adequately simulate the processes behind these teleconnections (Conway et al. 2007; Copsey et al. 2011), and therefore difficult to establish whether increasing SSTs might lead to a drier (wetter) west (east) Africa as the models might seem to suggest. This appraisal is hampered by background understanding: there is still debate as to what extent there is a complete zonal cell over the Indian Ocean, and in which seasons (Hastenrath et al. 2011). Mistry and Conway (2003) find that the meridional circulation over the Indian Ocean may also exert a control over East African precipitation. Improved observations of

the large scale atmospheric dynamics would be beneficial, and might be considered a priority given that rapid warming of the Indian Ocean is a clear signal in twentieth century data (Williams and Funk 2011), and is projected to continue in future (Cook and Vizy 2006).

Temperature projections

The focus of the thesis has been on precipitation projections, due to the greater variation between modelled responses and the potential for impacts on society (see section 1.2.1). Changes in temperature are presented in Figure 4.2, 6.5, and 9.1; largely confirming the IPCC's assessment that the highest magnitude warming is projected in subtropical regions (Christensen et al. 2007; Collins et al. 2013). The temperature response would therefore appear to be modified by precipitation: the drying in regions of subsidence amplifying warming through soil moisture and/or cloud feedbacks. The largest dry signals found here, in west Sahel, and west equatorial Africa during JAS, are also associated with the largest temperature anomalies (>6°C for a 4°C ΔT_g in PRECIS-GCM and PRECIS-RCM), further highlighting the influence of precipitation on temperature. However, the analysis of atmospheric dynamics associated with drying in West Africa in Chapter 6 implies that the high amplitude warming of the heat low region might have feedback effects on the drying response via the AEJ or WAM (section 6.5.3.1). This finding suggests that the influence of the SHL on Sahel precipitation could be more complex than would be suggested by previous studies which associate a strengthened heat low with wetter futures (Biasutti et al. 2009). The role played by the SHL may be contingent on the

location of maximum warming, which varies between models, as discussed by Vizy et al. (2013). Investigation of intermodel variation in temperature change might therefore represent an important area for further research.

10.3.2 Degrees of global warming

The preceding section summarises the key findings relating to the magnitude and direction of change in African temperature and precipitation. The dominant motivation of the thesis relates to the rate of change: how do regional climates evolve with ΔT_g? As noted in the summary of papers (section 10.2) the models show gradual evolution of local anomalies with increasing global temperature. This is a key finding, therefore in this section further evidence to substantiate the result will be summarised and discussed, after a brief examination of the value of the ΔT_g approach.

10.3.2.1 Value of the ΔT_g approach

The investigation of projected changes at 1°C, 2°C, 3°C, etc. is based on the contention that the more traditional approach to impacts assessment, using time-slices, conceals differences between ΔT_g increments; and therefore projections from a time-slice cannot be used to inform an assessment of whether 2°C, or any other degree of warming, is dangerous. Analysis of ΔT_g over time, presented for CMIP3 in Figure 4.1, but also examined for the other transient ensembles, shows that for the same GHG forcing models project different ΔT_g; due to variation in feedbacks (Bony

et al. 2006) and forcings (Kiehl 2007). For a 1985-99 time-slice, the average ΔT_g among the 24 CMIP3 models run in A1B ranges from 1.8°C to 4.2°C. Projections from this time-slice would not be useful for investigating the impacts of 2°C or other degrees of warming, verifying the importance of extracting ΔT_g increments directly.

An additional outcome of relevance to the approach itself is that the regional changes at each ΔT_g interval are consistent between emission scenarios. In Chapter 4 changes at 1-3°C are presented for the same models run in A2 and A1B, and are very similar in magnitude and spatial pattern (Figure 4.2-5). The result is in agreement with Tang and Lettenmaier (2012) who find that the rate of change per °C of warming is stable between A2, A1B, and B1, with reference to runoff in major river basins. An approach based on global warming might therefore allow emissions uncertainty to be bypassed in regional climate change assessments (as proposed by e.g. Darbyshire et al. 2013), at least for those scenarios which are most commonly used for impacts assessment, with increasing GHGs.

10.3.2.2 Key findings

The models consistently show that temperature and precipitation anomalies are enhanced progressively with global warming. At 1°C, there is little significant change, but from 1.5°C or 2°C anomalies develop which grow in magnitude and spatial extent with global temperature (Figure 4.3, 5.1, 6.1). The projected decrease in precipitation in Angola during SON is a typical example: 6% at 1°C, 10% at 2°C, and 15% at 3°C in the CMIP3 A2 ensemble mean (Table 4.2). The drying at the Guinea

Coast in AO-PPE demonstrates the extension of anomalies with global warming (Figure 5.1): at 1.5°C most ensemble members agree on a decrease in precipitation over Sierra Leone and Mali, but at 3°C there is a dry signal for much of southern West Africa, and by 5°C this extends to 20°N. The results from Chapter 6, in which changes in circulation are investigated at each degree of warming (Figure 6.4, 6.5); suggest a gradual transformation of atmospheric dynamics to match the gradual changes in precipitation.

The main difference between ΔT_g intervals is therefore in the magnitude and spatial extent of change. There do not appear to be rapid accelerations in the rate of change or trend reversals. This is not only true for lower levels of anthropogenic forcing, but also at higher degrees of warming (Figure 5.1, 5.6). The finding of approximately linear change is corroborated by linear regression of global temperature against local temperature and precipitation (see section 3.2), which is a good fit for the data. The slope of the regression line is significant across a large proportion of the continent according to the t-test (Figure 5.5, 9.1).

10.3.2.3 Discussion

Progressive local change with global temperature might have been to some extent expected from previous literature. Many projection studies using time-slices have shown that changes at the end of the twenty-first century are similar, but higher amplitude than, changes at mid-century (e.g. Hulme et al. 2001; Vizy et al. 2013). The IPCC AR5 noted the stability in large scale patterns of change from transient

experiments, in both CMIP3 and CMIP5 (Collins et al. 2011). However, there has been a lack of previous work which directly investigates change at 1°C, 2°C, 3°C, 4°C; and none which addresses changes to 6°C. The finding of progressive change from 1-6°C therefore makes an important contribution to the literature.

The results suggest that, in principal, pattern scaling (Mitchell 2003) might be a reasonable methodology to represent what the models show. However, given the spatial extension of anomalies with global warming it would be important to incorporate data which represent the influence of larger GHG levels, and not, for example, to calculate changes at 2°C and then multiply these to get 4°C anomalies. In addition, this would only give an approximation of the changes at each ΔT_g. This thesis has not sought to examine the extent to which the relationship with global temperature is exactly linear. Trend analysis has identified step changes in regional warming in southeastern Australia (Jones 2012), and an increase in the pace of shifting climate zones (Mahlstein et al. 2013). The techniques used in thesis are sufficient to show that, for Africa, there are no large shifts or accelerations, but thorough trend analysis might reveal more subtle nonlinearities.

10.3.2.4 Potential policy implications

The finding of progressive change has potential implications for policy. Given that larger changes in climate are likely to generate greater challenges for society, it suggests that global temperature should be limited to the lowest level possible. However, it does not imply that 2°C, or any other ΔT_g increment, should be

a preferred target from the perspective of regional climate. If there were trend reversals or step changes these could be used as initial evidence for mitigating to a ΔT_g level which avoids the onset of rapid transformations. However, as change is approximately linear, it is not possible to distinguish between ΔT_g intervals, such as 1.5°C and 2°C, on the basis of mean temperature and precipitation alone. Further impacts assessment would be needed, and the output from this investigation has the potential to provide a basis for such work.

10.4 Appraisal of the evidence base: *To what extent do available climate model experiments provide a trustworthy source to investigate the implications of global warming for African climate?*

The principal objective of the thesis was to reveal *what the models show* in terms of the evolution of African climate with degrees of global warming, and this has been summarised in section 10.3. Yet, if climate model experiments are to support decision making, it is important to consider the level of confidence in their projections. To what extent do they provide a credible evidence base? This is a weighty question, a full discussion of which is beyond the scope of this thesis. However, having made comparisons between different climate model datasets, and after exploring methods for appraising models using PPEs, reanalysis, and satellite data; the thesis can deliver some relevant insights.

This section will first return to the finding which has just been discussed: progressive change in local anomalies with global warming. How credible is the

representation of the *rate* of change in the model simulations? Then, the range of projected futures is considered: how far can we trust the representation of uncertainty in the *magnitude and direction* of change from available model runs?

10.4.1 Relationship between global temperature and local climate

The approximately linear relationship between global warming and local climate change implied by the model experiments analysed in this thesis might be undermined by two issues: emissions scenarios and model complexity.

10.4.1.1 Emissions scenarios

The majority of climate projection research to date, including all of the studies in section 1.2.1, and all of the analysis in this thesis, has been based on SRES scenarios with gradually increasing GHGs (Nakicenovic et al. 2000), which are not are not designed to represent mitigation (as highlighted by e.g. Arnell et al. 2013). These were the main experiments available in CMIP3 and were used for many other modelling projects (including Murphy et al. 2007; Buontempo et al. 2013). Most of the RCPs specified for CMIP5 are also dominated by increasing GHGs (Meinshausen et al. 2011).

Limiting to 2°C would necessitate a reduction in emissions (see e.g. Mackintosh 2010), which might generate a different the relationship between global temperature and local climate. Using experiments in which CO_2 is raised to 4x

preindustrial levels and then reduced back to 1xCO_2, Wu et al. (2010) find that there are two possible hydrological states for a given surface warming. 2°C might be associated with different global and regional precipitation anomalies depending on whether temperatures (and CO_2 concentrations) are rising or falling, due to the inertia generated by accumulated heat in the ocean. Further work using more realistic scenarios would be of interest to compare regional changes at 2°C stabilisation with changes at 2°C from increasing GHGs. RCP 2.6 provides an opportunity for such work using CMIP5 models (van Vuuren et al. 2011; Meinshausen et al. 2011); however, a variety of pathways to 2°C, and other ΔT_g increments, might be required to establish the extent to which the projections at 1°C, 2°C, 3°C, etc. are robust to the emissions trajectory.

10.4.1.2 Model complexity

The finding of progressive change with global warming brings into question the models' ability to represent nonlinearities in the earth system. The majority of regional climate change assessments are based on experiments which do not produce >3°C ΔT_g (see section 1.2.2). The fact that tipping points have not been reached in models run in A1B to 2050 or 2100 might be assumed to be due to the relatively low forcing: tipping points have not been reached *yet*. By investigating the evolution of change to 4°C and beyond, Chapter 5 shows that the models do not produce nonlinearities even for very large forcing. The fact that we do not see tipping points at 2100 in A1B is not because the forcing is too small to trigger them. It is because the models do not produce nonlinear change (at least to 4°C, and to 6°C in

versions of HadCM3). This may be because warming doesn't lead to nonlinear change, or it may be that the models cannot simulate the feedbacks involved due to their resolution and complexity.

Analysis of state-of-the-art models is a priority to test the findings based on CMIP3 and AO-PPE. The most complex or highest resolution CMIP5 models run in a high emissions scenario (RCP 8.5; Meinshausen et al. 2011) would make a good starting point. It would be particularly relevant to focus on the models which demonstrate the ability to incorporate important feedbacks, for example those models which have a better representation of the Mid-Holocene transition (see Braconnot et al. 2007). If more advanced models also show progressive regional changes with warming it will give more confidence in the result, but assessment of the likelihood of nonlinear change need not be based on climate models alone.

Expert elicitation suggests that there is >56% probability of crossing at least one large scale tipping point if warming exceeds 4°C; and some systems, in particular the Greenland Ice Sheet, might be sensitive to lower levels of ΔT_g (Kriegler and Hall 2009). Observational and land surface modelling studies of African environments also demonstrate strong regional feedback effects on climate; for example the role of inundation in the Niger inland delta (Dadson et al. 2010; Taylor 2010), which might be expected to modify the precipitation response to warming, but is not adequately represented in climate change experiments. The importance of such hydrological feedbacks provides an incentive to improve the realism of ESMs (Dadson et al. 2013). In the interim, climate change impact assessments should acknowledge the potential

for nonlinear responses in regional climate which is not represented by model projections.

10.4.2 Range of responses at each ΔT_g level

If impacts assessments are to inform policy decisions, they should incorporate uncertainty in the magnitude and direction of future climate change. Many impacts studies are based on projections from only one or two GCMs (e.g. Delire et al. 2008), and the use of different projections has often generated quite different outcomes (Conway and Schipper 2011). Recently there has been an emphasis on representing the range of climate model projections, either taking the full range from an ensemble, or seeking to identify a subset of models which characterise the full range (e.g. Darbyshire et al. 2013; Paton et al. 2013). However, the spread of responses from available climate model experiments may not approximate the full range of possible futures given current understanding. There could be alternative plausible futures which are not represented, and therefore risks which might be overlooked. And, some of the variation between available models could be due to identifiable model errors rather than limited understanding. Incorporating implausible futures may unnecessarily restrict the options considered for adaptation.

The thesis has compared the range of projections from three datasets, offering insights into the relative value of MMEs and PPEs, GCMs and RCMs for representing uncertainty. In addition, methods for constraining ensembles and appraising specific precipitation responses have been considered, with lessons about

the ability to exclude implausible models. Together the findings have implications for the use of current model data to measure uncertainty in the climatic response at each ΔT_g level.

10.4.2.1 Which sources of evidence should be consulted to investigate the range of possible futures?

MMEs and PPEs

As noted in section 10.2.1, the PPEs project responses to global warming which are not represented in CMIP3. Although the largest precipitation anomaly outside the CMIP3 range, the high magnitude drying of west Sahel in AO-PPE, has been brought into question (Chapter 6), important differences between the ensembles remain. Previous work has shown that PPEs extend the range of projections from MMEs (e.g. Fung et al. 2011; McSweeney et al. 2012), and Chapter 5 confirms that this is also true for Africa. The result implies that climate change impacts assessments should not be based on CMIP3 alone, and that further systematic exploration of parameters would be necessary to be more confident in the modelled range of responses. Most PPEs to date have been based on Hadley Centre models (Stainforth et al. 2005; Rougier et al. 2009) and PPEs using other base models may produce different projections. "Super-ensembles" of PPEs from each modelling centre would be the most comprehensive approach (Murphy et al. 2004), although the net benefits are a subject for debate given the large computing power which would be required.

GCMs and RCMs

The finding that RCMs produce different, but not necessarily more credible, projections to GCMs (section 10.2.1) has important connotations. The CORDEX simulations have been put forward as a tool to provide finer scale data to support decision making (Giorgi et al. 2009; Jones et al. 2011; Hewitson et al. 2012). However, Chapter 6 substantiates the conclusions from previous studies (Mariotti et al. 2011; Sylla et al. 2012; Laprise et al. 2013) that RCMs do not merely provide higher resolution versions of GCM output. The potential futures represented by GCMs should therefore not be excluded from impacts assessment unless the RCMs can be demonstrated to be more trustworthy. Appraisal of RCM vs. GCM projections has been limited to date (except Mariotti et al. 2011; Sylla et al. 2012; Saeed et al. 2013), in part because the experiments are still being run, but possibly also because of the difficultly of diagnosing differences between CORDEX RCMs and GCMs given the countless distinctions in model physics. Chapter 6 therefore makes an important contribution to the literature, by examining five RCMs which differ only in small perturbations to the driving GCMs, allowing inference about the value of regional modelling based on consistency between model versions. The results are specific to this dataset and to west Sahel, but demonstrate that RCMs do not necessarily produce more trustworthy projections, and highlight the importance of process-based analysis of other regional responses and using other RCMs.

The similarity in the dynamical response between the GCMs and RCMs illustrated in Figures 6.3-6.8 also suggests that the decrease in grid-cell size to 50km may not be large enough to improve modelled responses. More work is needed to

better understand the role of resolution: to assess the extent to which it inhibits GCMs' reliability, and how far it might produce alternative plausible futures. RCMs run at a range of resolutions would be a good starting point. In Chapter 8 RCM simulations of the historical period show a different spatial distribution of precipitation over the Congo Basin when run at a finer resolution, but in this case it is not possible to establish whether this constitutes progress due to observational uncertainty.

Discussion

The results therefore suggest that mitigation decisions should not be based on data from MMEs alone, and that RCMs should not supercede GCMs without further assessment of their value. Combining data from MMEs and PPEs, GCMs and RCMs has the potential to provide more conservative estimates of uncertainty in the climatic response, but a more thorough understanding would require PPEs using different base models and investigation of the role of resolution.

Another source of evidence which has not been considered here are initial condition ensembles, which might produce alternative plausible futures. Whilst the importance of natural variability is larger for shorter time scales, Deser et al. (2010) demonstrate that varying initial conditions can lead to divergence in projected futures which is equivalent to the uncertainty from different models. This effect is greater outside of the tropics (see also Deser et al. 2012), but it would be useful to test the influence on African precipitation, using the available initial condition ensembles in

CMIP5 (Taylor et al. 2012a), or the NCAR CCSM3 Large Ensemble of 40 runs (as used in Deser et al. 2010, 2012).

10.4.2.2 Can implausible futures be identified from the range of model projections?

Three approaches for constraining ensembles and appraising specific responses have been explored in this thesis.

PPEs

The difficulty of constraining MMEs was discussed in section 1.3.1. It arises partly because each model differs from the next in myriad ways. In PPEs differences between ensemble members are small and well understood, and in large ensembles this can facilitate understanding of the influence of different parameters (e.g. Rougier et al. 2009). The constraints applied to AS-PPE in Chapter 5, which removed 168 of 280 model versions, were enabled by the size and systematic nature of the ensemble (section 5.5.1). Previous studies have used Bayesian statistics to produce probabilistic projections from PPEs (Sexton et al. 2012). Chapter 5 demonstrates the potential for a simpler approach, which also allows for a more specific understanding of the causes of intermodel variability.

Comparison to observations

Comparison of models' historical climatologies to observations may not be sufficient to constrain ensembles (see section 1.2.3; Whetton et al. 2012), but it is a good first step towards understanding their weaknesses. Model biases which have been identified in previous research were summarised in Chapter 2, however this literature does not cover the entire continent, with a notable lack of work for the Congo Basin. The comparison of data products over Central Africa in Chapter 8 demonstrates for the first time the large observational uncertainty in both precipitation and moisture flux climatologies. This finding reveals that appraising the range of projections is limited by the scarcity of observations in this region.

Mechanisms for precipitation change

Models' twentieth century climatologies do not necessarily relate to their future projections (e.g. Abe et al. 2009). It is therefore important to directly investigate the credibility of their climate change signals. The analysis of atmospheric dynamics over west Sahel in Chapter 6 demonstrates that examination of mechanisms for precipitation change has the potential to deliver process-based understanding of projections and, through composite analysis and comparison to reanalyses, an assessment of the associated confidence. In this case the work casts doubt on the extreme drying in versions of HadCM3 and HadRM3P.

Discussion

The thesis therefore establishes that it is possible to identify implausible or questionable projections within the range provided from the available model experiments. It suggests the potential for further work to better understand the confidence in the modelled range using PPEs and through analysis of mechanisms for precipitation change on a regional basis. However, it may not be possible to assess modelled circulation in regions where there is a scarcity of observations. The value of the models is therefore easier to determine for some regions (West Africa, Chapter 6), than others (the Congo Basin).

10.5 Future outlook

Over twenty years after the establishment of the UNFCCC (UN 1992), politicians are still debating how to avoid dangerous anthropogenic interference (DAI) in the climate system (UNFCCC 2013), but with very little evidence to assess what degree of global warming (ΔT_g) would constitute DAI for vulnerable regions. Scientific assessment of the regional impacts associated with ΔT_g increments has the potential to inform the selection of appropriate mitigation goals, and influence the level of ambition to meet these targets.

10.5.1 Contributions of this thesis

This thesis takes a vital first step towards understanding the implications of ΔT_g for Africa, using climate model data to investigate the evolution of seasonal temperature and precipitation change with increasing degrees of global warming; and demonstrating a gradual amplification of local anomalies with global temperature. The modelled changes identified at 1°C, 2°C, 3°C, 4°C and beyond could potentially be used as a basis for impacts research to provide information for policy-makers.

However, comparison of MMEs and PPEs, GCMs and RCMs reveals that the implications of global warming for African climate are different depending on which dataset is consulted. MOHC PPEs show risks which are not represented in CMIP3, implying that perturbation of other base models might produce alternative futures. RCMs fail to provide more trustworthy responses to warming than their driving GCMs in west Sahel, suggesting that the role of resolution on projection requires further investigation. The thesis does suggest that there is potential to better understand modelled responses, which is demonstrated through examination of variation between models in PPEs and investigation of atmospheric dynamics associated with precipitation changes; however model evaluation is shown to be restricted by observational uncertainty in the case of the Congo Basin.

These findings imply that the model simulations are a limited source of evidence for understanding uncertainty in the response to global warming. The range of projections at each ΔT_g increment may include implausible responses, as process-based understanding of precipitation signals is currently limited, and appraisal is difficult using MMEs and for poorly observed regions. In addition, there may be

alternative plausible futures which are not represented in the modelled range, as model physics and resolution have not been systematically explored for most base models, and both have been shown to modify projections. Current climate models may also fail to represent the risk of nonlinear change: in demonstrating that the models show gradual evolution of regional change to 6°C, the lack of nonlinear behaviour has been revealed, which may be due to limited complexity or coarse resolution. This thesis therefore suggests that impacts assessment to inform policy decisions should not measure uncertainty in the climatic response to global warming using the range of current model projections alone.

10.5.2 Outlook for future research

To what extent will developments in climate modelling infrastructure improve the usefulness of the evidence base? Three issues are worthy of discussion. First, the dominant emphasis in climate research is on the creation of state-of-the-art models rather than on understanding uncertainty in more simple models (Smith 2002). The comparison of the newest GCMs and RCMs from each modelling centre in MMEs (CMIP5 and CORDEX) has been a recent focus. MMEs of hydrological models (WaterMIP; Haddeland et al. 2011) and other impacts models (ISIMIP; e.g. Davie et al. 2013) are also being generated. These ensembles are highly important but are not designed to systematically explore uncertainty and so are unlikely to produce a defensible range of future responses to global warming.

The second issue relates to model resolution. Results from Chapter 6 suggest that changes in grid-spacing have the potential to influence projections, but that 50km might not be sufficient to generate an improvement (see section 10.4.2). Further increases in resolution or further development of model physics may be needed. Testing the sensitivity of projections to resolution is an important step before RCM projections can be considered a higher quality product than those of GCMs. CORDEX runs provide an unprecedented resource for regional climate research, but they have not been designed to question the role of resolution, as GCMs and RCMs have many differences in physics, and simulations are generally only run at one resolution over Africa (Giorgi et al. 2009; Hewitson et al. 2012). Computer time has been invested in generating detailed data for users, rather than in experiments which might be used to determine the usefulness of that data.

The third concern is the disconnect between research into tipping points (e.g. Lenton et al. 2008; Scheffer et al. 2009) and regional impacts assessment. The majority of climate impacts research has been based on models which may lack the complexity to incorporate feedbacks. Earth System Models (ESMs) within CMIP5 (Friedlingstein and Jones 2011) provide an opportunity to investigate regional climate change using more complex models, but the extent to which the ESMs produce different projections has so far received little attention, as most existing CMIP3 studies combine information from AOGCMs and ESMs (e.g. Monerie et al. 2012a; Taylor et al. 2012b).

Contemporary developments in climate projection research are therefore unlikely to engender substantial progress in the representation of uncertainties

associated with global warming. So what are the connotations for impacts assessment at 1°C, 2°C, 3°C, etc.? It is important that model results are used with consideration for the level of associated confidence. The thesis has explored several approaches for better understanding credibility in model projections (see section 10.4.2), but has not addressed the challenge of how to combine such information with model output. This might be achieved through a pre-defined confidence scale, such as that used by the IPCC (Mastrandrea et al. 2010), which could be in the form of a qualitative expression of confidence ("very low," "low," "medium," "high," and "very high.") or a quantitative, probabilistic measure of uncertainty. Previous studies have quantified uncertainties and produced probabilistic projections using Bayesian statistics and observational constraints (e.g. Tebaldi et al. 2005; Shongwe et al. 2009; Sexton et al. 2012), including the UK Climate Projections 2009 (UKCP09) (Jenkins et al. 2009), however the results are still guided by the models, and do not necessarily incorporate the possibility of alternative futures or nonlinear change.

Subjective estimates of confidence and explanations of sources of uncertainty to decision makers might be a more comprehensive approach. Alternatively, rather than seeking to provide defensible error bars, climate model data could be used to generate a large number of plausible future scenarios to test mitigation goals or adaptation options, as advocated by e.g. Dessai et al. (2009). The difficulties of measuring uncertainty demonstrated by this thesis highlight the importance of this kind of creative application of climate information, as in, for example, "Robust Decision Making" approaches (see Hall et al. 2012; Weaver et al. 2013).

The most useful role for climate scientists might be to improve process-based understanding of model projections: to provide a better assessment of confidence or to determine which scenarios should be considered plausible. The potential for appraising projections via analysis of atmospheric circulation has been demonstrated in the case of the Sahel (Chapter 6). Similar investigation for other regions represents an important area for further research, but its utility is contingent on an understanding of the background climate, which is missing for some African regions. The contrast between datasets over the Congo Basin demonstrates for the first time the extent to which the knowledge of the basic features of the background climate is limited. Field campaigns to observe the circulation over Central Africa, in combination with analysis of modelled dynamics, might therefore be the most worthwhile investment to improve understanding of the implications of global warming for this region.

References

Abe, M., Shiogama, H., Hargreaves, J.C., et al. 2009, "Correlation between Inter-Model Similarities in Spatial Pattern for Present and Projected Future Mean Climate", vol. 5, pp. 5-8, doi:10.2151/sola.2009.

Ackerley, D., Booth, B.B.B., Knight, S.H.E., et al. 2011, "Sensitivity of Twentieth-Century Sahel Rainfall to Sulfate Aerosol and CO_2 Forcing", *Journal of Climate,* vol. 24, no. 19, pp. 4999-5014, doi:10.1175/JCLI-D-11-00019.1.

Adler, R.F., Huffman, G.J., Chang, A., et al. 2003, "The version-2 global precipitation climatology project (GPCP) monthly precipitation analysis (1979-present)", *Journal of Hydrometeorology,* vol. 4, no. 6, pp. 1147-1167.

Aguilar, E., Barry, A.A., Brunet, M., et al. 2009, "Changes in temperature and precipitation extremes in western central Africa, Guinea Conakry, and Zimbabwe, 1955-2006", *Journal of Geophysical Research D: Atmospheres,* vol. 114, no. 2.

Albrecht, B.A. 1989, "Aerosols, cloud microphysics, and fractional cloudiness", *Science,* vol. 245, no. 4923, pp. 1227-1230.

Allan, R.P. 2012, "Regime dependent changes in global precipitation", *Climate Dynamics,* doi:10.1007/s00382-011-1134-x.

Allan, R.P. & Soden, B.J. 2007, "Large discrepancy between observed and simulated precipitation trends in the ascending and descending branches of the tropical circulation", *Geophysical Research Letters,* vol. 34, no. 18, pp. 1-6, doi:10.1029/2007GL031460.

Allan, R.P., Soden, B.J., John, V.O., et al. 2010, "Current changes in tropical precipitation", *Environmental Research Letters,* vol. 5, no. 2, pp. 025205, doi:10.1088/1748-9326/5/2/025205.

Allen, M.R. & Stainforth, D.A. 2002, "Towards objective probabalistic climate forecasting", *Nature,* vol. 419, no. 6903, pp. 228-228.

Allen, M. 1999, "Do-it-yourself climate prediction", *Nature,* vol. 401, no. 6754, pp. 642-642.

Allen, M.R., Frame, D.J., Huntingford, C., et al. 2009, "Warming caused by cumulative carbon emissions towards the trillionth tonne", *Nature,* vol. 458, no. 7242, pp. 1163-6.

Allen, M.R. & Ingram, W.J. 2002, "Constraints on future changes in climate and the hydrologic cycle", *Nature,* vol. 419, no. 6903, pp. 224-32, doi:10.1038/nature01092.

Anderson, B.T. 2011, "Intensification of seasonal extremes given a 2°C global warming target", *Climatic Change,* doi:10.1007/s10584-011-0213-7.

Andrews, T., Forster, P.M., Boucher, O., et al. 2010, "Precipitation, radiative forcing and global temperature change", *Geophysical Research Letters,* vol. 37, no. 14, doi:10.1029/2010GL043991.

Andrews, T., Gregory, J.M., Webb, M.J., et al. 2012, "Forcing, feedbacks and climate sensitivity in CMIP5 coupled atmosphere-ocean climate models", *Geophysical Research Letters,* vol. 39, no. 9, pp. 1-7, doi:10.1029/2012GL051607.

Arnell, N.W., Lowe, J., Brown, S., et al. 2013, "A global assessment of the effects of climate policy on the impacts of climate change", *Nature Climate Change,* vol. 3, no. 2, pp. 1-8, doi:10.1038/nclimate1793.

Bala, G., Caldeira, K. & Nemani, R. 2009, "Fast versus slow response in climate change: implications for the global hydrological cycle", *Climate Dynamics,* vol. 35, no. 2-3, pp. 423-434.

Balas, N., Nicholson, S.E. & Klotter, D. 2007, "The relationship of rainfall variability in West Central Africa to sea-surface temperature fluctuations", *International Journal of Climatology,* vol. 1349, no. June, pp. 1335-1349, doi:10.1002/joc.

Barnett, D.N., Brown, S.J., Murphy, J.M., et al. 2006, "Quantifying uncertainty in changes in extreme event frequency in response to doubled CO2 using a large ensemble of GCM simulations", *Climate Dynamics,* vol. 26, no. 5, pp. 489-511, doi:10.1007/s00382-005-0097-1.

Beighley, R.E., Ray, R.L., He, Y., et al. 2011, "Comparing satellite derived precipitation datasets using the Hillslope River Routing (HRR) model in the Congo River Basin", *Hydrological Processes,* vol. 25, no. 20, pp. 3216-3229.

Ben Mohamed, A. 2011, "Climate change risks in Sahelian Africa", *Regional Environmental Change,* vol. 11, pp. 117, doi:10.1007/s10113-010-0172-y.

Betts, R.A., Collins, M., Hemming, D.L., et al. 2011, "When could global warming reach 4°C?", *Philosophical Transactions of the Royal Society A: Mathematical, Physical and Engineering Sciences,* vol. 369, no. 1934, pp. 67-84.

Betts, R.a., Cox, P.M., Collins, M., et al. 2004, "The role of ecosystem-atmosphere interactions in simulated Amazonian precipitation decrease and forest dieback under global climate warming", *Theoretical and Applied Climatology,* vol. 78, no. 1-3, pp. 157-175, doi:10.1007/s00704-004-0050-y.

Bewket, W. & Conway, D. 2007, "A note on the temporal and spatial variability of rainfall in the droughtâ€ prone Amhara region of Ethiopia", *International Journal of Climatology,* vol. 1477, pp. 1467-1477, doi:10.1002/joc.

Biasutti, M., Sobel, A.H. & Camargo, S.J. 2009, "The Role of the Sahara Low in Summertime Sahel Rainfall Variability and Change in the CMIP3 Models", *Journal of Climate,* vol. 22, no. 21, pp. 5755-5771, doi:10.1175/2009JCLI2969.1.

Biasutti, M. & Giannini, A. 2006, "Robust Sahel drying in response to late 20th century forcings", *Geophysical Research Letters,* vol. 33, no. 11, pp. 10-13.

Biasutti, M. & Sobel, A.H. 2009, "Delayed Sahel rainfall and global seasonal cycle in a warmer climate", *Geophysical Research Letters,* vol. 36, no. 23, pp. 1-5.

Bindoff, N.L., Stott, P.A., AchutaRao, K.M., et al. 2013, "Detection and Attribution of Climate Change: from Global to Regional" in *Climate Change 2013: The Physical Science Basis. Contribution of Working Group I to the Fifth Assessment Report of the Intergovernmental Panel on Climate Change*, eds. T. Stocker, Q. Dahe, G. Plattner, et al, Cambridge University Press, Cambridge, United Kingdom and New York, NY, USA.

Black, E., Slingo, J. & Sperber, K.R. 2003, "An observational study of the relationship between excessively strong short rains in coastal East Africa and Indian Ocean SST", *Monthly Weather Review,* vol. 131, no. 1, pp. 74-94.

Boko, M., Niang, I., Nyong, A., et al. 2007, "Africa" in *Climate Change Adaptation and Vulnerability: Contribution of Working Group II to the IV Assessment Report of the IPCC Panel on Climate Change*, eds. M. Parry, O. Canziani, J. Palutikof, et al, Cambridge University Press, Cambridge and New York, pp. 433-467.

Bony, S., Colman, R., Kattsov, V.M., et al. 2006, "How well do we understand and evaluate climate change feedback processes?", *Journal of Climate,* , pp. 3445-3482.

Braconnot, P., Otto-Bliesner, B., Harrison, S., et al. 2007, "Results of PMIP2 coupled simulations of the Mid-Holocene and Last Glacial Maximum - Part 1: experiments and large-scale features", *Climate of the Past,* vol. 3, no. 2, pp. 261-277, doi:10.5194/cp-3-261-2007.

Brncic, T.M., Willis, K.J., Harris, D.J., et al. 2007, "Culture or climate? The relative influences of past processes on the composition of the lowland Congo rainforest.", *Philosophical transactions of the Royal Society of London.Series B, Biological sciences,* vol. 362, no. 1478, pp. 229-242, doi:10.1098/rstb.2006.1982.

Brooks, N., Neil Adger, W. & Mick Kelly, P. 2005, "The determinants of vulnerability and adaptive capacity at the national level and the implications for adaptation", *Global Environmental Change,* vol. 15, no. 2, pp. 151-163.

Buontempo, C., Mathison, C., Williams, K., et al. 2013, "Regional Climate Modelling for Africa with PRECIS", *in prep.*

Camberlin, P., Janicot, S. & Poccard, I. 2001, "Seasonality and atmospheric dynamics of the teleconnection between African rainfall and tropical sea-surface

temperature: Atlantic vs. ENSO", *International Journal of Climatology,* vol. 21, no. 8, pp. 973-1005, doi:10.1002/joc.673.

Caminade, C., Terray, L. & Maisonnave, E. 2006, "West African monsoon response to greenhouse gas and sulphate aerosol forcing under two emission scenarios", *Climate Dynamics,* vol. 26, no. 5, pp. 531-547.

Caricom 2009, *Press Release: Climate Change, A Clear and Present Danger: 1.5 to Stay Alive*. Available: http://www.caricom.org/jsp/pressreleases/pres487_09.jsp [Accessed: 2013, 7 September].

Chadwick, R., Boutle, I. & Martin, G. 2013, "Spatial Patterns of Precipitation Change in CMIP5: Why the Rich Do Not Get Richer in the Tropics", *Journal of Climate,* vol. 26, no. 11, pp. 3803-3822, doi:10.1175/JCLI-D-12-00543.1.

Chou, C. & Neelin, J.D. 2004, "Mechanisms of Global Warming Impacts on Regional Tropical Precipitation*", *Journal of Climate,* vol. 17, no. 13, pp. 2688-2701, doi:10.1175/1520-0442(2004)017<2688:MOGWIO>2.0.CO;2.

Chou, C., Neelin, J.D., Chen, C., et al. 2009, "Evaluating the "Rich-Get-Richer" Mechanism in Tropical Precipitation Change under Global Warming", *Journal of Climate,* vol. 22, no. 8, pp. 1982-2005, doi:10.1175/2008JCLI2471.1.

Chou, C., Neelin, J.D., Tu, J., et al. 2006, "Regional Tropical Precipitation Change Mechanisms in ECHAM4/OPYC3 under Global Warming*", *Journal of Climate,* vol. 19, no. 17, pp. 4207-4223, doi:10.1175/JCLI3858.1.

Chou, C., Tu, J. & Tan, P. 2007, "Asymmetry of tropical precipitation change under global warming", *Geophysical Research Letters,* vol. 34, no. 17, pp. 1-5, doi:10.1029/2007GL030327.

Christensen, J.H., Hewitson, B., Busuioc, A., et al. 2007, "Regional Climate Projections" in *Climate Change 2007: The Physical Science Basis. Contribution of Working Group I to the Fourth Assessment Report of the Intergovernmental Panel on Climate Change*, eds. S. Solomon, D. Qin, M. Manning, et al, Cambridge University Press, Cambridge and New York, pp. 847-940.

Christensen, J.H., Kanikicharla, K.K., Aldrian, E., et al. 2013, "Climate Phenomena and their Relevance for Future Regional Climate Change " in *Climate Change 2013: The Physical Science Basis. Contribution of Working Group I to the Fifth Assessment Report of the Intergovernmental Panel on Climate Change*, eds. T. Stocker, Q. Dahe, G. Plattner, et al, Cambridge University Press, Cambridge, United Kingdom and New York, NY, USA, .

Ciais, P., Sabine, C., Bala, G., et al. 2013, "Carbon and Other Biogeochemical Cycles" in *Climate Change 2013: The Physical Science Basis. Contribution of Working Group I to the Fifth Assessment Report of the Intergovernmental Panel on Climate Change*, eds. T.

Stocker, Q. Dahe, G. Plattner, et al, Cambridge University Press, Cambridge, United Kingdom and New York, NY, USA.

Clark, C.O., Webster, P.J. & Cole, J.E. 2003, "Interdecadal variability of the relationship between the Indian Ocean zonal mode and East African coastal rainfall anomalies", *Journal of Climate,* vol. 16, no. 3, pp. 548-554.

Clark, R.T., Murphy, J.M. & Brown, S.J. 2010, "Do global warming targets limit heatwave risk?", *Geophysical Research Letters,* vol. 37, no. 17, pp. 1-5, doi:10.1029/2010GL043898.

Clement, A.C., Baker, A.C. & Leloup, J. 2010, "Climate change: Patterns of tropical warming", *Nature Geoscience,* vol. 3, no. 1, pp. 8-9, doi:10.1038/ngeo728.

Collins, M. 2007, "Ensembles and probabilities: a new era in the prediction of climate change", *Philosophical Transactions of the Royal Society A: Mathematical, Physical and Engineering Sciences,* vol. 365, no. 1857, pp. 1957-70.

Collins, M., Knutti, R., Arblaster, J.M., et al. 2013, "Long-term Climate Change: Projections, Commitments and Irreversibility" in *Climate Change 2013: The Physical Science Basis. Contribution of Working Group I to the Fifth Assessment Report of the Intergovernmental Panel on Climate Change*, eds. T. Stocker, Q. Dahe, G. Plattner, et al, Cambridge University Press, Cambridge, United Kingdom and New York, NY, USA.

Collins, M., Tett, S. & Cooper, C. 2001, "The internal climate variability of HadCM3, a version of the Hadley Centre coupled model without flux adjustments", *Climate Dynamics,* vol. 17, no. 1, pp. 61-81.

Collins, M., Booth, B.B.B., Glen, B.B., et al. 2011, "Climate model errors, feedbacks and forcings: a comparison of perturbed physics and multi-model ensembles", *Climate Dynamics,* vol. 36, pp. 1737-1766, doi:10.1007/s00382-010-0808-0.

Conway, D. 2011, "Adapting climate research for development in Africa", *Wiley Interdisciplinary Reviews: Climate Change,* vol. 2, no. 3, pp. 428-450.

Conway, D., Hanson, C.E., Doherty, R., et al. 2007, "GCM simulations of the Indian Ocean dipole influence on East African rainfall: Present and future", *Geophysical Research Letters,* vol. 34, no. 3, pp. 1-6, doi:10.1029/2006GL027597.

Conway, D., Allison, E., Felstead, R., et al. 2005, "Rainfall variability in East Africa: implications for natural resources management and livelihoods.", *Philosophical transactions.Series A, Mathematical, physical, and engineering sciences,* vol. 363, no. 1826, pp. 49-54, doi:10.1098/rsta.2004.1475.

Conway, D., Mould, C. & Bewket, W. 2004, "Over one century of rainfall and temperature observations in Addis Ababa, Ethiopia", *International Journal of Climatology,* vol. 24, no. 1, pp. 77-91, doi:10.1002/joc.989.

Conway, D., Persechino, A., Ardoin-Bardin, S., et al. 2009, "Rainfall and Water Resources Variability in Sub-Saharan Africa during the Twentieth Century", *Journal of Hydrometeorology,* vol. 10, no. 1, pp. 41-59, doi:10.1175/2008JHM1004.1.

Conway, D. & Schipper, E.L.F. 2011, "Adaptation to climate change in Africa: Challenges and opportunities identified from Ethiopia", *Global Environmental Change,* vol. 21, no. 1, pp. 227-237, doi:10.1016/j.gloenvcha.2010.07.013.

Cook, K.H. 2008, "Climate science: the mysteries of Sahel droughts", *Nature Geoscience,* vol. 1, no. 10, pp. 647-648.

Cook, C., Reason, C. & Hewitson, B. 2004, "Wet and dry spells within particularly wet and dry summers in the South African summer rainfall region", *Climate Research,* vol. 26, pp. 17-31.

Cook, K.H. 2000, "The South Indian convergence zone and interannual rainfall variability over southern Africa", *Journal of Climate,* vol. 13, pp. 3789-3804.

Cook, K.H. & Vizy, E.K. 2013, "Projected Changes in East African Rainy Seasons", *Journal of Climate,* doi:10.1175/JCLI-D-12-00455.1.

Cook, K.H. & Vizy, E.K. 2012, "Impact of climate change on mid-twenty-first century growing seasons in Africa", *Climate Dynamics,* doi:10.1007/s00382-012-1324-1.

Copsey, D., Sutton, R. & Knight, J.R. 2006, "Recent trends in sea level pressure in the Indian Ocean region", *Geophysical Research Letters,* vol. 33, no. 19, pp. L19712-L19712, doi:10.1029/2006GL027175.

Corlett, R.T. 2011, "Impacts of warming on tropical lowland rainforests", *Trends in ecology & evolution,* vol. 26, no. 11, pp. 606-13, doi:10.1016/j.tree.2011.06.015.

Corti, S., Molteni, F. & Palmer, T. 1999, "Signature of recent climate change in frequencies of natural atmospheric circulation regimes", *Nature,* vol. 398, no. 6730, pp. 799-802.

Cox, P.M., Betts, R.a., Collins, M., et al. 2004, "Amazonian forest dieback under climate-carbon cycle projections for the 21st century", *Theoretical and Applied Climatology,* vol. 78, no. 1-3, pp. 137-156, doi:10.1007/s00704-004-0049-4.

CSC 2013, *Climate Change Scenarios for the Congo Basin [Haensler A., Jacob D., Kabat P., Ludwig F. (eds.)] Climate Service Centre Report No. 11*, Hamburg, Germany, ISSN: 2192-4058.

Dadson, S., Acreman, M. & Harding, R. 2013, "Water security, global change and land–atmosphere feedbacks", *Philosophical Transactions of the Royal Society A: Mathematical, Physical and Engineering Sciences,* vol. 371, no. 2002, pp. 20120412.

Dadson, S.J., Ashpole, I., Harris, P., et al. 2010, "Wetland inundation dynamics in a model of land surface climate: Evaluation in the Niger inland delta region", *Journal of Geophysical Research,* vol. 115, D23114-D23114, doi:10.1029/2010JD014474.

Dai, A., Lamb, P.J., Trenberth, K.E., et al. 2004, "The recent Sahel drought is real", *International Journal of Climatology,* vol. 24, no. 11, pp. 1323-1331.

Dai, A. 2006, "Precipitation Characteristics in Eighteen Coupled Climate Models", *Journal of Climate,* vol. 19, no. 18, pp. 4605-4630.

Darbyshire, R., Webb, L., Goodwin, I., et al. 2013, "Impact of future warming on winter chilling in Australia", *International journal of biometeorology,* vol. 57, no. 3, pp. 355-66, doi:10.1007/s00484-012-0558-2.

Davie, J., Falloon, P.D., Kahana, R., et al. 2013, "Comparing projections of future changes in runoff and water resources from hydrological and ecosystem models in ISI-MIP", *Earth System Dynamics Discussions,* vol. 4, no. 1, pp. 279-315.

Dee, D.P., Uppala, S.M., Simmons, A.J., et al. 2011, "The ERA-Interim reanalysis: Configuration and performance of the data assimilation system", *Quarterly Journal of the Royal Meteorological Society,* vol. 137, no. 656, pp. 553-597, doi:10.1002/qj.828.

Delire, C., Ngomanda, A. & Jolly, D. 2008, "Possible impacts of 21st century climate on vegetation in Central and West Africa", *Global and Planetary Change,* vol. 64, no. 1-2, pp. 3-15.

Deser, C., Knutti, R., Solomon, S., et al. 2012, "Communication of the role of natural variability in future North American climate", *Nature Climate Change,* vol. 2, no. 11, pp. 775-779.

Deser, C., Phillips, A., Bourdette, V., et al. 2010, "Uncertainty in climate change projections: the role of internal variability", *Climate Dynamics,* vol. 38, no. 3-4, pp. 527-546, doi:10.1007/s00382-010-0977-x.

Dessai, S., Adger, W.N., Hulme, M., et al. 2004, "Defining and experiencing dangerous climate change", *Climatic Change,* vol. 64, no. 1-2, pp. 11-25.

Dessai, S., Hulme, M., Lempert, R., et al. 2009, "Do We Need Better Predictions to Adapt to a Changing Climate?", *Eos, Transactions American Geophysical Union,* vol. 90, no. 13, pp. 111, doi:10.1029/2009EO130003.

Dezfuli, A.K. 2010, "Spatio-temporal variability of seasonal rainfall in western equatorial Africa", *Theoretical and Applied Climatology,* vol. 104, no. 1-2, pp. 57-69, doi:10.1007/s00704-010-0321-8.

Dezfuli, A.K. & Nicholson, S.E. 2013, "The Relationship of Rainfall Variability in Western Equatorial Africa to the Tropical Oceans and Atmospheric Circulation.

Part II: The Boreal Autumn", *Journal of Climate,* vol. 26, no. 1, pp. 66-84, doi:10.1175/JCLI-D-11-00686.1.

Diallo, I., Sylla, M.B., Giorgi, F., et al. 2012, "Multimodel GCM-RCM Ensemble-Based Projections of Temperature and Precipitation over West Africa for the Early 21st Century", *International Journal of Geophysics,* vol. 2012, pp. 1-19, doi:10.1155/2012/972896.

Dickinson, R.E., Meleshko, V., Randall, D., et al. 1995, "Climate Processes" in *Climate Change 1995: The Science of Climate Change. Contribution of Working Group I to the Second Assessment Report of the Intergovernmental Panel on Climate Change*, eds. J.T. Houghton, L.G. Meira Filho, B.A. Callander, et al, Cambridge University Press, Cambridge, UK, New York, USA, and Melbourne, Australia.

Diro, G., Grimes, D.I.F. & Black, E. 2011, "Teleconnections between Ethiopian summer rainfall and sea surface temperature: part I—observation and modelling", *Climate Dynamics,* vol. 37, no. 1-2, pp. 103-119.

Dixon, R.K., Smith, J. & Guill, S. 2003, "Life on the Edge: Vulnerability and Adaptation of African Ecosystems to Global Climate Change", *Mitigation and Adaptation Strategies for Global Change,* vol. 8, no. 2, pp. 93-113.

Druyan, L.M., Feng, J., Cook, K.H., et al. 2010, "The WAMME regional model intercomparison study", *Climate Dynamics,* vol. 35, no. 1, pp. 175-192, doi:10.1007/s00382-009-0676-7.

Druyan, L.M. 2011, "Studies of 21st-century precipitation trends over West Africa", *International Journal of Climatology,* vol. 31, no. 10, pp. 1415-1424, doi:10.1002/joc.2180.

Duvel, J.P. 1990, "Convection over tropical Africa and the Atlantic Ocean during northern summer. Part II: Modulation by easterly waves", *Monthly Weather Review,* vol. 118, no. 9, pp. 1855-1868.

Easterbrook, S. 2012, *Some CMIP5 Statistics*. Available at: http://www.easterbrook.ca/steve/2012/04/some-cmip5-statistics/ [Accessed: 2013, 7 September] .

Elkin, C., Gutiérrez, A.,G., Leuzinger, S., et al. 2013, "A 2°C warmer world is not safe for ecosystem services in the European Alps", *Global Change Biology,* vol. 19, no. 6, pp. 1-14, doi:10.1111/gcb.12156.

Endris, H.S., Omondi, P., Jain, S., et al. 2013, "Assessment of the Performance of CORDEX Regional Climate Models in Simulating East African Rainfall", *Journal of Climate,* vol. 26, no. 21, pp. 8453-8475, doi:10.1175/JCLI-D-12-00708.1.

Fisher, J.B., Sikka, M., Sitch, S., et al. 2013, "African tropical rainforest net carbon dioxide fluxes in the twentieth century", *Philosophical Transactions of the Royal Society B: Biological Sciences,* vol. 368, no. 1625, pp. 20120376.

Flato, G., Marotzke, J., Abiodun, B., et al. 2013, "Evaluation of Climate Models" in *Climate Change 2013: The Physical Science Basis. Contribution of Working Group I to the Fifth Assessment Report of the Intergovernmental Panel on Climate Change*, eds. T. Stocker, Q. Dahe, G. Plattner, et al, Cambridge University Press, Cambridge, United Kingdom and New York, NY, USA.

Folland, C., Palmer, T. & Parker, D. 1986, "Sahel rainfall and worldwide sea temperatures, 1901–85", *Nature,* vol. 320, no. 6063, pp. 602-607.

Fontaine, B., Roucou, P. & Monerie, P. 2011, "Changes in the African monsoon region at medium-term time horizon using 12 AR4 coupled models under the A1B emissions scenario", *Atmospheric Science Letters,* vol. 12, no. 1, pp. 83-88, doi:10.1002/asl.321.

Foster, G. & Rahmstorf, S. 2011, "Global temperature evolution 1979–2010", *Environmental Research Letters,* vol. 6, no. 4, pp. 044022.

Fowler, H.J. 2007, "Linking climate change modelling to impacts studies: recent advances in downscaling techniques for hydrological modelling", *International Journal of â€¦,* vol. 1578, pp. 1547-1578, doi:10.1002/joc.

Frame, D.J., Faull, N.E., Joshi, M.M., et al. 2007, "Probabilistic climate forecasts and inductive problems", *Philosophical Transactions of the Royal Society A: Mathematical, Physical and Engineering Sciences,* vol. 365, no. 1857, pp. 1971-92.

Friedlingstein, P. & Jones, C. 2011, "Climate-carbon interactions in the CMIP5 Earth System models", *CLIVAR Exchanges No. 56,* vol. 16, pp. 27-29.

Frieler, K., Meinshausen, M., Golly, A., et al. 2012, "Limiting global warming to 2°C is unlikely to save most coral reefs", *Nature Climate Change,* vol. 3, no. 2, pp. 165-170, doi:10.1038/nclimate1674.

Fung, F., Lopez, A. & New, M. 2011, "Water availability in +2°C and +4°C worlds", *Philosophical Transactions of the Royal Society A: Mathematical, Physical and Engineering Sciences,* vol. 369, no. 1934, pp. 99-116.

Gbobaniyi, E., Sarr, A., Sylla, M.B., et al. 2013, "Climatology, annual cycle and interannual variability of precipitation and temperature in CORDEX simulations over West Africa", *International Journal of Climatology,* doi:10.1002/joc.3834.

Giannakopoulos, C., Le Sager P., Bindi, M., et al. 2009, "Climatic changes and associated impacts in the Mediterranean resulting from a 2°C global warming", *Global and Planetary Change,* vol. 68, no. 3, pp. 209-224, doi:10.1016/j.gloplacha.2009.06.001.

Giannini, A., Saravanan, R. & Chang, P. 2003, "Oceanic forcing of Sahel rainfall on interannual to interdecadal time scales", *Science,* vol. 302, no. 5647, pp. 1027-1030.

Giannini, A., Biasutti, M., Held, I.M., et al. 2008, "A global perspective on African climate", *Climatic Change,* vol. 90, no. 4, pp. 359-383, doi:10.1007/s10584-008-9396-y.

Giorgi, F. & Bi, X. 2005, "Updated regional precipitation and temperature changes for the 21st century from ensembles of recent AOGCM simulations", *Geophysical Research Letters,* vol. 32, no. 21.

Giorgi, F. & Mearns, L. 2003, "Probability of regional climate change based on the Reliability Ensemble Averaging (REA) method", *Geophysical Research Letters,* vol. 30, no. 12, pp. 1629.

Giorgi, F. & Mearns, L.O. 2002, "Calculation of average, uncertainty range, and reliability of regional climate changes from AOGCM simulations via the "reliability ensemble averaging"(REA) method", *Journal of Climate,* vol. 15, no. 10, pp. 1141-1158.

Giorgi, F. & Francisco, R. 2000, "Uncertainties in regional climate change prediction: a regional analysis of ensemble simulations with the HADCM2 coupled AOGCM", *Climate Dynamics,* vol. 16, no. 2-3, pp. 169-182, doi:10.1007/PL00013733.

Giorgi, F. & Coppola, E. 2010, "Does the model regional bias affect the projected regional climate change? An analysis of global model projections", *Climatic Change,* vol. 100, no. 3-4, pp. 787-795, doi:10.1007/s10584-010-9864-z.

Giorgi, F., Jones, C. & Asrar, G.R. 2009, "Addressing climate information needs at the regional level : the CORDEX framework", vol. 58, pp. 175-183.

Goddard, L. & Graham, E. 1999, "Importance of the Indian Ocean for simulating rainfall anomalies over eastern and southern Africa", *Journal of Geophysical Research,* vol. 104, pp. 19,099-19,116.

Gond, V., Fayolle, A., Pennec, A., et al. 2013, "Vegetation structure and greenness in Central Africa from Modis multi-temporal data", *Philosophical Transactions of the Royal Society B: Biological Sciences,* vol. 368, no. 1625, pp. 20120309.

Good, P., Ingram, W., Lambert, F.H., et al. 2012, "A step-response approach for predicting and understanding non-linear precipitation changes", *Climate Dynamics,* vol. 39, no. 12, pp. 2789-2803, doi:10.1007/s00382-012-1571-1.

Gupta, J. & Vanasselt, H. 2006, "Helping operationalise Article 2: A transdisciplinary methodological tool for evaluating when climate change is dangerous", *Global Environmental Change,* vol. 16, no. 1, pp. 83-94.

Haarsma, R.J., Selten, F.M., Weber, S.L., et al. 2005, "Sahel rainfall variability and response to greenhouse warming", *Geophysical Research Letters,* vol. 32, no. 17, doi:10.1029/2005GL023232.

Haddeland, I., Clark, D.B., Franssen, W., et al. 2011, "Multimodel Estimate of the Global Terrestrial Water Balance: Setup and First Results", *Journal of Hydrometeorology,* vol. 12, no. 5, pp. 869-884, doi:10.1175/2011JHM1324.1.

Haensler, A., Saeed, F. & Jacob, D. 2013, "Assessing the robustness of projected precipitation changes over central Africa on the basis of a multitude of global and regional climate projections", *Climatic Change,* , doi:10.1007/s10584-013-0863-8.

Hall, J.W., Lempert, R.J., Keller, K., et al. 2012, "Robust climate policies under uncertainty: a comparison of robust decision making and info-gap methods", *Risk analysis : an official publication of the Society for Risk Analysis,* vol. 32, no. 10, pp. 1657-72, doi:10.1111/j.1539-6924.2012.01802.x.

Haltiner, G.J. & Williams, R.T. 1980, *Numerical prediction and dynamic meteorology,* Wiley New York.

Hansen, J., Sato, M., Kharecha, P., et al. 2008, "Target Atmospheric CO2: Where Should Humanity Aim?", *The Open Atmospheric Science Journal,* vol. 2, no. 1, pp. 217-231.

Harris, I., Jones, P.D., Osborn, T.J., et al. 2013, "Updated high-resolution grids of monthly climatic observations: the CRU TS3.10 Dataset", *International Journal of Climatology,* , doi:10.1002/joc.3711.

Hartmann, D., Klein Tank, A.M.G., Rusticucci, M., et al. 2013, "Observations: Atmosphere and Surface " in *Climate Change 2013: The Physical Science Basis. Contribution of Working Group I to the Fifth Assessment Report of the Intergovernmental Panel on Climate Change*, eds. T. Stocker, Q. Dahe, G. Plattner, et al, Cambridge University Press, Cambridge, United Kingdom and New York, NY, USA, .

Hastenrath, S., Nicklis, A. & Greischar, L. 1993, "Atmospheric-hydrospheric mechanisms of climate anomalies in the western equatorial Indian Ocean", *Journal of Geophysical Research: Oceans (1978–2012),* vol. 98, no. C11, pp. 20219-20235.

Hastenrath, S. 2000, "Interannual and longer term variability of upper-air circulation over the tropical Atlantic and West Africa in boreal summer", *International Journal of Climatology,* vol. 20, no. 12, pp. 1415-1430, doi:10.1002/1097-0088(200010)20:12<1415::AID-JOC550>3.0.CO;2-C.

Hastenrath, S., Polzin, D. & Mutai, C. 2011, "Circulation Mechanisms of Kenya Rainfall Anomalies", *Journal of Climate,* vol. 24, no. 2, pp. 404-412, doi:10.1175/2010JCLI3599.1.

Hawkins, E. & Sutton, R. 2009, "The potential to narrow uncertainty in regional climate predictions", *Bulletin of the American Meteorological Society,* vol. 90, no. 8, pp. 1095-1107.

Hayashi, A., Akimoto, K., Sano, F., et al. 2009, "Evaluation of global warming impacts for different levels of stabilization as a step toward determination of the long-term stabilization target", *Climatic Change,* vol. 98, no. 1-2, pp. 87-112, doi:10.1007/s10584-009-9663-6.

Held, I.M., Delworth, T.L., Lu, J., et al. 2005, "Simulation of Sahel drought in the 20th and 21st centuries", *Proceedings of the National Academy of Sciences of the United States of America,* vol. 102, no. 50, pp. 17891-6.

Held, I.M. & Soden, B.J. 2006, "Robust Responses of the Hydrological Cycle to Global Warming", *Journal of Climate,* vol. 19, no. 21, pp. 5686-5699, doi:10.1175/JCLI3990.1.

Herceg, D., Sobel, A.H. & Sun, L. 2007, "Regional modeling of decadal rainfall variability over the Sahel", *Climate Dynamics,* vol. 29, no. 1, pp. 89-99, doi:10.1007/s00382-006-0218-5.

Herrmann, S.M. & Mohr, K.I. 2011, "A continental-scale classification of rainfall seasonality regimes in Africa based on gridded precipitation and land surface temperature products", *Journal of Applied Meteorology and Climatology,* vol. 50, no. 12, pp. 2504-2513.

Hewitson, B., Lennard, C., Nikulin, G., et al. 2012, "CORDEX-Africa: a unique opportunity for science and capacity building", *CLIVAR Exchanges,* vol. 60.

Hewitson, B.C. & Crane, R.G. 2006, "Consensus between GCM climate change projections with empirical downscaling: precipitation downscaling over South Africa", *International Journal of Climatology,* vol. 26, no. 10, pp. 1315-1337, doi:10.1002/joc.1314.

Hoerling, M., Hurrell, J., Eischeid, J., et al. 2006, "Detection and Attribution of Twentieth-Century Northern and Southern African Rainfall Change", *Journal of Climate,* vol. 19, no. 16, pp. 3989-3989.

Hu, Y. & Fu, Q. 2007, "Observed poleward expansion of the Hadley circulation since 1979", *Atmospheric Chemistry and Physics Discussions,* vol. 7, no. 4, pp. 9367-9384.

Huebener, H., Sanderson, M.G. & Höschel, I. 2013, "Regional hydrological cycle changes in response to an ambitious mitigation scenario", *Climatic Change,* vol. 120, pp. 389-403, doi:10.1007/s10584-013-0829-x.

Huffman, G.J., Adler, R.F., Bolvin, D.T., et al. 2007, "The TRMM Multisatellite Precipitation Analysis (TMPA): Quasi-global, multiyear, combined-sensor

precipitation estimates at fine scales", *Journal of Hydrometeorology,* vol. 8, no. 1, pp. 38-55.

Hulme, M. 1992, "Rainfall changes in Africa: 1931–1960 to 1961–1990", *International Journal of Climatology,* vol. 12, no. 7, pp. 685-699.

Hulme, M., Doherty, R., Ngara, T., et al. 2001, "African climate change: 1900-2100", *Climate Research,* vol. 17, pp. 145-168, doi:10.3354/cr017145.

Huntingford, C. & Cox, P. 2000, "An analogue model to derive additional climate change scenarios from existing GCM simulations", *Climate Dynamics,* vol. 16, no. 8, pp. 575-586.

Hurrell, J., Visbeck, M. & Pirani, A. 2011, "WCRP Coupled Model Intercomparison Project - Phase 5 - CMIP5", *CLIVAR Exchanges,* vol. 16, no. 56.

Indeje, M., Semazzi, F.H.M. & Ogallo, L.J. 2000, "ENSO signals in East African rainfall seasons", *International Journal of Climatology,* vol. 20, no. 1, pp. 19-46, doi:10.1002/(SICI)1097-0088(200001)20:1<19::AID-JOC449>3.0.CO;2-0.

IPCC (ed) 2007, *Climate Change 2007: Synthesis Report. Contribution of Working Groups I, II and III to the Fourth Assessment Report of the Intergovernmental Panel on Climate Change [Core Writing Team, Pachauri, R.K and Reisinger, A. (eds.)]*, IPCC, Geneva, Switzerland.

IPCC 2012, "Managing the Risks of Extreme Events and Disasters to Advance Climate Change Adaptation. A Special Report of Working Groups I and II of the Intergovernmental Panel on Climate Change" in , ed. [Field, C.B., V. Barros, T.F. Stocker, D. Qin, D.J. Dokken, K.L. Ebi, M.D. Mastrandrea, K.J. Mach, G.-K. Plattner, S.K. Allen, M. Tignor, and P.M. Midgley, Cambridge University Press, Cambridge, UK, and New York, NY, USA.

Jackson, B., Nicholson, S.E. & Klotter, D. 2009, "Mesoscale Convective Systems over Western Equatorial Africa and Their Relationship to Large-Scale Circulation", *Monthly Weather Review,* vol. 137, no. 4, pp. 1272-1294, doi:10.1175/2008MWR2525.1.

Jaeger, C.C. & Jaeger, J. 2010, "Three views of two degrees", *Regional Environmental Change,* 1, no. 3, 145-166.

Jenkins, G.J., Murphy, J.M., Sexton, D.M.H., et al 2009, *UK Climate Projections: Briefing report.*, Met Office Hadley Centre, Exeter, UK.

Jenkins, G.S., Gaye, A.T. & Sylla, B. 2005, "Late 20th century attribution of drying trends in the Sahel from the Regional Climate Model (RegCM3)", *Geophysical Research Letters,* vol. 32, no. 22, pp. L22705-L22705, doi:10.1029/2005GL024225.

Jolliffe, I.T. 2002, *Graphical Representation of Data Using Principal Components,* Springer.

Jones, C., Giorgi, F. & Asrar, G. 2011, "The Coordinated Regional Downscaling Experiment: CORDEX An international downscaling link to CMIP5 ", *CLIVAR Exchanges,* vol. No. 56, Vol. 16, No.2, pp. 34-40.

Jones, R.G., Noguer, M., Hassel, D.C., et al. 2004, *Generating high resolution climate change scenarios using PRECIS,* Met Office Hadley Centre, Exeter, UK.

Jones, R.N. 2012, "Detecting and attributing nonlinear anthropogenic regional warming in southeastern Australia", *Journal of Geophysical Research,* vol. 117, pp. D04105-D04105, doi:10.1029/2011JD016328.

Jordan, A., Rayner, T., Schroeder, H., et al. 2013, "Going beyond two degrees? The risks and opportunities of alternative options", *Climate Policy,* vol. 13, no. 6, pp. 751-769, doi:10.1080/14693062.2013.835705.

Joshi, M.M., Gregory, J.M., Webb, M.J., et al. 2007, "Mechanisms for the land/sea warming contrast exhibited by simulations of climate change", *Climate Dynamics,* vol. 30, no. 5, pp. 455-465, doi:10.1007/s00382-007-0306-1.

Joshi, M., Hawkins, E., Sutton, R., et al. 2011, "Projections of when temperature change will exceed 2°C above pre-industrial levels", *Nature Climate Change,* vol. 1, no. 8, pp. 407-412, doi:10.1038/nclimate1261.

Joyce, R.J. & Janowiak, J.E. 2004, "CMORPH: A method that produces global precipitation estimates from passive microwave and infrared data at high spatial and temporal resolution", *Journal of Hydrometeorology,* vol. 5, pp. 487-503.

Jun, M., Knutti, R. & Nychka, D.W. 2008, "Spatial analysis to quantify numerical model bias and dependence: How many climate models are there?", *Journal of the American Statistical Association,* vol. 103, no. 483, pp. 934-947.

Jury, M.R., Matari, E. & Matitu, M. 2009, "Equatorial African climate teleconnections", *Theoretical and Applied Climatology,* vol. 95, no. 3-4, pp. 407-416.

Jury, M.R. & Mpeta, E.J. 2009, "African climate variability in the satellite era", *Theoretical and Applied Climatology,* vol. 98, no. 3-4, pp. 279-291.

Jury, M.R. 2013, "A return to wet conditions over Africa: 1995-2010", *Theoretical and Applied Climatology,* vol. 111, no. 3-4, pp. 471-481, doi:10.1007/s00704-012-0677-z.

Kalnay, E., Kanamitsu, M., Kistler, R., et al. 1996, "The NCEP/NCAR 40-year reanalysis project", *Bulletin of the American Meteorological Society,* vol. 77, no. 3, pp. 437-471.

Kalognomou, E., Lennard, C., Shongwe, M., et al. 2013, "A Diagnostic Evaluation of Precipitation in CORDEX Models over Southern Africa", *Journal of Climate,* vol. 26, no. 23, pp. 9477-9506, doi:10.1175/JCLI-D-12-00703.1.

Kanamitsu, M., Ebisuzaki, W., Woollen, J., et al. 2002, "NCEP-DOE AMIP-II reanalysis (R-2)", *Bulletin of the American Meteorological Society,* vol. 83, no. 11, pp. 1631-1643+1559.

Kaplan, J.O. & New, M. 2006, "Arctic climate change with a 2°C global warming: Timing, climate patterns and vegetation change", *Climatic Change,* vol. 79, no. 3-4, pp. 213-241, doi:10.1007/s10584-006-9113-7.

Kattenberg, A., Giorgi, R., Grassl, H., et al. 1995, "Climate Models – Projections of Future Climate" in *Climate Change 1995: The Science of Climate Change. Contribution of Working Group I to the Second Assessment Report of the Intergovernmental Panel on Climate Change*, eds. J.T. Houghton, L.G. Meira Filho, B.A. Callander, et al, Cambridge University Press, Cambridge, UK, New York, USA, and Melbourne, Australia.

Kay, G. & Washington, R. 2008, "Future southern African summer rainfall variability related to a southwest Indian Ocean dipole in HadCM3", *Geophysical Research Letters,* vol. 35, no. 12, pp. 1-5.

Kaye, N.R., Hartley, a. & Hemming, D. 2012, "Mapping the climate: guidance on appropriate techniques to map climate variables and their uncertainty", *Geoscientific Model Development,* vol. 5, no. 1, pp. 245-256, doi:10.5194/gmd-5-245-2012.

Kiehl, J.T. 2007, "Twentieth century climate model response and climate sensitivity", *Geophysical Research Letters,* vol. 34, no. 22, pp. 1-4, doi:10.1029/2007GL031383.

Kniveton, D.R., Layberry, R., Williams, C.J.R., et al. 2009, "Trends in the start of the wet season over Africa", vol. 1225, pp. 1216-1225, doi:10.1002/joc.

Knutti, R. 2010, "The end of model democracy?", *Climatic Change,* vol. 102, no. 3-4, pp. 395-404, doi:10.1007/s10584-010-9800-2.

Knutti, R. 2008, "Should we believe model predictions of future climate change?", *Philosophical transactions.Series A, Mathematical, physical, and engineering sciences,* vol. 366, no. 1885, pp. 4647-4664, doi:10.1098/rsta.2008.0169.

Knutti, R., Furrer, R., Tebaldi, C., et al. 2010, "Challenges in Combining Projections from Multiple Climate Models", *Journal of Climate,* vol. 23, no. 10, pp. 2739-2758, doi:10.1175/2009JCLI3361.1.

Knutti, R. & Sedlacek, J. 2012, "Robustness and uncertainties in the new CMIP5 climate model projections", *Nature Climate Change,* doi:10.1038/nclimate1716.

Koren, I., Kaufman, Y.J., Washington, R., et al. 2006, "The Bodélé depression: a single spot in the Sahara that provides most of the mineral dust to the Amazon forest", *Environmental Research Letters,* vol. 1, no. 1, pp. 014005.

Koster, R.D., Dirmeyer, P.a., Guo, Z., et al. 2004, "Regions of strong coupling between soil moisture and precipitation", *Science (New York, N.Y.),* vol. 305, no. 5687, pp. 1138-40, doi:10.1126/science.1100217.

Koteswaram, P. 1958, "The Easterly Jet Stream in the tropics*", *Tellus,* , no. 1952.

Kriegler, E. & Hall, J.W. 2009, "Imprecise probability assessment of tipping points in the climate system", *PNAS*, doi:10.1073/pnas.0809117106.

Kuhnel, I. 1989, "Tropical-extratropical cloudband climatology based on satellite data", *International Journal of Climatology,* vol. 9, no. 5, pp. 441-463, doi:10.1002/joc.3370090502.

Lafon, T., Dadson, S., Buys, G., et al. 2013, "Bias correction of daily precipitation simulated by a regional climate model: a comparison of methods", *International Journal of Climatology,* vol. 33, no. 6, pp. 1367-1381, doi:10.1002/joc.3518.

Lambert, F.H., Webb, M.J. & Joshi, M.M. 2011, "The Relationship between Land-Ocean Surface Temperature Contrast and Radiative Forcing", *Journal of Climate,* vol. 24, no. 13, pp. 3239-3256, doi:10.1175/2011JCLI3893.1.

Laprise, R., Hernández-Díaz, L., Tete, K., et al. 2013, "Climate projections over CORDEX Africa domain using the fifth-generation Canadian Regional Climate Model (CRCM5)", *Climate Dynamics,* vol. 41, no. 11-12, pp. 3219-3246, doi:10.1007/s00382-012-1651-2.

Lau, K.M., Shen, S.S.P., Kim, K., et al. 2006, "A multimodel study of the twentieth-century simulations of Sahel drought from the 1970s to 1990s", *Journal of Geophysical Research,* vol. 111, no. D7, pp. 1-9, doi:10.1029/2005JD006281.

LBA 1996, "Concise Experiment Plan", INPE, Sao Jose´ dos Campos, Brazil, Available at: http://lba.cptec.inpe.br.

Le Quéré, C.L. & Andres, R.J. 2013, "The global carbon budget 1959-2011", *Earth System â€¦,* vol. 5, pp. 165-185, doi:10.3334/CDIAC/GCP.

Lebel, T. & Ali, A. 2009, "Recent trends in the Central and Western Sahel rainfall regime (1990-2007)", *Journal of Hydrology,* vol. 375, no. 1-2, pp. 52-64, doi:10.1016/j.jhydrol.2008.11.030.

Lebel, T., Diedhiou, A. & Laurent, H. 2003, "Seasonal cycle and interannual variability of the Sahelian rainfall at hydrological scales", *Journal of Geophysical Research,* vol. 108, pp. 8389-8389, doi:10.1029/2001JD001580.

Lee, H., Beighley, R.E., Alsdorf, D., et al. 2011, "Characterization of terrestrial water dynamics in the Congo Basin using GRACE and satellite radar altimetry", *Remote Sensing of Environment,* vol. 115, no. 12, pp. 3530-3538.

Leiserowitz, A.A. 2005, "American risk perceptions: Is climate change dangerous?", *Risk Analysis,* vol. 25, no. 6, pp. 1433-1442.

Lenton, T.M. 2011a, "Beyond 2°C: redefining dangerous climate change for physical systems", *Wiley Interdisciplinary Reviews: Climate Change,* vol. 2, no. 3, pp. 451-461, doi:10.1002/wcc.107.

Lenton, T.M. 2011b, "Early warning of climate tipping points", *Nature Climate Change,* vol. 1, no. 4, pp. 201-209, doi:10.1038/nclimate1143.

Lenton, T.M., Held, H., Kriegler, E., et al. 2008, "Tipping elements in the Earth's climate system", *Proceedings of the National Academy of Sciences of the United States of America,* vol. 105, no. 6, pp. 1786-93.

Leroux, S. & Hall, N.M. 2009, "On the relationship between African easterly waves and the African easterly jet", *Journal of the Atmospheric Sciences,* vol. 66, no. 8, pp. 2303-2316.

Lewis, S.L., Lopez-Gonzalez, G., Sonke, B., et al. 2009, "Increasing carbon storage in intact African tropical forests", *Nature,* vol. 457, no. 7232, pp. 1003-6, doi:10.1038/nature07771.

Lindesay, J. 1988, "South African rainfall, the Southern Oscillation and a Southern Hemisphere semi-annual cycle", *International Journal of Climatology,* vol. 8, no. 1, pp. 17-30.

Liverman, D.M. 2009, "Conventions of climate change: constructions of danger and the dispossession of the atmosphere", *Journal of Historical Geography,* vol. 35, no. 2, pp. 279-296.

Lorenzoni, I., Pidgeon, N.F. & O'Connor, R.,E. 2005, "Dangerous climate change: the role for risk research", *Risk analysis : an official publication of the Society for Risk Analysis,* vol. 25, no. 6, pp. 1387-98.

Lott, F.C., Christidis, N. & Stott, P.a. 2013, "Can the 2011 East African drought be attributed to human-induced climate change?", *Geophysical Research Letters,* vol. 40, no. 6, pp. 1177-1181, doi:10.1002/grl.50235.

Lough, J.M. 1986, "Tropical Atlantic sea surface temperatures and rainfall variations in Subsaharan Africa", *Monthly Weather Review,* vol. 114, no. 3, pp. 561-570.

Luo, J. 2011, "Ocean dynamics not required?", *Nature,* vol. 477, pp. 544.

Lyon, B. & DeWitt, D.G. 2012, "A recent and abrupt decline in the East African long rains", *Geophysical Research Letters,* vol. 39, doi:10.1029/2011GL050337.

Macintosh, A. 2010, "Keeping warming within the 2°C limit after Copenhagen", *Energy Policy,* vol. 38, no. 6, pp. 2964-2975.

Mahlstein, I., Knutti, R., Solomon, S., et al. 2011, "Early onset of significant local warming in low latitude countries", *Environmental Research Letters,* vol. 6, no. 3, pp. 034009-034009, doi:10.1088/1748-9326/6/3/034009.

Mahlstein, I., Daniel, J.S. & Solomon, S. 2013, "Pace of shifts in climate regions increases with global temperature", *Nature Climate Change,* vol. 3, no. 5, pp. 1-5, doi:10.1038/nclimate1876.

Malhi, Y., Adu-Bredu, S., Asare, R.A., et al. 2013, "The past, present and future of Africa's rainforests", *Philosophical Transactions of the Royal Society B: Biological Sciences,* vol. 368, no. 1625, doi:10.1098/rstb.2012.0293.

Malhi, Y., Aragao, L.E.O.C., Galbraith, D., et al. 2009, "Exploring the likelihood and mechanism of a climate-change-induced dieback of the Amazon rainforest.", *Proceedings of the National Academy of Sciences of the United States of America,* vol. 106, no. 49, pp. 20610-20615, doi:10.1073/pnas.0804619106.

Malhi, Y. & Wright, J. 2004, "Spatial patterns and recent trends in the climate of tropical rainforest regions.", *Philosophical transactions of the Royal Society of London.Series B, Biological sciences,* vol. 359, no. 1443, pp. 311-329, doi:10.1098/rstb.2003.1433.

Mariotti, L., Coppola, E., Sylla, M.B., et al. 2011, "Regional climate model simulation of projected 21st century climate change over an all-Africa domain: Comparison analysis of nested and driving model results", *Journal of Geophysical Research,* vol. 116, doi:10.1029/2010JD015068.

Markovic, M., de Elia, R., Frigon, A., et al. 2013, "A transition from CMIP3 to CMIP5 for climate information providers: the case of surface temperature over eastern North America", *Climatic Change,* pp. 197-210, doi:10.1007/s10584-013-0782-8.

Marsham, J.H., Dixon, N.S., Garcia-Carreras, L., et al. 2013, "The role of moist convection in the West African monsoon system: Insights from continental-scale convection-permitting simulations", *Geophysical Research Letters,* vol. 40, pp. 1-7, doi:10.1002/grl.50347.

Mason, S. & Jury, M. 1997, "Climatic variability and change over southern Africa: a reflection on underlying processes", *Progress in Physical Geography,* vol. 21, no. 1, pp. 23-50.

Mason, S.J. & Goddard, L. 2001, "Probabilistic precipitation anomalies associated with ENSO", *Bulletin of the American Meteorological Society,* vol. 82, pp. 619-638, doi:http://dx.doi.org/10.1175/1520-0477(2001)082<0619:PPAAWE>2.3.CO;2.

Masson, D. & Knutti, R. 2011, "Climate model genealogy", *Geophysical Research Letters,* vol. 38, no. 8, pp. 1-4, doi:10.1029/2011GL046864.

Mastrandrea, M.D., Field, C.B., Stocker, T.F., et al 2010, *Guidance Note for Lead Authors of the IPCC Fifth Assessment Report on Consistent Treatment of Uncertainties. Intergovernmental Panel on Climate Change (IPCC).*

Matthews, H.D. & Weaver, A.J. 2010, "Committed climate warming", *Nature Geoscience,* vol. 3, no. 3, pp. 142-143.

May, W. 2011, "Assessing the strength of regional changes in near-surface climate associated with a global warming of 2°C", *Climatic Change,* , doi:10.1007/s10584-011-0076-y.

May, W. 2008, "Climatic changes associated with a global "2°C-stabilization" scenario simulated by the ECHAM5/MPI-OM coupled climate model", *Climate Dynamics,* vol. 31, no. 2-3, pp. 283-313.

McCollum, J.R., Gruber, A. & Ba, M.B. 2000, "Discrepancy between gauges and satellite estimates of rainfall in equatorial Africa", *Journal of Applied Meteorology,* vol. 39, pp. 666-679.

McSweeney, C.F. & Jones, R.G. 2013, "No consensus on consensus: the challenge of finding a universal approach to measuring and mapping ensemble consistency in GCM projections", *Climatic Change,* vol. 119, no. 3-4, pp. 617-629, doi:10.1007/s10584-013-0781-9.

McSweeney, C.F., Jones, R.G. & Booth, B.B.B. 2012, "Selecting Ensemble Members to Provide Regional Climate Change Information", *Journal of Climate,* vol. 25, no. 20, pp. 7100-7121, doi:10.1175/JCLI-D-11-00526.1.

Meehl, G.A., Stocker, T.F., Collins, W.D., et al. 2007a, "Global Climate Projections" in *Climate Change 2007: The Physical Science Basis. Contribution of Working Group I to the Fourth Assessment Report of the Intergovernmental Panel on Climate Change*, ed. Solomon, S., D. Qin, M. Manning, Z. Chen, M. Marquis, K.B. Averyt, M. Tignor and H.L. Miller, Cambridge University Press, Cambridge, United Kingdom and New York, NY, USA.

Meehl, G.a., Covey, C., Delworth, T., et al. 2007b, "The WCRP CMIP3 Multimodel Dataset: A New Era in Climate Change Research", *Bulletin of the American Meteorological Society,* vol. 88, no. 9, pp. 1383-1383.

Meinshausen, M., Meinshausen, N., Hare, W., et al. 2009, "Greenhouse-gas emission targets for limiting global warming to 2 degrees C", *Nature,* vol. 458, no. 7242, pp. 1158-62.

Meinshausen, M., Smith, S.J., Calvin, K., et al. 2011, "The RCP greenhouse gas concentrations and their extensions from 1765 to 2300", *Climatic Change,* , pp. 213-241, doi:10.1007/s10584-011-0156-z.

Messager, C., Parker, D.J., Reitebuch, O., et al. 2010, "Structure and dynamics of the Saharan atmospheric boundary layer during the West African monsoon onset: Observations and analyses from the research flights of 14 and 17 July 2006", *Quarterly Journal of the Royal Meteorological Society,* vol. 136, pp. 107-124, doi:10.1002/qj.469.

Mistry, V.V. & Conway, D. 2003, "Remote forcing of East African rainfall and relationships with fluctuations in levels of Lake Victoria", *International Journal of Climatology,* vol. 23, no. 1, pp. 67-89, doi:10.1002/joc.861.

Mitchell, T.D., Carter, T.R., Jones, P.D., et al. 2004, "A comprehensive set of high-resolution grids of monthly climate for Europe and the globe: the observed record (1901–2000) and 16 scenarios (2001–2100)", *Tyndall Centre for Climate Change Research Working Paper,* vol. 55, pp. 25.

Mitchell, T.D. 2003, "Pattern scaling: an examination of the accuracy of the technique for describing future climates", *Climatic Change,* vol: 60, no. 3, pp. 217-242.

Mitchell, T.P. & Wallace, J.M. 1992, "The annual cycle in equatorial convection and sea surface temperature", *Journal of Climate,* vol. 5, no. 10, pp. 1140-1156.

Mohino, E., Janicot, S. & Bader, J. 2011, "Sahel rainfall and decadal to multi-decadal sea surface temperature variability", *Climate Dynamics,* vol. 37, no. 3-4, pp. 419-440, doi:10.1007/s00382-010-0867-2.

Monerie, P., Fontaine, B. & Roucou, P. 2012a, "Expected future changes in the African monsoon between 2030 and 2070 using some CMIP3 and CMIP5 models under a medium-low RCP scenario", *Journal of Geophysical Research,* vol. 117, pp. 1-12, doi:10.1029/2012JD017510.

Monerie, P., Roucou, P. & Fontaine, B. 2012b, "Mid-century effects of Climate Change on African monsoon dynamics using the A1B emission scenario", *International Journal of Climatology,* , doi:10.1002/joc.3476.

Mortimore, M.J. & Adams, W.M. 2001, "Farmer adaptation, change and 'crisis' in the Sahel", *Global Environmental Change,* vol. 11, no. 1, pp. 49-57.

Morton, J.F. 2007, "The impact of climate change on smallholder and subsistence agriculture", *Proceedings of the National Academy of Sciences of the United States of America,* vol. 104, no. 50, pp. 19680-5.

Mupangwa, W., Walker, S. & Twomlow, S. 2011, "Start, end and dry spells of the growing season in semi-arid southern Zimbabwe", *Journal of Arid Environments,* vol. 75, no. 11, pp. 1097-1104, doi:10.1016/j.jaridenv.2011.05.011.

Murphy, J.M., Booth, B.B.B., Collins, M., et al. 2007, "A methodology for probabilistic predictions of regional climate change from perturbed physics

ensembles.", *Philosophical transactions.Series A, Mathematical, physical, and engineering sciences,* vol. 365, no. 1857, pp. 1993-2028, doi:10.1098/rsta.2007.2077.

Murphy, J.M., Sexton, D.M.H., Barnett, D.N., et al. 2004, "Quantification of modelling uncertainties in a large ensemble of climate change simulations", *Nature,* vol. 430, pp. 769-772.

Nakicenovic, N., Alcamo, J., Davis, G., et al 2000, *Special report on emissions scenarios: a special report of Working Group III of the Intergovernmental Panel on Climate Change.* , Pacific Northwest National Laboratory, Richland, WA (US), Environmental Molecular Sciences Laboratory (US).

Neelin, J.D. 2003, "Tropical drought regions in global warming and El Nino teleconnections", *Geophysical Research Letters,* vol. 30, no. 24, pp. 1-4, doi:10.1029/2003GL018625.

Neelin, J.D., Munnich, M., Su, H., et al. 2006, "Tropical drying trends in global warming models and observations.", *Proceedings of the National Academy of Sciences of the United States of America,* vol. 103, no. 16, pp. 6110-6115, doi:10.1073/pnas.0601798103.

Neupane, N. & Cook, K.H. 2013, "A Nonlinear Response of Sahel Rainfall to Atlantic Warming", *Journal of Climate,* vol. 26, no. 18, pp. 7080-7096, doi:10.1175/JCLI-D-12-00475.1.

New, M., Hewitson, B., Stephenson, D.B., et al. 2006, "Evidence of trends in daily climate extremes over southern and west Africa", *Journal of Geophysical Research D: Atmospheres,* vol. 111, no. 14, doi:10.1029/2005JD006289.

New, M. 2011, "Four degrees and beyond: the potential for a global temperature increase of four degrees and its implications", *Philosophical Transactions of the Royal Society A: Mathematical, Physical and Engineering Sciences,* vol. 369, no. 1934, pp. 4-5, doi:10.1098/rsta.2010.0304.

New, M., Liverman, D.M. & Anderson, K. 2009, "Mind the Gap: Policymakers must aim to avoid a 2°C temperature rise, but plan to adapt to 4°C", *Nature Reports Climate Change,* vol. 3, pp. 143-144.

Nicholson, S.E. 1986, "The spatial coherence of African rainfall anomalies: interhemispheric teleconnections", *Journal of climate and applied meteorology,* vol. 25, no. 10, pp. 1365-1381.

Nicholson, S.E., Kim, J. & Hoopingarner, J. 1988, *Atlas of African rainfall and its interannual variability,* Department of Meteorology, the Florida State University.

Nicholson, S. 2005, "On the question of the "recovery" of the rains in the West African Sahel", *Journal of Arid Environments,* vol. 63, no. 3, pp. 615-641, doi: http://dx.doi.org/10.1016/j.jaridenv.2005.03.004.

Nicholson, S. & Entekhabi, D. 1986, "The quasi-periodic behavior of rainfall variability in Africa and its relationship to the Southern Oscillation", *Meteorology and Atmospheric Physics,* vol. 34, no. 3, pp. 311-348.

Nicholson, S.E. 2009, "A revised picture of the structure of the monsoon and land ITCZ over West Africa", *Climate Dynamics,* vol. 32, no. 7-8, pp. 1155-1171, doi:10.1007/s00382-008-0514-3.

Nicholson, S.E. 2010, "A low-level jet along the Benguela coast, an integral part of the Benguela current ecosystem", *Climatic Change,* vol. 99, no. 3-4, pp. 613-624, doi:10.1007/s10584-009-9678-z.

Nicholson, S.E. & Dezfuli, A.K. 2013, "The Relationship of Rainfall Variability in Western Equatorial Africa to the Tropical Oceans and Atmospheric Circulation. Part I: The Boreal Spring", *Journal of Climate,* vol. 26, no. 1, pp. 45-65, doi:10.1175/JCLI-D-11-00653.1.

Nicholson, S.E. & Grist, J.P. 2003, "The Seasonal Evolution of the Atmospheric Circulation over West Africa and Equatorial Africa", *Journal of Climate,* vol. 16, no. 7, pp. 1013-1030, doi:10.1175/1520-0442(2003)016<1013:TSEOTA>2.0.CO;2.

Nicholson, S.E. & Palao, I.M. 1993, "A re-evaluation of rainfall variability in the sahel. Part I. Characteristics of rainfall fluctuations", *International Journal of Climatology,* vol. 13, no. 4, pp. 371-389, doi:10.1002/joc.3370130403.

Nikulin, G., Jones, C., Giorgi, F., et al. 2012, "Precipitation Climatology in an Ensemble of CORDEX-Africa Regional Climate Simulations", *Journal of Climate,* vol. 25, no. 18, pp. 6057-6078, doi:10.1175/JCLI-D-11-00375.1.

North, G.R., Bell, T.L., Cahalan, R.F., et al. 1982, "Sampling errors in the estimation of empirical orthogonal functions", *Mon.Wea.Rev,* vol. 110, no. 7, pp. 699-706.

O'Neill, B.C. & Oppenheimer, M. 2002, "Dangerous Climate Impacts and the Kyoto Protocol", *Science,* vol. 296, pp. 1971-1972.

Oppenheimer, M. 2005, "Defining dangerous anthropogenic interference: the role of science, the limits of science", *Risk analysis : an official publication of the Society for Risk Analysis,* vol. 25, no. 6, pp. 1399-407, doi:10.1111/j.1539-6924.2005.00687.x.

Oslisly, R., White, L., Bentaleb, I., et al. 2013, "Climatic and cultural changes in the west Congo Basin forests over the past 5000 years", *Philosophical Transactions of the Royal Society B: Biological Sciences,* vol. 368, no. 1625, pp. 20120304.

Paeth, H., Hall, N.M., Gaertner, M.A., et al. 2011, "Progress in regional downscaling of west African precipitation", *Atmospheric Science Letters,* vol. 12, no. 1, pp. 75-82, doi:10.1002/asl.306.

Paeth, H. & Hense, A. 2004, "SST versus Climate Change Signals in West African Rainfall: 20th-Century Variations and Future Projections", *Climatic Change,* vol. 65, no. 1/2, pp. 179-208, doi:10.1023/B:CLIM.0000037508.88115.8a.

Parry, M.L., Canziani, O.F., Palutikof, J.P., et al. (eds) 2007, *Contribution of Working Group II to the Fourth Assessment Report of the Intergovernmental Panel on Climate Change*, Cambridge University Press, Cambridge, United Kingdom and New York, NY, USA.

Parry, M.L., Carter, T.R. & Hulme, M. 1996, "What is a dangerous climate change?", *Global Environmental Change,* vol. 6, no. 1, pp. 1-6.

Paton, F.L., Maier, H.R. & Dandy, G.C. 2013, "Relative magnitudes of sources of uncertainty in assessing climate change impacts on water supply security for the southern Adelaide water supply system", *Water Resources Research,* vol. 49, no. 3, pp. 1643-1667, doi:10.1002/wrcr.20153.

Patricola, C.M. & Cook, K.H. 2011, "Sub-Saharan Northern African climate at the end of the twenty-first century: forcing factors and climate change processes", *Climate Dynamics,* vol. 37, pp. 1165-1188, doi:10.1007/s00382-010-0907-y.

Patricola, C.M. & Cook, K.H. 2010, "Northern African climate at the end of the twenty-first century: an integrated application of regional and global climate models", *Climate Dynamics,* vol. 35, no. 1, pp. 193-212, doi:10.1007/s00382-009-0623-7.

Peters, G.P., Marland, G., Le Quéré, C., et al. 2011, "Rapid growth in CO2 emissions after the 2008-2009 global financial crisis", *Nature Climate Change,* vol. 2, no. 1, pp. 2-4, doi:10.1038/nclimate1332.

Piani, C., Frame, D.J., Stainforth, D., et al. 2005, "Constraints on climate change from a multi-thousand member ensemble of simulations", *Geophysical Research Letters,* vol. 32, no. 23, pp. 1-5.

Pokam, W.M., Djiotang, L.a.T. & Mkankam, F.K. 2011, "Atmospheric water vapor transport and recycling in Equatorial Central Africa through NCEP/NCAR reanalysis data", *Climate Dynamics,* vol. 38, no. 9-10, pp. 1715-1729, doi:10.1007/s00382-011-1242-7.

Pope, V., Brown, S., Clark, R., et al. 2007, "The Met Office Hadley Centre climate modelling capability: the competing requirements for improved resolution, complexity and dealing with uncertainty", *Philosophical transactions.Series A, Mathematical, physical, and engineering sciences,* vol. 365, no. 1860, pp. 2635-57, doi:10.1098/rsta.2007.2087.

Pope, V.D., Gallani, M.L., Rowntree, P.R., et al. 2000, "The impact of new physical parametrizations in the Hadley Centre climate model: HadAM3", *Climate Dynamics,* vol. 16, no. 2-3, pp. 123-146, doi:10.1007/s003820050009.

Poulter, B., AragÃ£o, L., Heyder, U., et al. 2010, "Net biome production of the Amazon Basin in the 21st century", *Global Change Biology,* vol. 16, no. 7, pp. 2062-2075, doi:10.1111/j.1365-2486.2009.02064.x.

Power, S.B., Delage, F., Colman, R., et al. 2012, "Consensus on Twenty-First-Century Rainfall Projections in Climate Models More Widespread than Previously Thought", *Journal of Climate,* vol. 25, no. 11, pp. 3792-3809, doi:10.1175/JCLI-D-11-00354.1.

Prospero, J.M. & Lamb, P.J. 2003, "African droughts and dust transport to the Caribbean: Climate change implications", *Science,* vol. 302, no. 5647, pp. 1024-1027.

Räisänen, J. 2007, "How reliable are climate models?", *Tellus A,* vol. 59, no. 1, pp. 2-29.

Ramanathan, V. & Feng, Y. 2008, "On avoiding dangerous anthropogenic interference with the climate system: formidable challenges ahead", *Proceedings of the National Academy of Sciences of the United States of America,* vol. 105, no. 38, pp. 14245-50.

Randall, D.A., Wood, R.A., Bony, S., et al. 2007, "Climate Models and their Evaluation" in *Climate Change 2007: The Physical Science Basis. Contribution of Working Group I to the Fourth Assessment Report of the Intergovernmental Panel on Climate Change*, eds. S. Solomon, D. Qin, M. Manning, et al, Cambridge University Press, Cambridge and New York, pp. 589-662.

Randalls, S. 2010, "History of the 2°C climate target", *Wiley Interdisciplinary Reviews: Climate Change,* vol. 1, no. 4, pp. 598-605, doi:10.1002/wcc.62.

Rayner, N. 2003, "Global analyses of sea surface temperature, sea ice, and night marine air temperature since the late nineteenth century", *Journal of Geophysical Research,* vol. 108, pp. 4407-4407, doi:10.1029/2002JD002670.

Reason, C.J.C. 2002, "Sensitivity of the southern African circulation to dipole sea-surface temperature patterns in the south Indian Ocean", *International Journal of Climatology,* vol. 22, no. 4, pp. 377-393.

Reason, C.J.C., Allan, R.J., Lindesay, J.a., et al. 2000, "ENSO and climatic signals across the Indian Ocean Basin in the global context: part I, interannual composite patterns", *International Journal of Climatology,* vol. 20, no. 11, pp. 1285-1327, doi:10.1002/1097-0088(200009)20:11<1285::AID-JOC536>3.0.CO;2-R.

Redelsperger, J.-., Thorncroft, C.D., Diedhiou, A., et al. 2006, "African Monsoon Multidisciplinary Analysis: An international research project and field campaign", *Bulletin of the American Meteorological Society,* vol. 87, no. 12, pp. 1739-1746.

Reichler, T. & Kim, J. 2008, "How Well Do Coupled Models Simulate Today's Climate?", *Bulletin of the American Meteorological Society,* vol. 89, no. 3, pp. 303-311, doi:10.1175/BAMS-89-3-303.

Richman, M.B. 1986, "Rotation of Principal Components", *Journal of Climatology,* vol. 6, pp. 293-335, doi:10.1007/BF00118735.

Rodhe, H. & Virji, H. 1976, "Trends and periodicities in East African rainfall data", *Monthly Weather Review,* vol. 104, no. 3, pp. 307-315.

Rodwell, M. & Palmer, T. 2007, "Using numerical weather prediction to assess climate models", *Quarterly Journal of the Royal Meteorological Society,* vol. 133, no. 622, pp. 129-146, doi:10.1002/qj.

Roehrig, R., Bouniol, D., Guichard, F., et al. 2013, "The Present and Future of the West African Monsoon: A Process-Oriented Assessment of CMIP5 Simulations along the AMMA Transect", *Journal of Climate,* vol. 26, no. 17, pp. 6471-6505, doi:10.1175/JCLI-D-12-00505.1.

Rogelj, J., Hare, W., Lowe, J., et al. 2011, "Emission pathways consistent with a 2°C global temperature limit", *Nature Climate Change,* vol. 1, no. 8, pp. 413-418.

Rogelj, J., McCollum, D., O'Neill, B., et al. 2012a, "2020 emissions levels required to limit warming to below 2°C", *Nature Climate Change,* vol. 3, pp. 405-412, doi:10.1038/nclimate1758.

Rogelj, J., Meinshausen, M. & Knutti, R. 2012b, "Global warming under old and new scenarios using IPCC climate sensitivity range estimates", *Nature Climate Change,* vol. 2, no. 4, pp. 248-253, doi:10.1038/nclimate1385.

Ropelewski, C.F. & Halpert, M.S. 1987, "Global and regional scale precipitation patterns associated with the El Niño/Southern Oscillation", *Monthly Weather Review,* vol. 115, no. 8, pp. 1606-1626.

Rotstayn, L.D. & Lohmann, U. 2002, "Tropical rainfall trends and the indirect aerosol effect", *Journal of Climate,* vol. 15, no. 15, pp. 2103-2116.

Rougier, J., Sexton, D.M.H., Murphy, J.M., et al. 2009, "Analyzing the Climate Sensitivity of the HadSM3 Climate Model Using Ensembles from Different but Related Experiments", *Journal of Climate,* vol. 22, no. 13, pp. 3540-3557, doi:10.1175/2008JCLI2533.1.

Rowell, D., Booth, B. & Nicholson, S. 2013, "The East African Climate Paradox: Characteristics and Hypotheses", *Africa Climate Conference, Arusha, Tanzania, 15-18th October 2013*.

Rowell, D.P. 2012, "Sources of Uncertainty in Future Changes in Local Precipitation", *Climate Dynamics,* vol. 39, no. 7-8, pp. 1929-1950, doi:10.1007/s00382-011-1210-2.

Rowell, D.P. 2013, "Simulating SST Teleconnections to Africa: What is the State of the Art?", *Journal of Climate,* vol. 26, no. 15, pp. 5397-5418, doi:10.1175/JCLI-D-12-00761.1.

Rowlands, D.J., Frame, D.J., Ackerley, D., et al. 2012, "Broad range of 2050 warming from an observationally constrained large climate model ensemble", *Nature Geoscience,* vol. 5, no. 4, pp. 256-260, doi:10.1038/ngeo1430.

Saeed, F., Haensler, A., Weber, T., et al. 2013, "Representation of Extreme Precipitation Events Leading to Opposite Climate Change Signals over the Congo Basin", *Atmosphere,* vol. 4, no. 3, pp. 254-271, doi:10.3390/atmos4030254.

Saha, S., Moorthi, S. & Pan, H.L. 2010, "The NCEP climate forecast system reanalysis", *Bulletin of the American Meteorological Society,* doi:10.1175/2010Bams3001.1.

Sanderson, B.M., Knutti, R., Aina, T., et al. 2008a, "Constraints on Model Response to Greenhouse Gas Forcing and the Role of Subgrid-Scale Processes", *Journal of Climate,* vol. 21, no. 11, pp. 2384-2400.

Sanderson, B.M., Piani, C., Ingram, W.J., et al. 2008b, "Towards constraining climate sensitivity by linear analysis of feedback patterns in thousands of perturbed-physics GCM simulations", *Climate Dynamics,* vol. 30, no. 2-3, pp. 175-190.

Sanderson, B.M., O'Neill, B.,C., Kiehl, J.T., et al. 2011, "The response of the climate system to very high greenhouse gas emission scenarios", *Environmental Research Letters,* vol. 6, no. 3, pp. 034005-034005, doi:10.1088/1748-9326/6/3/034005.

Sanderson, M. 2008, *Regional Assessment of QUMP 17 member ensemble*, Met Office Documents, Exeter, UK.

Santer, B.D., Taylor, K.E., Gleckler, P.J., et al. 2009, "Incorporating model quality information in climate change detection and attribution studies", *Proceedings of the National Academy of Sciences of the United States of America,* vol. 106, no. 35, pp. 14778-83, doi:10.1073/pnas.0901736106.

Scheffer, M., Bascompte, J., Brock, W.a., et al. 2009, "Early-warning signals for critical transitions", *Nature,* vol. 461, no. 7260, pp. 53-9, doi:10.1038/nature08227.

Schellnhuber, H.J., Hare, B., Serdeczny, O., et al *Turn down the heat : climate extremes, regional impacts, and the case for resilience - full report*, World Bank, Washington DC.

Schmidt, G. & Archer, D. 2009, "Too much of a bad thing", *Nature,* vol. 458, pp. 1117-1118.

Schneider, S.H. & Mastrandrea, M.D. 2005, "Probabilistic assessment of "dangerous" climate change and emissions pathways", *Proceedings of the National Academy of Sciences of the United States of America,* vol. 102, no. 44, pp. 15728-35.

Servat, É., Paturel, J.E., Lubès-Niel, H., et al. 1999, "Regarding rainfall in non sahelian western and central Africa", *Revue des Sciences de l'Eau,* vol. 12, no. 2, pp. 363-387.

Seth, A., Rauscher, S.a., Rojas, M., et al. 2011, "Enhanced spring convective barrier for monsoons in a warmer world?", *Climatic Change,* vol. 104, no. 2, pp. 403-414, doi:10.1007/s10584-010-9973-8.

Sexton, D.M.H., Murphy, J.M., Collins, M., et al. 2012, "Multivariate probabilistic projections using imperfect climate models part I: outline of methodology", *Climate Dynamics,* vol. 38, no. 2, pp. 2513-2542, doi:10.1007/s00382-011-1208-9.

Shongwe, M.E., van Oldenborgh, G.J., van, d.H., et al. 2009, "Projected Changes in Mean and Extreme Precipitation in Africa under Global Warming. Part I: Southern Africa", *Journal of Climate,* vol. 22, no. 13, pp. 3819-3837.

Shongwe, M.E., van Oldenborgh, G.J., van, d.H., et al. 2011, "Projected changes in mean and extreme precipitation in Africa under global warming, Part II: East Africa", *Journal of Climate,* vol. 24, pp. 3718-3733, doi:10.1175/2010JCLI2883.1.

Simpson, M.C., Scott, D., New, M., et al 2009, *An overview of modelling climate change impacts in the Caribbean Region with contribution from the Pacific Islands*, United Nations Development Programme (UNDP), Barbados, West Indies.

Skeie, R., Berntsen, T., Myhre, G., et al. 2011, "Anthropogenic radiative forcing time series from pre-industrial times until 2010", *Atmospheric Chemistry and Physics,* vol. 11, no. 22, pp. 11827-11857.

Smith, L. 2012, "Distinguishing Uncertainty, Diversity and Insight", *Uncertainty in Climate Change Research: An Integrated Approach, August 6-17, NCAR, Boulder, Colorado*.

Smith, L.a. 2002, "What might we learn from climate forecasts?", *Proceedings of the National Academy of Sciences of the United States of America,* vol. 99 Suppl 1, pp. 2487-92.

Stainforth, D.A., Downing, T.E., Washington, R., et al. 2007, "Issues in the interpretation of climate model ensembles to inform decisions", *Philosophical Transactions of the Royal Society A: Mathematical, Physical and Engineering Sciences,* vol. 365, no. 1857, pp. 2163-77.

Stainforth, D.a., Aina, T., Christensen, C., et al. 2005, "Uncertainty in predictions of the climate response to rising levels of greenhouse gases", *Nature,* vol. 433, no. 7024, pp. 403-6.

Stone, D., Weaver, A.J. & Stouffer, R.J. 2001, "Projection of climate change onto modes of atmospheric variability", *Journal of Climate,* vol. 14, no. 17, pp. 3551-3565.

Stott, P.a., Tett, S.F., Jones, G.S., et al. 2000, "External control of 20th century temperature by natural and anthropogenic forcings", *Science (New York, N.Y.),* vol. 290, no. 5499, pp. 2133-7.

Suzuki, T. 2010, "Seasonal variation of the ITCZ and its characteristics over central Africa", *Theoretical and Applied Climatology,* vol. 103, no. 1-2, pp. 39-60, doi:10.1007/s00704-010-0276-9.

Sylla, M.B., Gaye, a.T. & Jenkins, G.S. 2012, "On the Fine-Scale Topography Regulating Changes in Atmospheric Hydrological Cycle and Extreme Rainfall over West Africa in a Regional Climate Model Projections", *International Journal of Geophysics,* vol. 2012, pp. 1-15, doi:10.1155/2012/981649.

Sylla, M.B., Gaye, a.T., Jenkins, G.S., et al. 2010, "Consistency of projected drought over the Sahel with changes in the monsoon circulation and extremes in a regional climate model projections", *Journal of Geophysical Research,* vol. 115, pp. 1-9.

Tadross, M.a., Gutowski, W.J., Hewitson, B.C., et al. 2006, "MM5 simulations of interannual change and the diurnal cycle of southern African regional climate", *Theoretical and Applied Climatology,* vol. 86, no. 1-4, pp. 63-80, doi:10.1007/s00704-005-0208-2.

Tadross, M.A., Hewitson, B.C. & Usman, M.T. 2005a, "The interannual variability of the onset of the maize growing season over South Africa and Zimbabwe", *Journal of Climate,* , pp. 3356-3372.

Tadross, M., Jack, C. & Hewitson, B. 2005b, "On RCM-based projections of change in southern African summer climate", *Geophysical Research Letters,* vol. 32, no. 23, pp. L23713-L23713, doi:10.1029/2005GL024460.

Tanaka, T.Y. & Chiba, M. 2006, "A numerical study of the contributions of dust source regions to the global dust budget", *Global and Planetary Change,* vol. 52, no. 1, pp. 88-104.

Tang, Q. & Lettenmaier, D.P. 2012, "21St Century Runoff Sensitivities of Major Global River Basins", *Geophysical Research Letters,* vol. 39, no. 6, pp. L06403-L06403, doi:10.1029/2011GL050834.

Tarhule, A. & Lamb, P.J. 2003, "Climate Research and Seasonal Forecasting for West Africans: Perceptions, Dissemination, and Use?", *Bulletin of the American Meteorological Society,* vol. 84, no. 12, pp. 1741-1759, doi:10.1175/BAMS-84-12-1741.

Tarnavsky, E., Grimes, D., Maidment, R., et al. 2013, "Development of the 30-year TAMSAT African Rainfall Time Series And Climatology (TARCAT) Dataset Part I: improved calibration and operational validation", *in prep.*

Tate, E., Sutcliffe, J., Conway, D., et al. 2004, "Water balance of Lake Victoria: update to 2000 and climate change modelling to 2100/Bilan hydrologique du Lac Victoria: mise à jour jusqu'en 2000 et modélisation des impacts du changement climatique jusqu'en 2100", *Hydrological Sciences Journal,* vol. 49, no. 4.

Taylor, C.M. 2010, "Feedbacks on convection from an African wetland", *Geophysical Research Letters,* vol. 37, no. 5, doi:10.1029/2009GL041652.

Taylor, K.E., Stouffer, R.J. & Meehl, G.a. 2012a, "An Overview of CMIP5 and the Experiment Design", *Bulletin of the American Meteorological Society,* vol. 93, no. 4, pp. 485-498, doi:10.1175/BAMS-D-11-00094.1.

Taylor, R.G., Todd, M.C., Kongola, L., et al. 2012b, "Evidence of the dependence of groundwater resources on extreme rainfall in East Africa", *Nature Climate Change,* vol. 2, no. 11, pp. 1-5, doi:10.1038/nclimate1731.

Tebaldi, C., Smith, R.L., Nychka, D., et al. 2005, "Quantifying uncertainty in projections of regional climate change: A Bayesian approach to the analysis of multimodel ensembles", *Journal of Climate,* vol. 18, no. 10, pp. 1524-1540.

Tebaldi, C., Arblaster, J.M. & Knutti, R. 2011, "Mapping model agreement on future climate projections", *Geophysical Research Letters,* vol. 38, no. 23, pp. 1-5, doi:10.1029/2011GL049863.

Tebaldi, C. & Knutti, R. 2007, "The use of the multi-model ensemble in probabilistic climate projections.", *Philosophical transactions.Series A, Mathematical, physical, and engineering sciences,* vol. 365, no. 1857, pp. 2053-2075, doi:10.1098/rsta.2007.2076.

Thorncroft, C.D., Nguyen, H., Zhang, C., et al. 2011, "Annual cycle of the West African monsoon: regional circulations and associated water vapour transport", *Quarterly Journal of the Royal Meteorological Society,* vol. 137, no. 654, pp. 129-147, doi:10.1002/qj.728.

Thornton, P.K., Jones, P.G., Ericksen, P.J., et al. 2011, "Agriculture and food systems in sub-Saharan Africa in a 4°C+", *Philosophical transactions.Series A, Mathematical, physical, and engineering sciences,* vol. 369, no. 1934, pp. 117-136, doi:10.1098/rsta.2010.0246.

Todd, M.C. & Washington, R. 2004, "Climate variability in central equatorial Africa: Influence from the Atlantic sector", *Geophysical Research Letters,* vol. 31, no. 23, pp. 2-5.

Tokinaga, H. & Xie, S. 2011, "Weakening of the equatorial Atlantic cold tongue over the past six decades", *Nature Geoscience,* vol. 4, no. 4, pp. 222-226, doi:10.1038/ngeo1078.

Tol, R.S.J. 2007, "Europe's long-term climate target: A critical evaluation", *Energy Policy,* vol. 35, no. 1, pp. 424-432, doi:10.1016/j.enpol.2005.12.003.

Trenberth, K.E., Dai, A., Rasmussen, R.M., et al. 2003, "The Changing Character of Precipitation", *Bulletin of the American Meteorological Society,* vol. 84, no. 9, pp. 1205-1205.

Tubiello, F.N. & Fischer, G. 2007, "Reducing climate change impacts on agriculture: Global and regional effects of mitigation, 2000-2080", *Technological Forecasting and Social Change,* vol. 74, no. 7, pp. 1030-1056, doi:10.1016/j.techfore.2006.05.027.

Tyson, P.D., Dyer, T.G. & Mametse, M. 1975, "Secular changes in South African rainfall: 1880 to 1972", *Quarterly Journal of the Royal Meteorological Society,* vol. 101, no. 430, pp. 817-833.

Tyson, P.D. & Preston-Whyte, R. 2000, *The weather and climate of Southern Africa,* Oxford University Press, Cape Town.

UN 1992, *The United Nations Framework Convention on Climate Change*, United Nations, Rio de Janeiro.

UNFCCC 2010, Decision 1/CP.15 Outcome of the work of the Ad Hoc Working Group on Long-term Cooperative Action under the Convention at its fifteenth session, held in Copenhagen.

UNFCCC 2011, Decision 1/CP.16 The Cancun Agreements: Outcome of the work of the Ad Hoc Working Group on Long-term Cooperative Action under the Convention.

UNFCCC 2012, Report of the Conference of the Parties on its seventeenth session, held in Durban from 28 November to 11 December 2011. Addendum. Part Two: Action taken by the Conference of the Parties at its seventeenth session.

UNFCCC 2013, Report of the Conference of the Parties on its eighteenth session, held in Doha from 26 November to 8 December 2012. Addendum. Part Two: Action taken by the Conference of the Parties at its eighteenth session.

Uppala, S.M., Kållberg, P., Simmons, A., et al. 2005, "The ERA-40 re-analysis", *Quarterly Journal of the Royal Meteorological Society,* vol. 131, no. 612, pp. 2961-3012.

van Vuuren, D.P., Stehfest, E., Elzen, M.G.J., et al. 2011, "RCP2.6: exploring the possibility to keep global mean temperature increase below 2°C", *Climatic Change,* vol. 109, pp. 95-116, doi:10.1007/s10584-011-0152-3.

Vecchi, G.a. & Soden, B.J. 2007, "Global Warming and the Weakening of the Tropical Circulation", *Journal of Climate,* vol. 20, no. 17, pp. 4316-4340.

Vecchi, G.a., Soden, B.J., Wittenberg, A.T., et al. 2006, "Weakening of tropical Pacific atmospheric circulation due to anthropogenic forcing.", *Nature,* vol. 441, no. 7089, pp. 73-76, doi:10.1038/nature04744.

Vizy, E.K. & Cook, K.H. 2002, "Development and application of a mesoscale climate model for the tropics : Influence of sea surface temperature anomalies on the West African monsoon", *Journal of Geophysical Research,* vol. 107. D3

Vizy, E.K., Cook, K.H., Crétat, J., et al. 2013, "Projections of a Wetter Sahel in the Twenty-First Century from Global and Regional Models", *Journal of Climate,* vol. 26, no. 13, pp. 4664-4687, doi:10.1175/JCLI-D-12-00533.1.

Vondou, D.a., Nzeukou, A., Lenouo, A., et al. 2010, "Seasonal variations in the diurnal patterns of convection in Cameroon-Nigeria and their neighboring areas", *Atmospheric Science Letters,* vol. 11, no. 4, pp. 290-300, doi:10.1002/asl.297.

Waliser, D. & Gautier, C. 1993, "A Satellite-derived Climatology of the ITCZ", *Journal of Climate;(United States),* vol. 6, pp. 2162-2174.

Walker, G.T. 1910, "Correlation in seasonal variations of weather", *Mem. Indian Meteor. Dep.,* vol. 21, no. 2, pp. 22-45.

Wang, B., Wu, R. & Li, T. 2003, "Atmosphere-warm ocean interaction and its impacts on Asian-Australian monsoon variation", *Journal of Climate,* vol. 16, no. 8, pp. 1195-1211.

Ward Jr, J.H. 1963, "Hierarchical grouping to optimize an objective function", *Journal of the American statistical association,* vol. 58, no. 301, pp. 236-244.

Ward, M.N. 1998, "Diagnosis and short-lead time prediction of summer rainfall in tropical North Africa at interannual and multidecadal timescales", *Journal of Climate,* vol. 11, no. 12, pp. 3167-3191.

Warren, R., Price, J., Fischlin, A., et al. 2010, "Increasing impacts of climate change upon ecosystems with increasing global mean temperature rise", *Climatic Change,* , pp. 1-37.

Washington, R., Bouet, C., Cautenet, G., et al. 2009, "Dust as a tipping element: the Bodele Depression, Chad", *Proceedings of the National Academy of Sciences,* vol. 106, no. 49, pp. 20564-20571.

Washington, R., Todd, M., Middleton, N.J., et al. 2003, "Dust-storm source areas determined by the total ozone monitoring spectrometer and surface observations", *Annals of the Association of American Geographers,* vol. 93, no. 2, pp. 297-313.

Washington, R., Harrison, M., Conway, D., et al. 2006, "African Climate Change: Taking the Shorter Route", *Bulletin of the American Meteorological Society,* vol. 87, no. 10, pp. 1355, doi:10.1175/BAMS-87-10-1355.

Washington, R. & Preston, A. 2006, "Extreme wet years over southern Africa: Role of Indian Ocean sea surface temperatures", *Journal of Geophysical Research,* vol. 111, pp. 1-15.

Washington, R. & Todd, M. 1999, "Tropical-temperate links in southern African and southwest Indian Ocean satellite-derived daily rainfall", *International Journal of Climatology,* vol. 19, no. 14, pp. 1601-1616.

Watson, R.T., Zinyowera, M.C. & Moss, R.H. (eds) 1995, *Climate Change, 1995: Impacts, Adaptations, and Mitigation of Climate Change: Scientific-technical Analyses: Contribution of Working Group II to the Second Assessment Report of the Intergovernmental Panel on Climate Change*, Cambridge.

Watterson, I.G. 2011, "Understanding and partitioning future climates for Australian regions from CMIP3 using ocean warming indices", *Climatic Change,* doi:10.1007/s10584-011-0166-x.

Weaver, C.P., Lempert, R.J., Brown, C., et al. 2013, "Improving the contribution of climate model information to decision making: the value and demands of robust decision frameworks", *Wiley Interdisciplinary Reviews: Climate Change,* vol. 4, no. 1, pp. 39-60, doi:10.1002/wcc.202.

Webb, M.J., Senior, C., Sexton, D.M.H., et al. 2006, "On the contribution of local feedback mechanisms to the range of climate sensitivity in two GCM ensembles", *Climate Dynamics,* vol. 27, no. 1, pp. 17-38.

Webster, P.J. 1983, "The large-scale structure of the tropical atmosphere" in *Large Scale Dynamical Processes in the Atmosphere*, eds. B. Hoskins & R. Pearce, Academic Press, .

Whetton, P., Hennessy, K., Clarke, J., et al. 2012, "Use of Representative Climate Futures in impact and adaptation assessment", *Climatic Change,* vol. 115, no. 3-4, pp. 433-442, doi:10.1007/s10584-012-0471-z.

Wilby, R.L. & Wigley, T. 1997, "Downscaling general circulation model output: a review of methods and limitations", *Progress in Physical Geography,* vol. 21, no. 4, pp. 530-548.

Wilby, R.L. & Dessai, S. 2010, "Robust adaptation to climate change", *Weather,* vol. 65, no. 7, pp. 176-180, doi:10.1002/wea.504.

Wilks, D.S. 2006, *Statistical Methods in the Atmospheric Sciences,* 2nd edn, Elsevier, Oxford.

Williams, a.P. & Funk, C. 2011, "A westward extension of the warm pool leads to a westward extension of the Walker circulation, drying eastern Africa", *Climate Dynamics,* doi:10.1007/s00382-010-0984-y.

Williams, a.P., Funk, C., Michaelsen, J., et al. 2011, "Recent summer precipitation trends in the Greater Horn of Africa and the emerging role of Indian Ocean sea surface temperature", *Climate Dynamics,* , doi:10.1007/s00382-011-1222-y.

Williams, C.a., Hanan, N.P., Neff, J.C., et al. 2007, "Africa and the global carbon cycle", *Carbon balance and management,* vol. 2, pp. 3-3, doi:10.1186/1750-0680-2-3.

World Bank 2012, *Turn Down the Heat: Why a 4 warmer world must be avoided*, World Bank, Washington DC.

Wu, P., Wood, R., Ridley, J., et al. 2010, "Temporary acceleration of the hydrological cycle in response to a CO2 rampdown", *Geophysical Research Letters,* vol. 37, no. 12, pp. 1-5, doi:10.1029/2010GL043730.

Xie, P. & Arkin, P.A. 1997, "Global precipitation: A 17-year monthly analysis based on gauge observations, satellite estimates, and numerical model outputs", *Bulletin of the American Meteorological Society,* vol. 78, no. 11, pp. 2539-2558.

Yarnal, B. 1993, *Synoptic climatology in environmental analysis: a primer,* Belhaven press London.

Yip, S., Ferro, C.A., Stephenson, D.B., et al. 2011, "A simple, coherent framework for partitioning uncertainty in climate predictions", *Journal of Climate,* vol. 24, no. 17, pp. 4634-4643.

Zelazowski, P., Malhi, Y., Huntingford, C., et al. 2011, "Changes in the potential distribution of humid tropical forests on a warmer planet.", *Philosophical transactions.Series A, Mathematical, physical, and engineering sciences,* vol. 369, no. 1934, pp. 137-160, doi:10.1098/rsta.2010.0238.

Zeng, N., Neelin, J.D., Lau, K., et al. 1999, "Enhancement of interdecadal climate variability in the Sahel by vegetation interaction", *Science,* vol. 286, no. 5444, pp. 1537-1540.